THE USE OF OPTICAL ACTIVITY MEASUREMENTS IN OIL SHALE PROCESSING

Dale L. Lawlor*, D. R. Latham*, T. C. Bartke*, and R. O. Asplund**

*Laramie Energy Research Center
P. O. Box 3395
Laramie, Wyo. 82071

**University of Wyoming
Chemistry Department
Laramie, Wyo. 82071

INTRODUCTION

Shale oil reserves are more than three and one-half times the amount of world petroleum reserves (1). But because of overburden, most of the reserves cannot be mined conventionally; an in-situ process must be used for oil recovery. The in-situ process has advantages over aboveground, conventional processes because transporting or crushing the shale is unnecessary before retorting; and spent shale disposal is no problem after retorting. But a disadvantage is the difficulty of monitoring the relatively deep underground conversion changes. One developing method for following these changes is optical activity measurements on the shale oil during its production because we know the optical activity of shale oil decreases with increasing heating rate (2). Shale oil is optically active because oil shale contains optically active biological markers derived from life forms existing during the formation of the shale deposit (3). Known biological markers--steranes, diterpanes, gammacerane, and perhydro-β-carotene--are reduction products from diagenesis of former living systems. Despite the rigors of heating, in most retorting systems these optically active molecules survive in sufficient quantities to allow their detection with a sensitive spectropolarimeter. These measurements show promise in studying large-scale field retorting systems.

This study at the Laramie Energy Research Center (LERC) shows examples of optical activity measurements in a controlled-state retort system, in the Site 9 in-situ field experiment, located at Rock Springs, Wyo., and in differing retorting systems using Green River, Antrim, and Moroccan oil shales.

EXPERIMENTAL

Optical activity measurements were made on the saturate fraction from the shale oil and bitumen, as described in detail earlier (2). Briefly, 1/2 g of dried oil in a 50-ml beaker was dissolved in 20 ml of cyclohexane (Burdick and Jackson Laboratories, Inc.). The solution was cooled to 0°C in a circulating cold bath, and 10 ml of 15 percent phosphorous pentoxide in sulfuric acid was slowly added with stirring. Stirring was continued for 1 hour, then the mixture was transferred and centrifuged for 1/2 hour at 3000 RPM. The cyclohexane layer was drawn off, and the bottom layer was twice more mixed with 10 ml of cyclohexane and centrifuged. Then the combined solution was decolorized by passing it over 10 gm of "powdered" silica gel (Baker, 60-200 mesh), eluting with cyclohexane, and collecting the first 10 ml of solution. The solution was evaporated under nitrogen to 20 ml. The optical activity was determined on this solution in the ORD mode with a Jasco J-20 spectropolarimeter. Optical activity data were determined in the 300- to 600-nm wavelength range and the solution was evaporated to dryness to determine the total saturates. The optical activity data were calculated based upon the amount of total saturates.

Shale oils and bitumens from an interrupted, controlled-state retort experiment (4) were analyzed. Green River formation oil shale, 1/8-to 1/2-in. particle

size, was packed into a vertical 3-in. stainless steel pipe and was externally electrically heated in 6-in. increments at a 2°F-per-minute heating rate with a zone travel rate of 3 in. per hour. Produced oil flowed downward with assistance from a nitrogen sweep gas. After approximately half of the shale column had reached a temperature of 1000°F (about 36 hours), the experiment was stopped; the pipe was cooled with water and cut into 24 6-in. segments. The shale samples from the 24 segments consisted of 14 spent-shale samples and 10 samples of oil-wet shale, with varying temperature exposures from 730°F to ambient. The oil-wet shale samples were rinsed with cyclohexane to recover the surface oil samples. The rinsed samples were dried at room temperature, crushed to 200 mesh, and Soxhlet extracted for 48 hours with cyclohexane to obtain the bitumen samples. The surface oil and bitumen samples were prepared and analyzed for optical activity as described.

Optical activity analyses were made on several retorting systems using the described method. Nine composite samples of shale oil were analyzed, representing 6 months of operation at the LERC Site 9 in-situ field experiment (5). Shale oils were analyzed from the bench-scale controlled-state retort system; from five aboveground, semi-works retort systems; and from two large-block systems.

RESULTS AND DISCUSSION

Only data from the 450-nm wavelength are presented in Figures 1 and 2 for ease of interpretation. Shale oil optical activity changes as the retort heating rate changes (2). And since heating rate consists of two components, temperature and time, optical activity changes should be related to each of these components. Data from analysis of oils and bitumens from the interrupted controlled-state retort are shown in Figure 1. Oils rinsed from the surface of the cooler shale have, except for samples 15 and 24, a specific rotation of about 4 units. Sample 15, having been exposed to the hottest temperature (730°F), shows only a trace of activity; and the last sample, 24, has about nine degrees of rotation, possibly because the cooler end of the retort causes dilution by accumulations of saturates. The wavelike distribution of the data is probably real in that it is well within the testing limits. The receiver oil, from about one-half of the total charged shale, shows an optical rotation of about four degrees, approximating the values from the surface oils.

The optical activity of the bitumens extracted from the partly retorted shale (samples 15 to 19) and from the unretorted shale (samples 20 to 24) is also shown in Figure 1. A smooth curve evolves, proceeding from sample 20 to 15, indicating that the effect of heat on the shale produces a uniform loss of optical activity in the bitumen. An induction period before the retorting of the shale (estimated to occur at about 400°F) occurs in the low-temperature loss of activity in samples 19 to 17. Sample 19 has a rotation of approximately 12 degrees; number 17 approximately 10 degrees. This 2-degree difference apparently results from increasing the temperature from 110 to 190°F over a 4-hour period. Samples 15 and 16 reflect a rapid loss of activity as the shale becomes heated to retorting temperature with subsequent emergence of oil. The rapid increase in optical activity from sample 20 to 23 cannot be satisfactorily explained at this time but approaches the optical activity of Green River natural bitumen--typically 30 units.

Oils from the Site 9 in-situ field experiment were analyzed for optical activity. The results in Figure 2 show that the oils produced during the first part of the 6-month experiment were more optically active than those in the second half. The lower optical activity in the second half of the experiment probably results from a different thermal history. The results may reflect change in the air-injection system when on the 60th day the injection well was changed from well No. 1 (located at the center of the site) to well No. 10 (located nearer the edge of the site), thereby moving the air injection closer to the moving combustion front, possibly further decomposing previously accumulated oil. The general decrease in

optical activity for all the composite oils indicates that after 6 months of production a "steady state" oil was not produced. The general indication of oil decomposition is not evident in 10 other physical or chemical tests, as shown in Table 1. Traditional indications of oil thermal decomposition such as increasing olefin, aromatic, and naphtha contents or decreasing viscosity and pour point, are not unequivocally present. In some instances, as in olefin content, the last four samples are in opposition to the optical activity data by having generally lower amounts of olefins--less oil decomposition. The optical activity data indicate that the last four samples are decomposed the most.

TABLE 1. - Properties of Site 9 composite oils

Property	Sample number								
	1	2	3	4	5	6	7	8	9
Naphtha, percent*	9	6	6	8	10	10	11	12	14
Olefins, percent in naphtha	36	32	25	19	--	19	14	27	9
Olefins, percent in light distillate	22	37	38	35	--	15	13	12	33
Paraffins, percent in naphtha	43	17	51	57	--	54	59	45	63
Paraffins, percent in light distillate	22	46	49	52	49	52	57	56	38
Aromatics, percent in naphtha	21	22	24	24	--	27	27	28	28
Aromatics, percent in light distillate	35	17	13	13	34	33	30	32	29
Residuum, percent*	6	6	6	7	5	4	5	8	7
Viscosity, SUS 100°F	53	58	57	53	50	46	47	56	45
Pour point, °F	35	40	40	45	45	40	45	40	35
Optical activity $[\alpha]^{25}_{450}$	3.2	2.1	1.9	1.8	1.6	0.8	0.6	0.3	0.2

*Determined by simulated distillation

Oils from different retorting systems were analyzed for optical activity to determine the possibility of observing basic differences among retorting systems. The results in Figure 3 show that differences are observable. Data from the entire 300- to 600-nm range are presented in Figures 3 and 4 for more comprehensive data evaluation. Generally, the optical activity data may be categorized into three groups. First, the least decomposed oils are derived from the controlled-state system where small shale particles, gravity flow, and nitrogen gas sweeping allowed the produced oil to escape from the shale easily thereby minimizing secondary oil decomposition. The second group of oils was produced from large, aboveground,

semi-works retorts with relatively medium shale particles (1 to 6 in.) and moderate capability for the oil to escape the shale. The third group of oils was produced from LERC's aboveground, simulated in-situ 150-ton retort and the Site 9 in-situ system that may be characterized as large-block systems; therefore, slow escape of oil from the shale would be probable. Slow escape of oil would presumably cause considerable decomposition.

Optical activity comparisons were made among oils produced in the LERC 10-ton retort using Green River, Antrim, and Moroccan shales. Figure 4 shows the Green River shale oil to be the most optically active by at least a factor of 2 at all wavelengths. The Antrim and Morrocan shale oils have essentially identical activity probably reflecting the amounts of optically active components in the original shales. These shales have, interestingly, a marine origin, while the Green River shale has a nonmarine origin.

SUMMARY

Optical activity measurements of shale oils allow insights into retorting conditions that are not observable by traditional analytical methods. With a bench-scale retort, a low-temperature induction period in the shale before retorting can be observed. The retorting phase itself may be observed by following changes in bitumen and in surface oil optical activity. Optical activity data from Site 9 composite oils, representing 6 months of production, reflect two distinct retorting phases of the experiment. The second, lower optically active phase, may have resulted from secondary degradation of previously accumulated oil. Despite 6 production months, a "steady state" oil was not produced. Optical activity data from 10 different retorting system oils show decreasing optical activity with increasing shale size.

REFERENCES

1. D. C. Duncan, Ind. Petrol. Assoc. Am., pp. 22, 49-51, Aug. 1958.

2. D. L. Lawlor, Preprints, Amer. Chem. Soc., Div. Fuel Chem., v. 22, (3), 100 (1977).

3. D. E. Anders and W. E. Robinson, Geochim. et Cosmochim. Acta, v. 35, 661 (1977).

4. J. J. Duvall and H. B. Jensen, Quart. Colo. School of Mines, v. 70, (3), 187 (1975).

5. A. Long, Jr., N. W. Merriam, and C. G. Mones, Ibid. (1977). (In press).

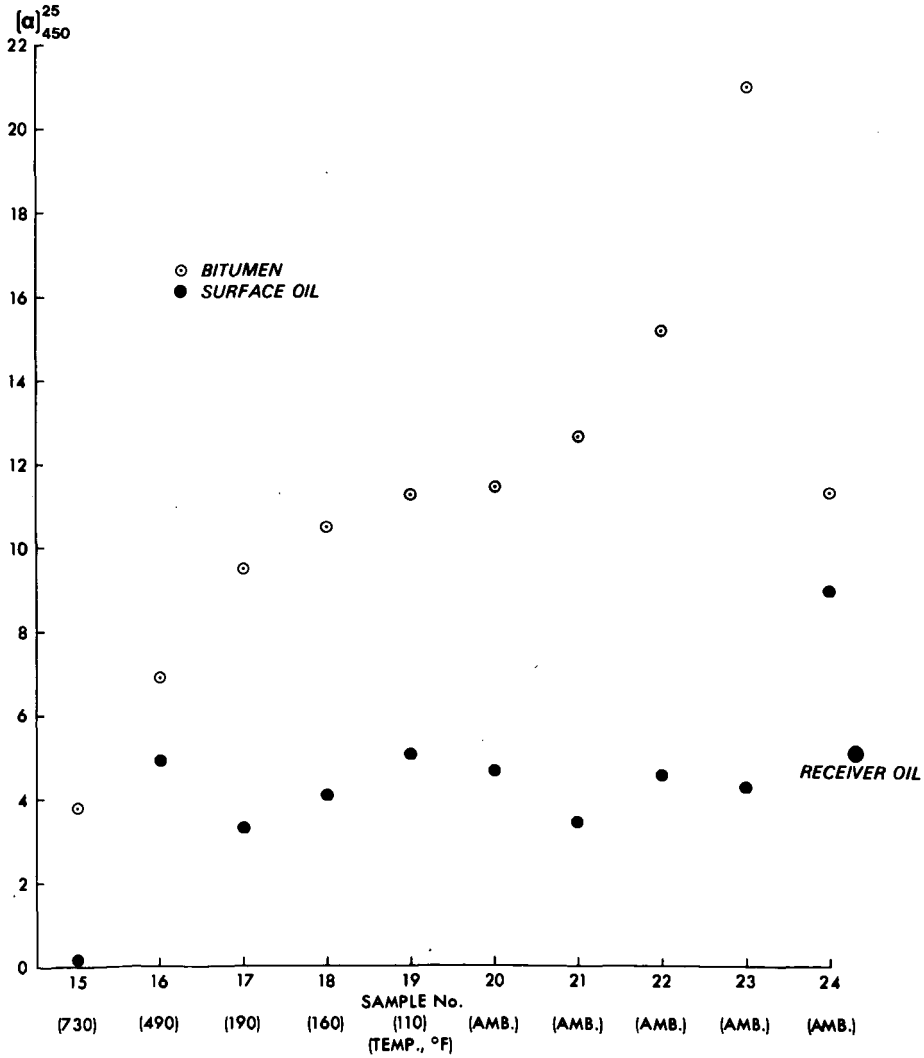

FIGURE 1. - OPTICAL ACTIVITY OF SATS. (450nm.), INTERRUPTED CONTROLLED STATE RETORT.

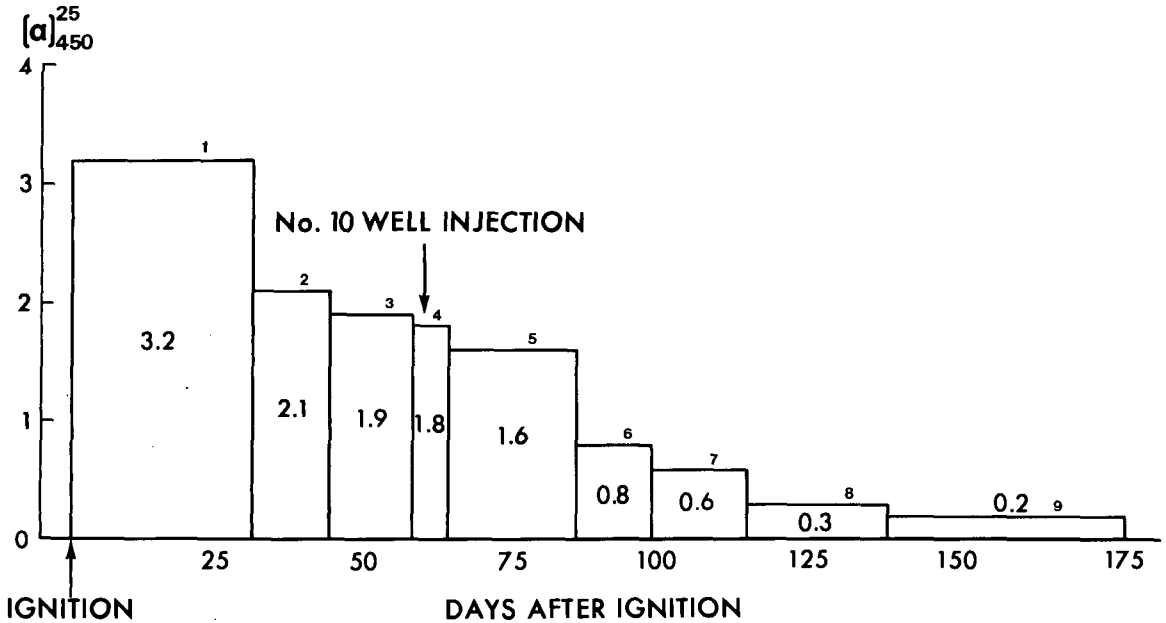

FIGURE 2. - OPTICAL ACTIVITY OF SITE 9 COMPOSITE OILS.

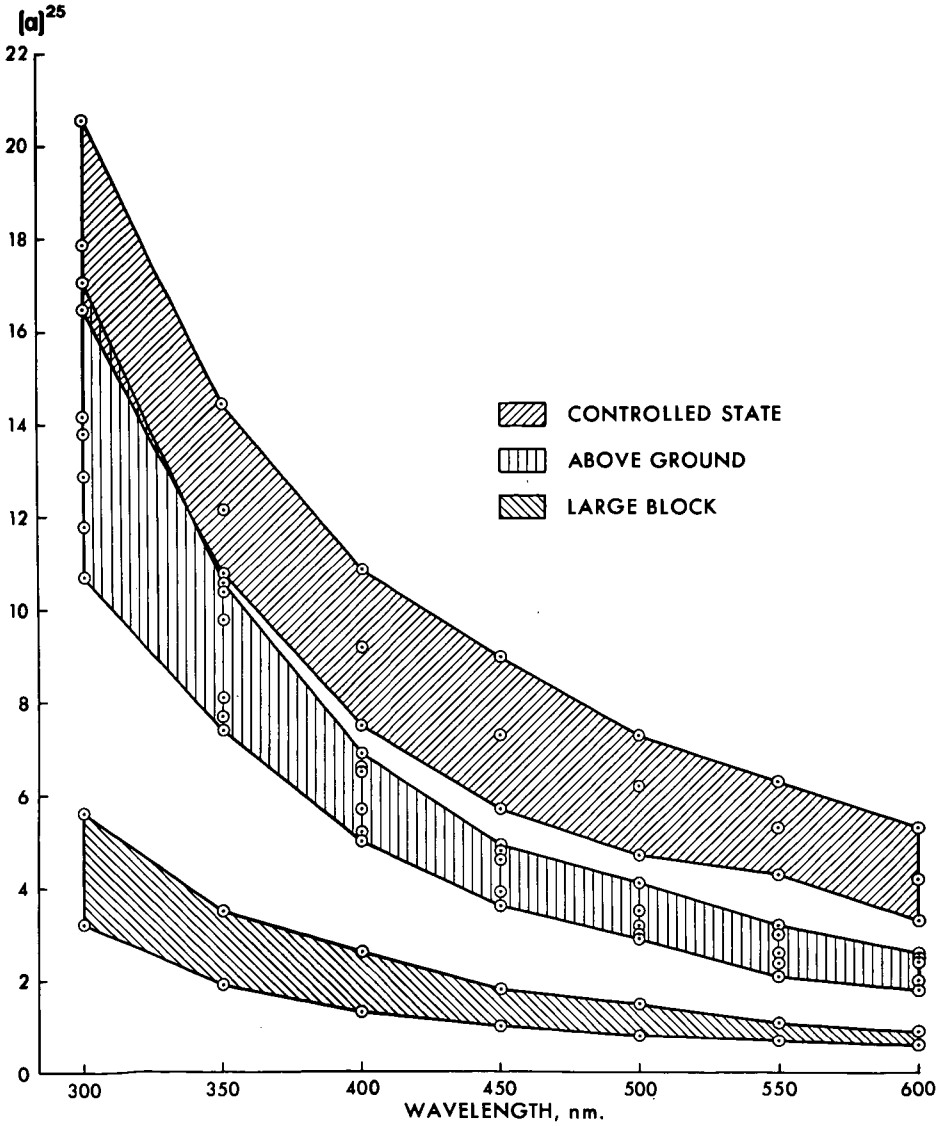

FIGURE 3. - OPTICAL ACTIVITY OF OILS FROM DIFFERENT RETORTS, GREEN RIVER FORMATION SHALES.

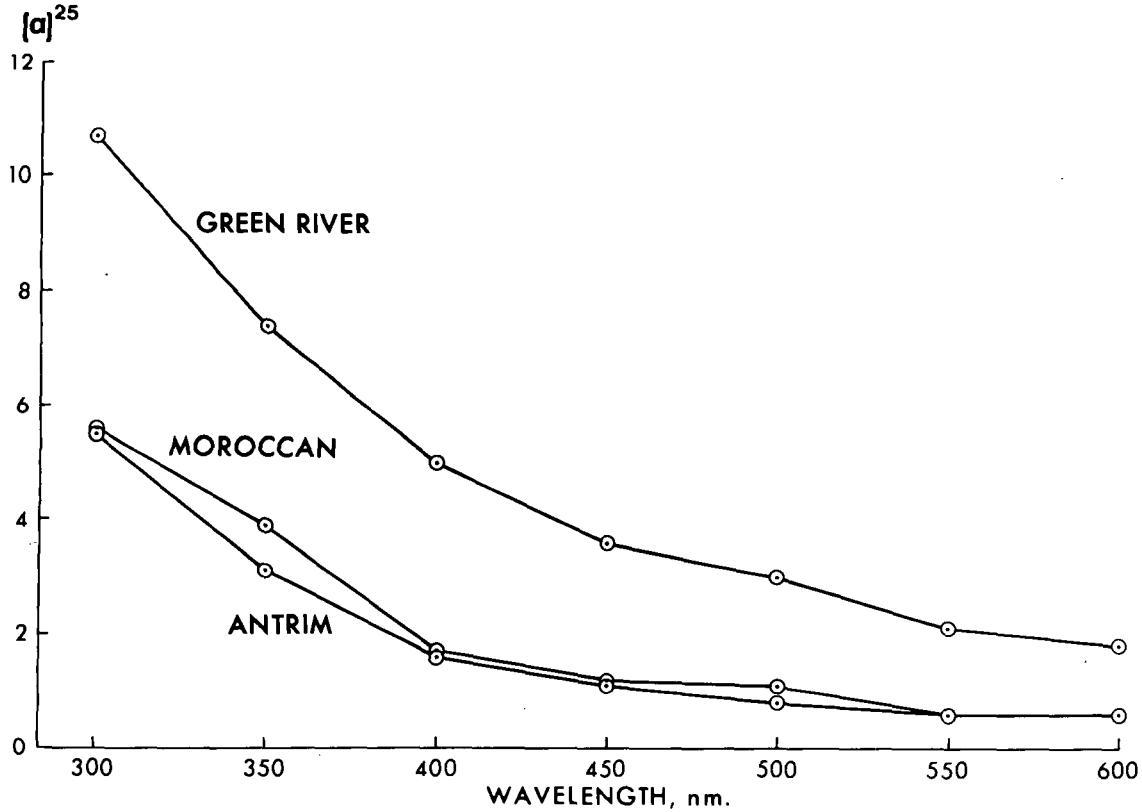

FIGURE 4. - OPTICAL ACTIVITY OF GREEN RIVER, ANTRIM AND MOROCCAN SHALE OILS, 10 TON RETORT.

PETROGRAPHIC METHOD FOR SELECTIVE DETERMINATION OF A COMPONENT (RAW COAL) IN A MIXTURE OF PRODUCTS FROM PROCESSING OF COAL

D. M. Mason
Y. Julian

Institute of Gas Technology
3424 S. State Street
Chicago, Illinois 60616

Introduction

In the HYGAS® pilot plant gasification reactor, fine particles from each reactor stage become entrained in the gas and are carried into the exit-gas cyclone and are removed from the gas. Thus, the dust removed by the pilot plant cyclone includes particles from the steam-oxygen-gasification fluidized bed, the second-stage hydrogasification fluidized bed, the first-stage hydrogasification entrained reactor, and the slurry drier fluidized bed. (See Figure 1.) For an understanding of the process, it is desirable to estimate the amount of feed coal carried out of the reactor from the slurry drier bed. To fill this need, we have developed a petrographic method for determining the feed coal content of samples of dust collected from the cyclone. The method was developed on samples obtained when the pilot plant was operating on lignite, but it should also be applicable to samples from the processing of other ranks of coal.

If the dust collected from the cyclone were composed of material from only two sources and the two components differed in character, it would be possible to estimate their relative proportions from the elemental composition or other test property of the sample and its two sources. This situation would also apply in effect if some test property were sufficiently uniform among all sources but the one of interest. This is not the case here, as shown by analyses of typical bed samples from the different stages of the reactor (Table 1). Table 1 also shows that the cyclone dust is much finer than the samples of source materials, as might be expected. One should, therefore, analyze corresponding fines fractions of the source materials if this approach appeared fruitful. However, note that the composition of the fines elutriated from a particular bed may differ from the composition of particles of the same size range sampled from the bed. Thus, one can only surmise, from the composition data of Table 1, that the amount of feed coal in the cyclone dust is probably between zero and 25 weight percent.

Development of Method

In the customary form of petrographic quantitative analysis for the organic components (macerals) of coal, the sample is mixed with epoxy resin and pressed in a mold to obtain a cylindrical briquet. After hardening, the briquet is sectioned and polished in a manner such that the macerals can be identified under the microscope (ASTM Methods D2797 and D2799) (1). Using an eyepiece with crosshairs, successive areas of the polished surface are examined, and the macerals that appear under the crosshair intersection are counted. (A crosshair grid with multiple intersection points can also be used.) The number of counts of each component is proportional to its area in the section and its volume in the sample; with a sufficient number of counts, the percentage of counts for a component is a satisfactory measure of its volume percent in the sample. Points appearing on mineral matter and the resin matrix are ignored. The volume percent of each maceral on the mineral-matter-free basis is customarily reported, but can be converted to an ash- or mineral-matter-containing basis by calculation from ash content and estimated densities.

We concluded that application of this method to the cyclone fines would be very difficult because of the nature of some of the components other than the coal feed.

As gasification progresses the particles become increasingly porous and the proportion of mineral matter increases. Mineral matter other than iron sulfides is sometimes difficult to distinguish from the mounting medium, and clay particles especially are subject to plucking during the grinding and polishing. Instead we investigated a variant procedure in which we gravimetrically determine the weight percent of the sample in the briquet and, by a point count analysis, determine the volume percent of feed coal in the briquet, lumping all other components and mounting medium together. The densities of the feed coal and of the briquet are then needed to convert the volume percent of feed coal in the briquet to weight percent. From the weight percents of feed coal and sample in the briquet we obtain the weight percent of feed coal in the sample.

Some extra care in the mounting procedure is required to obtain briquets of known and uniform sample content. The usual technique in which the sample-resin mixture is pressed in a mold is not applicable because the clearances of the mold may allow liquid resin and some of the small particles to escape and thus change the composition of the mixture and resulting briquet. For this reason, we limit the sample content to obtain a mixture that is easily mixed and that will retain a minimum of air bubbles after hand stirring with a wooden splint. Note that the presence of bubbles is not deleterious provided they are uniformly distributed. Removing the bubbles by centrifuging, for example, is likely to cause sample concentration. Stirring with a propellor stirrer is satisfactory if done without breaking the surface of the mixture.

The density of the briquet can be determined very simply by weighing it in air and in water. Determining the appropriate density of the feed coal is not so simple. True (solid phase) density is easily determined by helium or water displacement or can be estimated from the hydrogen and ash content (3). However, some coals, especially high volatile C bituminous rank and lower, contain a substantial volume of submicroscopic pores. The density we use should include these pores but not those that are visible under the microscope, such as shrinkage cracks in lignite and the lower ranks of subbituminous coals. Particle density determined by mercury displacement is suitable if most of the particles are larger than about 100-mesh sieve size and if they do not contain an appreciable volume of microscopically observable pores or cracks. On our cyclone fines we determined true density by helium displacement on a Beckman Air Pycnometer; from this and porosity obtained from an equilibrium moisture determination, we calculated particle density. Note that use of this porosity value on our dried lignite feed is based on the conclusion, from unpublished work at IGT, that the dried lignite does not swell appreciably when immersed in water. However, we need to apply a correction to the pore volume because of the enhanced density of water (or actually of the water-coal complex) in the pores of low rank coal (4). This is the reason that density determined by water displacement on low rank coals is higher than density determined by helium displacement. Later we realized that if we had used apparent density in water, no correction would be necessary as the effect then cancels out. The respective equations for the particle density, d, of dry coal are —

$$d = [1/(d_{He} + 0.10) + M/(100 - M)]^{-1} \qquad 1)$$

and

$$d = [1/(d_w) + M/(100 - M)]^{-1} \qquad 2)$$

where d_{He} and d_w are densities in g/cm^3 determined by helium and water displacement, respectively, and M is the weight percent of equilibrium moisture. The quantity 0.10 in the first of these equations is our value for the difference between the two densities for this coal (2).

In the point count analysis of the briquet the feed coal is recognized principally by the low reflectance of its vitrinite and exinite, ranging below about 0.4%, compared with the substantially higher reflectance of vitrinite that has been heated to 800°

to 900°F in the first stage of hydrogasification and to even higher temperatures in succeeding stages. However, some particles darken as gasification progresses in the later stages; perhaps these particles contain dispersed clay that becomes more concentrated and thus lowers the reflectance. However, these particles also become grainy, so they can still be distinguished from the feed coal rather easily. We have not been able to distinguish whether particles composed of inertinite only or mineral matter only originate from the feed coal or from one of the reaction stages. Accordingly, we count as feed coal the points falling on any maceral or on mineral matter if the particle that the point is on contains any recognizable vitrinite. Then, to correct for the presence of particles from the feed coal containing inertinite or mineral matter only, we analyze by point count the fines of the feed coal that pass a 100-mesh USS sieve to obtain the volume fraction of such particles.

The weight percent of coal in the cyclone sample is calculated according to the formula –

$$\text{Coal, wt \%} = \frac{100\ dV}{d_b(1 - I_c)W} \qquad 3)$$

where d is the particle density of the coal, d_b is the density of the sample briquet, V is the determined volume percent of coal in the sample briquet, I_c is the volume fraction of particles in the coal fines containing inertinite or mineral matter only, and W is the weight percent of sample in the sample briquet.

Apparatus and Procedures

The sample was dried enough that the retained moisture did not interfere with the curing of the epoxy resin. Weighed amounts of epoxy resin, sample, and activator were mixed to yield a briquet of accurately known and uniformly dispersed dry sample content of 30 to 40 weight percent. After curing in a mold overnight the density of the briquet was determined by weighing in air and water, and the briquet was ground and polished according to the methods of ASTM D2797 (1). Feed coal briquets were prepared in the same way.

For the point count analysis a Zeiss Universal microscope was used with a 40X Achromat objective giving a magnification of 625X with a 12.5X eyepiece. Points were counted at the corners of a Whipple disk to a total of 1000 on each of two briquets. Points were counted on the feed coal fines in the same manner except that inertinite and mineral matter were also counted.

Equilibrium moisture was determined according to a modification of ASTM D1412 (1) in which a 10 g sample was used and the temperature was maintained near room temperature by placing the equilibrium vessel in an insulated box.

Results and Conclusions

The helium density of the feed coal fines was 1.63 g/cm^3 and the equilibrium moisture content 21.1 weight percent; these give a particle density of 1.18 g/cm^3. The point count analysis of six briquets of the feed coal is shown in Table 2; two briquets each were prepared from three different coal-resin mixtures. The average content of vitrinitic particles (from the six analyses) was 91.0 volume percent. The amount of feed coal found in each briquet by the point count analysis, when calculated according to this average content of vitrinitic particles and expressed as percent of the amount determined gravimetrically in our preparation, ranged from 90% to 112% with an average of 102%.

Replicate determinations on some cyclone dusts (Table 3) indicates the repeatability that was obtained in the point count. Only one resin-sample mixture was prepared for each sample because of the limited quantity of sample available; for two of

them only one briquet could be made. A new section of each briquet was exposed by regrinding and repolishing to obtain a duplicate point count analysis of each briquet.

The good average recovery on the feed coal briquets lends support to the principles of the method and indicates that systematic errors have been reduced to a satisfactory level.

With the analysis for feed coal in the cyclone dust in hand we can attempt to draw some additional conclusions about the source of the remainder of the dust. For example, if we take the analyses in Table 1 to be representative of the fines elutriated from each bed, then about 45% to 55% of the cyclone dust must come from the steam-oxygen gasifier. However, note that sampling of such streams at about 1200 psi presents severe difficulties and the analyses shown may not fully represent the composition (or size distribution) of the actual process solids.

Acknowledgments

This work was conducted as part of the HYGAS® coal gasification program jointly sponsored by the United States Energy Research and Development Administration (ERDA) and the American Gas Association. This program is under the technical direction of Mr. Stephen C. Verikios of ERDA (now DOE) and Dr. Ab Flowers of the American Gas Association.

References

1. American Society for Testing and Materials, 1974 Annual Book of ASTM Standards, Part 26, "Gaseous Fuels: Coal and Coke; Atmospheric Analysis." Philadelphia, 1974.

2. Institute of Gas Technology, "Pipeline Gas From Coal — Hydrogenation (IGT Hydrogasification Process)," Project 8907 Interim Report No. 2 for the Period July 1974 to June 1975, No. FE-1221-144, pp. 286-90. Washington, D.C.: U.S. Energy Research and Development Administration, July 1976.

3. Institute of Gas Technology, "Preparation of a Coal Conversion Systems Technical Data Book," Project 8964 Final Report for the Period October 31, 1974 to April 30, 1976, No. FE-1730-21, Section PMa.44.1.2. Washington, D.C.: U.S. Energy Research and Development Administration, 1976.

4. Institute of Gas Technology, "Preparation of a Coal Conversion Systems Technical Data Book," Project 8979 Quarterly Status Report for the Period May 1 to July 31, 1976, No. FE-2286-4, pp. I-1 to I-15. Washington, D.C.: U.S. Energy Research and Development Administration, November 1976.

RBC/PC

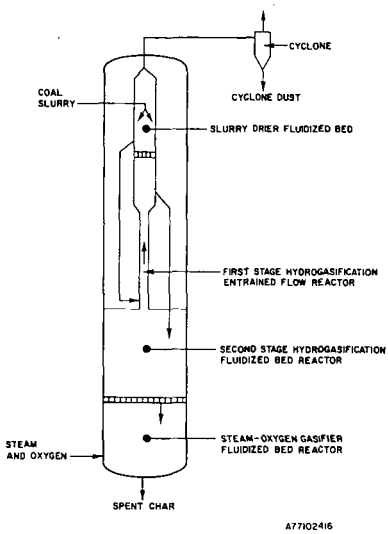

Figure 1. SCHEMATIC DIAGRAM OF HYGAS® PILOT-PLANT REACTOR SHOWING FLOW OF SOLIDS

Table 1. TYPICAL COMPOSITION OF SOLIDS IN THE HYGAS REACTOR DURING RUN 37 ON LIGNITE

	Feed Coal (Lignite)	After First Stage*†	Second Stage Bed†	Spent Char From Steam-Oxygen Gasifier†	Cyclone Dust
	wt%				
Proximate Analysis (as received)					
Moisture	17.0	3.7	2.6	7.0	2.6
Volatile Matter	35.2	19.2	8.5	9.3	15.5
Ash	9.7	22.9	28.2	46.1	36.5
Fixed Carbon	38.1	54.2	60.7	37.6	45.4
Ultimate Analysis (dry basis)					
Carbon	61.9	62.8	65.2	44.9	52.9
Hydrogen	4.31	2.70	1.56	0.94	2.00
Nitrogen	1.01	1.02	0.55	0.22	0.67
Sulfur	0.86	0.48	0.17	0.10	0.38
Ash	11.74	23.76	28.93	49.58	37.52
Oxygen (by difference)	20.18	9.24	3.59	4.26	6.53
Sieve Analysis, USS					
Retained on No.					
12	11.0	2.5	6.5	0.1	0.0
20	23.6	11.5	19.6	2.9	0.0
30	11.1	6.7	9.7	4.4	0.6
40	10.3	6.3	10.7	6.4	0.6
60	14.9	13.4	16.9	16.5	2.1
80	6.9	7.4	8.4	11.4	2.5
100	2.8	5.5	4.3	7.6	3.5
200	8.3	16.9	13.2	19.7	24.7
325	4.1	15.4	7.2	12.5	30.9
Pan	7.0	14.4	3.5	18.5	35.1

*Sampled from the spouting bed above the lift line reactor.

†Because of high-pressure sampling difficulties, these analyses may not be representative of the composition or size distribution of the process solids.

Table 2. ANALYSIS OF FEED COAL

Briquet No.	1A	1B	2A	2B	3A	3B
Density of Briquet, g/cm^3	1.216	1.210	1.198	1.198	1.209	1.209
Feed Coal in Briquet, as Prepared, wt %	33.7	33.7	28.8	28.8	26.5	26.5
Point Count Analysis						
Vitrinitic Particles, vol % of Briquet	28.5	31.9	29.9	27.2	24.6	27.1
Vitrinitic Particles, % of Whole Coal	88.8	92.1	94.0	91.0	92.1	91.2
Whole Coal, wt % of Briquet*	30.2	34.0	32.2	29.2	26.2	28.9
Whole Coal by Point Count/ Whole Coal by Gravimetric Preparation, %	90	101	112	102	99	109

*Based on average vitrinitic particle content of whole coal = 91.6 vol %.

Table 3. ANALYSIS OF CYCLONE DUSTS

Sample No.	Briquet No.	Feed Coal Content, wt % Initial	Reground	Average
1	1013	5.0	4.4	4.7
2	1015	8.2	6.3	6.6
	1016	5.7	6.0	
3	1014	5.8	4.5	5.2
4	1005	2.9	3.2	4.4
	1008	6.6	5.0	
5	1007	6.6	6.6	7.1
	1009	7.1	8.1	
6	1011	7.8	8.5	8.0
	1012	7.1	8.6	
7	1006	7.0	7.3	7.8
	1010	9.3	7.4	

Developments in Solid State NMR and Potential Applications to Fuel Research*

Alex Pines and David E. Wemmer

Department of Chemistry and Materials and Molecular Research Division,
Lawrence Berkeley Laboratory, University of California
Berkeley, California 94720

The high resolution NMR of two important nuclei (^{13}C and ^{2}D) in the solid state is now a practical possibility. This adds a useful tool to the arsenal of analytical chemistry in the area of solid materials which are insoluble or otherwise not amenable to classical spectroscopic techniques. The study of ^{13}C is made possible by a double resonance method (Proton Enhanced NMR) due to Pines, Gibby and Waugh and has now reached the stage where analysis of some functional groups in coal is possible. A simple physical picture of the method will be given in the talk. As an example, Figure 1 shows spectra on our spectrometer and our computer from a sample of coal from Dr. F. Mayo at SRI working on an ERDA fossil energy related project. At top is the ^{13}C proton enhanced NMR spectrum. At bottom are the computer generated lineshape analyses for four carbon types (aliphatic 26%, ether 13%, aromatic 53% and polycondensed aromatic 8%). In the center is the computer simulation done by adding the four shapes at the bottom and adding some noise--you must agree that there is some similarity with the experimental spectrum. We thus believe the method is quick and reasonably reliable ($\sim$ 10%) for studying whole coals, coal processing, coal by-products and other fuel related materials. We shall show several examples of this in the talk and discuss the advantages and limitations of the method.

The study of ^2D NMR in the solid adds a new possible dimension since isotopic labeling during processing could be followed directly in the solid state. This was considered until recently a particularly nasty nucleus since ^2D linewidth are typically 200 KHz ($\sim$ 1000 ppm wide) in the solid state. A method due to Vega, Shattuck and Pines (Fourier Transform Double Quantum NMR) now brings this nucleus into the realm of high resolution and the possibility of analytical applications. Again, a simple physical picture of the method will be presented in the talk. As an example, Figure 2 shows the first resolution of deuterium chemical shifts in the solid state. At top is an NMR free induction decay taken by the double quantum method. The Fourier transform spectrum at the bottom shows true ^2D chemically shifted lines, one due to the COOD and one due to HDO. Several recent examples of this solid state ^2D spectroscopy will be described and its possibilities and limitations discussed.

---

* Supported by U.S. Energy Research and Development Administration.

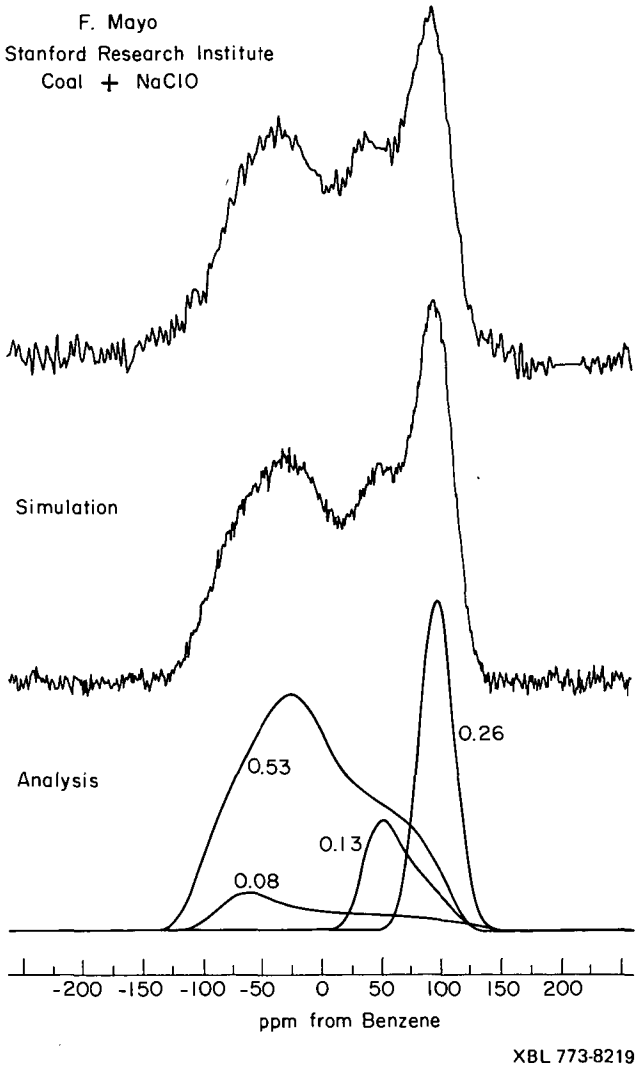
F. Mayo
Stanford Research Institute
Coal + NaClO
Simulation
Analysis
0.26
0.53
0.13
0.08
-200 -150 -100 -50 0 50 100 150 200
ppm from Benzene
XBL 773-8219

Figure 1

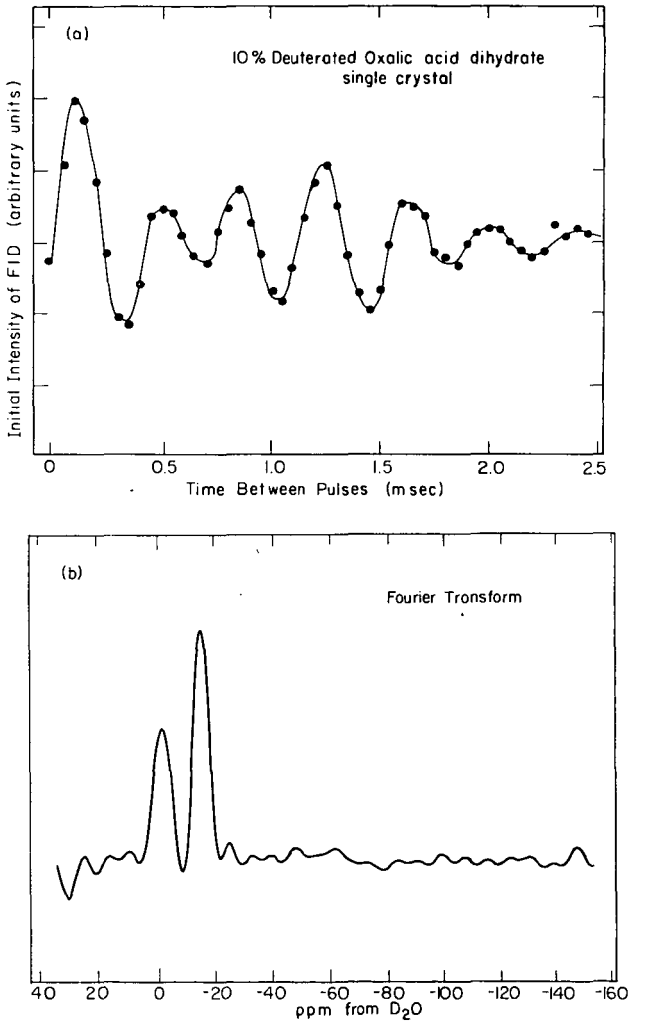

XBL 763-722A

Figure 2

^{13}C NMR Studies of Coals and Oil Shales

Victor J. Bartuska and Gary E. Maciel
Department of Chemistry, Colorado State University
Fort Collins, Colorado U.S.A. 80523

and

Francis P. Miknis, Laramie Energy Research Center
U.S. Department of Energy
Laramie, Wyoming 82070

INTRODUCTION

The "standard" ^{13}C nmr techniques, including pulse Fourier transform (FT) approaches[1] have not been generally useful for solid samples because of (1) the excessive line broadening due to dipole-dipole interactions between ^{13}C and ^{1}H magnetic dipoles, (2) chemical shift anisotropies (different shielding values for the many different orientations of the molecules in an amorphous state with respect to the magnetic field direction), and (3) long ^{13}C spin-lattice relaxation times (T_1).[2] All of these problems are eliminated in liquids (or in the case of long T_1 values, at least greatly reduced) by the normal tumbling motions occurring randomly in the liquid state.

For an analytical technique in the field of fossil fuels, the constraint to liquid samples has been very restrictive. For many types of samples, e.g., oil shales and typical coals, only a small fraction of the organic substances can be extracted from a solid under mild conditions that would be expected to retain the primary structural integrity of the organic compounds.

The recently developed techniques used to narrow the lines of ^{13}C nmr signals in solids are high power ^{1}H decoupling[3] and magic-angle spinning.[4-7] The former involves irradiation of the proton manifold at the ^{1}H resonance frequency. It is analogous to the common "spin-decoupling" technique for eliminating splittings due to indirect spin-spin coupling in standard high-resolution nmr experiments; but it requires much higher radio frequency power, because direct dipolar $^{13}C,^{1}H$ interactions are much larger than indirect $^{13}C,^{1}H$ coupling constants.

The importance of magic-angle spinning is that rapid sample spinning at the magic angle eliminates the effects of chemical shift anisotropy, i.e., averaging the resonance positions corresponding to the various orientations of a particular type of carbon atom in the solid sample to the isotropic limit that would be observed if the sample were in a nonviscous liquid state.[7,8] This is because the anisotropic part of the shielding tensor involves a trigonometric factor which vanishes at a value 54.7° (the magic angle) for the angle between a shielding tensor axis and the magnetic field axis.

The remaining source of line broadening expected of ^{13}C resonances in solid fuels is the dispersion of (isotropic) chemical shifts of a given class of carbon atoms over a range due to subtle structural differences associates with the complex structural variations in such samples. This dispersion of chemical shifts is not removed by the techniques discussed in this paper, and is ultimately a genuine source of structural information.

The third problem mentioned above, the long spin-lattice relaxation times in solids, is circumvented by the development by Waugh and coworkers of cross polarization methods, or Proton Enhanced Nuclear Induction Spectroscopy.[3] In cross polarization an enhanced ^{13}C magnetization is achieved at a rate much faster than the rate of reestablishment of an equilibrium ^{13}C magnetization via ^{13}C spin-lattice relaxation. This is achieved by the ^{1}H spin-lock procedure[3] and the establishment of Hartmann-Hahn conditions, $\gamma_C H_1^C = \gamma_H H_1^H$, where γ_C and γ_H are the magnetogyric ratios of ^{13}C and ^{1}H, respectively.

Although several variations of the general type of cross polarization experiment have been suggested, the form employed in this work is that originally described by Pines, Gibby and Waugh[3] for ^{13}C; it is shown schematically in Fig. 1. The key feature responsible for the success of the cross polarization experiment for ^{13}C in solid samples is the rapid transfer of magnetization from the proton spin set to the ^{13}C spin set under the Hartmann-Hahn condition. This transfer permits the establishment and repetitive reestablishment of the ^{13}C spin polarization needed for ^{13}C nmr detection, without waiting the long times (three to five ^{13}C T_1's) required for establishment of the polarization via normal ^{13}C spin-lattice relaxation processes. The experiment can be repeated after waiting for the protons to repolarize (three to five ^{1}H T_1's). This repolarization is generally a much more efficient process than ^{13}C repolarization by spin-lattice processes.

Using the cross-polarization/high-power ^{1}H decoupling technique, ^{13}C spectra of the type shown in Fig. 2 were obtained. A variety of factors preclude using spectra obtained in this way directly for the quantitative determination of the aliphatic carbon/aromatic carbon ratio.[7,9] These factors include chemical shift anisotropies and related peak overlaps, unequal cross-polarization efficiencies and the undetermined distribution of relevant proton relaxation times. This current limitation can be eliminated only by overcoming or characterizing these factors, a subject of continuing research in these laboratories. Nevertheless, we have observed a very interesting and useful correlation obtained directly from the raw spectra.

In the spectra of the type shown in Fig. 2, the region to the right (higher shielding) of the arbitrarily-drawn vertical dashed line can be identified largely with the resonances of aliphatic carbons, while the region to the left is associated mainly with aromatic carbons (perhaps some olefinic carbons and carbonyl carbons). If the area under the spectrum to the left of the line is referred to as A, the area to the right as B, and the total area (A+B) as C, then A/C is roughly the fraction of total organic carbon that is aromatic and B/C

is roughly the fraction which is aliphatic. Then, if P is the percent (by weight) organic carbon in the sample, measured independently (by total carbon minus carbonate and bicarbonate), the quantity AP/C is an indication of the percent aromatic carbon in the sample and BP/C is the percent aliphatic carbon. Figures 3 and 4 show the results of plotting these fractions against oil yield (gal/ton). For the twenty oil shales and kerogens examined in this study, the total organic carbon content (P) ranged from 11 to 81 percent (by weight) and the (apparent) fraction of aliphatic carbon (B) ranged from 0.37 to 0.85.

Fig. 3 indicates that there is little correlation between the amount of aromatic carbon in an oil shale and its oil yield. By contrast, Fig. 3 shows a high level of correlation between the amount of aliphatic carbon in an oil shale and the yield of oil obtained in retorting. These results support the thesis that it is the aliphatic part of the kerogen that is largely responsible for the oil retorted from oil shale. The results are also consistent with earlier evidence that higher H/C ratios in oil shales are associated with higher oil yields.[10] Furthermore, the results suggest that refined ^{13}C nmr measurements (faster and more accurate) may provide a convenient method for determining not only the structural characteristics of kerogen, but also the economic potential of individual shales.

Similar experiments on a wide range of coal samples are underway and will be described in the talk. The resolution of aromatic and aliphatic carbons can be improved from what is shown in Fig. 2 by magic-angle spinning. The consequences of this improvement are also discussed.

Acknowledgement

The authors gratefully acknowledge support of this research by the U.S. Energy Research and Development Administration, Laramie Energy Research Center, and valuable discussions with Drs. J. Schaefer, E.O. Stejskal and D.L. VanderHart.

References

1. T.C. Farrar and E.D. Becker, "Pulse and Fourier Transform NMR," Academic Press, New York, 1971.

2. J.A. Pople, W.G. Schneider and H.J. Bernstein, "High-resolution Nuclear Magnetic Resonance," Ch. 3, McGraw-Hill, New York, 1959.

3a. A. Pines, M.G. Gibby and J.S. Waugh, 1972, J. Chem. Phys., 56, 1776.
b. A. Pines, M.G. Gibby and J.S. Waugh, 1973, ibid., 59, 569.

4. I.J. Lowe, 1959, Phys. Rev. Letters, 2, 285.

5. H. Kessemeier and R.E. Norberg, 1967, Phys. Rev., 155, 321.

6. E.R. Andrew, 1971, Progr. Nucl. Magn. Reson. Spectrosc., 8, 1.

7. V.J. Bartuska, G.E. Maciel, J. Schaefer and E.O. Stejskal, 1977, Fuel, 56, 0000.

8a. J. Schaefer, S.H. Chin and S.I. Weissman, 1972, Macromol., 5, 798.
b. E.O. Stejskal, J. Schaefer, J.M.S. Henis and M.K. Tripodi, 1975, J. Chem. Phys., 61, 2352.

9. D.L. VanderHart, H.L. Retcofsky, Fuel, 1976, 55, 202.

10a. F.P. Miknis, A.W. Decora, and G.L. Cook, Pulsed Nuclear Magnetic Resonance Studies of Oil Shales - Estimation of potential oil yields. U.S. Bureau of Mines, RI 7984 (1974).

b. E.W. Cook, Fuel, 1974, 53, 16.

Figure Captions

Figure 1. Timing sequence of ^{1}H and ^{13}C irradiation and ^{13}C observation in a typical cross polarization experiment.

Figure 2. Cross polarization spectra of three oil shales with different aliphatic C/aromatic C ratios. The arbitrary vertical line roughly separates the aliphatic from the aromatic regions of the spectra.

Figure 3. A plot of the apparent percent aromatic carbon (AP/C) of twenty oil shales and kerogens vs. the oil yields of the oil shales in gal/ton.

Figure 4. A plot of the apparent percent aliphatic carbon (BP/C) of twenty oil shales and kerogens vs. the oil yields of the oil shales in gal/ton.

Fig. 1

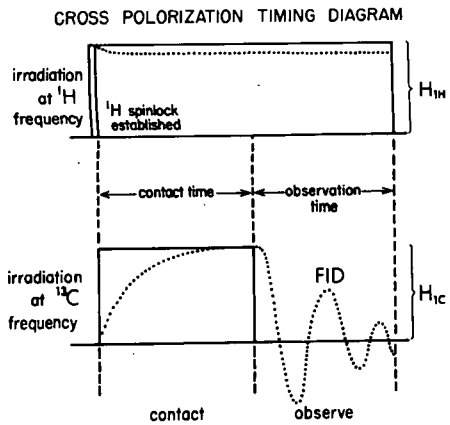

Fig. 2

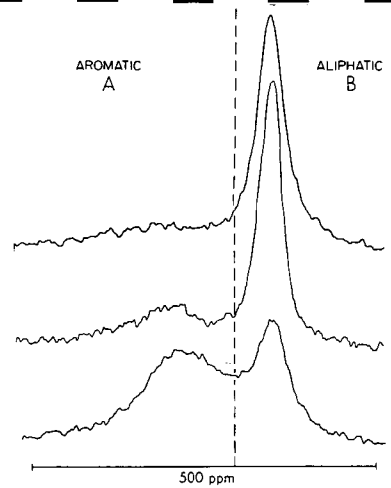

Fig. 3

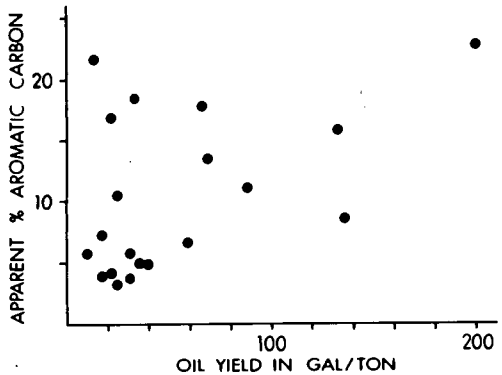

Fig. 4

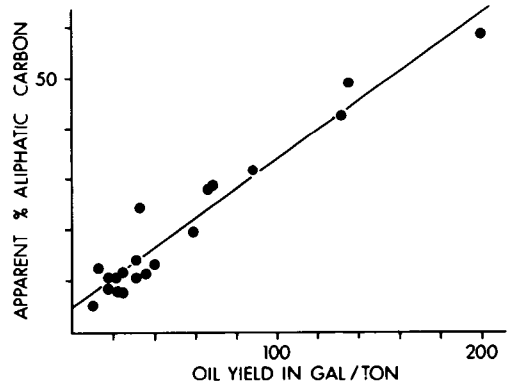

A CARBON-13 NMR INVESTIGATION OF THE CHEMICAL COMPOSITION OF COAL DERIVED LIQUIDS

Ronald J. Pugmire, Kurt W. Zilm, David H. Bodily
David M. Grant, Hironori Itoh, Susumu Yokoyama

Departments of Chemistry, and Mining, Metallurgy and Fuels Engineering
University of Utah, Salt Lake City, Utah 84112

The recent increased importance of coal as an energy source has dictated that more knowledge be obtained about the basic molecular properties of the solid and its conversion properties. Starting as early as 1966, Carbon-13 NMR spectroscopy has been employed on a limited basis for the analysis of coal derived liquids as well as petroleum samples. Extensive C-13 NMR work has been carried out in our laboratories on Utah coal derived liquid samples which have been subjected to LC and GPC separation techniques. NMR data taken at 25 MHZ and 75 MHZ have been analyzed on the acidic, basic, and neutral portions of the oils in question. These data have demonstrated that valuable chemical information can be readily obtained on aromatic and hydroaromatic ring structures and ring substituents in coal liquids obtained from different sources. The chemical significance of these results will be discussed.

I. Introduction

The recent increased importance of coal as an energy source has dictated that more knowledge be obtained about the basic molecular properties of the solid and its conversion products. In the solid form, coal does not readily lend itself to a detailed molecular characterization. However, recent advances in experimental techniques[1] have been quite encouraging and promise to shed new light on this chemical structural characteristic of solid hydrocarbons.

Starting with the work of Friedel and Retcofsky,[2,3] Carbon-13 nuclear magnetic resonance has been employed on a limited basis for the analysis of coal derived liquids as well as petroleum samples.[2,4] Early works were somewhat hampered in these investigations due to such complicating factors as: 1) instrument sensitivity and techniques; 2) the lack of an extensive reservoir of Carbon-13 magnetic resonance (CMR) data on which to base detailed spectral interpretation; and 3) the extremely complex chemical composition of the materials under investigation. The problems associated with adequate instrumentation for the analysis of complex hydrocarbon investigation have largely been overcome in the past 5-7 years with the advent of fourier transform NMR techniques.[5] Many early workers in the CMR field concentrated their efforts on hydrocarbons and by the early 1970s a fairly extensive body of chemical shift data on fossil fuel derived hydrocarbons was emerging.[6] Advances in instrumentation has significantly aided in this interpretation of the composition of complex hydrocarbon mixtures. Whereas, early studies were concerned with such problems as aromaticity of various coal samples[2,3,4,6,7,8] and average molecular parameters,[9] only limited progress was made in increasing the sophistication of the analytical results obtained by means of CMR. More recent workers focused on analysis of the extracts from coal.[10,11] However, recognition of the necessity to fractionate coal derived liquids in order to enhance sample analysis has provided useful new information regarding the chemical structure of the liquid.[12,13] While LC and GPC separation schemes required to fractionate the coal liquids are well known, they involve significant effort.

This work is the first in a series describing the chemical information derived from the LC and GPC chromatographic separation and CMR analysis of the liquefication products of Hiawatha high volatile bituminous coal.

II. Experimental

A. Liquefication and Separation Procedure

The coal used in this study was Utah high volatile bituminous B rank. The details of the hydrogenation procedure have been given elsewhere.[14] The coal hydrogenation product was initially obtained as a "light liquid" and "heavy liquid" product in the two condenser units of the reactor. The heavy coal hydrogenated product was separated into saturates, monoaromatic, diaromatic, triaromatic, and polyaromatic/polar fractions using gradient elution through dual-packed (silica gel-alumina gel) absorption columns according to the technique described by Hirsch et al.[15] Further separation of these fractions was obtained by means of gel permeation chromatography (GPC) in accordance with the procedure of Haines and Thompson.[16] The separation scheme employed is portrayed in Figure 1.

B. NMR Procedures

Proton spectra for each sample was obtained on a Varian EM-390 spectrometer. Carbon-13 NMR spectra were obtained on Varian XL-100 and SC-300 sepectrometers, operating in the fourier transform mode. At 25 MHZ, an 8K spectra was obtained on each sample using 0.8 sec. acquisition time, a 45° pulse angle and no pulse delay. At 75 MHZ, a 16 K spectra was obtained utilizing 0.9 sec. acquisition time, a 45° pulse angle, and no pulse delay. Deuterochloroform was used as solvent and samples were run in 5 or 10 mm tubes, depending on quantity of sample available. Standard broad-band decoupling was used and no attempts were made to compensate for differences in carbon NOE or T_1 values.

III. Results and Discussion

The distribution of materials derived from gradient elution through silica-alumina gel columns are given in Table 1. The asphaltene and oil samples were further separated by GPC techniques into seven subfractions. The acidic fraction was further separated by both GPC and LC techniques into five GPC and five LC fractions. The CMR data of selected fractions of the saturate, monoaromatic, diaromatic, triaromatic, poly/polar aromatic and asphaltene fractions are shown in Figures 2-10. It was noted that in GPC fraction number one of all aromatic species, the saturates region is dominated by the spectral lines associated with normal paraffin groups. With subsequent fractions one observes a marked decrease in unbranched paraffinic structure with little or no evidence of such side chains in the last fractions (smallest molecular size) eluted from the column. These results can be rationalized by considering the volume occupied by flexible alkyl substituents on the aromatic rings in question, which, on the basis of effective molecular size, would be quickly eluted from the column.

By closely examining the spectra of each GPC fraction and comparing the line positions with those of model compounds, it is possible to derive structural features which can be used to arrive at types of molecular species that may be present. For instance, comparison of Figure 4 with Figure 6, 7, 9 and 10 illustrates that only a restricted number of possible aliphatic and/or cycloaliphatic structures are present in substantial amounts in the smaller molecular weight fractions of the polynuclear aromatic and asphaltene compounds as compared with

the monoaromatic family of compounds. In fact, the banding structure in the aliphatic region of Figures 6, 7, 9, and 10 correspond to the lines predicted for hydroaromatic species that do not contain a large number of alkyl side chains on the cycloaliphatic moeity. With the exception of GPC fractions 1 and 2 of all samples examined, which have a relatively high percentage of n-alkyl side chains, one observes a general preponderance of aliphatic line patterns similar to those in Figures 6, 7, 9, and 10.

The data in Table 2-6 provide a convenient summary of the general structural features of the individual oil fractions examined. No attempt has been made to portray all the structural features that may be present nor to attempt to quantify the results. Rather, structural features are given for the most easily identified molecular species.

It is interesting to note that electronegative functional groups containing oxygen and nitrogen usually shift adjacent carbon atoms sufficiently downfield, compared to carbons which do not bear a substituent, to enable ready identification. Of the 34 GPC fractions of the oil fractions examined in detail, only 3 fractions exhibit evidence of such functional groups. GPC fraction number one in the 3-ring aromatic fraction was the only sample exhibiting carbons contained in or adjacent to an ester functional group; i.e., $R-\overset{O}{\overset{\|}{C}}-O-C-R$. In the case of the polyaromatic/polar fraction, GPC fractions four and seven display resonance lines indicative of the presence of ethers and/or alcohols. The functional groups could not be present in more than a few tenths percent. Hence, the CMR data suggests that the majority of the oxygen and, perhaps the nitrogen compounds as well, are not present in the oils but, rather, have probably concentrated in the other fractions (acids, bases, and asphaltenes). The CMR data does not permit comment on the presence of absence of nitrogen or sulfur species.

With the exception of GPC fractions 1, 2, and 3 of the saturates fraction, which contain almost entirely normal paraffins, the spectral lines are so complex that at 25 MHZ only a small fraction of the chemical information available can be interpreted. An illustration example of the power of carbon-13 NMR techniques to simplify the problem somewhat is illustrated in Figures 11, 12 and 13. In this case the light liquid, which has not been subjected to any further separation, was examined at 75 MHZ (Figure 12) with the corresponding 25 MHZ spectrum (Figure 11) included for purposes of comparison. The increased field of the superconducting spectrometer not only provides a three-fold increase in line dispersion but also greatly increases the sensitivity. Hence, with this higher field one can resolve nearly all of the lines in the spectrum in Figure 11. (It is admitted that the light liquid is less complex than the GPC fractions considered in this paper but the comparison is informative). A 250 Hz plot (Figure 13) of a portion of the aromatic region in Figure 12 demonstrates the wealth of chemical information that is available in this sample. This light liquid sample has been subjected to a GC separation using glass capillary column techniques by Dr. F. J. Yang.[17] Using a flame ionization detector, 306 peaks in the chromatogram were resolved and measured by means of computer techniques.[17,18] However, only 30-40 compounds are present in significant amounts (ca. 1%). Dr. J. N. Shoolery has employed ^{13}C NMR analysis, using microsampling techniques,[19] to identify toluene as the most prominent component in the light liquid.[20] The resonance positions of toluene are marked in Figure 12.

It is interesting to point out, without further comment, that the resonance lines for alkenes are observed in nearly all GPC fractions studied.

The GPC and LC subfractions of the acid fraction were examined in detail. GPC fractions 4 and 5 were not studied due to solubility problems in a solvent suitable for CMR studies. GPC fractions 1-3 exhibited resonance lines in the aromatic region associated with phenolic and carbazolic structures. However, little significant change was observed in either the aromatic or aliphatic regions as a function of molecular size. The five LC fractions examined also exhibited aromatic lines characteristic of phenol and carbozole derivatives. However, the relative changes in resonance line patterns were quite distinct, especially in the saturate region, between the various fractions that were eluted from the column. Perhaps the most significant result is that only in sample LC-3 (the third sample collected from the column) one observes resonance lines from both ester and ether functional groups. Inasmuch as silica-alumina gel columns have functional separation characteristics, it is not surprising that such discrimination is noted.

The basic fraction was subjected to LC separation techniques only and exhibited the resonance lines in the aromatic region characteristic of pyridine type compounds and their derivatives.

The CMR data obtained demonstrates the utility of Carbon-13 NMR techniques in obtaining chemical structural information on coal derived liquids. As with any analytical technique, the detail of the information obtained is dependent, to some extent, on the sophistication of the separations scheme employed in order to reduce the number of compounds or compound types to a manageable level. However, even the most elaborate separation scheme renders individual compound identification very tedious if it must be carried out manually. Fortunately, the advent of sophisticated data processing equipment may soon allow significant progress in this area as archival files and data manipulating sub-routines replace the inadequacies of human data analysis. The status of these techniques will be discussed.

ACKNOWLEDGEMENTS

Support for this work was provided by the Energy Research and Development Administration through contract E(949-18)2006.

REFERENCES

1. See for instance, M. Melring, High Resolution NMR Spectroscopy in Solids, Springer-Verlog, Berlin, Heidelberg, New York 1976. This monograph is part of the series NMR II, Basic Principles and Progress, Editors P. Diebl, E. Fluck, and R. Kosfeld.
2. R. A. Friedel and H. L. Retcofsky, Chem. and Ind., 455 (1966).
3. R. A. Friedel and H. L. Retcofsky in Coal Science, Advances in Chemistry Series 55, American Chemical Soceity, Washington, D. C., 1966. Page 503-515.
4. S. A. Knight, Chem. and Ind., 1020 (1967).
5. See for instance, T. C. Forror and E. D. Becker, Pulse and Fourier Transform NMR. Instruction to Theory and Methods, Academic Press, New York and London, 1971.
6. See for instance: a) H. L. Retcofsky and R. A. Friedel, Spectrometer of Fuels, edited by R. A. Friedel, Plerum Press, New York, London, 1070, p. 90-119. b) J. Stothers Carbon-13 NMR Spectroscopy, Academic Press, New York, London, 1972. c) G. C. Levy and G. L. Nelson, Carbon-12 Nuclear Magnetic Resonance for Organic Chemistry, Wiley Interscience, New York, London, Sydney, Toronto, 1972.
7. H. L. Retcofsky and R. A. Friedel, Anal. Chem., 43, 485 (1971).
8. H. L. Retcofsky and R. A. Friedel, 5, Phys. Chem., 77, 68 (1973).
9. D. R. Clutter, L. Petrakis, R. L. Stenger, Jr., and R. K. Jensen, Anal. Chem. 44, 1395 (1972).
10. H. L. Retcofsky and R. A. Friedel, Fuel, 55, 363 (1976).
11. J. A. Franz, J. R. Morrey, J. R. Campbell, G. L. Tingey, R. J. Pugmire, D. M. Grant, Am. Chem. Soc., Div. of Fuel Chem., Preprints, 1975, 70, No. 3, Page 12.
12. F. K. Scheveighardt, H. L. Retcofsky, and R. A. Friedel, Fuel, 55, 313 (1976).
13. R. J. Pugmire, D. M. Grant, K. W. Zilm. L. L. Anderson, A. G. Oblad, and R. E. Wood, Fuel, 56, 0000 (1972).
14. R. E. Wood and W. H. Wiser, Ind. Engng. Chem. - Process Design Dev., 15, 144 (1976).
15. D. E. Hirsch, R. L. Hopkins, H. J. Coleman, and F. O. Cotton, Anal. Chem., 44, 915 (1972).
16. W. E. Haines and C. J. Thompson, Separating and Characterizing High-Boiling Petroleum Distillates: The USBM-AI Procedure, Laramie Energy Research Center, RI 7414.
17. F. J. Yang, Varian Associates, Instrument Division, Private Communication, August 1977.
18. S. P. Cram, F. J. Yang, A. C. Brown, III, and R. N. McCoy, Preprint, 1977 Pettsburgh Conference on Analytical Chemistry and Applied Spectroscopy, Cleveland, Ohio, March 2, 1977.
19. J. N. Shoolery and R. E. Majors, American Laboratory, May 1977, page 51.
20. J. N. Shoolery, Varian Instrument Division, Varian Associates, Private Communication, September 1977.

FIGURE 1

SEPARATION SCHEME

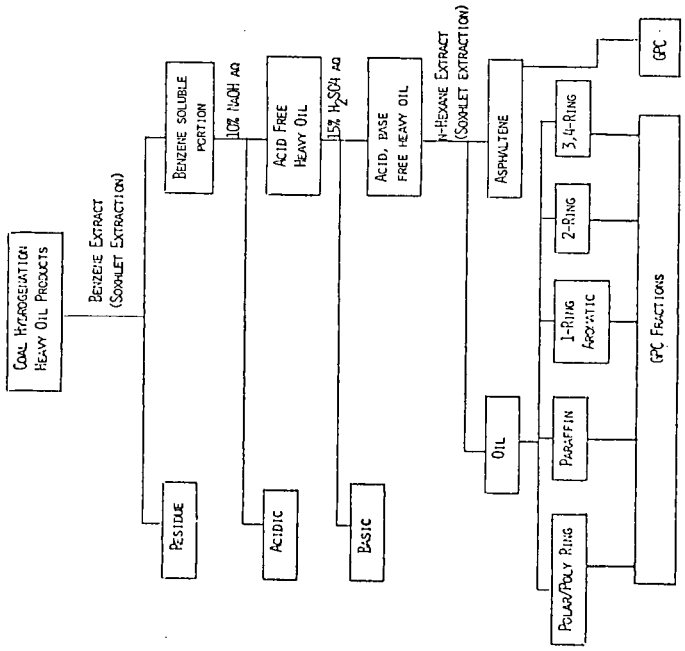

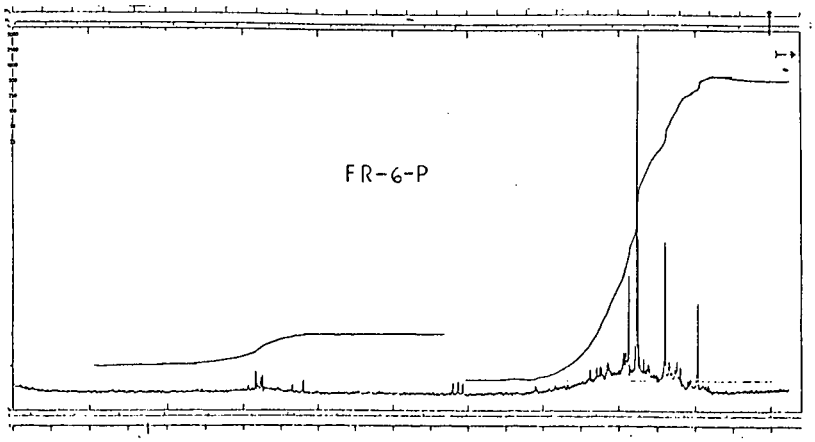

FIGURE 2 GPC subfraction number 6 of the saturates fraction of the heavy oil. UV data indicate that aromatic species are present. However, line positions in the unsaturates regional also indicate the presence of alkenes. Predominant lines are due to normal alkanes. Spectra was taken at 25 MHz.

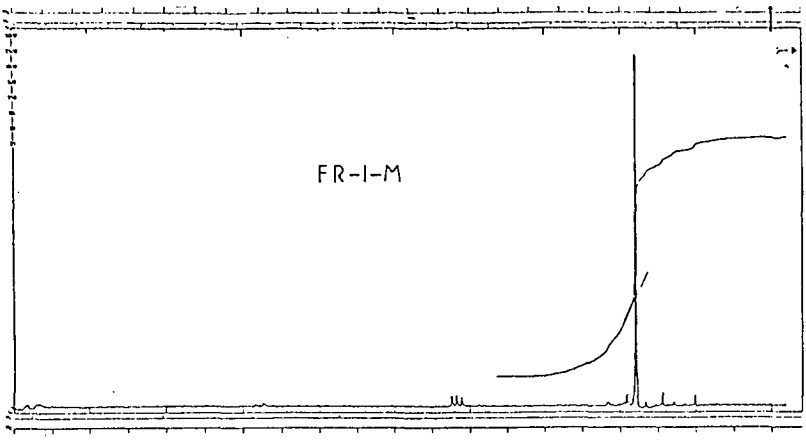

FIGURE 3 GPC subfraction number 1 of the monoaromatic fraction. Little structure is observable except in the aliphatic region where n-alkyl substituents dominate.

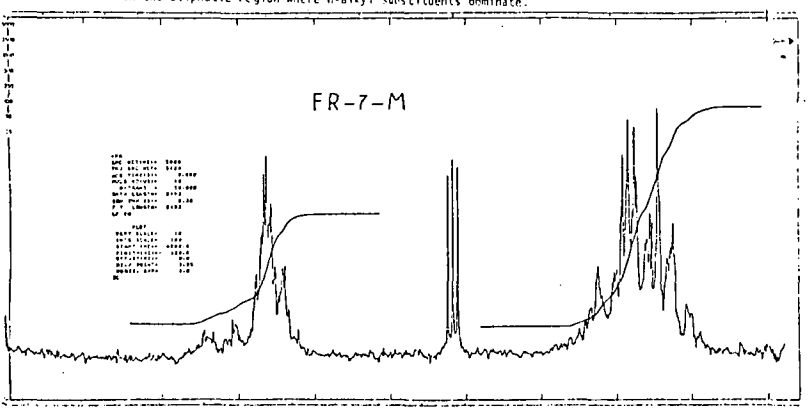

FIGURE 4 GPC subfraction number 7 of the monoaromatic fraction.

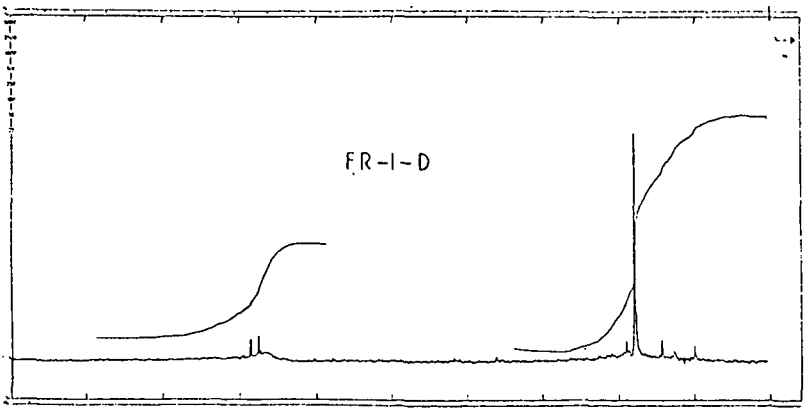

FIGURE 5 GPC subfraction number 1 of the diaromatic fraction. The structural features of the aliphatic region are dominated by n-alkyl substituents.

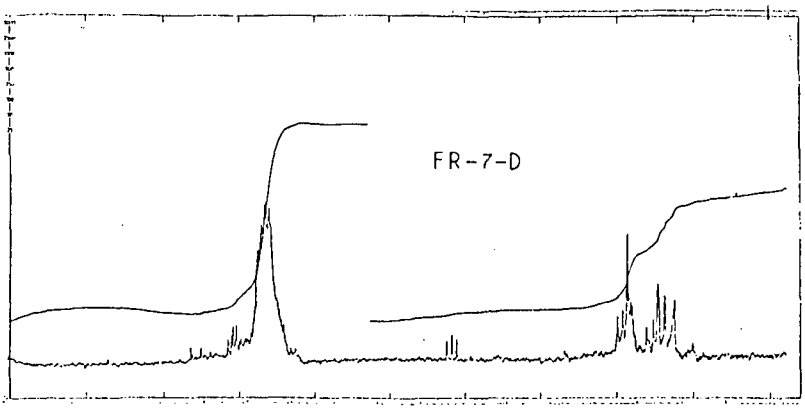

FIGURE 6 GPC subfraction number 7 of the diaromatic fraction. The aliphatic structure displays evidence of hydroaromatic species.

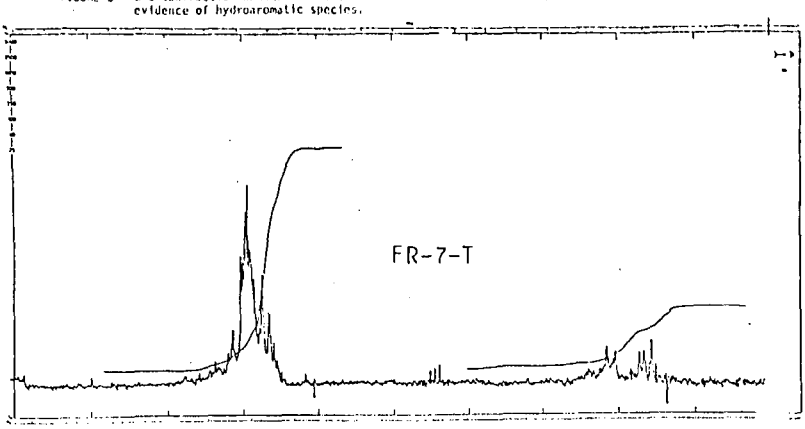

FIGURE 7 GPC subfraction number 7 of the three/four ring aromatic fraction.

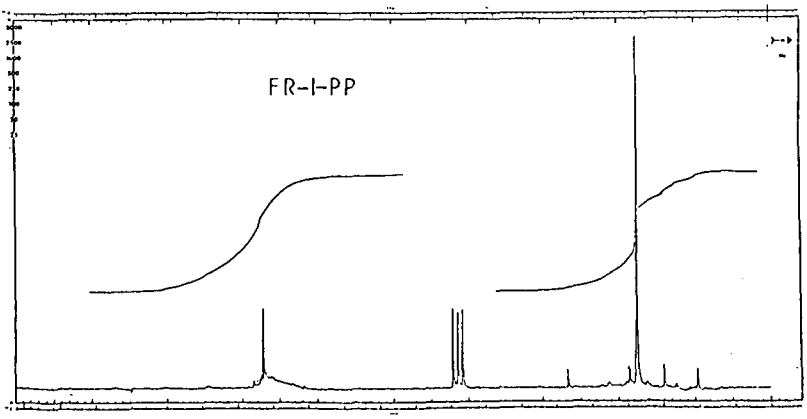

FIGURE 8 GPC subfraction number 1 of the poly/polar aromatic fraction. Note the presence of resonance lines due to n-alkyl substituents.

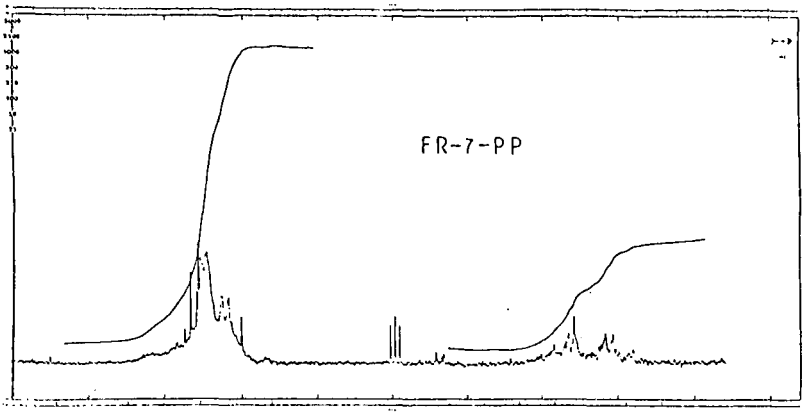

FIGURE 9 GPC subfraction number 7 of the poly/polar aromatic fraction.

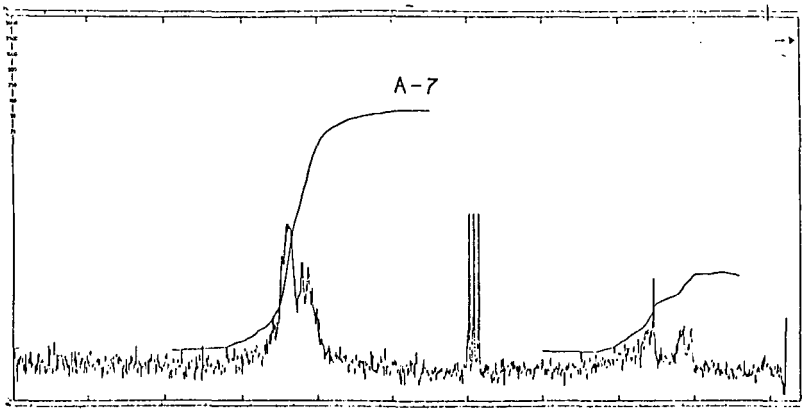

FIGURE 10 GPC subfraction number 7 of the asphaltenes. The signal to noise is too low to permit observation of minor structural features. The aliphatic region is similar to that observed in Figure 6, 7, and 9.

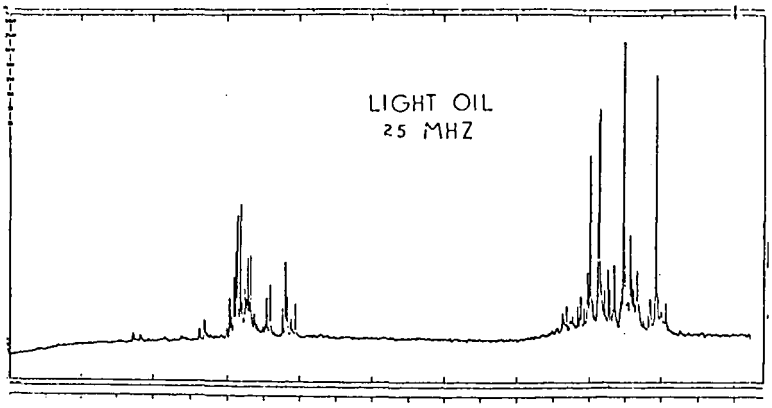

FIGURE 11 CMR spectra of light oil taken at 25 MHz. A D_2O capillary was used as external lock. A total of 35,445 transients were accumulated. Total time required was 8 hours.

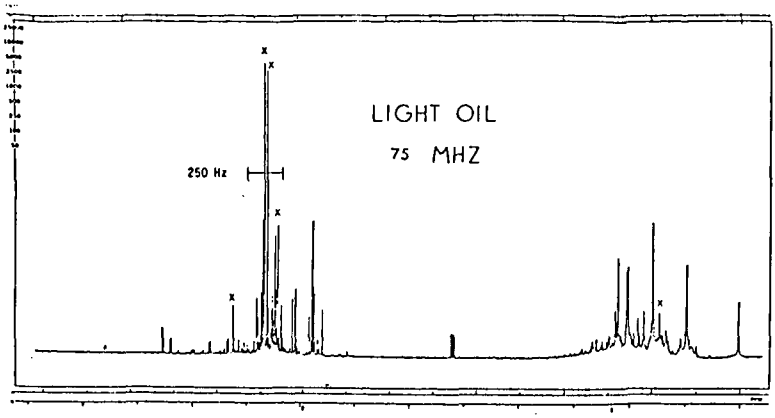

FIGURE 12 CHR spectra of sample shown in Figure 11. Data was taken using DCl_3 as an internal lock. TMS was added as a reference. The lines designated by x correspond to the lines found in toluene. Spectra width was 15 KHz. The spectra was obtained from accumulation of 203 transients requiring approximately 0.1 hour.

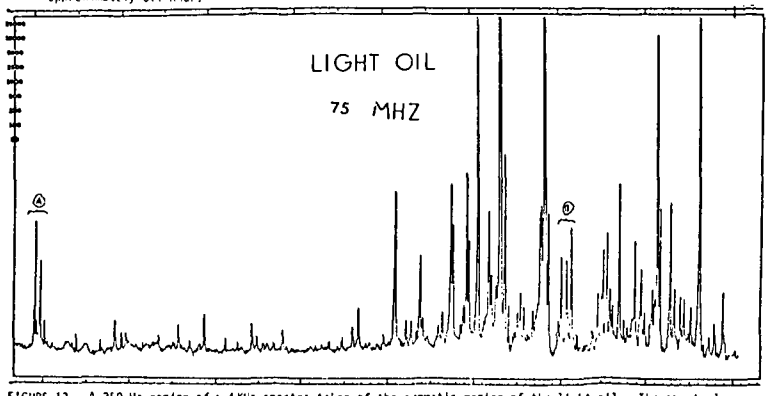

FIGURE 13 A 250 Hz region of a 4KHz spectra taken of the aromatic region of the light oil. The spectral region is that indicated in Figure 12. 1194 transients were obtained with an aquisition time of 4.096 sec. for a total spectrometer time of 1.4 hours.

TABLE 1. DISTRIBUTION OF HEAVY OIL FRACTIONS

SAMPLE: HIAWATHA H.V. BITUMINOUS COAL

YIELD: HEAVY OIL 31.3% W/W COAL

PRODUCTS

	% HEAVY OIL	% COAL
ASPHALTENE	6	1.8
OIL	62.2	19.6
SATURATES	6.29	1.97
ONE-RING AROMATIC	7.76	2.43
TWO-RING AROMATIC	8.05	2.52
THREE-FOUR-RING AROMATIC	8.72	2.73
POLAR/POLY RING AROMATIC	29.65	9.28
ACIDIC	12.9	4.0
BASIC	2.2	0.7
RESIDUE (BENZENE INSOLUBLE)	3.3	1.0
LOSS	12.9	4.0

TABLE 2. SUGGESTED COMPOSITION OF SATURATES FRACTIONS

GPC FRACTION	UNSATURATES: R-C-C-R[1] OR AROMATICS	R-C=C	RC=C-C	⬡	⬡ R	SATURATES: %N-P[2]	N[2]	C R-C-C-C-R	C R-C-C	R R-C-C-C-C R	ISO-PARAFFINS	CYCLIC PARAFFINS	% OF OIL
FR-1-P	X					60	24	X		X		X	0.54
FR-2-P	X SIMILAR TO FR-1-P					85-90	25	MOST OF BRANCHED AND CYCLIC PARAFFIN LINES GONE					1.21
FR-3-P	X SIMILAR TO FR-1-P					85-90	24	MOST OF BRANCHED AND CYCLIC PARAFFIN LINES GONE					1.05
FR-4-P	X SIMILAR TO FR-1-P					64	18				X	X	1.09
FR-5-P		X	X			45-50	14			X	X	X	1.12
FR-6-P	X			X	X	20	14	OTHER THAN N-PARAFFINS, LITTLE DEFINITIVE STRUCTURE PRESENT					1.28
												TOTAL	6.29

[1]These spectral lines correspond with those of monosubstituted benzenes as well as long chain alkenes. UV data exhibits absorption bands characteristic of aromatic rings indicating that the separations procedure does not eliminate all aromatic material from the saturates fraction.

[2]%N-P represents the percent of normal paraffins present in the sample while N represents the number average length of the alkyl chains.

TABLE 3A

SUGGESTED COMPOSITION OF MONOAROMATIC FRACTIONS
UNSATURATES

GPC FRACTION	C ⬡	C ⬡	R R C R ⬡	R ⬡	C-C=C-R	R ⬡	R-C=C-R	⬡⬡	% OF OIL
FR1-M	X								0.93
FR2-M	X								1.02
FR3-M	X	X	X	X	X	X	X		1.12
FR4-M	X	X		X	X				1.12
FR5-M	X	X		X	X				1.04
FR6-M	X	X	X	X		X			1.18
FR7-M	X	X	X	X	X	X	X	X	1.37
								TOTAL	7.79

TABLE 3B

SUGGESTED COMPOSITION OF MONOAROMATIC FRACTIONS
SATURATES

GPC FRACTION	%N-P[1]	N[1]	φ-C	φ-C-C	φ-C-C-R	φ-C-C-R	⬡⬡⬡	CYCLIC PARAFFINS	C R-C-C-C	% OF OIL
FR1-M	~60	~31	X	X	X	X				0.93
FR2-M	A	>10	X		X	X				1.02
FR3-M	15-20	~8	X	X	X	X				1.12
					BROAD BAND RICH IN STRUCTURE					
FR4-M	A	~5	X	BROAD BAND WITH LITTLE STRUCTURE						1.12
FR5-M	A	~5	X	BROAD BAND WITH MUCH BRANCHED AND CYCLIC ALIPHATIC STRUCTURE						1.04
FR6-M	A		X	X			X	X	X	1.18
FR7-M	A		X				X	X	X	1.37
									TOTAL	7.79

[1]Same as N in Table 2 except in the aromatic fractions N is used to designate the n-alkyl substituents.

[2]Not measured.

TABLE 4

SUGGESTED COMPOSITION OF DIAROMATIC FRACTIONS

	Unsaturates						Saturates						
GPC Fraction	R-C=C	C-C=C-C-R	C-C=C-R				% n-P[1]	n[1]	ϕ-C	ϕ-Iso Paraffin	Cyclic Paraffins	ϕ-R-C	% of Oil
FR-1D							25	13				X	0.95
FR-2-D	X	X	X	X	X	X		5	X	X	X	X[2]	0.99
FR-3-D		X	X	X	X	X			X	X	X	X[2]	1.02
FR-4-D		X	X	X	X	X			X	X	X	X[2]	1.12
FR-5-D		X	X	X	X	X			X	X	X	X[2]	1.44
FR-6-D		X	X	X	X	X			X	X	X	X[2]	1.34
FR-7-D		X	X	X	X	X			X	X	X	X[2]	1.25
												TOTAL	8.02

[1]See Footnote 2 in Table 2.

[2]Decreasing amounts as molecular weight decreases.

TABLE 5

SUGGESTED COMPOSITION OF 3-RING AROMATIC FRACTIONS

	Unsaturates					Saturates							
GPC Fraction	R-C=C	C-C=C-R				% n-P[1]	n[1]	O R-C-O-C-R	O R-C-O-C-R	ϕ-C			Iso-Paraffins	% of Oil
FR-1-T	X	---BANDS WITH NO RESOLVABLE STRUCTURE---				16	9	X	X	X			X	1.21
FR-1-T	X	X	X		X						X	X	X	1.27
FR-3-T	X	X	X	X	X					X	X	X	X	1.15
FR-4-T	X	X	X	X	X					X	X	X	X	1.41
FR-5-T	X	X	X	X	X					X	X	X	X	1.37
FR-6-T	X	X	X	X						X	X		X	1.05
FR-7-T	X	X	X	X						X	X	X		1.15
													TOTAL	8.74

[1]See Footnote 2 in Table 2.

TABLE 6

SUGGESTED COMPOSITION OF POLYAROMATIC/POLAR FRACTIONS

	Unsaturates						Saturates							
GPC Fraction	R-C=C	C-C=C-R	C-C=C-R				% n-Par.[1]	n[1]	ϕ-C	ϕ-Iso-Paraffins		ϕ-R-C	R-CH2-OR[2]	% of Oil
FR-1-PP	Broad band of low intensity						25	13	X			X		4.15
FP-2-PP	X	X	X	X	X	X	-	5	X	X	X	X		5.02
FP-3-PP		X	X	X	X	X			X	X	X	X		3.93
FP-4-PP		X	X	X	X	X			X	X	X	X	X	3.50
FP-5-PP		X	X	X	X	X			X	X	X			4.09
FP-6-PP		X	X	X	X	X			X	X	X			4.22
FP-7-PP		X			X	X			X	X	X		X	4.44
													TOTAL	29.55

[1]See Footnote 2 in Table 2.

[2]The resonance lines observed are probably due mainly to ethers but the line positions do not preclude the possibility of secondary or tertiary alcohols.

FIELD DESORPTION MASS SPECTROMETRY - APPLICATION TO THE ELUCIDATION OF THE STRUCTURE OF HUMIC ACID by R. L. Wershaw, U.S. Geological Survey, Denver Federal Center, Denver, CO, 80225, D. F. Barofsky and E. Barofsky, Oregon Graduate Center, Beaverton, Oregon, 97005

Progress in the elucidation of the structure of humic acids has been impeded, in part, by our inability to dissociate humic acid aggregates into analyzable units and, in part, to the nonavailability of adequate analytical tools to monitor the chemical procedures. Field desorption mass spectrometry (FDMS) has two properties that make it ideally suited to the analysis of relatively large molecular aggregates such as humic acids. These are: (1) The FDMS of most compounds exhibit predominantly molecular or pseudomolecular ions and (2) sample volatilization is not required prior to ionization.

Field desorption mass spectrometry allows us to monitor the chemical reactions that we have used to dissociate humic acid fractions by enabling us to observe the dissociated fragments. The most significant result arising out of this work to date, has been the observation of humic acid fragments following either chlorination or permethylation; in untreated samples we get no spectra. The disaggregation on permethylation is attributed to a reduction in hydrogen bonding.

The first part of this paper will present a brief survey of FDMS, that is, its theory, instrumentation, and techniques The second part will present the results of the application of FDMS to the structural elucidation of humic acid and the general applicability of FDMS to similar problems.

NOVEL APPROACHES FOR DETERMINATION OF DEGREE OF ASSOCIATION OF COAL-DERIVED PRODUCTS BY VAPOR PRESSURE OSMOMETRY

W.C. Lee, I. Schwager, T.F. Yen

University of Southern California, Chemical Engineering Department
University Park, Los Angeles, California 90007

INTRODUCTION

Vapor Pressure Osmometry (VPO) molecular weights of coal-derived asphaltenes obtained from coal liquids produced in five major coal liquefaction demonstration processes have been determined as a function of concentration in the solvents tetrahydrofuran (THF) and benzene (1). It was shown that association of coal-derived asphaltenes takes place in both solvents over the concentration range of 4-36g/l. In this study, the VPO molecular weights of the same asphaltenes have been obtained over a wider concentration range of 4-60g/l and a self-association model of asphaltenes in solution has been derived and the dissociation constants, one for the dissociation of dimeric complexes and one for the dissociation of higher order complexes, have been calculated with the aid of a modern computer.

This is the first time that VPO has been used to quantitatively correlate the degree of association of coal-derived asphaltenes in solution, although a number of other techniques have been used in the past (2-8, 13, 14).

THEORETICAL

In order to investigate the self-association of phenol in carbon tetrachloride solution, Coggeshall and Saier (2) carried out an IR study of the hydroxyl stretching region of phenol and obtained very good agreement between theory and experiment by using two equilibrium constants. They derived the following two expressions:

$$\alpha_n = n\alpha \frac{K}{K_1} \left[\frac{\alpha C}{K} \right]^{n-1} \qquad 1)$$

$$K = \frac{C\alpha}{2(K_1 - \bar{K})} \left[2K_1 - \frac{\bar{K}}{2} + \sqrt{2K_1 \bar{K} + \frac{\bar{K}^2}{4}} \right] \qquad 2)$$

where

- n = integer
- α_n = fraction of monomer bound in nth polymer
- α = fraction of monomer unassociated
- C = concentration in moles per liter
- K_1 = dissociation constant of dimer
- K = dissociation constant of all other polymers $=K_2=K_3\ldots$
- $\bar{K}$ = $2\alpha^2 C/(1-\alpha)$

If C is the initial concentration of monomer before any association, at equilibrium the concentrations of monomer, dimer, trimer, etc., are C, $\frac{\alpha_2 C}{2}$, $\frac{\alpha_3 C}{3}$, ... $\frac{\alpha_n C}{n}$ and the molecular weights are Mo, 2Mo, 3Mo,... and nMo.

Since the molecular weight measured in VPO is the number average molecular weight, it is given that

$$MW_{obs} = \frac{Mo\ \alpha C + 2Mo \bullet \frac{\alpha_2 C}{2} + 3Mo \bullet \frac{\alpha_3 C}{3} + \ldots + nMo\ \frac{\alpha_n C}{n}}{C \bullet \left[\alpha + \frac{\alpha_2}{2} + \frac{\alpha_3}{3} + \ldots + \frac{\alpha_n}{n} \right]} \qquad 3)$$

where MW_{obs} is the number average molecular weight from VPO.
With the use of the relationship $\sum \alpha_n = 1$, $\frac{1}{1-x} = 1 + x + x^2 + \ldots$, and Equation 1, one may simplify Equation 3 and get

$$MW_{obs} = \frac{Mo}{\alpha \left[1 + \frac{K}{K_1} \frac{1}{\frac{K}{\alpha C} - 1} \right]} \qquad 4)$$

In theory, the equilibrium constants K and K_1 can be obtained by solving Equations 2 and 4 simultaneously at two different concentrations. The approach will be discussed in the next section.

EXPERIMENTAL

Coal-derived asphaltenes were separated by solvent fractionation (9, 10) from coal liquids produced in five major demonstration liquefaction processes: Synthoil, HRI H-Coal, FMC-COED, Catalytic Inc. SRC, and PAMCO SRC.

A Mechrolab Model 301A Vapor Pressure Osmometer was used to determine molecular weights with benzil employed as a standard. Both the non-aqueous probe and the thermostat were designed for 37°C. In normal runs, 6-8 molecular weights over the range 4-60 g/l were measured in the solvents benzene or THF.

A modern computer was used to solve the calculation problem according to the following steps:

(a) Assume values of K and K_1.
(b) Calculate for α and β at two concentrations, C_1 and C_2, from Equation 4 where MW_{obs} is the molecular weight from VPO. When the concentration is C_1, the fraction of monomer unassociated at equilibrium is α, and when the concentration is C_2, it is β.
(c) Substituting C_1, C_2, α and β into Equation 2 and get

$$K = \frac{C_1 \alpha}{2(K_1 - \bar{K}_1)} \left[2K_1 - \frac{\bar{K}_1}{2} + \sqrt{2K_1\bar{K}_1 + \frac{\bar{K}_1^{\,2}}{4}} \right] \qquad 5)$$

$$K = \frac{C_2 \beta}{2(K_1 - \bar{K}_2)} \left[2K_1 - \frac{\bar{K}_2}{2} + \sqrt{2K \bullet \bar{K}_2 + \frac{\bar{K}_2}{4}} \right] \qquad 6)$$

where $\bar{K}_1 = 2\alpha^2 C_1/(1-\alpha)$

$\bar{K}_2 = 2\beta^2 C_2/(1-\beta)$

Since K is independent of concentration, by combining Equations 5 and 6, it is given that

$$\frac{\alpha C_1}{2(K_1 - \bar{K}_1)}\left[2K_1 - \frac{\bar{K}_1}{2} + \sqrt{2K_1\bar{K}_1 + \frac{\bar{K}_1^{\,2}}{4}}\right]$$

$$= \frac{C_2\beta}{2(K_1 - \bar{K}_2)}\left[2K_1 - \frac{\bar{K}_2}{2} + \sqrt{2K_1\bar{K}_2 + \frac{\bar{K}_2^{\,2}}{4}}\right] \qquad 7)$$

(d) Solve Equation 7 for K_1 by the Newton-Raphson method.
(e) Calculate K from Equation 5 or 6.
(f) Repeat the same procedures until the calculated values of K and K_1 are close enough to the assumed values.
(g) Using the equilibrium constants obtained above the molecular weights over the concentration range of 4-65 g/l can be calculated based on this model. The fraction of monomer unassociated at each concentration is obtained by solving Equation 2 and the fraction of monomer bound in any degree of polymer can be also obtained from Eqaation 1.

A number of different equilibrium constant pairs, K and K_1, have been tried for five asphaltenes in benzene. The ones which afford the minimum standard deviations between the experimental and calculated molecular weights have been chosen.

RESULTS AND DISCUSSION

The VPO molecular weights for all five coal-derived asphaltenes, in benzene are shown in Figs. 1 to 5. The results indicate that association of coal-derived asphaltenes takes place in both solvents over the concentration range of 4-60 g/l. The calculated equilibrium constants, together with the standard deviations are summarized in Table I where the % Dev. is defined as:

$$\frac{\text{Standard Deviation of MW}}{\text{MW of Monomer}} \times 100\%$$

All % Dev. values are less that 5.5%. This suggests that this two parameter model is efficient in describing the self-association of asphaltenes from five different processes in benzene and THF. The calculated molecular weights, fraction of monomer and monomer bound in dimer and trimer are also plotted in Figs. 1 to 5 for the five asphaltenes.

It is interesting to note from Equation 4 that $MW_{obs} \doteq Mo/\alpha$ as $C \longrightarrow 0$ and $Mo/\alpha \doteq Mo$ since $\alpha \longrightarrow 1$ as $C \longrightarrow 0$. This agrees with the experimental results obtained from VPO and reported in Reference (1) that molecular weight values found in different solvents, by extrapolating the plots to infinite dilution are in accordance. These infinite dilution molecular weight values approximate the true monomer molecular weights and were used as Mo throughout this study.

The association of petroleum asphaltenes has been studied by a variety of techniques (3-8) and the mechanism of self-association has been described largely in terms of electronic association. The mechanism of bonding in coal-

derived asphaltenes is important and is under study (11). The association of these species has been reported in terms of hydrogen bonded complexes which can be separated into acidic and basic components (12). The hydrogen bonding of these two components and some model complexes has been further studied by NMR (13,14). Unfortunately, all of the reports on coal-derived asphaltenes contain only qualitative results. However, these studies tend to support the self-association model derived here, since it is very likely that in solution dimer could be formed through the bondings between the acidic proton and basic nitrogen or oxygen of two molecules or trimer could be formed through the bondings between those of three molecules. The association of monomer into dimer, trimer in solution depends on the solvent used. It is more significant in the less polar solvent benzene than THF, so the variation of molecular weights vs. concentration in benzene is greater.

This study is significant because, based on this model, the heat of formation of the polymers can be calculated from equilibrium constants at various temperatures and the mechanism of the bonding can be studied. This is the first time that VPO has been used to quantitatively correlate the degree of association of coal-derived asphaltenes in solution.

Comparing the equilibrium constants K_1 and K of these five different asphaltenes in benzene, it is found that Synthoil and PAMCO SRC asphaltenes have stronger association between molecules while FMC-COED and Cat. Inc. SRC asphaltenes have less. The equilibrium constants in THF are generally larger than in benzene, since THF is more polar solvent and tends to dissociate the asphaltene molecules as they are dissolved. But this dissociation tends to go to completion in either solvent at infinite dilution.

The curves labeled 1,2,3 in Figs. 1 to 5 show the distribution of asphaltene between monomer, dimer and trimer as a function of total asphaltene concentration. For example, if 20 gm of Cat. Inc. SRC asphaltene is dissolved in 1 ℓ benzene at 37°C, the fractions of monomer, dimer and trimer are 0.70, 0.18, 0.07 (from Fig. 1), while the remaining 0.05 is contained as polymers higher than trimer . The concentrations of monomer, dimer and trimer can be calculated and are:

$$\text{concentration of monomer (moles/l)} = \frac{20}{483} \times 0.7 = 2.9 \times 10^{-2}\text{M}$$

$$\text{concentration of dimer (moles/l)} = \frac{20}{483} \times 0.18 \times {}^{1}/_{2} = 3.7 \times 10^{-3}\text{M}$$

$$\text{concentration of trimer (moles/l)} = \frac{20}{483} \times 0.07 \times {}^{1}/_{3} = 9.7 \times 10^{-4}\text{M}$$

If the rest is assumed tetramer then concentration of tetramer (moles/l) = $\frac{20}{483} \times 0.05 \times {}^{1}/_{4} = 5.2 \times 10^{-4}\text{M}$ where the number 483 is the molecular weight of monomer.

In benzene solution, as the concentration increases, the fraction of asphaltene existing as the dimer reaches a maximum, and then decreases, and higher multimers become increasingly important. In highly concentrated solutions these larger multimers start to precipitate. Evidence for association of monomeric asphaltenes into 4-6 average layers in the solid state has been found by x-ray diffraction spectroscopy (15).

(1) I. Schwager, W.C. Lee, T.F. Yen, to be published, Anal. Chem., Vol. 49, Nov. 1977.

(2) N.D. Coggeshall and E.L. Saier, J. Am. Chem. Soc., 73, 5414 (1951).

(3) G.A. Sill and T.F. Yen, Fuel, 48, 61 (1969).

(4) E.C. Tynan and T.F. Yen, Fuel, 48, 191 (1969).

(5) T.F. Yen, E.C. Tynan, G.B. Vaughan, and L.J. Boucher, "Spectrometry of Fuels," (edited by R.A. Friedel) Plenum Press, N.Y. 1970, Chapter 14.

(6) J.P. Dickie, M.N. Haller, and T.F. Yen, J. of Colloid and Interface Science, 29, 475 (1969).

(7) J.P. Dickie and T.F. Yen, Anal. Chem., 39, 1847 (1967).

(8) S.E. Moschopedis, J.F. Fryer and J.G. Speight, Fuel, 55, 227 (1976).

(9) I. Schwager and T.F. Yen, Am. Chem. Soc., Div. Fuel Chem., Preprints, 21 (5), 199 (1976).

(10) I. Schwager and T.F. Yen, in Liquid Fuels from Coal (R.T. Ellington, ed.), Academic Press, New York, N.Y., 1977, pp. 233-248.

(11) T.F. Yen, in Workshop on Coal Chemistry Preprint, Stanford Research Institute, 1976, pp. 144-164.

(12) H.N. Sternberg, R. Raymond and F.K. Schweighardt, Science, 188, 49 (1975).

(13) F.K. Schweighardt, R.A. Friedel, and H.L. Retcofsky, Applied Spectroscopy, 30, 291 (1976).

(14) S.R. Taylor, L.G. Galya, B.J. Brown, and N.C.Li, Spectroscopy Letters, 9, 733 (1976).

(15) ERDA Report No. FE-2031-4, June 1976.

ACKNOWLEDGEMENT

This work was sponsored by U.S. DOE under contract no. E(49-18)2031, to whom the authors wish to express their appreciation.

Table 1. Calculated Equilibrium Constants and Standard Deviations of Coal - Derived Asphaltenes in Benzene

Process	Monomer MW **	K_1	K	Standard Deviation	% Dev.
Synthoil Asphaltene	560	0.0762	0.0671	13.7	2.4
IRI Asphaltene	492	0.118	0.0866	9.0	1.8
FMC-COED Asphaltene	375	0.210	0.0813	20.7	5.5
Cat. Inc. SRC * Asphaltene	485	0.225	0.109	12.2	2.5
PAMCO SRC * Asphaltene	532	0.0610	0.0971	18.6	3.5

*Isolated from vacuum distillated bottom product.

** From Ref. (1).

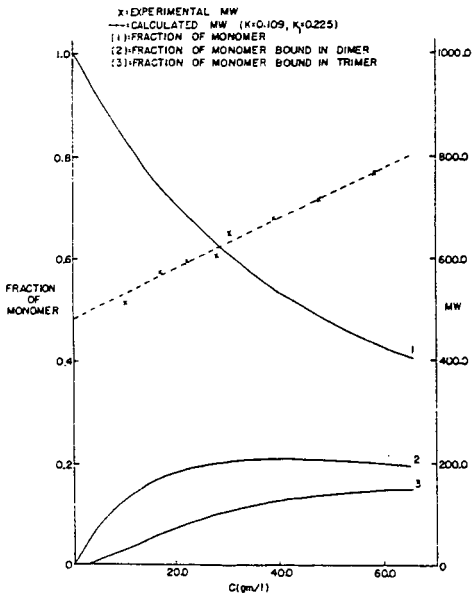

FIG. 1 FRACTIONS OF MONOMER AND VPO MW VS CONCENTRATION CAT. INC. ASPHALTENE IN BENZENE

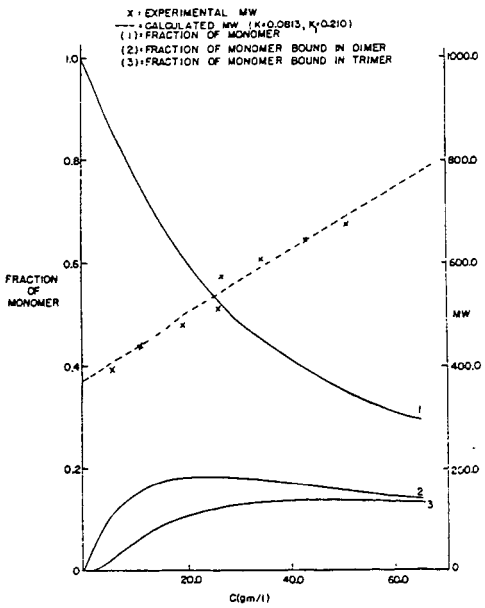

FIG. 2 FRACTIONS OF MONOMER AND VPO MW VS CONCENTRATION FMC-COED ASPHALTENE IN BENZENE

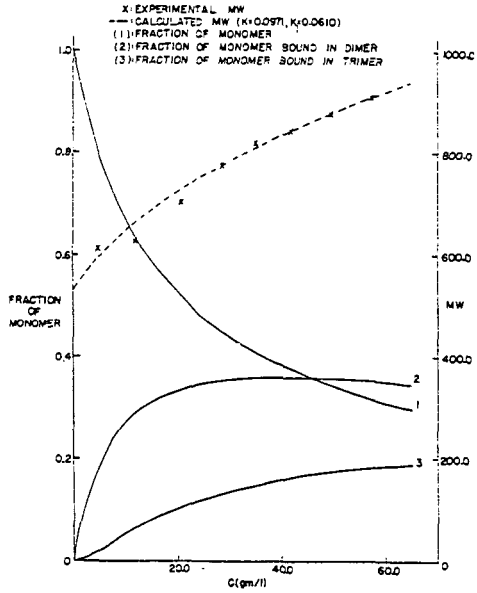

FIG. 3 FRACTIONS OF MONOMER AND VPC MW VS CONCENTRATION PAMCO ASPHALTENE IN BENZENE

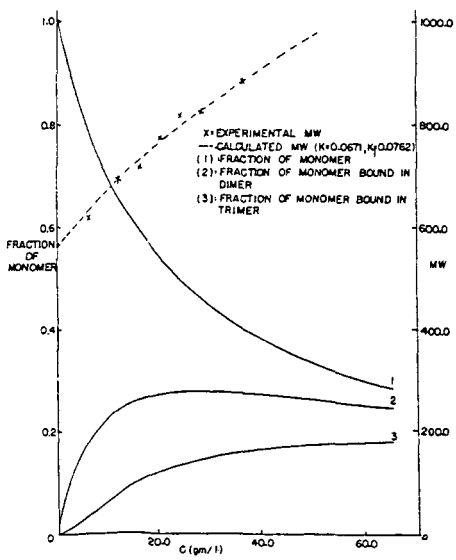

FIG. 4 FRACTIONS OF MONOMER AND VPO MW VS CONCENTRATION SYNTHOIL ASPHALTENE IN BENZENE

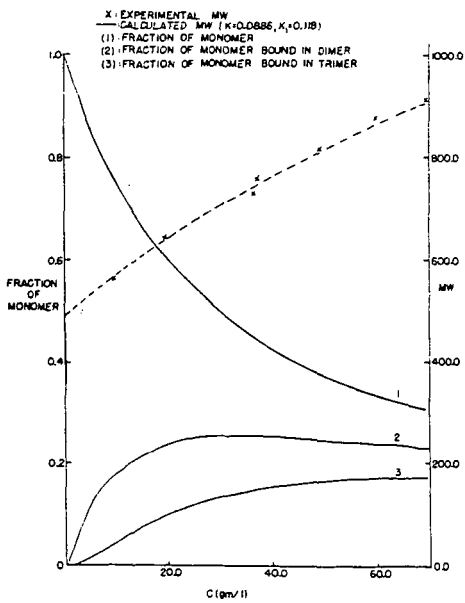

FIG. 5 FRACTIONS OF MONOMER AND VPO MW VS CONCENTRATION HRI ASPHALTENE IN BENZENE

On the Distribution of Organic Sulfur Functional Groups in Coal.

Amir Attar and Francois Dupuis, Department of Chemical Engineering,
University of Houston, Houston, Texas 77004.

1. SULFUR IN COAL

Traditionally, the sulfur in coal has been considered in two classes: 1) inorganic sulfur and 2) organic sulfur. In the class of inorganic sulfur, two types of compounds were considered: the disulfides and the sulfates. The organic sulfur is all the sulfur which is connected to the hydrocarbon matrix. Standard analytical techniques (1)(2)(3) are used to estimate the concentration of each class of sulfur in coal samples.

The inorganic sulfur, which is mainly iron pyrite, FeS_2, is present in the form of isolated crystals. Part of the FeS_2 particles are usually separated from the coal by simple physical separation. However, the organic sulfur can be removed from coal only if the chemical bond between carbon and sulfur is broken. The chemistry, the thermodynamics and the kinetics of the reactions of sulfur in coal have been reviewed recently (4)(5)(6) and the reader is referred to these manuscripts for details.

The chemistry of the reactions of FeS_2 and their rate are obviously different from that of the organic sulfur. Moreover, since the organic sulfur is present in the form of different functional groups, each functional group reacts at a different rate (6)(7).

2. ORGANIC SULFUR FUNCTIONAL GROUPS IN COAL

Very little data on the functional groups in which the organic sulfur appear and on their distribution has been derived by direct observation on coal. However, it is plausible to assume that the organic sulfur is present in coal in the same types of sulfur functional groups that can be found in oils and in other organic sulfur containing molecules. Moreover, if a general rule that applies throughout organic chemistry is applied to the sulfur in coal, we can say that the organic sulfur groups in coal react in the same way as their low molecular weight homologs and produce the same types of reaction products. For example, organic thiols, RSH, can be reduced by hydrogen to hydrogen sulfide, H_2S:

$$R - SH + H_2 \rightarrow RH + H_2S \qquad (1)$$

Thus, all the thiols, irrespective of the size and the shape of the radicals, R, can be reduced by H_2 to RH and H_2S. Variations in the rate of the reduction may, however, exist for different R's.

The most important sulfur functional groups in coal are believed to be:

1. derivatives of thiophenes and alkyl thiophenes

The most important parent structures are:

Thiophene

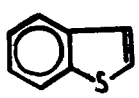

Thianaphene

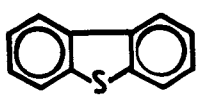

Dibenzothiophene

2. aryl sulfides: Ar-S-Ar'
3. aliphatic sulfides: R-S-R
4. cyclo sulfides, e.g.,
5. thiaphenoles

The presence of disulfides, sulfoxides, and sulfones were never demonstrated. It is believed that disulfides and sulfoxides are too unstable to survive the coalification process. Most of the organic sulfur is present in the forms of thiophenes and alkyl, aryl, and cyclic sulfides (4)(5)(6)(7). Most of the information was obtained from examination of the smaller molecular products

which were obtained by breaking the organic coal matrix (depolymerization). Obviously, the technique which is used to depolymerize the coal would have a deterministic effect on the results, since drastic depolymerization techniques may change the structures of the sulfur constituents as well as that of the hydrocarbon parts. Several reviews of the chemistry of sulfur in coal can be found in the older literature (8)(9)(10)(11)(12). Some aspects of the organic sulfur groups have recently been discussed by Attar and Corcoran (7).

3. THE PRINCIPLE OF THE PROPOSED METHOD OF ANALYSIS

All the sulfur groups in coal can be reduced by hydrogen to hydrogen sulfide, H_2S:

$$FeS_2 + H_2 \rightarrow FeS + H_2S \quad (3)$$

$$FeS + H_2 \rightarrow Fe + H_2S \quad (4)$$

$$R\text{-}S\text{-}R' + 2H_2 \rightarrow RH + R'H + H_2S \quad (5)$$

$$Ar\text{-}S\text{-}Ar' + 2H_2 \rightarrow ArH + Ar'H + H_2S \quad (6)$$

$$+ 4H_2 \rightarrow C_4H_{10} + H_2S \quad (7)$$

Each of these reactions has a given activation energy and a frequency factor which vary in a limited range for each group of sulfur compounds, when the structure of the organic radical is changed. Other reducing agents which contain hydrogen can be used with the same effective results.

These observations lead to the following important deductions: 1. If the activation energy Eai and the frequency factor Ai for the rate of reduction of the i-th functional group are determined, the i-th group is uniquely characterized. In other words, a particular value of Eai and Ai can belong only to the i-th group, and therefore they define the i-th group and 2. The exact amount of H_2S that evolves when the i-th group is reduced is proportional to the amount of the i-th sulfur group that has been reduced. If all the amount of the i-th group in the sample was reduced, then the amount of H_2S that evolved is proportional to the amount of the i-th group in the sample.

In order to be able to determine the total amount of each sulfur group in a fixed sample of coal, the following problems have to be solved:

1. How to determine the activation energy and the frequency factor for each sulfur group.

2. How to quantitatively reduce all the sulfur in a coal sample to H_2S and how to determine its amount.

The activation energies and the frequency factors can be determined using Juntgen method. Juntgen method and the methods which we proved that can be used to quantitize the H_2S are discussed in the next sections.

3.1 JUNTGEN METHOD FOR THE DETERMINATION OF Eai AND Ai

Consider a sample which contains a fixed quantity of sulfur in the form of different functional groups. Let us assume that each group can be reduced to H_2S by a first order reaction. For example, consider the reduction of the aliphatic sulfides:

$$R\text{-}S\text{-}R' \rightarrow RH + R'H + H_2S \quad (8)$$

$$\frac{d[H_2S]_1}{dt} = k_1 \, [R\text{-}S\text{-}R'] \quad (9)$$

The index 1 was used to denote the sulfidic functional group; R-S-R'. Let's assume further that the rate constant, k_1, depends on the temperature according to Arrhenius equation:

$$k_1 = A_1 e^{-\frac{E_{a1}}{RT}} \tag{10}$$

where A_1 is the frequency factor and E_{a1} the activation energy for the reduction. Then:

$$\frac{d[H_2S]_1}{dt} = A_1 e^{-\frac{E_{a1}}{RT}} [R-S-R'] \tag{11}$$

The rate constant of the reduction becomes larger at higher temperatures. That means that the rate of depletion of sulfide becomes larger at higher temperatures. The rate of evolution of H_2S from a sample with a fixed amount of the sulfide, which temperature is gradually increased, will increase initially due to the increase in the temperature, but since the concentration of the sulfur is depleted in the process, due to the evolution of H_2S, the rate will begin to decrease after most of the sulfur was reduced. The mathematical equation which describes the rate of evolution of gas as a function of the temperature of the sample, where the temperature is increased linearly with the time were developed by Juntgen (13)(14). Suppose that the temperature is increased according to:

$$T = T_o + \alpha t \tag{12}$$

where T_o is the initial temperature (°K), α the rate of heating, °K/min, and t the time, min. Then the volume of H_2S, V_i, that evolves when the i-th group is reduced, follows the equation:

$$\frac{dV_i}{dt} = \frac{A_i V_{i\infty}}{\alpha} \exp\left[-\frac{E_i}{RT} + \frac{A_i RT^2}{E_i}\left(1 - \frac{2RT}{E_i}\right) e^{-\frac{E_i}{RT}}\right] \tag{13}$$

where $V_{i\infty}$ denotes the total volume of H_2S that will evolve as a result of the complete reduction of the i-th group. The graph of this function is sketched in Figure 1.

The temperature at which the rate of evolution of H_2S from the i-th group reaches its maximum is denoted by T_{mi}, and is a unique function of E_{ai} and A_i and the rate of heating, α:

$$\frac{RT_{mi}^2 A_i}{\alpha E_{ai}} = e^{-\frac{E_{ai}}{RT_{mi}}} \tag{14}$$

Equation (14) means that if the sample is heated at the constant rate α, the apex of the H_2S peak from the i-th group, which is reduced with activation energy E_{ai} and frequency factor A_i, will be different from that of the j group which is reduced with different parameters, E_{aj} and A_j.

When a mixture which contains several functional groups is reduced, the behavior of each sulfur group is similar, except that each peak will appear at a different Tm. Figure 2 shows the graph for a mixture of several groups.

The reduction curve, or the "kinetogram" can be used to derive the following data:

1. The location of T_{mi} is characteristic of the i-th functional group.
2. The integral of the peak of each group is the exact stoichiometric equivalent of the sulfur group that has been reduced. The activation energy and the frequency factor of the reaction can be determined by curve pitting of the data to equation 12.
3. Slightly different variations of this method were used by Juntgen and co-workers to study the rates of coal pyrolysis and gasification (13)(14)(15),

by Campbell and Stephen (16) to study the rates of coal pyrolysis, and by Yergey et al. (17) and Bauman et al. (18) to study the rate of evolution of H_2S during coal hydrogenation. In the latter studies, not all the sulfur was removed from the coal, therefore, quantitation of the sulfur groups cannot be done from the data. A more detailed discussion of the quantitation is presented below.

3.2 QUANTITATION OF THE DATA

The most important problems that should be solved so that the analysis of the sulfur groups in coal will be quantitative are:

1. COMPLETE reduction of each sulfur group.
2. COMPLETE recovery of all the H_2S from each sulfur group.

The major difficulty on the road to obtain complete reduction of the sulfur groups are mass transfer limitations. The diffusion of the reducing agent into the coal particle is slow and so is the diffusion of the H_2S out of the coal particles. These processes result in incomplete reduction of the sulfur and in the spreading of the peak from one group over a large interval of temperature. To reduce the effect of mass transfer, we used finely divided coal particles and conducted the reduction in a solvent which partially liquefies the coal. In addition, we added Co-Mo catalyst to the cell to enhance the rate of reduction of sulfur groups.

Complete recovery of all the H_2S was impossible when lignite with a large content of calcium carbonate was examined. Apparently, some of the H_2S reacted with the carbonate according to:

$$CaCO_3 + H_2S \rightarrow CaS + CO_2 + H_2O \qquad (15)$$

Most of the basic carbonates in coal, e.g., calcite, dolomite, and sidrite can, however, be easily dissolved in dilute hydrochloric acid and removed from the sample.

The application of the special solvent permitted us to reduce most of the organic sulfur below 370°C and 100 psi.

4. EXPERIMENTAL SYSTEM

The experimental system consists of five parts: 1) reduction cell, 2) hydrogen sulfide detectors, 3) gas flow systems, 4) heater and temperature programmer, and 5) recording and signed processing device.

Figure 3 shows the functional relation among the units. All the components except for the reduction cell are standard. Several prototypes of cells were built and tested in our laboratory. The first prototype is described in Figure 4.

One commercial detector and two modified detectors were tested: 1) the lead-acetate detector*, 2) the flame photometric detector, and 3) electrolytic detector. The first two are differential detectors, while the third is an integral detector. The data that are reported in this manuscript were derived using the lead acetate detector.

5. RESULTS AND DISCUSSION

Two questions are addressed: 1. the identification peaks which belong to a specific functional group. 2. the variation in the distribution of sulfur groups in different coals.

5.1 IDENTIFICATION OF PEAKS

The philosophy of the identification technique is that when solids are reduced peaks that belong to a specific sulfur group will appear at the same temperature, T_{mi}, provided that the same rate of heating is used, and that the mass

---

* The courtesy of Mr. C. Kimbell, President of Houston Atlas, who loaned us the equipment and helped us in its modification is greatly appreciated.

transfer does not limit the rate of reduction. Therefore, solid polymers that contain only one sulfur group, will produce one peak of sulfur only, the peak that corresponds to the sulfur group which they have. Thus, polythiophenes produce a peak which corresponds to the group 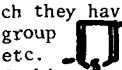 . Rubber produces a peak which corresponds to R-S-R and R-S-S-R, etc. Figure 5 shows the kinetoground rubber. Figure 6 shows the kinetogram of thiantrenes . Note that two different peaks appear. The authors believe that the first peak is due to H_2S from the reaction

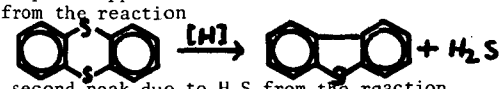

Process I

and the second peak due to H_2S from the reaction

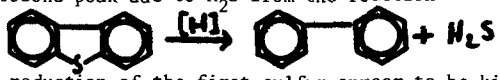

Process II

The reduction of the first sulfur appear to be kinetically equivalent to the reduction of aromatic sulfides. However, the reduction of dibenzothiophene occurs at a higher temperature. The reduction of FeS_2 occurs in two stages as expected:

$$FeS_2 \xrightarrow{[H]} FeS + H_2S \qquad \text{and} \qquad FeS \xrightarrow{[H]} Fe + H_2S$$

However, the "sharpness" of the peak depends on the particle size of the FeS_2. Small FeS_2 produce very sharp peaks and larger FeS_2 particles produce a "sluggish" peak. The FeS and Fe produce resistance to mass transfer.

6.2 TESTS OF COAL AND LIGNITE SAMPLES

Table 2 gives the distribution of sulfur in Illinois No. 6 coal, and in Texas lignite. Figure 7 shows the kinetogram of the Illinois No. 6 coal. A tentative assignment of functional groups to the peaks is given on the chart. Extraction of the coal with nitric acid removes the pyritic sulfur altogether, and slightly affects the organic sulfur as well. The latter is expected because nitric acid oxidizes organic sulfur to the corresponding sulfoxides (19). Figure 8 shows the kinetogram of HNO_3 extracted Illinois No. 6 coal. Table 2 shows a quantitative estimate of the distribution of sulfur groups in Illinois No. 6 and in Texas lignite.

Texas lignite (Milam Co.) is more porous than bituminous coal, and therefore its resistance to mass transport is smaller than that of bituminous coal. Most of the sulfur in the samples that were tested was organic. The kinetogram in Figure 9 shows that the organic sulfur in the lignite was essentially in the form of isolated single thiophenic rings, and not in the form of dibenzothiophenes or aliphatic sulfides. This indicates that the thiophenic structures are formed in coals in early stages of the geological coalification of wood. This thiophenic structure condenses latter to dibenzothiophenic structures etc. The latter observation was unexpected, and we searched for reaction mechanisms which may lead to the same experimental observation. One such mechanism involves the reaction:

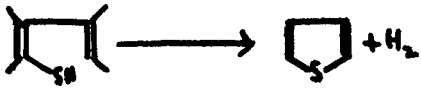

This reaction shows that isolated thiophenic structures can be produced from unstable sulfur-containing groups due to thermal decomposition. Thermally unstable sulfur groups are reduced to H_2S at much lower temperatures than stable groups, (see discussion in Ref. 6). However, if not all the unstable sulfur was reduced while the temperatures were still low, part of it may be converted into a more stable form during the analysis. Thus, if mass transfer limits the rate of reduction, the result of the analysis of coal samples will be biased, and will show a larger fraction of single-thiophenic rings.

Another observation which seems interesting is that the fraction of sulfidic sulfur is about the same in the lignite and in the bituminous coal. This observation can be accidental, however, similar results were noted by others (20).

6. CONCLUSION

A method has been developed which permits to conduct detailed quantitative analysis of the distribution of sulfur groups in coal. The method permits to determine qualitatively and quantitatively the distribution of organic sulfur groups in coal samples. Illinois No. 6 bituminous coal and Texas lignite were tested, and the results are consistent with accepted theories on the sulfur in coal.

ACKNOWLEDGEMENT

The authors wish to thank the Office of Research and the Energy Institute of the University of Houston for their support of this program.

REFERENCES

1. ASTM, part 26D2492, (1974), 507.
2. British Standards Institution, BS 1016, part II (1975).
3. *International Organization for Standardization*, R157 (1960).
4. Attar, A., "The Fundamental Reactions of Sulfur in Coal During Pyrolysis--Review" (presented in the AIChE Meeting, Houston, March, 1977).
5. Attar, A., "The Fundamental Reaction of Sulfur and Modeling the Distribution of Sulfur in Coal Pyrolysis and Hydrogenation", Review in print in a Chemical Engineering Progress, Technical Manual.
6. Attar, A., "The Chemistry, the Thermodynamics and the Kinetics of the Reactions of the Sulfur in Coal with Gases", Accepted for publication, Fuel.
7. Attar, A. and Corcoran, W. H., "Sulfur Functional Groups in Coal", Ind. Eng. Chem., Prod. Res. Dev., 16, 168 (1977).
8. Brook, J. D., J. Inst. Fuel, 29, 82 (1956).
9. Jones, J. R., "Some Aspects of the Chemistry of Sulfur in Relation to Its Presence in Coal", Ph.D. Thesis, The Pennsylvania State University, Dept. of Fuel Technology, Sept. (1976).
10. Wandless, A. M., J. Inst. Fuel, 32, 258 (1959).
11. Horton, L. and Randall, R. B., Fuel, 26, 127 (1947).
12. Given, P. H. and Wyss, W. F., BCURA Mont. Bull., XXV(5), 165 (1961).
13. Juntgen, H., Erdol and Kohle, 17, 180 (1964).
14. Juntgen, H. and Van Heek, K. H., Fuel, 47, 103 (1968).
15. Feistel, P. P., Van Heek, K. H., and Juntgen, H., Prep. Div. Fuel Chem., 22 (1), 53 (1977).
16. Campbell, J. H. and Stephens, D. R., IBID, 21 (7) 94 (1976).
17. Yergey, A. L., Lampe, F. W., Vestal, M. L., Day, A. G., Fergusson, G. J., Johnson, W. H., Snyderman, J. S., Essenhigh, R. H., and Hudson, J. E., Ind. Eng. Chem., Proc. Res. Dev., 13 (3), 233 (1974).
18. Bauman, H., Klein, J., and Juntgen, H., Erdol and Kohle, 30 (4), 159 (1977).
19. Suter, C. M., "The Organic Chemistry of Sulfur", Wiley, N.Y. (1944).
20. Bogdanova, V. A. and Boranski, A. O., C.A. 63, 17741 (1965) and Pretezhaeva, E. N. et al., C.A. 60, 6215 (1964).

Table 1: Sulfur Classes in Illinois #6 and in Texas Lignite

	Illinois #6	Texas Lignite
Total Sulfur	4.05	1.03
FeS_2 wt%	1.56	0.19
SO_4 wt%	0.38	0.07
Organic wt%	2.09	0.77

Table 2: Wt% of the Organic Sulfur in Different Functional Groups
Tentative assignment. ±15% error is possible.

Structure	Illinois No. 6 (Bituminous)	Texas Lignite
-SH	present in small amounts	
aliphatic or alicyclic -S- or	27.4	26.6
Dibenzothiophenic	41.8	16.3
Single thiophenic or other very stable group.	30.8	57.1

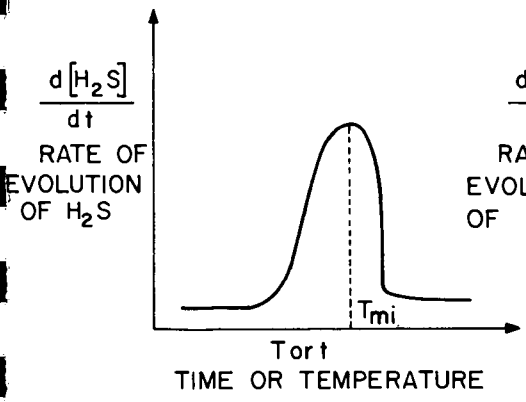

FIGURE 1: ANALYSIS OF MATERIAL WITH A SINGLE FUNCTIONAL GROUP

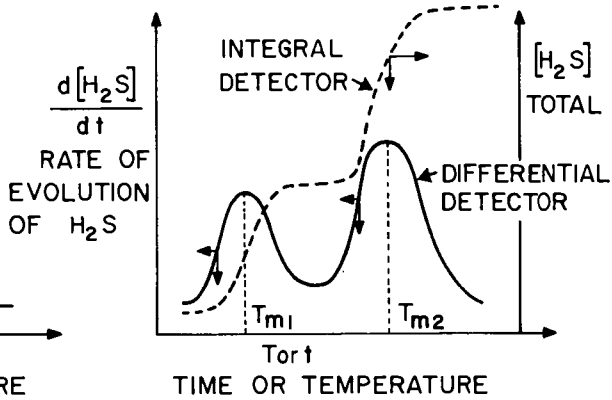

FIGURE 2: ANALYSIS OF A MIXTURE CONTAINING TWO GROUPS USING A DIFFERENTIAL AND AN INTEGRAL DETECTORS.

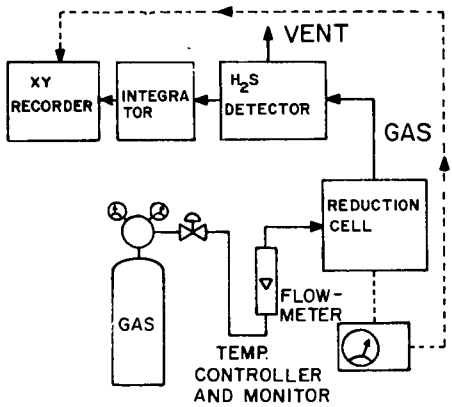

FIGURE 3: SCHEMATIC DIAGRAM OF EXPERIMENTAL SYSTEM.

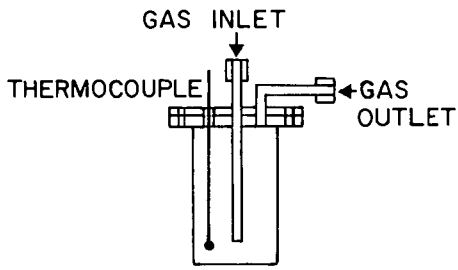

FIGURE 4: PROTOTYPE OF REDUCTION CELL.

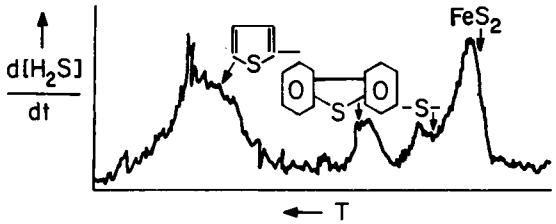

FIGURE 7: KINETOGRAM OF 32.6 mg ILLINOIS No. 6 BITUMINOUS COAL. THE GROUP ASSIGNMENT IS TENTATIVE.

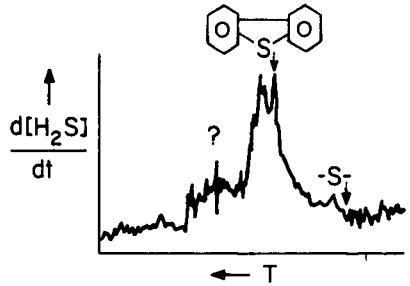

FIGURE 8: KINETOGRAM OF ILLINOIS No. 6 - EXTRACTED WITH HNO_3.

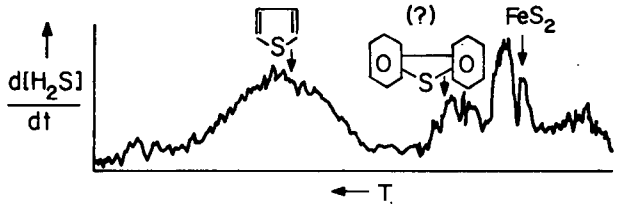

FIGURE 9: KINETOGRAM OF TEXAS LIGNITE. THE GROUP ASSIGNMENT IS TENTATIVE.

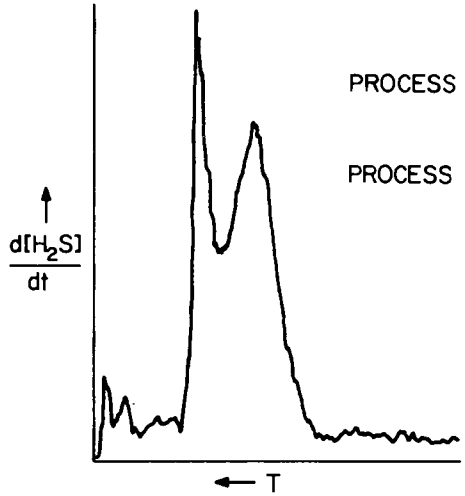

FIGURE 5: KINETOGRAM OF RUBBER.

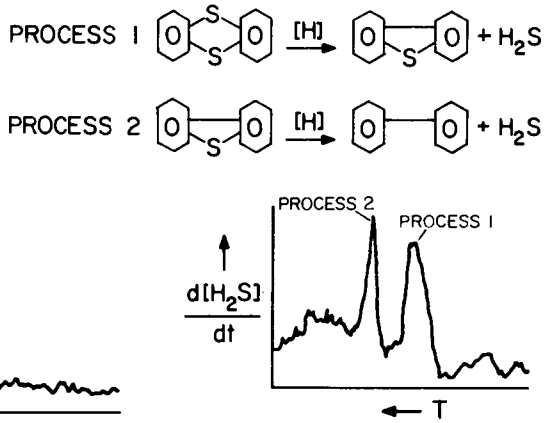

FIGURE 6: KINETOGRAM OF THIANTHRENE.

The Aliphatic Structures in Coal

N. C. Deno, Barbara A. Greigger, and Stephen G. Stroud

Department of Chemistry, The Pennsylvania State University
University Park, Pennsylvania 16802

Coals are varying and complex in their chemical structures. This type of situation is classically studied by degradative procedures which reduce the complexity to simpler component parts. This has been done with coal and four degradative methods have emerged to which we owe much of our concepts of coal structure. These are (a) destructive distillation of coal to benzene and pyridine derivatives, (b) alkyl transfer to phenol and determination of the alkylphenols, (c) liquifaction or solvent refining which reduces MW from the 5000 to 600 range, and (d) oxidation with the usual oxidizing agents (HNO_3, O_2, Mn VII, Cr VI) to produce benzene carboxylic acids.

We now introduce a 5th degradation procedure. This is oxidation with H_2O_2 in TFA (trifluoroacetic acid) with or without addition of H_2SO_4. This system has the capability of completely dissolving coal to form colorless or pale brown solutions in which all aromatic structures have been destroyed and most of the aliphatic structures preserved (1,2). The nature of its action is illustrated by three examples. Treatment of propylbenzene, isopropylbenzene, and 1,2-diphenylethane by the usual oxidizing agents (HNO_3, O_2, Mn VII, Cr VI) leads to attack at the benzylic positions, oxidative cleavage, and formation of benzoic acid. In contrast, the H_2O_2-TFA-H_2SO_4 oxidations attack the aromatic rings leaving the benzylic positions virtually untouched even when tertiary as in isopropyl and cyclohexyl benzenes. The products from the three examples are respectively butyric acid, isobutyric acid, and succinic acid (2). It is immediately evident that this new degradation procedure is particularly suited to cataloging and categorizing the aliphatic structures in coals.

The products from the H_2O_2-TFA-H_2SO_4 oxidations have been examined in two ways. The nmr (nuclear magnetic resonance) spectra of the reaction mixture provides an inventory of the hydrogen present in the products. Acetic acid, succinic acid, and methanol (as the trifluoroacetate) can be easily recognized because they generate sharp singlets and because they are dominant products. The absolute yields were determined using malonic acid as an internal standard. The non-volatile products can be isolated by evaporation in vacuo, conversion to methyl esters, and examination by nmr and gc (gas chromatography).

It must be emphasized that there has not been sufficient time or funding to optimize and standardize procedures. However, it has been found that acetic acid is produced from a wider variety of models in H_2O_2-TFA oxidations than in H_2O_2-TFA-H_2SO_4 oxidations. In the latter, acetic acid formation is mainly limited to arylmethyl groups. The current procedure is to add 0.8 g of <20 mesh coal to a mixture of 12 ml of TFA, 15 ml of 96% H_2SO_4, and 15 ml of 30% aq. H_2O_2. Addition is exothermic, but not enough to require any precautions with the above amounts. The mixture is heated for five hours at 60°. After cooling, it is important to destroy excess peroxide with 10% Pt on asbestos until O_2 evolution ceases and a KI test for peroxide is negative.

Table I summarizes data on products from oxidations of coal. Table II summarizes data on model compounds. The data has been submitted for publication in greater detail (2).

Despite the preliminary nature of the data, several conclusions are possible. No propionic acid, butyric acid, or isobutyric acid were observed in the products from any of the coals. This eliminates structures involving ethyl, propyl, and

Table I. NMR Spectra of Solutions of Coals in H_2O_2-TFA-H_2SO_4

Coal	H Obsvd. x 100/Total H in Coal			
	Acetic acid (2.18δ)	Succinic acid (2.78δ)	alkyl other than α or β (0-2.0δ)	Other bands
Pittsburgh Seam 79.5% H 5.2% H	1.0	3.3	0	3.5
Illinois #6 70.5% C 5.1% H	5.7	8.9	0.5	2.6
Illinois #6 Monterey 69.7% C 4.98% H	2.8	8.9	2.2	4.1
Illinois #6 Monterey solvent refined	4.4	2.4	1.0	2.8
Wyodak solvent refined 87.0% C 6.6% H	2.3	1.0	8.1	5.9
Lignite North Dakota 65.3% C 4.4% H	0	10.6	50.6	20.4[a]

[a] This was entirely methanol as its trifluoractate.

Table II. H_2O_2-TFA-H_2SO_4 Oxidations of Model Compounds

Compound	Predominant Product(s)	% Yield[a]
1,2-diphenylethane	succinic acid	73
9,10-dihydrophenanthrene	succinic acid	71
acenaphthene	succinic acid	64
indan	succinic acid	27
5-hydroxyindan	succinic acid	38
4,7-dimethylindan	succinic acid[b] acetic acid[b]	
toluene	acetic acid	68
1,4-dimethylbenzene	acetic acid	66
1,3-dimethylbenzene	acetic acid	66
1,2-dimethylbenzene	acetic acid	46
ethylbenzene	propionic acid	71
propylbenzene	butyric acid	73
isopropylbenzene	isobutyric acid	32
t-butylbenzene	$(CH_3)_3CCOOH$	
cyclohexylbenzene	c-$C_6H_{11}COOH$	
methoxybenzene	methanol	79
3-phenyl-1-propanol	butyrolactone	75
tetralin and 6-hydroxytetralin	cyclohexene-1,2-$(COOH)_2$	69
1,3-diphenylpropane	glutaric acid	

[a] Computed on the basis of one mol of substrate yields one mol of product except for the three dimethylbenzenes where the basis was 2 mols of acetic acid from one mol of substrate.

[b] Acetic acid : succinic acid = 1.1.

isopropyl attached to an aryl ring. These structures have been reported previously (3,4). While our results will be more reliable if confirmed by gc studies, they seem reasonably firm now. Furthermore, the past reports are in some doubt because they depended on Friedel-Crafts type of degradations (3) or tenuous analysis of broad absorption bands in nmr spectra of coal extracts (4).

None of the bituminous coals contained arylmethoxy as shown by the complete absence of methanol in the oxidation products. This agrees with results of Zeisel determinations which also showed no methoxyl (5). This is particularly interesting because lignite and lignin are well-known to contain arylmethoxy groups. In fact an H_2O_2-TFA-H_2SO_4 oxidation of lignin at 25° showed 14.0% by weight arylmethoxy which is typical for lignins (6-8). A sample of North Dakota lignite showed 9.6% arylmethoxy. Both yields were computed on the basis that each arylmethoxy went quantitatively to methanol. Neither lignin nor lignite produced acetic acid confirming the well-established absence of aryl methyl groups (6-8). Both produced succinic acid indicating unsubstituted $ArCH_2CH_2$-C components in the structure.

All coals produced acetic acid, but in widely varying amounts. The model studies indicate that this acetic acid comes from arylmethyl groups and the amount of arylmethyl can be estimated from the data in Table I. In making this estimate, it should probably be assumed that the yield of acetic acid from each arylmethyl is ~70% based on the models in Table II.

The succinic acid originates from diarylethane or indan structures. Since any indan components in coal would likely have alkyl, alkoxy, or hydroxy groups on the aryl ring, it was of particular concern to us to show that such substituents did not significantly alter the production of succinic acid. For this purpose both 4,7-dimethylindan and 5-hydroxyindan were studied and both gave succinic acid as the dominant product the same as indan itself.

The question remains as to whether the succinic acid arises from indan or diarylethane structures or from some other type of structure which has not been studied. One bit of evidence is suggestive that indans are predominantly responsible for succinic acid formation. Oxidation of indan with H_2O_2-TFA-H_2SO_4 gave no acetic acid whereas the amounts of acetic and succinic acids were comparable when H_2O_2-TFA was the oxidizing agent. Pittsburgh Seam and Illinois #6 coals showed similar effects. Leaving out the H_2SO_4 in H_2O_2-TFA oxidations caused the yield of acetic acid to more than double (2).

No aryl hydrogen appeared in the oxidation products despite the fact that benzoic acid is inert. This eliminates benzoate esters as components of coal structure.

The absence of cyclohexene-1,2-dicarboxylic anhydride shows that no tetralin structure can be present of the type which are unsubstituted on the aliphatic ring.

The solvent refining (liquifaction) of coal is thought to involve thermal cleavage of benzyl ethers and conversion of the benzyl radicals to arylmethyl by hydrogen abstraction (9-11). The data on Monterey Coal in Table I is in accord with this view in that the yield of acetic acid (reflecting arylmethyl) increased. The yield of succinic acid decreased presumably reflecting the aromatization or desaturation of indan, diarylethane, and partially reduced aromatic structures.

There is much to do in this field in the direction of varying the oxidation technique to make it more selective and to increase yields. Furthermore, no start has been made in identifying the other products of H_2O_2-TFA-H_2SO_4 oxidations although their aliphatic nature, small size, and simple nmr spectra suggests that their identification is facile.

The total %H observed can be calculated by adding the columns in Table I. The highest was 81.9% for North Dakota Lignite and the lowest was 7.8% for Pittsburgh Seam Coal. This largely reflects the aromaticity of the coal. The aromatic hydrogens are completely lost while the aliphatic are largely preserved. However, even in model compounds loss of 30% of the aliphatic H was typical and the loss is even greater in certain aliphatic structures such as those on benzyl derivatives. Thus, while the %H observed in a typical bituminous coal such as Illinois #6 is a respectable 17.7%, this represents no more than about half of the total aliphatic hydrogen.

We are deeply indebted to Dr. Malvina Farcasiu and Dr. Duayne Whitehurst for the last 4 substrates in Table 1, for a sample of lignin, and for stimulating discussions. They will be coauthors with us in future papers on solvent refined coal and on lignin. We are also deeply indebted to Mr. Philip Dolsen and the Coal Research Station at The Pennsylvania State University for the first two substrates in Table I. Complete analyses of these coals are available (2). We also wish to acknowledge stimulating discussions with Dr. Ron Liotta of Exxon Corp., Linden, New Jersey.

References

(1) N. Deno, B. A. Greigger, L. A. Messer, M. D. Meyer, and S. G. Stroud, Tetrahedron Lett., 1977, 1703.

(2) N. Deno, B. A. Greigger, and S. G. Stroud, submitted to Fuel.

(3) L. A. Heredy, A. E. Kostzo, and M. B. Neuworth, Fuel 1965, 44, 125.

(4) K. D. Bartle, T. G. Martin, and D. F. Williams, Fuel 1975, 54, 226.

(5) D. W. van Krevelen, "Coal," Elsevier Publishing Co., Amsterdam, 1961.

(6) "Lignin Structure and Reactions," Advances in Chemistry Series No. 59, Am. Chem. Soc., Washington, D. C., 1966.

(7) W. J. Schubert, "Lignin Biochemistry," Academic Press, N. Y., 1965.

(8) F. E. Brauns and D. A. Brauns, "The Chemistry of Lignin," Academic Press, N. Y., supplemental vol. 1960.

(9) R. G. Roberts, D. C. Cronauer, D. M. Jewell, and K. S. Seshadri, Fuel 1977, 56, 17.

(10) B. S. Ignasiak and M. Gawlak, Fuel 1977, 56, 216.

(11) D. D. Whitehurst, M. Farcasiu, T. O. Mitchell, and J. J. Dickert, Jr., "The Nature and Origin of Asphaltenes in Processed Coals," Mobil Research and Development Corp., Princeton, N.J., July 1977, report submitted to Electric Power Research Institute.

CHROMATOGRAPHIC SEPARATION OF COAL LIQUIDS

By

T. E. Cogswell and D. R. Latham

Laramie Energy Research Center
P. O. Box 3395
Laramie, Wyo. 82071

INTRODUCTION

Coal liquefaction is a major attempt to meet certain energy requirements and at the same time protect the environment. If coal liquefaction is to be successful, a technology must be developed that provides analytical data on both feed coals and liquid products. Refining procedures could then be altered to accommodate syncrudes of different composition. Thus, efficient processing and utilization require a knowledge of the chemical composition of coal liquids.

Interest in the chemical structure of coal and coal conversion products has increased greatly in recent years. This interest has produced two general approaches to the study of coal liquids. One is the detailed characterization of a particular coal liquid by extensive separation followed by elaborate spectroscopic characterization of the various compound types (1). The other approach emphasizes a rapid and simple method of separation in which fewer fractions are generated (2). The latter is more amenable to on-stream control, where fast procedures are required.

Our approach to the analysis of coal liquids incorporates the most attractive features of the two approaches. Five chemically meaningful fractions are generated from a total coal liquid. These fractions are separated on a chemical functionality basis and are suitable for detailed characterization. Asphaltene and pre-asphaltene fractions are purposefully avoided because of their lack of chemical definition.

This paper describes the separation of a coal liquid into five fractions by liquid chromatography. The fractions are generated by ion exchange, coordination complex, and adsorption chromatography. The nonhydrocarbon fractions account for most of the coal liquid and were emphasized in the characterization work that is reported here.

EXPERIMENTAL

Coal Liquid Sample

The coal liquid used in this investigation was obtained from the Pittsburgh Energy Research Center's Synthoil process (3). The feed was a high-sulfur West Virginia coal slurried in 65 percent product recycle oil. The process used a 14-ft catalytic reactor operated at 450°C and 4000 psig of hydrogen. The liquid product was centrifuged to reduce water and solids.

Apparatus

Infrared spectra were recorded using a Perkin-Elmer 621* infrared spectrophotometer; low-resolution mass spectra were recorded on a Varian CH-5 single-focusing mass spectrometer. The columns used for chromatographic separations were similar to those used by Jewell et al. (4). They were gravity flow columns, 1.4-cm i.d. by 119-cm, with a recycling arrangement that permits the continuous elution of the sample without the need for large quantities of solvent.

Reagents

All solvents were flash distilled. The ion-exchange resins and other chromatographic materials were prepared according to previously reported methods (5).

Routine Methods of Nitrogen, Sulfur, and Oxygen Analyses

Elemental analyses were performed at a commercial laboratory; nitrogen was determined by the micro-Dumas method; sulfur, by combustion followed by titration of oxidation product with barium perchlorate to a colorimetric endpoint; and oxygen, by a modified Unterzaucher method.

Quantitative Infrared Analyses

Quantitative infrared measurements and calculations were performed in a manner similar to that used by McKay et al. (6).

Separation Procedure

The coal liquid (0.5 g) was dissolved in methylene chloride (20.0 ml) and passed through a 10- to 15-micron filter to remove inorganic solids and any undissolved organics. The material retained on the glass filter amounted to less than 2 percent of the total coal liquid. The separation was performed by sequentially passing the coal liquid through four chromatographic columns to obtain five fractions: acids, bases, neutral nitrogen compounds, saturate hydrocarbons, and aromatic hydrocarbons as shown in Figure 1.

Separation of Acids--Anion Exchange Chromatography. - The sample of filtered coal liquid was chromatographed on anion resin (100 g) that had been wet packed in the column with methylene chloride. Unreactive material was washed from the resin with methylene chloride (700 ml) for 3 hours or until the eluant was clear. After the unreactive materials were removed, the reactive compounds (acids) were recovered in two steps. The column was first eluted with 60% benzene-40% methanol (350 ml); the resin was then removed from the column and placed in an extractor; the remaining acid was removed by elution with 60% benzene-40% methanol (350 ml) saturated with carbon dioxide.

Separation of Bases--Cation Exchange Chromatography. - The sample of acid-free coal liquid (about 350 mg) was taken to dryness by evaporation under a nitrogen atmosphere and redissolved in benzene (25 ml). The benzene solution was chromatographed on cation resin (50 g) that had been wet packed in the column with benzene. Unreactive material was eluted from the resin with benzene (500 ml) for 1 hour or until the eluant was clear. The reactive material (bases) was removed from the resin in two steps. The column was first eluted with 60% benzene-40% methanol (350 ml); the resin was then removed from the column and placed in an extractor; the remaining bases were removed from the resin with 54% benzene-38% methanol-8% isopropylamine (200 ml).

Separation of Neutral Nitrogen Compounds--Ferric Chloride Coordination Chromatography. - Ferric chloride-Attapulgus clay (80 g) was placed above anion resin (120 g) in a single column. After the column was washed with cyclohexane (100 ml), the acid- and base-free material, freed of benzene and redissolved in cyclohexane (50 ml), was passed through the column. The column was eluted with cyclohexane (300 ml) to remove hydrocarbons. The nitrogen compound-ferric chloride complexes were removed from the clay with 1,2-dichloroethane (200 ml). These complexes were subsequently broken by passing the solution over the anion resin; the ferric chloride salt was retained on the resin, and the neutral nitrogen compounds were recovered in the eluate.

Separation of Hydrocarbons--Silica Gel Chromatography. - The acid-, base-, and neutral-nitrogen-free coal liquid, freed of cyclohexane and redissolved in n-pentane (50 ml), was placed on a silica gel column (150 g). The column was eluted with n-pentane (approximately 500 ml or until UV monitor showed absorbance greater than 10 percent of full scale at 254 nm) to remove the saturate hydrocarbons. The aromatic hydrocarbons were then recovered by elution with benzene (approximately 300 ml).

RESULTS AND DISCUSSION

Recovery and precision data for three different runs are presented in Table 1. Recoveries from 96 to 98 percent may be expected from the separation scheme. The precision data in the last column of Table 1 show a reproducibility of ± 3 wt. percent for each of the five fractions.

TABLE 1. - Three separations showing weight percent and precison for each fraction

	Weight percent			
Fraction	Run 1	Run 2	Run 3	Precision
Acid	27	33	31	30 ± 3
Base	20	18	22	20 ± 2
Neutral nitrogen	12	10	11	11 ± 1
Saturate	10	13	11	11 ± 2
Aromatics	27	22	23	24 ± 3
Recovery	96	96	98	97 ± 1

The data in Table 1 show that for each separation run the acids, bases, and neutral nitrogen compounds represent about 60 percent of the total coal liquid. Acids and bases alone amount to about 50 percent of the total liquid showing the highly polar nature of the coal liquid. This relatively high amount of polar material compared with amounts found in petroleum poses problems in developing separation methods and in processing these liquids into useful fuels.

The saturate and aromatic hydrocarbon fractions represent about 35 percent of the total liquid. The content of aromatic hydrocarbons is about twice that of saturate hydrocarbons, reflecting the aromatic character of the coal feedstock.

Elemental analyses in Table 2 show that oxygen and nitrogen are the primary heteroatoms present in the polar fractions. The acid fraction contains about 5 percent oxygen, primarily due to large amounts of phenolic compounds as discussed later. The bases are high in nitrogen, having about 4 percent nitrogen. Reproducible data for the neutral nitrogen fraction were not obtained so they are not included in Table 2. The saturate hydrocarbons contain only small amounts of heterocompounds, but the aromatic hydrocarbons contain large amounts of oxygen heterocompounds. The aromatic fraction shows 3.4 percent oxygen, which is high for a hydrocarbon fraction. This might be explained by the presence of furan or dibenzofuran-type oxygen compounds that are not removed by the resins or the ferric chloride. Data on sulfur are too limited to determine whether sulfur is evenly distributed among the fractions or whether sulfur compounds are concentrated in any one fraction(s). Molecular-weight data on the total coal liquid and on selected fractions from the separation show average molecular weights ranging from 210 to 250.

TABLE 2. - Elemental analyses and molecular weights of Synthoil and fractions

Sample	Weight percent					Molecular wt.
	Carbon	Hydrogen	Nitrogen	Oxygen	Sulfur	LRMS*
Total Synthoil	86.09	7.4	1.6	3.9	0.7	225
Acid	79.4	6.7	1.0	5.5	0.8	250
Base	81.5	7.4	3.9	1.9	-	225
Saturates	88.1	11.6	0.3	-	-	230
Aromatic	87.6	7.6	0.1	3.4	0.6	210

*Low-resolution mass spectrometry.

Characterization of Acid Fraction

The acid fraction represents about 30 percent of the total coal liquid. This fraction has 5.5 percent oxygen (Table 2) and an average molecular weight of 250. Calculations from these data, assuming one oxygen atom per molecule, show that 86 percent of the molecules contain one oxygen atom. Similarly, one percent nitrogen and a molecular weight of 250 calculates to 15 percent of the molecules containing one nitrogen atom.

The infrared spectrum of the acid fraction, Figure 2, shows a strong band of free phenolic O-H stretching vibration at 3590 cm^{-1}. The lack of significant absorption in the carbonyl region (1650-1750 cm^{-1}) indicates the absence of carboxylic acids. Quantitative infrared analysis shows that approximately 85 percent of the fraction is represented by the phenolic O-H stretching band. The remaining material can be accounted for by quantitative analysis of the N-H absorption at 3460 cm^{-1}, showing the presence of pyrrolic nitrogen compounds.

Two different methods give the same values for oxygen compounds (phenols) and for nitrogen compounds(pyrroles). Thus, the elemental analysis suggests 86 percent oxygen compounds, and infrared shows that these compounds, 85 percent of the fraction, are phenols. Similarly, elemental analysis shows 15 percent nitrogen compounds and infrared shows about the same amount of pyrrolic nitrogen compounds.

Characterization of Base Fraction

The base fraction represents about 20 percent of the coal liquid. A nitrogen content of almost 4 percent reflects a successful attempt to concentrate nitrogen compounds. From the average molecular weight and the nitrogen content it appears that about 70 percent of the molecules contain one nitrogen atom. This is not as easy to substantiate with infrared spectroscopy as it was in the acid fraction. The problem results from overlapping bands, as shown in Figure 3. Pyrrolic N-H stretching at 3460 cm^{-1} overlaps with amide-type N-H stretching at 3410 cm^{-1}, prohibiting quantitative determinations by infrared spectrometry. The infrared spectrum shows carbonyl absorption in the region 1650-1700 cm^{-1}, which may be due to small amounts of amides. A shoulder on the low-frequency side of the 1600 cm^{-1} band may indicate the presence of pyridines in this fraction.

Neutral Nitrogen Fraction

This fraction represents only about 10 percent of the total coal liquid. The infrared spectrum of this fraction is given in Figure 4. The spectrum shows an absorption band at 3460 cm^{-1} due to pyrrolic N-H stretching vibrations and a shoulder around 3410 cm^{-1} probably due to N-H stretching of amide types. Carbonyl absorption between 1700 and 1750 cm^{-1} also suggests the presence of amides.

Saturate Hydrocarbon Fraction

Saturated hydrocarbon compounds comprise 11 percent of the total coal liquid and less than one-third of the total hydrocarbon material. A gas chromatogram of this fraction is presented in Figure 5. The figure shows that normal paraffins, ranging in carbon number from 13 to 35, are major components of this fraction.

Aromatic Hydrocarbon Fraction

About one-fourth of the total coal liquid is defined by the separation method as the aromatic hydrocarbon fraction. However, this fraction has been shown to have over 3 percent oxygen. The compound types containing oxygen have not been defined in this work. Calculations using 3.4 percent oxygen and an average molecular weight of 210, assuming one oxygen atom per molecule, show that about 45 percent of the molecules contain oxygen. This oxygen is probably of the furan or dibenzofuran type which is nonreactive to resins or ferric chloride. Thus, these compounds are isolated with aromatic hydrocarbons in the final separaton step.

SUMMARY

A Synthoil coal liquid that had not been solvent deasphaltened was separated into fractions of acids, bases, neutral nitrogen compounds, saturate hydrocarbons, and aromatic hydrocarbons using ion exchange, coordination, and adsorption chromatography. The separation method is reproducible, and recovery of material was better than 95 percent. The method separates compounds according to chemical functionality and generates fractions that are suitable for detailed characterization. The Synthoil coal liquid used in this investigation contains about 30 percent acids and 20 percent bases, according to the ion exchange resin definition of acids and bases. The acids were characterized as being about 85 percent phenolic compounds and 15 percent compounds containing pyrrolic nitrogen. The bases were found to be largely pyridine and pyrrolic nitrogen compound types. The saturate hydrocarbons were 11 percent of the total coal liquid, and the aromatic hydrocarbons were about 24 percent; however, oxygen compounds, probably of the dibenzofuran type, were also found in the aromatic hydrocarbon fraction. The average molecular weight of the coal liquid sample was determined by low resolution mass spectrometry to be about 225.

CONCLUSIONS

This separation method, a modification of a previous method, may be useful for separating other coal liquids according to chemical functionality. An important advantage of this method over other separation schemes used for coal liquids is that the total coal liquid is separated and a minimum number of fractions is generated. A practical application of the separation scheme may be found in monitoring the amounts of acids and bases produced in coal liquification processes. Such information is important because acids and bases are known to cause both chemical and physical problems in the processes.

REFERENCES

1. T. Aczel, R. B. Williams, R. J. Pancirov, and J. H. Karchmer, "Chemical Properties of Synthoil Products and Feeds," report prepared for U.S. Energy Research and Development Administration, FE 8007, 1977.

2. J. E. Schiller and D. R. Mathiason, Anal. Chem. 49, 1225 (1977).

3. S. Akhtar, N. J. Mazzocco, M. Weintraub, and P. M. Yavorsky. "Synthoil Process for Converting Coal to Nonpolluting Fuel Oil," presented at Fourth Synthetic Fuels from Coal Conference, Oklahoma State University, Stillwater, Okla. May 6-7, 1974.

4. D. M. Jewell, J. H. Weber, J. W. Bunger, H. Plancher, and D. R. Latham, Anal. Chem. 44, 1391 (1972).

5. J. F. McKay, P. J. Amend, T. E. Cogswell, P. M. Harnsberger, R. B. Erickson, and D. R. Latham, Preprints, Div. Petrol. Chem., ACS, 22, (2), 708 (1977).

6. J. F. McKay, T. E. Cogswell, J. H. Weber, and D. R. Latham, Fuel 54, 50 (1975).

*Mention of specific brand names or models of equipment is made for identification only and does not imply endorsement by the Department of Energy.

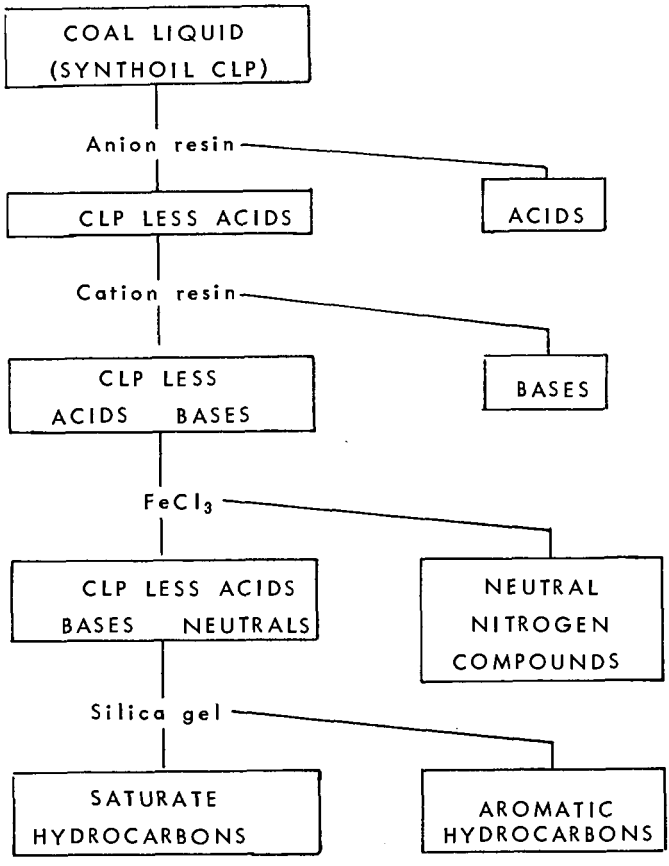

Figure 1- SEPARATION PROCEDURE

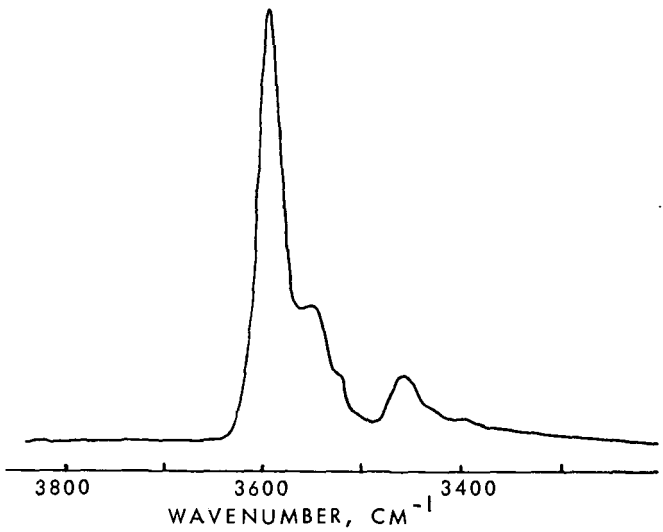

Figure 2- PARTIAL INFRARED SPECTRUM OF ACID FRACTION

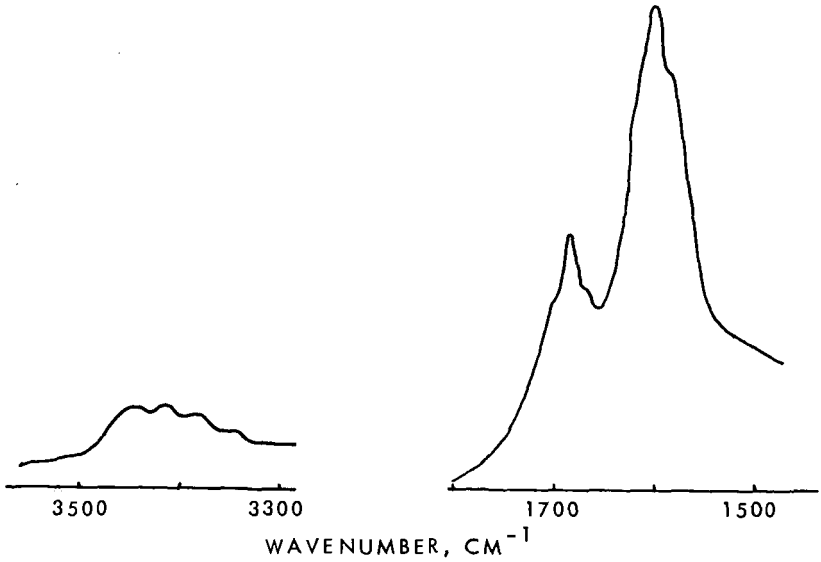

Figure 3 - PARTIAL INFRARED SPECTRUM OF BASE FRACTION

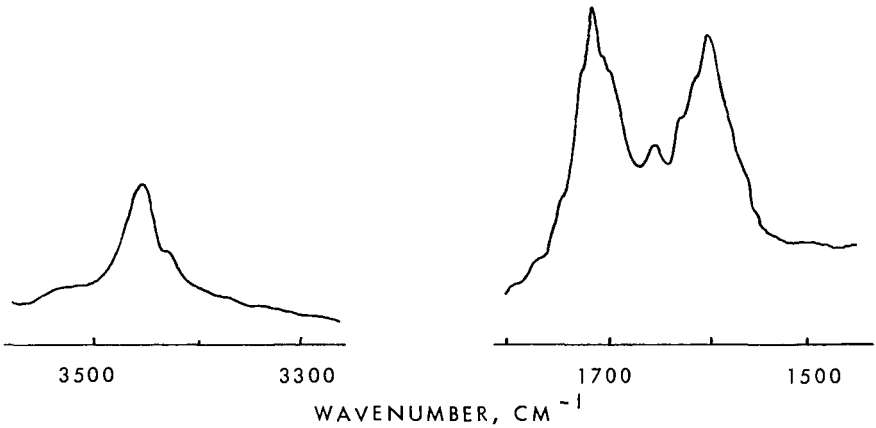

Figure 4 - PARTIAL INFRARED SPECTRUM OF NEUTRAL NITROGEN FRACTION

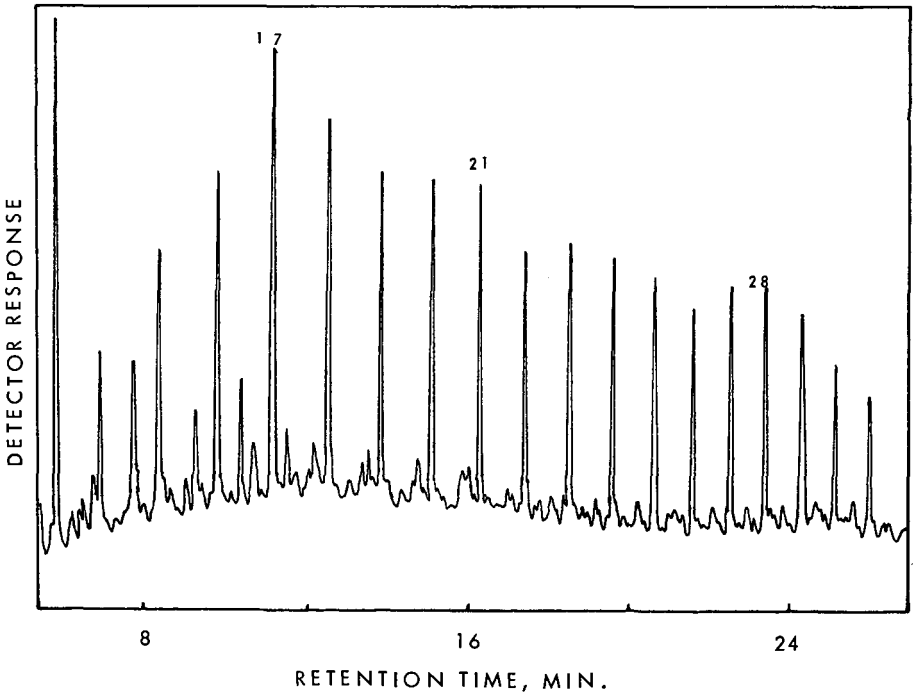

Figure 5 - GC CHROMATOGRAM OF SATURATE FRACTION

CO-Steam Process: Functional Group Analysis of Non-Distillables in Lignite-Derived Liquids

Bruce W. Farnum and Curtis L. Knudson

Grand Forks Energy Research Center
Grand Forks, North Dakota 58202

The CO-Steam process for conversion of lignite to boiler fuel consists of reaction of a finely ground slurry of lignite in hydrocarbon donor solvent with carbon monoxide and hydrogen at about 450° C and pressures up to 5000 psi (1). Recent studies at the Grand Forks Energy Research Center (GFERC) have utilized a preheated batch autoclave with gas and slurry phase sampling to establish optimum reaction conditions for reduction in molecular weight of the non-distillables in CO-Steam product (2,3). A study of the effect of the nature and quantity of non-distillables on coal liquid viscosity has pointed out the importance of reducing the quantity and molecular weight of non-distillables (4). This study also pointed out a relationship between weak acid concentration and percent oxygen in non-distillables, and product quality as indicated by solution viscosity.

CO-Steam products were separated into four fractions based on solubility in hexane, toluene, and tetrahydrofuran. The acidity of each fraction was determined by non-aqueous titration with tetramethyl ammonium hydroxide. The end point obtained indicated total oxygen acids (phenols) plus nitrogen acids (carbazoles). Table 1 lists the weight percent of each solubility fraction, and their measured acidities. Close agreement was obtained between measured acidities of total products and weighted sums of the acidities of the individual fractions. CO-Steam products A and B were produced in continuous reactors at Pittsburgh Energy Research Center using recycled CO-Steam oil as the slurry vehicle, while CO-Steam C was produced in our batch autoclave using 9:1 anthracene oil - tetralin as vehicle. Higher acidity of the oil fractions of A and B can be attributed to the buildup of phenols content during recycle of the solvent. Higher acidity of the other fractions of A and B can be partially explained by their higher molecular weight resulting from lower processing temperature. Figure 1 illustrates the relative acidity of the CO-Steam fractions in Meq H^+ per fraction per gram of total product.

CO-Steam products were separated by column chromatography on alumina into three fractions using a simplification of the method of Schiller and Mathiason (5). Fraction 1 (eluted by toluene) consisted of hydrocarbons, fraction 2 (eluted by chloroform, 1% ethanol) consisted primarily of nitrogen compounds, and fraction 3 (eluted by 9:1 tetrahydrofuran - methanol) consisted primarily of hydroxyl compounds as confirmed by mass spectrometry of the volatile constituents. Acid and base titrations confirmed the absence of acid-base reactivity in the hydrocarbon fractions. The nitrogen compound fractions were more acidic and more basic than the hydroxyl fractions, indicating the concentration of nitrogen acids and bases in fraction 2.

A matrix of parameters was developed to provide separate estimates of oxygen acids and nitrogen acids content from non-aqueous titration and elemental analysis data, regardless of mineral content of the sample. When applied to a set of SRCs and CO-Steam distillation residues, it was found that oxygen acids decreased linearly with molecular weight by gel permeation high pressure liquid chromatography, while nitrogen acids remained at a constant concentration (Figure 2). When model solutions were prepared from the SRCs and CO-Steam distillation residues with anthracene oil, it was found that log viscosity of 25 percent solutions decreased linearly with acidity due to oxygen acids, as well as total acidity in a parallel fashion. The constant difference in curves represents the unchanging concentration of nitrogen acids, despite the varying degree of depolymerization represented in the range of samples. These results imply that during coal

depolymerization: (1) the stable core of a preasphaltene or asphaltene molecule includes a carbazole, benzocarbazole, dibenzocarbazole or related nitrogen acid, and (2) extended processing to lower molecular weight (and thus lower viscosity) involves scission of bonds linking a phenolic oxygen acid to the stable core of the molecule. The calculation method is summarized as follows:

% Basic N = 1.4 B
% Acidic N = 100 N - 1.4 B
% Acidic O = 1.6 A - 16/14 (100 N - 1.4 B)
% Neutral O = 100 X - (1.6 A - 16/14 (100 N - 1.4 B))

where:

A = (meq acid/g sample) -- by non-aqueous titration.
B = (meq base/g sample) -- by non-aqueous titration.
N = (g nitrogen/g sample) -- by Kjeldahl method.
X = (g oxygen/g sample) -- by Neutron Activation Analysis.

Assumptions:

Neutral N = 0
Basic O = 0
Mineral content is neither acidic nor basic
N and O are not amphoteric

Analysis of the recycle solvents of these SRC samples indicated that the concentration of carbazole and its methylated derivatives remained essentially constant, while the concentration of phenol and its methylated derivatives increased sixfold between SRC I and SRC II process conditions (6). These results are consistent with the hypothesis presented here.

REFERENCES

1. Appell, H.R. and I. Wender. Div. Fuel Chem. preprints. Amer. Chem. Soc. 12 (3) 220 (1968).

2. Knudson, C.L., J.E. Schiller, and A.L. Ruud. Div. Fuel Chem. preprints. Amer. Chem. Soc. 22 (6) 49 (1977).

3. Sondreal, E.A., C.L. Knudson, J.E. Schiller, and T.H. May. Proc. Ninth Biennial Lignite Symposium, Grand Forks, ND, May 1977.

4. Schiller, J.E., B.W. Farnum, and E.A. Sondreal. Div. Fuel Chem. preprints. Amer. Chem. Soc. 22 (6) 33 (1977).

5. Schiller, J.E. and D.R. Mathiason. Anal. Chem. 49, 1225 (1977).

6. Schiller, J.E. Hydrocarbon Processing 56, 147 (1977).

Table 1. Properties of Solubility Fractions of CO-Steam Products

CO-Steam Product	A		B		C	
Solubility fractions	Wt. %	MW	Wt. %	MW	Wt. %	MW
Oil (hexane soluble)	55.9	403	48.7	385	52.3	281
Asphaltene (toluene soluble hexane insoluble)	22.6	554	18.4	542	22.8	345
Preasphaltene (THF soluble toluene insoluble)	20.9	747	17.9	611	4.7	501
Tetrahydrofuran insoluble	0.6	---	15.0	---	20.2	---
Process Temp. (°C)	425		450		470	
Acidity (Meq H^+/g):						
Oil	1.587		1.361		0.513	
Asphaltene	1.945		2.449		0.873	
Preasphaltene	1.974		2.052		1.058	
THF insoluble	1.518		1.027		0.266	
Total Product	1.729		1.725		0.544	
Calculated Acidity[a]	1.748		1.635		0.571	

[a] Acidity calculated as the weighted sum of the acidities of the individual fractions.

Table 2. Acid-Base Content of Column Chromatography Fractions

	CO-Steam A		CO-Steam B	
	Acidity (Meq/g)	Basicity (Meq/g)	Acidity (Meq/g)	Basicity (Meq/g)
1. Hydrocarbons	0	0	0	0
2. N Fraction	---	0.724	3.687	0.942
3. OH Fraction	2.98	0.217	2.806	0.216

Table 3. Acid-Base Properties of Non-Distillables

Sample	Acidity (Meq/g)	Pct O	Basicity (Meq/g)	Pct N	Pct N Basic	Pct N Acidic	Pct O Acidic	Pct O Neutral
SRC 115	1.481	1.55	0.711	1.70	0.995	0.718	1.55	0
CO-Steam Residue B	1.938	3.72	0.476	1.23	0.67	0.56	2.46	1.26
CO-Steam Residue A	1.661	7.03*	0.449	1.15	0.63	0.52	2.07	4.96*
SRC 308	2.285	4.32	0.786	1.78	1.10	0.68	2.88	1.44
SRC 122	2.531	4.69	0.713	1.55	1.00	0.55	3.42	1.27

* Not deashed; illustrates mineral oxygen.

Figure I.

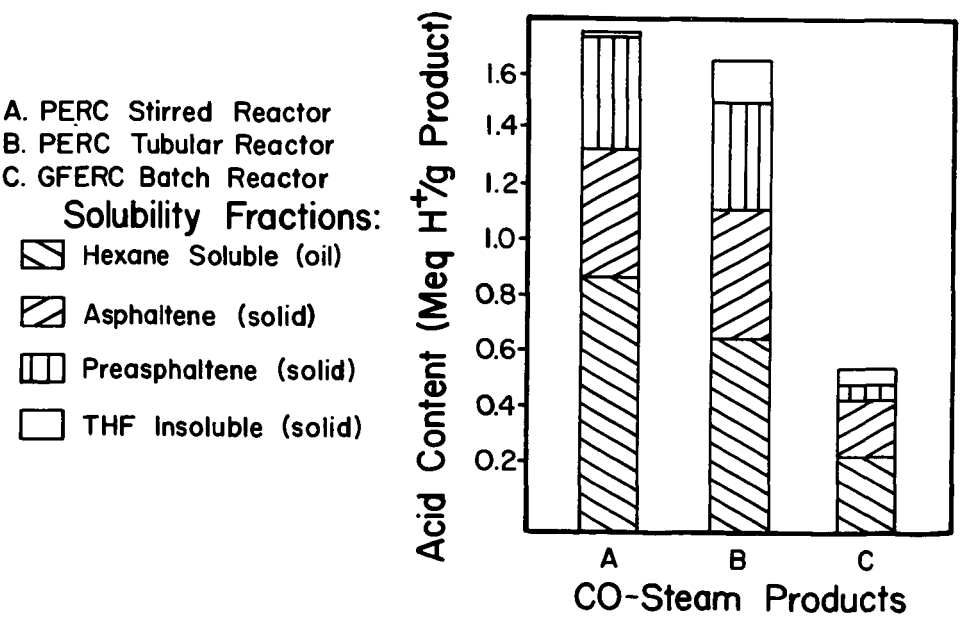

FIGURE 2

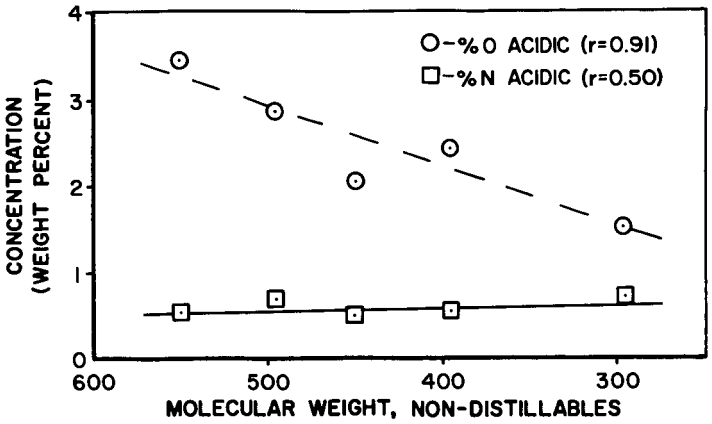

FIGURE 3

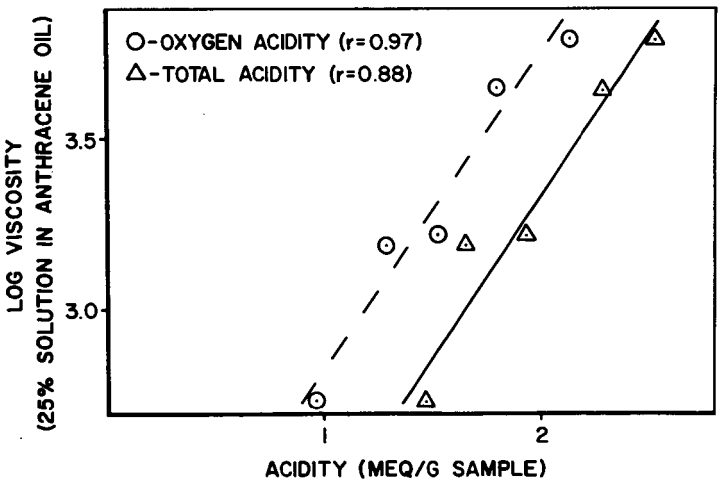

LIQUID CHROMATOGRAPHIC CHEMICAL CLASS ANALYSIS OF BITUMEN AND HEAVY PETROLEUM CRUDES

C. Reichert and L. Grant
Oil Sands Research Centre
Alberta Research Council
Edmonton, Alberta T6G 2C2

INTRODUCTION

The importance of bitumen and heavy crudes is steadily increasing as reserves of conventional crudes diminish around the world producing an increased emphasis upon the development of methods of recovery for bitumens and heavy crudes. Because of the extremely high viscosities encountered, a variety of novel in-situ recovery methods using combinations of steam, solvents, surfactants, and combustion are being investigated.

Conventional and heavy petroleum crudes consist of a large variety of organic molecules generally classified into four major groups identified as saturates, aromatics, resins and asphaltenes. Each of these classes have individual uses and their relative ratios determine the upgrading processes employed. Bitumen and heavy crudes tend to have larger proportions of resins and asphaltenes that are less economically converted to usable products. Precipitation of asphaltenes in the formation or production of asphaltenes from other compounds can occur during the recovery process necessitating some monitoring of process streams for changes in the relative ratios of these classes of compounds.

Numerous methods are used to separate petroleum hydrocarbons into their type and classes. The most common method utilizes pentane precipitation of the asphaltenes in a procedure similar to ASTM D 893-69. A variety of procedures (1-6) are employed for the subsequent fractionation of the remaining oil. Many of the procedures for the separation of the aromatics and saturates using silica and/or alumina columns are modifications of ASTM D 2549-75. Some of the methods achieve separations into subgroupings such as monoaromatics, diaromatics, polyaromatics and polar compounds.

Each of the procedures however has the disadvantage that a total class analysis requires several steps and to obtain the data regarding the distribution of the fractions requires several days.

The procedure discussed here enables the separation of the bitumen or heavy petroleum crude into three groupings namely asphaltenes, resins and a mixture of aromatics and saturates with no prior separation of the polar constituents or of backflushing of the columns. Using a 254 nm UV detector it is possible to quantify each of the fractions in the bitumen.

EXPERIMENTAL

The liquid chromatograph used in this study was a Varian Model 8500 dual syringe pump instrument equipped with a Varian Aerograph 254 nm UV detector connected to a Varian CDS 111 Data System. The columns used were a 25 cm Varian Aerograph Micropak CH-10 connected in series with a 25 cm Varian Aerograph Micropak CN-10.

Two mobile phase systems can be used to achieve the separation. One system employed 99% methanol-1% isopropanol for 4 minutes, 40% of the 99% methanol-1% isopropanol mixture-60% tetrahydrofuran for 10 minutes and finally 100% THF for 10 minutes. The second system used 90% acetonitrile-10% water for 5 minutes followed by 50% acetonitrile mixture-50% methylene chloride for 10 minutes followed finally by 100% methylene chloride for 10 minutes. Separation achieved by the two methods is comparable and is accomplished in 25-30 minutes using a flow rate of 60 cc/hr.

The bitumen/heavy crude samples are dissolved in methylene chloride at a concentration of 10-20 mg/ml with 2-5 µl of sample being injected on the columns.

DISCUSSION AND RESULTS

Figure 1 shows a typical chromatogram of the separation of saturates and aromatics, resins, and asphaltenes in samples of Athabasca Bitumen. Superimposed on the chromatogram is a plot of the change in the solvent gradient during the analysis.

Chromatograms of aromatics and resins material obtained by separation on passage through attapulgus clay and silica-alumina columns successively are given in Figures 2 and 3 respectively. The chromatograms show that the aromatics produced by column chromatography contain material that we classified as resins by this procedure while the resin samples contain some aromatic material and also some asphaltene material. A chromatogram of an asphaltene sample obtained by pentane precipitation is given in Figure 4 which shows the presence of a resins peak. It is evident from these chromatograms that a very similar fractionation of the bitumen is obtained in our HPLC method as compared to the conventional column separation. Saturates material in the bitumen is eluted with the aromatics fraction however since saturates absorption at 254 nm is negligible they are not detected. By evaluation of the amount of aromatics, resins and asphaltenes the percentage of each of the four fractions in a bitumen sample can be determined.

CONCLUSIONS

The HPLC method discussed in this paper achieves a separation of bitumen into its class components i.e., asphaltenes, resins and mixture of aromatics and saturates, in proportions comparable to that obtained in classical separation by asphaltene precipitation with pentane and subsequent successive passage through attapulgus clay and silica alumina columns.

ACKNOWLEDGMENT

This study was funded by the Alberta Oil Sands Technology and Research Authority.

LITERATURE CITED

(1) G.L. Brown and A.L. Jones, Hydrocarbon Processing Petrol Refiner, 39, 156 (1960).

(2) J. Coleman, J.E. Dooly, D.E. Hirsch and C.J. Thompson, Analytical Chemistry, 45, 1724 (1973).

(3) H. Sawtzky, A.E. George, G.T. Smiley and D.S. Montgomery, Fuel, 54, 16 (1976).

(4) G.N. Pozdnyshev, R.I. Masurov and R.M. Ruchkina, Chemical Technology of Fuel and Oils, 10, 806 (1974).

(5) J.C. Suatoni and H.R. Garber, J. Chromatog, Science, 14, 546 (1976).

(6) U.S. Bureau of Mines, API-RP-60 (1974).

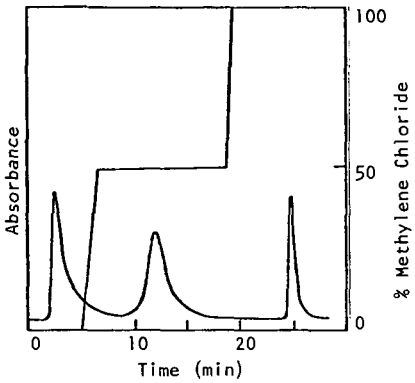

FIGURE 1 Chromatogram of Toluene Extracted Bitumen

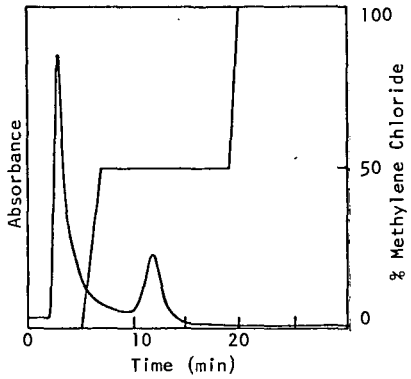

FIGURE 2 Chromatogram of an Aromatics Fraction Separated on Silica-Alumina

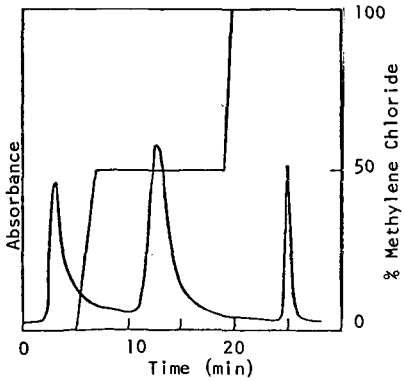

FIGURE 3 Chromatogram of a Resins Fraction Separated on Attapulgus Clay

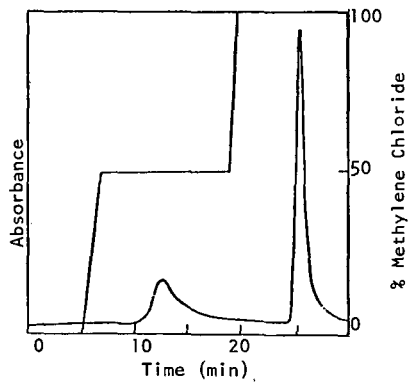

FIGURE 4 Chromatogram of an Asphaltene Fraction Precipitated by Pentane

COMPARISON OF METHODS FOR DETERMINING ASPHALTENES IN COAL-DERIVED LIQUID FUELS

H. Schultz and M. J. Mima

DEPARTMENT OF ENERGY
PITTSBURGH ENERGY RESEARCH CENTER
4800 Forbes Avenue
Pittsburgh, Pennsylvania 15213

There is at present no standard method for the determination of asphaltenes in the products of coal conversion, nor is there any known relationship between the values for asphaltene concentration produced by the various analytical methods currently in use. Lacking a standard method of analysis, are comparisons of the coal conversion products of the various processes possible? The research described in this paper attempts to answer this question at least in part.

Five different solvent separation methods which are currently in use for determining asphaltenes in coal-derived liquids have been studied in the analytical chemistry laboratory of the Pittsburgh Energy Research Center of the U. S. Department of Energy. The material chosen for the tests was a liquid product which was produced from the Center's 0.5 ton-per-day hydrodesulfurization plant. The material was produced using a fixed-bed cobalt-molybdenum catalyst, 4,000 psi hydrogen, and a temperature of 450 °C. The Homestead, Kentucky coal was slurrried in coal-derived oil (35% by weight coal) and fed to the plant at 25 pounds per hour. A single sample of the liquid product was taken, separated into five portions, and stored in the refrigerator under nitrogen.

Twenty replicate determinations of asphaltenes were made with each test method, relying not only on written procedures but also on personal contacts with the authors of each method. Data collected include weight percent asphaltenes, insolubles, and oils. Standard deviations were calculated for each method and statistical comparisons made between methods.

The following are short descriptions of the five procedures studied:

Method A: A ten-gram sample is extracted with benzene in a Soxhlet apparatus. The benzene is removed on a steam bath, and 5 ml. of benzene are added to the residue. Asphaltenes are precipitated with 250 ml of n-pentane, and separated by filtration through the paper.

Method B: A three-gram sample is frozen and pulverized in liquid nitrogen and n-pentane is added. The sample is mixed and crushed while in an ultrasonic bath, and then centrifuged. The supernatant liquid is decanted into a rotary evaporator flask and the pentane washing procedure and centrifugation repeated three times. The combined supernatant solutions are then evaporated with nitrogen to recover the oil. Benzene is added to the insoluble material in the centrifuge tubes and the mixing, sonication, and centrifugation are carried out in the same manner as with the n-pentane. The supernatant benzene solutions are combined, evaporated under nitrogen, and finally freeze-dried to obtain the asphaltenes.

Method C: A three-gram sample is extracted under nitrogen with toluene in a Soxhlet apparatus. The toluene is removed from the extract in a rotary evaporator using a water aspirator. Exactly two ml of toluene per gram of soluble material are added

and the asphaltenes are precipitated with a volume of n-pentane equal to twenty times the volume of toluene that was added. The precipitate is then extracted with n-pentane in a Soxhlet apparatus.

Method D: Ten grams of sample are mixed with benzene, stirred for 30-60 minutes at 30 °C, and centrifuged. The benzene solution is decanted and the residue is washed with fresh benzene four times. The solvent is stripped from the combined supernatant liquid in vacuo at 30 °C, and finally the material is freeze-dried. The residue is dissolved in five ml. of benzene and the asphaltenes are precipitated with a liter of hexane. The solids are separated by centrifugation, the supernatant is stripped of hexane, and the precipitation procedure is repeated. The supernatants are combined and stripped as before, and the asphaltenes are freeze-dried.

Method E: A 25-gram sample is refluxed with benzene. The supernatant liquid is centrifuged and then filtered through paper under cover of nitrogen. The residue in the centrifuge tubes is refluxed with benzene, centrifuged, and filtered three more times. The collected extracts are evaporated under vacuum in a rotary evaporator at 105 °F. Cyclohexane is added to precipitate the asphaltenes and the mixture is refluxed under nitrogen. Centrifugation and filtration are carried out as above and are repeated once or twice depending on the color of the supernatant liquid. The reflux flask, centrifuge bottles, and filter paper are dried in vacuo and weighed to obtain the weight of the asphaltenes.

Table 1 shows the results obtained with the first three methods described above:

Table 1. - Results with Methods A, B, and C

	% Insolubles ±1s	% Asphaltenes ±1s	% Oils ±1s
Method A	5.2 ±0.3	26.9 ±0.7	67.9 ±0.7 (by difference)
Method B	7.6 ±0.5	23.8 ±0.7	67.2 ±0.9
Method C	4.6 ±0.5	22 ±2	70 ±3

The data indicate that the relative standard deviations for asphaltenes range from 2.6 to 6.8%, well within the range of acceptability for a separation procedure for coal-derived materials. There was considerable variation between methods in the length of time necessary to complete an analysis, in the amount of time expended by the analyst, and in the production rate.

In order to determine if the analytical results produced by each of the methods were significantly different, Student's 't' test was applied to the average of the 20 replicate analyses. Table 2 shows the findings obtained with the first three methods.

Table 2. - Significance* of Differences Between Methods

Methods Compared	Insolubles	Asphaltenes	Oils
A vs. B	Significant	Significant	Not significant
A vs. C	Significant	Significant	Not significant
B vs. C	Significant	Not significant	Not significant

*Student's 't' test - at the 95% confidence level.

It is evident that in half the comparisons made the difference proved to be significant. From the results obtained in this study one can surmise that the conclusions drawn from the comparison of the analyses of coal-derived liquids produced by different analytical procedures are problematical at best. One can also conclude that some acceptable "standard" method for the determination of asphaltenes in coal-derived liquids is urgently needed.

Environmental Aspects of the HYGAS Process

L. J. Anastasia, W. G. Bair, D. P. Olson

Institute of Gas Technology
3424 South State Street
Chicago, Illinois 60616

As part of the development of second-generation coal gasification processes, the U. S. Department of Energy has commissioned an environmental assessment of the HYGAS process. The objective of this assessment is to establish systems for sampling, analysis, and data evaluation to determine the fate of potential pollutants generated during operation of the HYGAS pilot plant and to apply these data to demonstration and commercial plant designs.

HYGAS operates at high temperatures to obtain high reaction rates and at high pressure to increase the equilibrium methane yield. The most reactive coal fraction is hydrogasified to form methane while the less reactive fraction remains in the coal char and is used to generate hydrogen and heat. Of the total methane formed in the process, about 64% to 70% is formed in the gasifier.

Figure 1 shows the current processing steps in the HYGAS pilot plant. Lignite and subbituminous coals do not require pretreatment. However, with a caking coal such as Illinois No. 6 bituminous, a pretreatment step is used to destroy any agglomerating tendencies. The pretreatment is a mild surface oxidation carried out in a fluidized bed at 700° to 800°F and slightly above atmospheric pressure. For introduction into the high-pressure gasifier, up to 45 wt % coal is mixed in a light oil slurry which is pressurized with reciprocating piston pumps. Entrained solids in the crude gas which leave the gasifier are removed with a cyclone. Then the gas is quenched to condense steam and light oil. Next, water and oil are separated, recovered, and recycled. Acid gases (H_2S and CO_2) are removed from the product gas with a diglycolamine-water solution which is regenerated and recycled. The product gas is further cleaned to reduce sulfur levels to <0.1 ppm. Then methanation is carried out in a packed-bed of nickel catalyst pellets sensitive to sulfur poisoning. The methanation step upgrades the product gas to essentially pure methane (SNG).

PILOT PLANT HYDROGASIFIER REACTOR

The hydrogasifier reactor vessel is shown schematically in Figure 2. The reactor vessel has four internally connected fluidized-bed contact stages which operate at 1000 psig, with different temperatures in the various fluidized beds. The reactor is designed to accept 3 ton/hr coal feed and to produce 1.5 x 10^6 SCF/day of pipeline-quality gas.

The feed slurry is introduced into the upper fluidized bed (the slurry-drying bed) which operates at 600°F. The dried coal flows by gravity into a vertical lift line where the first stage of hydrogasification occurs. Here, coal particles are heated by hot gases from the lower stage, and hydrogen contained in the gases reacts with about 20% of the coal to produce methane.

The partially reacted coal (now called a char) then flows to the second-stage gasifier and is further gasified by the steam and hydrogen-rich gas rising from the steam-oxygen gasification stage below. About 25% of the original coal is converted in this reaction stage, making the total conversion about 45% in the first and second stages of hydrogasification. The char then flows to the final reactor stage where steam and oxygen are introduced to convert the char to

hydrogen and carbon oxides and to provide the necessary heat for operation of the gasifier during self-sustained steady plant operation.

SAMPLE COLLECTION

Sampling of pilot plant streams specifically for environmental assessment began with Test 55 with Montana subbituminous coal. Process water streams were sampled every 8 hours and three of these samples were composited to represent 24 hours of plant operation. Water samples were analyzed for total dissolved solids (TDS), total suspended solids (TSS), total organic carbon (TOC), total phenols, total sulfur, ammonia, cyanide, thiocyanate, sulfide, chloride, and oil. Solids samples were collected once per day and analyzed for sulfur species and trace elements. The solids streams sampled included the coal feed, the first and second stages of gasification, and the spent char. Samples of oils in the coal feed slurry were also taken once per day to determine organic compositions using a gas chromatograph mass spectrometer.

HYGAS WATER COMPONENTS

Before the environmental assessment program began with subbituminous coal, HYGAS tests were carried out with both Montana lignite and Illinois No. 6 bituminous coals. In these tests, a single water sample was taken once every 24 hours. Process engineering data from these tests have been examined to determine the water compositions corresponding to periods of self-sustained, steady operation and to normalize pollutant generation to a uniform basis for the three types of coal.

Compositions of the gasifier feed coals used to calculate pollutant generation in HYGAS Test 37 with Montana lignite, Tests 46 and 54 with Illinois No. 6 bituminous, and Test 55 and 58 with Montana subbituminous are given in Table 1. These compositions were derived from the routine ultimate and proximate analyses made during operation of the HYGAS plant and correspond to the coal feeds when the water samples were taken. Carbon conversions in these HYGAS tests ranged from 44% to 88%. Complete carbon conversion was not one of the objectives in these HYGAS tests; consequently, interpretation of this pollutant data is subject to the constraint that more complete carbon conversion will be obtained in future pilot plant tests.

Effluent production in the quench condensate slurry (from the water quenching of the gasifier crude product gas) is reported in Table 2 as a function of coal type and carbon in the feed on a moisture and ash-free basis (MAF). This stream is a major source of pollutants and has a relatively high water inventory (~2600 gallons) which generally contributes to more precise analytical results. Each of the pollutants was correlated with the carbon in the feed by a linear regression analysis, and the linear correlation coefficients are also given in Table 2. The correlation coefficients were then tested for significance from zero using Fisher's Z test with a two-sided probability at 95% confidence and (n–2) degrees of freedom. According to this test, the strongest significance from zero (77%) is the effect of carbon in the feed on thiocyanate, while the weakest significance (50%) is the effect of carbon on ammonia. What is perhaps most interesting is the negative slopes (meaning pollutant production is inversely proportional to carbon content in the feed) for all pollutants except sulfide and ammonia. This result occurs primarily because of the influence of pretreatment on the bituminous coals, which lowers the levels of total dissolved solids, phenol, total organic carbon, thiocyanate, and total sulfur in the gasifier quench condensate. Significant quantities of these pollutants were found in the pretreater quench waters. The sulfides and ammonia however, appear to be generated primarily in the gasifier.

Table 3 presents the results of linear regression analyses for feed constituents other than carbon and their effect upon selected pollutants in the crude gas quench. These analyses include oxygen on phenol, sulfur on sulfide and thiocyanate, nitrogen on ammonia and thiocyanate, and hydrogen on phenol and ammonia. The regression analysis for hydrogen in the coal feed on phenol production in the gasifier gave the strongest indication of a linear correlation. The correlation coefficient for this regression was 0.921 with a significance from zero of 85%. About 40% of the total phenol from bituminous coal was produced during pretreatment, which appeared to significantly reduce phenol production in the gasifier. Total phenols produced with bituminous coals were 2.9 lb/ton feed (MAF) in Test 46 and 5.6 lb/ton feed (MAF) in Test 54. This total was much less than the phenol production of 11.2 lb/ton feed (MAF) with lignite coal (Test 37) and approximately 16 lb/ton feed (MAF) with subbituminous coal (Tests 55 and 58).

HYGAS OIL COMPONENTS

A net make of light oil (benzene, toluene, and xylene) is produced in the HYGAS process and toluene is used in the pilot plant to represent this product. Coal feed is slurried with the oil for introduction into the high-pressure gasifier. Essentially all the oil is recycled by recovery from the product gas quench condensate and the product gas cyclone slurry. Toluene is added only for losses which are specific to the pilot plant, i.e., pump seals, storage tanks, vent gases, and vapor in product gas. The oil used in the coal feed slurry represents a concentrated source of polynuclear aromatics, potential carcinogens, and potentially toxic organic compounds. Consequently, it is necessary to screen the chemical composition of this oil for possible health and safety hazards. As each HYGAS test progresses, this oil changes in composition as a function of operating time and gasification conditions. Presumably, equilibrium compositions will be reached under extended steady-state conditions.

Compositions for oil samples taken during HYGAS Test 37 using lignite coal and Test 58 using subbituminous coal are shown in Table 4. The differences in compositions for the heavier three-, four-, and five-ring compounds may be due to the type of coal, to plant operation, and possibly other factors. The presence of many compounds in the initial samples occurs because the plant oil inventory of ~6000 gal remaining after one test is reused for coal slurry in the subsequent test.

Phenol composition is important because of the effects various water-soluble phenols may have on biosystems designed for wastewater cleanup. Phenols in the feed coal-oil slurry with lignite coal are characterized as major fractions, 40% each, C_1- and C_2-phenols (where C represents the methyl or alkyl groups, i.e., isomers were not separated) and 10% each for phenol and C_3-phenols. With the subbituminous coal, the major phenolic fractions consisted of C_1-, C_2-, and C_3-phenols (approximately 30% each) with minor fractions of phenol and C_4-phenols (about 10% each) and about 1% C_5-phenols.

HYGAS SOLIDS COMPOSITION

During gasification, transformation and elimination of sulfur from one class of compounds to another occurs as the coal chars move through the various gasification stages. For the subbituminous coal used in Test 58, about 91% of the total sulfur entered the gasifier as organic and pyritic sulfur in the coal feed. In the gasifier, sulfide sulfur increased significantly in the presence of hydrogen (from 1.2% in feed coal to 25% of total sulfur in first-stage char) while the remaining sulfur species all decreased. Table 5 lists the quantities

of each sulfur class during gasification. The normalized data, based upon 100 lbs of coal feed, show that the bulk of the sulfur (approximately 70%) is reacted during the first stage of gasification and that lesser amounts of 12% each are reacted in the second-stage and in the steam-oxygen bed. Overall, about 70% of the sulfide and sulfate species were gasified along with 95% of the organic and pyritic sulfurs for an overall sulfur removal of 92% from the coal feed to the spent char.

The trace elements in solids obtained from gasification of subbituminous coal during Test 55, can be split into several categories according to the quantities found in the feed coal as compared to those found in the spent char.

- Group 1: 90% to 100% recovery in the ash — Be, V, Mn, Zn, Li, Cr, Pb
- Group 2: 50% to 90% recovery in the ash — Fe, Ba, As, B, F, Tl, Ni, Cu, Mo
- Group 3: Less than 50% recovery in the ash — Cl, Se, Cd, Hg.
- Elements primarily released from char in the steam-oxygen zone — Fe, As, Se, Tl, Ni, Cu, Cd, Mo
- Elements primarily released from char in first and second stages of gasification — Ba, B, Cl, F, Hg
- Elements in chars from first and second stages of gasification with higher concentrations than in the feed coal — Fe, Tl, Ni, Cu, Cd, Pb, Mo, Cr.

For the latter group of elements, material balances indicated that $\geq$130% existed in gasifier chars compared with the feed coals. Two of these elements, Pb and Cr, showed essentially no net disappearance from coal feed to char ash. For three elements, Pb, Mo, and Cd, 208%, 247%, and 262%, respectively, of coal feed input was found in the upper stages of gasification. With the exception of As and Se, all of the elements released primarily in the steam-oxygen zone showed an increased concentration in chars from the upper stages of gasification. The trace element distribution reported here may have resulted from the large temperature differences used in the various zones of the reactor and in this respect, the HYGAS reactor is not unique but is comparable to other industrial processes (power plants, steel plants, and other coal gasification reactors) where large temperature gradients exist. Moreover, these trace element data represent a single test of the gasifier and additional testing is required to determine "average" distributions and also the ultimate fate of the trace elements.

Table 1. COAL COMPOSITIONS USED IN EFFLUENT ANALYSES FOR SELECTED HYGAS TESTS

Test No.:	37		46		54		55		58	
Type of Coal Feed:	Montana Lignite		Pretreated Ill. No. 6		Pretreated Ill. No. 6		Rosebud Subbituminous		Rosebud Subbituminous	
Number of Samples:	12		7		23		5		12	
	$\bar{x}$	$s_{\bar{x}}$*	$\bar{x}$	$s_{\bar{x}}$	$\bar{x}$	$s_{\bar{x}}$	$\bar{x}$	$s_{\bar{x}}$	$\bar{x}$	$s_{\bar{x}}$
	wt %									
Proximate Analysis										
Moisture	14.98	0.27	1.74	0.08	1.82	0.04	10.50	0.42	10.39	0.20
Ash	9.97	0.17	9.89	0.27	9.89	0.11	8.54	0.16	8.48	0.05
Volatile Matter	36.02	0.09	20.16	0.57	20.37	0.07	34.44	0.19	34.21	0.10
Fixed Carbon	39.03	0.16	68.21	0.43	67.91	0.12	46.52	0.21	46.92	0.13
Ultimate Analysis										
Carbon	61.35	0.16	74.44	0.31	74.27	0.10	67.12	0.22	67.55	0.05
Hydrogen	4.21	0.03	3.26	0.05	3.50	0.02	4.49	0.01	4.40	0.02
Nitrogen	0.99	0.01	1.85	0.02	1.74	0.01	0.93	0.01	0.93	0.01
Sulfur	0.84	0.02	2.41	0.11	2.10	0.02	0.96	0.04	0.92	0.01
Ash	11.71	0.17	10.06	0.28	10.07	0.11	9.54	0.14	9.47	0.06
Oxygen	20.90	0.14	7.98	0.43	8.32	0.07	16.96	0.20	16.73	0.08

*$s_{\bar{x}} = s/\sqrt{n}$ where s = standard deviation = $[\Sigma(x-\bar{x})^2/(n-1)]^{1/2}$.

A77041114

Table 2. EFFECT OF CARBON IN COAL FEED ON POLLUTANTS IN PRODUCT GAS QUENCH CONDENSATE STREAM FOR HYGAS REACTOR

Test 37: Montana Lignite
Tests 46, 54: Pretreated Illinois No. 6 Bituminous
Tests 55, 58: Montana Subbituminous (Rosebud)

Test	Carbon in Feed, wt %[a]	Total Dissolved Solids		Phenol		Total Organic Carbon		Thiocyanate		Sulfide		Ammonia		Total Sulfur	
		$\bar{x}$	$s_{\bar{x}}$[b]	$\bar{x}$	$s_{\bar{x}}$	$\bar{x}$	$s_{\bar{x}}$	$\bar{x}$	$s_{\bar{x}}$	$\bar{x}$	$s_{\bar{x}}$	$\bar{x}$	$s_{\bar{x}}$	$\bar{x}$	$s_{\bar{x}}$
		lb/ton feed (MAF)													
37	69.5	4.31	0.24	5.22	0.30	9.97	0.53	0.88	0.11	0.28	0.013	9.28	0.52	--	--
46	82.8	0.98	0.12	0.26	0.10	0.35	0.06	0.032	0.01	0.52	0.19	13.0	2.64	0.62	0.16
54	82.6	1.94	0.13	2.28	0.10	1.78	0.38	0.17	0.01	1.30	0.10	12.0	1.35	1.01	0.20
55	74.2	6.54	1.05	11.5	0.44	22.0	0.82	1.15	0.07	0.32	0.04	12.5	0.97	5.11	2.27
58	74.6	4.50	1.30	10.0	0.92	7.60	0.82	0.48	0.04	0.43	0.06	13.8	1.20	2.91	0.35
Linear Correlation Coefficient,[c] r		−0.782		−0.653		−0.659		−0.836		0.722		0.517		−0.912	
Significance[d] From Zero, %		72.4		61.6		62.1		77.0		67.4		49.6		63.3	

[a] Moisture- and ash-free (MAF) basis.

[b] $s_{\bar{x}} = s/\sqrt{n}$ where s = standard deviation = $[\Sigma(x-\bar{x})^2/(n-1)]^{1/2}$.

B77041132

[c] Perfect linear correlation is indicated at $r = \pm 1$; linear independence is indicated at $r = 0$.

[d] Using Fisher's Z test, two-sided T[0.95, (n − 2)DF].

Table 3. EFFECT OF COMPONENTS IN COAL FEED ON POLLUTANTS FOUND IN PRODUCT GAS QUENCH CONDENSATES FOR HYGAS TESTS 37, 46, 54, 55, AND 58

Regression[a]	Linear Correlation Coefficient,[b] r	Significance[c] From Zero, %
Oxygen on Phenol	0.676	--[d]
Sulfur on Sulfide	0.640	60.4
Sulfur on Thiocyanate	−0.855	78.7
Nitrogen on Ammonia	0.151	15.0
Nitrogen on Thiocyanate	−0.856	78.7
Hydrogen on Phenol	0.921	84.8
Hydrogen on Ammonia	−0.156	15.6

[a] Elements in coal feed (MAF) on pollutant levels (reported in Tables 1 and 2).

[b] r = 1 for perfect linear correlation, and r = 0 for linear independence.

[c] Using Fisher's Z test, two-sided T[0.95, (n − 2)DF].

[d] Oxygen in coal determined by difference; therefore, only 2 degrees of freedom and a very low significance.

A77040520

Table 4. COMPOSITION OF LIGHT OIL IN COAL FEED SLURRY TO HYGAS REACTOR
HYGAS TEST 37 USING MONTANA LIGNITE FEED
HYGAS TEST 58 USING MONTANA SUBBITUMINOUS FEED

Test No.	37		58	
Sample Age (Days of Plant Operation)	1	12	2	12
	wt %			
Aliphatics	0.49	1.08	6.85	7.27
Benzene	1.37	6.94	5.13	7.10
Toluene	94.9	85.2	71.3	69.8
C_2-C_5 Benzenes	0.98	1.90	3.98	3.98
Indenes	0.041	1.41	0.25	0.27
Indanes	--	--	1.27	1.02
Phenols	0.20	1.14	3.80	2.44
Napthalenes	0.62	1.65	4.47	5.00
Biphenyls	0.077	0.086	0.30	0.28
Acenaphthenes	0.020	0.11	0.11	0.11
Acenaphthalenes	--	--	0.10	0.092
Fluorenes	0.06	0.11	0.49	0.35
Phenanthrenes/Anthracenes	--	--	0.44	0.44
Pyrene	0.013	0.027	0.059	0.029
Flouranthenes	--	--	0.12	0.089
Benzofluorenes	--	--	0.006	0.003
Benzoflouroanthene	--	--	0.005	0.016
Benzo-Pyrene	--	--	0.005	0.002
Furans	--	--	0.62	0.67
Miscellaneous & Unknowns	1.22	0.34	0.67	0.90
Totals	99.99	100.0	99.98	99.86

Table 5. GASIFICATION OF SULFUR BY SPECIES DURING HYGAS TEST 58
USING ROSEBUD SUBBITUMINOUS COAL

From HYGAS Routine Ultimate Analyses*	Coal Feed	First-Stage Gasification	Second-Stage Gasification	Spent Char	
No. of Samples:	63	22	20	85	
	wt %				
Ash	9.48 ± 0.055	18.19 ± 0.71	23.61 ± 1.41	28.45 ± 0.68	
Sulfur	0.91 ± 0.012	0.48 ± 0.07	0.40 ± 0.08	0.16 ± 0.003†	
Sulfur Species	lb S/100 lb Coal Feed				Sulfur Gasified Spent Char/Feed, %
Sulfide	0.01	0.062	0.052	0.003	70.0
Sulfate	0.06	0.031	0.034	0.020	66.7
Organic	0.45	0.125	0.070	0.030	93.3
Pyritic	0.29	0.036	0.006	0.010	96.6
Sum	0.81	0.255	0.162	0.063	
Total Sulfur Gasified, %	0	68.5	80.0	92.2	

* Limits shown are 95% confidence levels determined by $(\bar{x} \pm \frac{1.96\sigma}{\sqrt{n}})$. Data are from normal HYGAS operations.

† 70 samples involved in sulfur analysis.

A77020324

Table 4. COMPOSITION OF LIGHT OIL IN COAL FEED SLURRY TO HYGAS REACTOR
HYGAS TEST 37 USING MONTANA LIGNITE FEED
HYGAS TEST 58 USING MONTANA SUBBITUMINOUS FEED

Test No.	37		58	
Sample Age (Days of Plant Operation)	1	12	2	12
	wt %			
Aliphatics	0.49	1.08	6.85	7.27
Benzene	1.37	6.94	5.13	7.10
Toluene	94.9	85.2	71.3	69.8
C_2-C_5 Benzenes	0.98	1.90	3.98	3.98
Indenes	0.041	1.41	0.25	0.27
Indanes	--	--	1.27	1.02
Phenols	0.20	1.14	3.80	2.44
Naphthalenes	0.62	1.65	4.47	5.00
Biphenyls	0.077	0.086	0.30	0.28
Acenaphthenes	0.020	0.11	0.11	0.11
Acenaphthalenes	--	--	0.10	0.092
Fluorenes	0.06	0.11	0.49	0.35
Phenanthrenes/Anthracenes	--	--	0.44	0.44
Pyrene	0.013	0.027	0.059	0.029
Flouranthenes	--	--	0.12	0.089
Benzofluorenes	--	--	0.006	0.003
Benzoflouroanthene	--	--	0.005	0.016
Benzo-Pyrene	--	--	0.005	0.002
Furans	--	--	0.62	0.67
Miscellaneous & Unknowns	1.22	0.34	0.67	0.90
Totals	99.99	100.0	99.98	99.86

Table 5. GASIFICATION OF SULFUR BY SPECIES DURING
HYGAS TEST 58 USING ROSEBUD SUBBITUMINOUS COAL

From HYGAS Routine Ultimate Analyses*	Coal Feed	First-Stage Gasification	Second-Stage Gasification	Spent Char	
No. of Samples:	63	22	20	85	
	wt %				
Ash	9.48 ± 0.055	18.19 ± 0.71	23.61 ± 1.41	28.45 ± 0.68	
Sulfur	0.91 ± 0.012	0.48 ± 0.07	0.40 ± 0.08	0.16 ± 0.003†	
Sulfur Species	lb S/100 lb Coal Feed				Sulfur Gasified Spent Char/Feed, %
Sulfide	0.01	0.062	0.052	0.003	70.0
Sulfate	0.06	0.031	0.034	0.020	66.7
Organic	0.45	0.125	0.070	0.030	93.3
Pyritic	0.29	0.036	0.006	0.010	96.6
Sum	0.81	0.255	0.162	0.063	
Total Sulfur Gasified, %	0	68.5	80.0	92.2	

* Limits shown are 95% confidence levels determined by $(\bar{x} \pm \frac{1.96\sigma}{\sqrt{n}})$. Data are from normal HYGAS operations.

† 70 samples involved in sulfur analysis.

A77020324

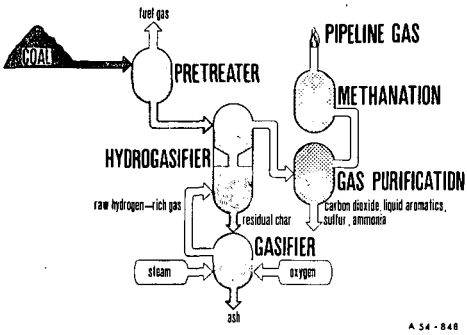

Figure 1. THE HYGAS PROCESS USING A STEAM-OXYGEN GASIFIER TO PRODUCE HYDROGEN-RICH GAS

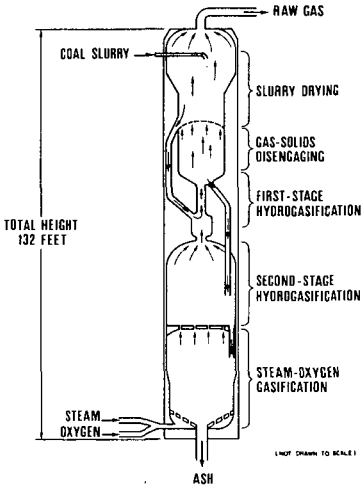

Figure 2. HYGAS PILOT PLANT REACTOR

MAJOR, MINOR AND TRACE ELEMENT BALANCES FOR THE SYNTHANE PDU GASIFIER - ILLINOIS NO. 6 COAL

S. J. Gasior, R. G. Lett, J. P. Strakey and W. P. Haynes

U. S. Department of Energy
Pittsburgh Energy Research Center
4800 Forbes Avenue
Pittsburgh, PA 15213

Summary

Two typical coal gasification tests were performed in the SYNTHANE process development unit (PDU) primarily to determine the distribution and quantity of trace elements in all process streams. For these tests, an Illinois No. 6 coal was gasified in a fluidized-bed with steam and oxygen at 40 atmospheres and a nominal 940° C. Sixty-five trace elements were identified by spark source mass spectrometry (SSMS) and quantified by computer assisted photoplate analysis. The distribution and quantities of only some potentially hazardous elements such as arsenic (As), beryllium (Be), cadmium (Cd), lead (Pb), mercury (Hg), nickel (Ni), selenium (Se) and vanadium (V) are discussed. Mercury (Hg) was determined by flameless atomic adsorption spectrometry (AAS) using double gold amalgamation. Within the precision of both these analytical techniques it was found that most of the trace elements in the feed coal were recovered in the char. The trace elements in the feed coal ranged from a low of 0.1 ppm of Hg to a high of 19 ppm of Ni. The major elements, carbon (C), hydrogen (H), nitrogen (N), oxygen (O), and sulfur (S) were determined by standard ASTM procedures while the minor elements, iron (Fe), aluminum (Al), silicon (Si), sodium (Na), calcium (Ca), potassium (K), magnesium (Mg) and chlorine (Cl) were determined by gravimetric or atomic adsorption techniques. Average overall recoveries of over 95 percent were obtained for the major elements, which were found primarily in the product gas. Recoveries of better than 87 percent were attained for the minor elements, found principally in the char except for Cl which was found principally in the condensate water.

Introduction

Conversion of coal to a high-energy gaseous fuel in an environmentally acceptable manner is an important part of the U. S. energy program. The Pittsburgh Energy Research Center's SYNTHANE process is one of these coal conversion processes. While this coal-to-gas conversion process was being developed in the Process Development Unit (PDU) the environmental aspects of the process were being studied. Forney et.al.(1) and Schmidt et.al. (2) first reported on the analysis of the various effluent streams discharging from this PDU. Later, Forney et.al (3) attempted to make a mass balance of the trace and major elements around the SYNTHANE PDU gasifier. While the balance of major elements was satisfactory, the recovery and balance of the trace elements was less so. This paper describes two coal gasification tests, performed in the same PDU gasifier, in which a several fold improvement in recovery and balance of a selected group of trace elements was made. Means were taken to obtain representative samples of the various solid, gas and liquid streams, followed by meticulous care in preparing the samples to prevent contamination.

The SYNTHANE PDU System

The system consists primarily of a fluid-bed gasifier, a free-fall carbonizer, and a fluid-bed pretreater, figure 1.

The gasifier is a 6-ft. long, 4-in. diameter, Schedule 40 pipe of 310 stainless steel. It is surrounded by three individually controlled, insulated, electric heaters that supply heat for startup and counter radiation loss during operation.

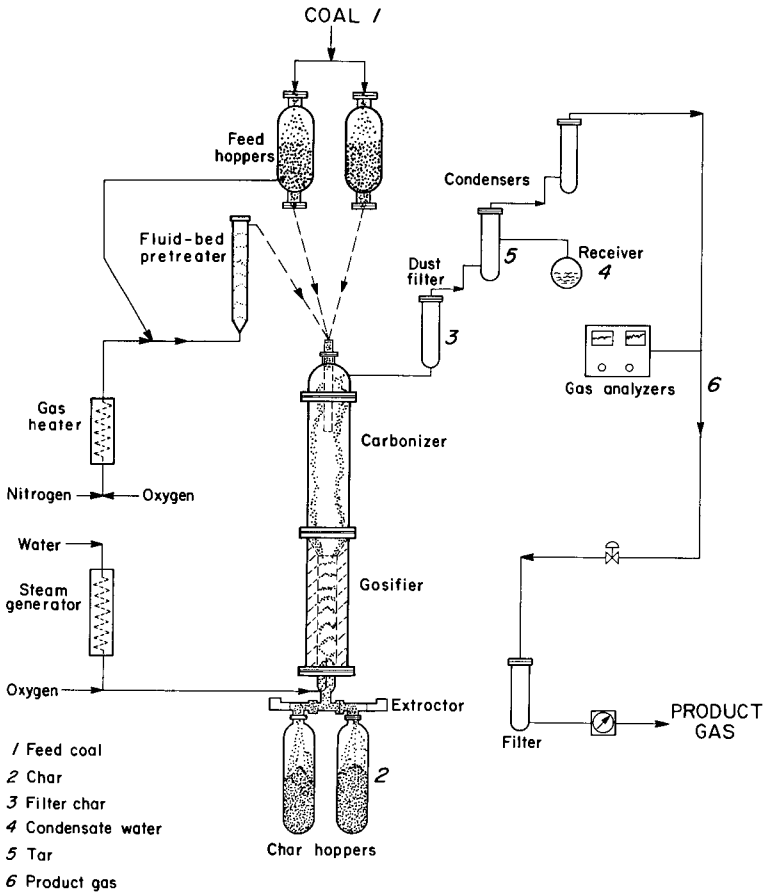

Figure 1.-Schematic flowsheet of the SYNTHANE PDU gasifier and sample points.

9-8-77 L-15584

The carbonizer is a 6-ft. long, 10-in. diameter Schedule 40 pipe of 304 stainless steel. Electric heaters surrounding the carbonizer maintain it at a nominal 560° C during gasification.

The pretreater is a 7.5-ft. long, 1-1/2-in. diameter Schedule 80 pipe of 304 stainless steel. Four individually controlled heaters enclose the pretreater and normally maintain heat for adiabatic conditions at 430° C.

Operations

When gasifying the caking Illinois No. 6 coal, the pulverized (20 x 0 mesh) coal is conveyed to the base of the pretreater and through the pretreater with nitrogen containing 10-15 vol.% oxygen at a fluidizing gas velocity of 0.3-0.5 ft/sec. Pretreating or decaking occurs at a nominal oxygen-to-coal ratio of 1.0 cu.ft. per lb., a temperature of 430° C and a coal-to-gas contact time of 8 mins. The decaked coal empties from the top of the pretreater and falls by gravity through the carbonizer countercurrent to the product gas exiting from the top of the fluidized-bed in the gasifier. A mixture of steam and oxygen enters the base of the gasifier and maintains the coal in a fluidized state at a nominal gas velocity of 0.3 ft/sec. A fluidized-bed height of 68 ins. is maintained by a combination of coal feed, gasification and extraction rates.

Sampling

Samples of the feed coal, char, tar, condensate water and gas were collected from the sampling points shown in figure 1. All samples for SSMS analysis were collected in polyethylene containers, those containers for condensate and tar were acid-cleaned. All coal and char samples were collected and prepared according to ASTM (D-2234-72 and D-2013-72) methods. To improve homogeneity the coal and char samples were further crushed to a fine powder using a boron carbide mortar and pestle. Due to the high hydrocarbon and low ash content of the tars they were examined as low temperature ash. Condensate samples were prepared by evaporation onto ultra-pure graphite. Product gas was passed through graphite-packed filters. Analysis of the filters by SSMS indicated low concentration of sulfur and no other elements above the instrument background levels.

Analysis

Spark source mass spectra were recorded as a series of graded exposures on ion-sensitive photoplates. Resolution was maintained near 1 part in 10,000 on ashed samples. A wider beam-defining slit giving resolution near 1 part in 4,000 was used on a few longer exposures for the ultra-trace elements in order to improve ion transmission and shorten the length of time required for ion collection. The lower resolution slit was also used on the condensate samples to avoid blockage by organic material. After developing, the photoplates were placed on a densitometer and the densitometer output transferred to a strip chart recording. Elemental concentrations were determined from the percent transmission of analytical mass lines by standard procedures, assuming validity of the Hull (4) equation. All calculations were done at PERC on a PDP-11/70 computer.

Elemental sensitivities for the SSMS analysis were determined, where possible, from runs of NBS SRM 1632 (fly ash). Sensitivities of a few minor elements were determined from USGS standard BCR-1 (basalt). A few sensitivities for elements such as Cd and Se were determined from prepared solutions evaporated onto graphite.

Results and Discussion

Operating conditions and results for the subject tests are shown in table 1. Major element analyses and amounts of coal and feed streams to the gasifier are shown in table 2. Major element analyses of the exit streams from the gasifier are shown

TABLE 1. - Operating conditions and results from gasification of an Illinois No. 6 coal with steam and oxygen at 40 atmospheres

Test No.	228	235
Time, hrs.	4.5	5.0
Input, kgs		
Coal	40.179	38.136
Steam	73.030	71.732
Oxygen	17.932	15.436
Nitrogen	69.149	80.340
Output, kgs		
Gas	119.297	131.468
Condensate	57.500	64.476
Char	11.613	10.930
Tar	1.599	.812
Temp., max. avg. °C		
Pretreater	428	430
Gasifier	947	933
Results		
Carbon gasified, %	67.9	75.5
Carbon converted, %	72.9	78.3
Steam converted, %	14.7	13.8
Make[1] gas SCM/kg coal	.96	1.0
Tar make, % of coal	3.98	2.13

1/ $H_2+CO+CH_4+C_2H_6$.

TABLE 2. - Major element analysis of feed stream to gasifier

Test No.	228	235
Coal feed, gms	40,179	38,136
Elements, wt.%		
Carbon	64.5	64.2
Hydrogen	5.0	6.0
Oxygen	9.9	12.3
Nitrogen	1.1	1.2
Sulfur	4.0	3.7
Ash	15.5	12.7
Moisture	3.8	4.3
Fixed Carbon	46.6	47.8
Volatile Matter	34.1	35.2
Water,[1] gms	73,030	71,732
Hydrogen, wt.%	11.1	11.1
Oxygen, wt.%	88.9	88.9
Oxygen,[2] gms	17,932	18,436
Nitrogen,[3] gms	69,149	80,340

1/Distilled water, less than 1.0 ppb Hg.
2/Cylinder oxygen, 99.5% O_2, 0.5% N_2+Ar less than .03 ppb Hg.
3/Liquid nitrogen, 99.9985% N_2, typically less than 3 ppm H_2, O_2 with trace of Ar and less than 0.2 ppb Hg.

in table 3 and the mass balances of the major elements around the gasifier are shown in table 4. The tabulated results reveal that, at the particular gasification conditions, the largest portions of the major elements appear in the product gas and condensate. The gas was analyzed by mass spectrometry and gas chromatography and the condensate by gravimetric, colorimetric and titrametric methods.

TABLE 3. - Major element analysis of exit streams from gasifier

	Gas gm	Extractor char, gm	Filter Char, gm	Tar gm	Condensate gm	Total gm
Test No. 228						
Carbon	16,495	6,545	417	1,290	920	25,667
Hydrogen	2,636	131	11	107	6,268	9,153
Oxygen	29,883	165	29	136	50,025	80,238
Nitrogen	69,149	42	4	22	218	69,435
Sulfur	1,134	81	7	43	288	1,553
Test No. 235						
Carbon	16,914	6,140	362	676	1,032	25,124
Hydrogen	2,698	198	13	59	7,028	9,996
Oxygen	30,355	136	14	58	56,094	86,657
Nitrogen	80,340	52	4	9	257	80,685
Sulfur	1,161	73	5	10	129	1,378

TABLE 4. - Mass balance of the major elements

	IN, kg	OUT, kg	% Recovery
Test No. 228			
Elements;			
Carbon	25.92	25.67	99.0
Hydrogen	10.18	9.15	89.9
Oxygen	86.77	80.24	92.5
Nitrogen	69.59	69.44	99.8
Sulfur	1.60	1.55	96.9
	194.06	186.05	95.8
Test No. 235			
Carbon	24.48	25.12	102.6
Hydrogen	10.32	10.00	96.9
Oxygen	83.83	86.66	103.4
Nitrogen	80.80	80.69	99.9
Sulfur	1.41	1.38	97.9
	200.84	203.85	101.5

The mass balance reveals a relatively good recovery, ranging from 90-97% for H to 99.8-99.9% for N. Even the recovery of the comparatively small amount of S was in the range of 96.9 to 97.9%. Most of it was found in the product gas.

Minor elements, (Al, Ca, Cl, Fe, Mg, K, Na, Si, and Ti) found in the ash of the coal were recovered in the gasified char except for Cl, which was found primarily in the condensate water, as shown in table 5. Analysis was done by AAS and gravimetric methods. Recovery of the minor elements ranged from a low of 62.5% for the least prevalent element in this group, Cl, to 101.6% for the most prevalent element, Si.

TABLE 5. - Minor element analysis of solids and mass balance

	IN gm	Coal wt.%	OUT gm	Char wt.%	Recovery percent
Test No. 228					
Elements:					
Silicon	1,665	4.14	1,694	14.6	101.6
Aluminum	753	1.87	754	6.5	100.1
Iron	1,173	2.92	1,033	8.9	88.1
Titanium	48	.12	45	.4	93.8
Calcium	418	1.04	409	3.5	97.8
Magnesium	41	.10	45	.4	93.8
Sodium	24	.06	21	.2	87.5
Potassium	112	.28	113	1.0	100.9
Chlorine 1/	16	.04	2	.02	12.5

1/8 gms found in condensate water, total recovery 62.5.

As in the case of the minor elements, the trace elements (As, Be, Cd, Ni, Pb, Se, V) from the coal were recovered in the gasified char, except for Hg. Only 12.5 to 20.0% of the Hg was recovered. In test 235, this represented a recovery of 0.6 mg of Hg out of the 3.0 mg present in the 38 KG of gasified coal, table 6. Of this amount 0.44 mg was found in the char and 0.16 mg was found in the tar and condensate. Although the whereabouts of the major portion of the Hg remains unresolved, it seems reasonable to assume that because of the volatility of Hg, it should be found in the product gas. For coal combustion Kalb (5) reports that the major portion of mercury was indeed detected in flue gas.

TABLE 6. - Trace element analysis of solids and liquid streams

	Coal ppm	Coal mg	Extractor char, mg	Filter ppm	Filter char, mg	Tar mg	Condensate mg
Test No. 228							
Arsenic	3.2	130	120	6.2	3.7	1.6	2.6
Beryllium	1.1	44	41	0.2	0.1	-	≤0.2
Cadmium	0.5	20	23	3.6	2.2	≤0.5	≤0.3
Lead	5.1	200	120	14.0	8.4	0.3	≤0.3
Mercury	0.10	4	.24	.02	.06	.01	.19
Nickel	16	640	600	11.0	6.6	7.6	0.5
Selenium	2.8	110	94	0.7	0.4	≤0.5	≤2.1
Vanadium	14	560	680	17.0	10	0.7	0.3
Test No. 235							
Arsenic	2.9	110	100	7.6	3.8	0.7	3.0
Beryllium	1.4	53	39	0.4	0.2	.02	≤0.4
Cadmium	0.5	19	17	5.9	3.0	0.1	≤1.0
Lead	8.5	320	150	25.0	13.0	1.2	≤3.0
Mercury	.08	3	.40	.03	.14	.03	.13
Nickel	19	720	400	17	8.5	6.1	2.0
Selenium	2.6	99	86	1.5	0.8	.09	≤20
Vanadium	13	500	380	24.0	12	0.2	0.6

Another unresolved condition was the relatively high ratio of As, Cd and Pb in the filter char as compared to that found in the coal. On a percentage basis, the char contained about twice the As, eight times the Cd and 3-50 times the Pb as was found in the coal. The filter char which has essentially the same ultimate analysis as does the coal, represents, however, only 1.3-1.5 percent of the coal feed. Whether the disparate ratio between the filter char and coal is caused by the volatilized material in the product gas, depositing onto the fine filter char or whether this represents particle size effect, i.e., the finer coal or char contains a greater percentage of these three elements, remains to be resolved.

Total recoveries ranged from a nominal low of 49% for Pb to a nominal high of 124% for Cd and V. The apparent low recovery of Pb may be an artifact arising from an inhomogeneity of Pb in the coal or chars.

Trace elements content of the coal as determined by our SSMS and flameless AAS analysis were reasonably close to those determined by AAS analysis, as reported by Attari (6), for a similar Illinois No. 6 coal.

Conclusions

Results from two typical coal gasification tests, performed in the SYNTHANE PDU, indicated that a mass balance of major and minor elements can be achieved with a relatively high degree of precision by standard analytical methods.

A reasonable degree of precision can be obtained for trace elements, with the exception of mercury.

References

1. Forney, A. J., W. P. Haynes, S. J. Gasior, G. E. Johnson, J. P. Strakey, Jr. Analysis of Tars, Chars, Gases and Water Found in Effluents from the SYNTHANE Process. U. S. BuMines TPR 76, January 1974, 9 pp.

2. Schmidt, C. E., A. G. Sharkey, Jr., R. A. Friedel. Mass Spectrometric Analysis of Product Water from Coal Gasification. U. S. BuMines, TPR-86, December 1974.

3. Forney, A. J., W. P. Haynes, S. J. Gasior, R. M. Kornosky, C. E. Schmidt and A. G. Sharkey, Jr. Trace Element and Major Component Balances Around the SYNTHANE PDU Gasifier. U. S. ERDA, PERC/TPR-75/1, August 1975.

4. Hull, C. W. Abstracts of 10th Annual Conference on Mass Spectrometry. ASTM Comm. E14, New Orleans, LA, June 1962, Paper 72, page 404.

5. Kalb, W. G. Trace Elements in Fuel, ACS Advances in Chemistry Series 141, 1975, pp. 155-174.

6. Attari, A., M. Mensinger and J. Paul. Initial Environmental Test Plan for Source Assessment of Coal Gasification. EPA-600/2-76-259, September 1976.

EFFECTS OF UNDERGROUND COAL GASIFICATION ON GROUND-WATER QUALITY

J. H. Campbell and V. Dalton

Lawrence Livermore Laboratory
P.O. Box 808, Livermore, CA 94550

J. Busby
United States Geological Survey
Cheyenne, Wyoming

INTRODUCTION

Although in-situ coal gasification offers important environmental advantages when compared with more conventional methods of coal recovery, there are certain environmental concerns that require careful evaluation. The possibility that undergound reaction products may cause adverse changes in ground-water quality is particularly important.

The Lawrence Livermore Labortory (LLL) is pursuing a 3-part program to clarify the nature and significance of the ground-water question. This program includes a laboratory investigation of gasification reaction products and their interaction with coal, a modeling study of the evolving plume of contaminated ground-water, and a ground-water sampling program at the site of an in-situ coal gasification experiment. The gasification experiment was conducted in North-East Wyoming (the Hoe Creek site) by LLL. This paper is focused on the results of our water-sampling program associated with the "Hoe Creek I" gasification experiment and results from recent laboratory experiments on ash leaching and pollutant transport.

The Hoe Creek gasification experiment[1,2] was conducted in the fall of 1976. The gasified coal seam (Felix II) is 25 feet thick and lies at a depth of 125 feet — well below the static water level. The Felix II coal is an aquifer, and is overlain by two additional aquifers. Although the overlying aquifers are also of importance environmentally, this initial study is concentrated on the gasified Felix II seam.

The water-quality investigations have two objectives: First, to determine the effects of in situ coal gasification experiments on the local ground water and second, to learn to predict, reliably, the ground-water effects that may result from commercial-sized gasification operations. It is important to emphasize that the effects of concern may develop over a period of several decades, or even centuries. This is a consequence of the relatively slow transport of contaminant materials through the slow-moving ground-water system. It is, therefore, essential to develop quantitative predictive capabilities based on a thorough understanding of the contaminant source and its chemical and physical evolution. The current water-sampling activities are aimed primary at source definition while the laboratory studies focus on providing data on pollutant leaching and transport.

The water quality field data were obtained principally from a series of wells completed into the Felix II coal and provided with pumps (Fig. 1). The designations EM, DW and OW in Fig. 1 are abbreviations for environmental monitoring well, dewatering well and observation well, respectively.

The curve surrounding the injection and production wells in Fig. 1 shows the estimated extent of coal gasified as deduced from thermocouple data.[1] DW-4 lies within two feet of the gasification boundary and hence provides a close look at the important region just outside the burn zone.

Work performed under the auspices of the U.S. Energy Research & Development Administration under contract No. W-7405-Eng-48.

Figure 2[3] is useful in interpreting the water-quality data obtained at Hoe Creek. In agreement with this model of the undergound source, a variety of inorganic materials have been found issuing from within the burn boundary and a high level of organics (particularly phenolic material) that appears to be concentrated in a thin ring that surrounds the burn zone.

EXPERIMENTAL

Details of the well pumping and sampling procedures used in the field are given elsewhere[4]. Water samples that were to be further analyzed in the laboratory were preserved using well known methods[5,6]. Water samples for field measurements were immediately refrigerated and usually analyzed within an hour of sampling. Methods and procedures used for analyses of the samples are found in references 5-8.

Details of the apparatus, procedure and analysis methods for both the ash leaching and pollutant transport experiments are given in reference 9. A schematic of the coal column apparatus used for the pollutant transport experiments is shown in Figure 3.

RESULTS AND DISCUSSION

A. Field Measurements

Pregasification (baseline data)

Prior to gasification, water from wells in the Felix II coal seam and in the overburden were sampled to provide baseline data with which to compare gasification and post-gasification water analyses. The results of the baseline data for the Felix II coal seam are presented in Table 1. Note that the principal cations are calcium, magnesium, potassium and sodium; the anions are bicarbonate, sulfate and chloride. On an equivalent basis, these seven species balance (i.e., form an electrically neutral solution) to within 3%.

The concentration of phenolic material present before gasification is in the range 0-2 ppb, and the dissolved organic carbon (DOC) is between 3 and 8.5 ppm. Fractionation of the DOC gives an approximately 50/50 distribution between hydrophobic and hydrophilic compounds. Results from further fractionation of the DOC into acid, base, and neutral compounds are discussed in refs. 4 and 10.

Qualitative GC-MS data for the volatile organic species in the water (pre-gasification) show the presence of trace amounts of low-molecular-weight chain hydrocarbons (C_4-C_{12}) as well as simple aromatics such as benzene, toluene and xylenes[8,10].

The amount of methane dissolved in the coal seam water was approximately 11 ± 4 mg/l, pre-gasification. As might be expected, this value was relatively high since coal seams often naturally contain large quantities of free-methane. Water from local ranch wells, which are not completed into the coal seam, contained undetectable amounts of methane (<0.2 mg/l).

Gasification

Although the major emphasis of this study is on the evaluation of the post-gasification ground-water contaminant source, we also analyzed water from several of the monitoring wells <u>during</u> the gasification process. These data provided an estimate of the rate of contaminant buildup in the coal which surrounds the gasifier, as well as the approximate areal extent of the contamination as a function of time.

TABLE 1

Results of water analyses before, during, and after the Hoe Creek I experiment. The baseline data represent an average of analyses from 7 wells completed into the Felix II coal seam. Only "during" and "after" data for EM-1 (100 ft from burn boundary) and DW-1 (10 ft from burn boundary) are shown here since they typify the general trends observed with increasing radial distance. Also given are post-gasification data for inside the burn boundary. Data for 182 and 280 days following gasification and complete data for all other wells are summarized elsewhere[10].

Species	Conc. Units	Pre-Gasif. Baseline Data[a]	Inside Burn Boundary (Injection Well) Post-Gasif.	Outside Burn Boundary					
				DW-1 (10 ft.)			EM-1 (100 ft.)		
				During Gasif.	Post Gasif.		During Gasif.	Post Gasif.	
			83d		3d	83d		3d	83d
Alkal.	mg/1	407 ± 30	63	595	693	430	837	686	636
Al^{+3}	µg/1	0 - 10	220	0	10	20	0	10	10
As^{+3}	µg/1	0 - 1	8	1	1	0	0	0	1
Ba^{+2}	µg/1	100 ± 100	0	200	600	0	0	0	1
HCO_3^-	mg/1	496 ± 40	0	725	845	524	1020	836	776
B^{+3}	µg/1	86 ± 30	710	90	110	360	90	90	70
Br^-	mg/1	0 - 0.1	1.0	0.2	0.3	0.7	0.0	0.1	0.1
Cd^{+2}	µg/1	0	0	0	0	0	1	0	1
Ca^{+2}	mg/1	36 ± 10	570	35	110	220	110	100	78
CO_3^{-2}	mg/1	0	24	0	0	0	0	0	0
Cl^-	mg/1	13 ± 5	37	10	10	22	6.6	7.4	9.5
CN^-	mg/1	0.00 - 0.01	0.43	7.0	48	0.14	4.0	5.0	0.01
Fe diss.	µg/1	0 - 10	30	380	37000	1700	4400	18000	160
Pb^{+2}	µg/1	0 - 1	1	2	0	0	2	2	7
Li^+	mg/1	34 ± 5	310	30	50	190	50	50	50
Mg^{+2}	mg/1	10 ± 4	19	8.1	28	55	26	26	18
NH_4^+ as N	mg/1	0.55 ± 0.05	19	0.49	2.1	20	0.80	0.77	0.84
NO_2 as N	mg/1	0.00	0.00	0.00	0.00	0.00	0.00	0.00	0.00
NO_3 as N	mg/1	0.02 ± .01	0.01	0.19	0.01	0.07	0.01	0.01	0.02
Phenols	µg/1	1 ± 1	41	15	1000	340	83	15	2
K^+	mg/1	5.4 ± 0.5	57	4.3	7.5	25	7.7	7.7	6.1
Diss. Solids	mg/1	703 ± 70	3390	699	989	2020	1170	1240	1050
Na^+	mg/1	214 ± 15	320	240	350	310	330	320	310
SO^{-2}	mg/1	154 ± 80	2200	37	67	1000	250	320	310
S^{-2}	mg/1	0.3 ± 0.2	4.0	0.7	1.1	—	0.3	2.6	0.6
Zn^{+2}	µg/1	224 ± 200	10	50	20	1200	120	30	20
CH_4	mg/1	11.5 ± 4	1.8	<0.2	0.4	—	<0.2	35.0	—

[a]The ± values indicate the approximate range of the results for the seven baseline wells.

Ignition took place October 15, 1976 and gasification continued for approximately 11 days. During that period, nearly 130 tons of coal were gasified, producing 19 MMSCF of gas (13.2 MMSCF dry) having an average heating value of 110 Btu/scf (1,2). On the seventh day of gasification, water samples were pumped from several of the wells outside the gasification burn boundary. Data from the analysis of two samples (DW-1 and EM-1) are summarized in Table 1 and compared with conditions prior to and following gasification.

It is interesting to note that although gasification had proceeded for only seven days at the time of this sampling, the gasification process had begun to affect the water quality at distances up to 100 feet from the burn zone. In particular, large increases in CN^-, phenols and electrical conductivity were observed.

Although the total amount of DOC also increased during gasification, the distribution of DOC (as determined from fractionation measurements) remained approximately the same as that observed in the baseline study[10]. The concentration of methane present in the water dropped from 11 mg/l to below detectable limits (<0.2 mg/l) in all the wells monitored. Thus, the amount of dissolved CH_4 in the water appears to be very sensitive to perturbations of the natural ground-water system.

Post-Gasification

Water sampling at the Hoe Creek site was carried out at periods of 3, 83, 182 and 280 days following gasification. (Only part of the data are currently available for the most recent (280-day) sampling expedition.) Shown in Table 1 are typical analyses for inside (Injection Well) and outside (DW-1 and EM-1) the burn-boundary. Complete data for all other wells are given elsewhere[10]. Data for some of the contaminants and characteristics showing large changes following gasification have been plotted as a function of distance from the burn-boundary (Figure 4-7). This method of displaying the data implies that the initial release of contaminants is independent of direction (cylindrical symmetry). This is not exactly true, of course, but the results suggest that it is a useful simplification. The assumption of cylindrical symmetry appears to be quite valid for the wells in the close proximity to the burn boundary (i.e., the DW wells), but at large radial distances (the outermost EM wells) the data suggest that the contaminants move more easily in the direction of highest permeability (N59E, See Fig. 1)[4].

Electrical Conductivity, Temperature and pH

An increase in electrical conductivity is a good measure of the increase in ionic species as a result of gasification. Our results show approximately a 2-fold increase in conductivity within 10 feet of the burn boundary, with a rapid drop off to nearly baseline values at a distance of 100 ft (Fig. 4). Also, there is a continuing drop in conductivity between the 83 and 280-day sampling period. As will be shown later, this may be an indication of contaminant sorption by the coal. Inside the burn boundary, the soluble coal ash species produce a highly conductive solution (3500 μmho/cm).

As might be expected, the total dissolved solids (TDS, the residue at 180°C) follows closely the changes observed in electrical conductivity. The TDS level decreases from ~2000 mg/l at 10 ft from the burn boundary to ~900 mg/l at 100 ft. Inside the gasified zone, TDS reaches a value near 3400 mg/l.

The measured temperature gradient near the gasifier was quite large 3 days after gasification (Fig. 4). After 83 days, the system had evolved to a rather slowly varying state with a much smaller temperature gradient. This approach to thermal equilibrium is probably driven by convection near the gasification site. In a later section, it is shown that the mixing caused by convection produces a rather large change in the near-gasifier contaminant distribution immediately following gasification.

The pH of the water remains near 7.0 at points sampled outside the burn boundary. Inside the burn zone, the dissolution of metal oxides remaining in the ash produces a high pH solution (~10 - 10.5). This observed pH value is very close to that predicted by our recent laboratory ash-leaching experiments (see next section and ref. 9).

The measured alkalinity of the water at first appears to contradict the observed pH values: inside the burn zone, the alkalinity is lower (60 mg/l) than it is outside the burn zone (400-600 mg/l). This apparent contradiction results from the fact that whereas pH is a measure of a specific ion concentration (H^+or OH^-), alkalinity is a measure of the ability to neutralize acids, and hence includes not only OH^- but also such species as HCO_3^- and CO_3^{2-}. The alkalinity of water samples taken outside the burn zone is almost totally due to the presence of high concentrations of bicarbonate ion. Inside the gasification zone, only OH^- and CO_3^{2-} contribute to the alkalinity and, because they are present in much lower molar concentrations, they produce a much lower alkalinity (Table 1).

Cation Species

The concentrations of many of the cation species — particularly Mg^{+2}, Ca^{+2}, Li^{+1}, NH_4^+, and K^+ — increased as a result of the gasification process. The metal ions presumably come from the ash material remaining in the burned-out zone, whereas the observed increases in NH_4^+ probably result from the evolution of NH_3 during the gasification process. Ammonia is a commonly observed coal pyrolysis product.

Figures 5 is a plot of Ca^{+2}, Mg^{+2}, K^+ and NH_4^+ concentrations as a function of distance from the gasification boundary for different sampling times following gasification. The fact that log-log or semi-log scales have been used is not meant to imply a particular relationship between concentrations and radius. These scales were chosen simply for convenience in showing a large range of values on a single plot.

The convective mixing that occurs as water re-enters the gasification zone causes a redistribution of soluble ash species into the surrounding coal seam. This accounts for the observed increases in metal ion concentrations which occur between the 3-day and 83-day post-gasification sampling periods (Fig. 5).

The Mg^{+2} concentration is found to be lower inside the burn boundary than it is outside. This apparent anomaly is associated with the suppression of the $Mg(OH)_2$ solubility due to the high pH inside the burn boundary. The solubility product of $Mg(OH)_2$ is 1.2×10^{-11} moles $^3/l^3$ at 18°C. Hence, a Mg^{+2} concentration of 18 mg/l, as measured inside the burn zone, (Fig. 5) can only exist in a solution of pH $\leq$10.1, which is within experimental error of the measured value (10.3). The higher concentrations of Mg^{+2} that occur outside the burn boundary evidently resulted from mixing at a time when the pH was slightly lower, specifically pH $\leq$ 10.

The variation in concentration with distance observed for other cations (e.g., B^{+3}, Li^+) is quite similar to that shown here for Mg^{+2}, Ca^{+2} and K^+. Furthermore, all species showed the effects of the convective mixing that occurred shortly following gasification.

Other cation species that showed some measurable increases in concentration as a result of gasification are Al^{+3}, As^{+3} and Ba^{+2}. In general, however, only a few close-in wells showed increases in these species.

Aluminum was detected at above baseline levels (220 μg/l) only inside the burn zone. This agrees with laboratory experiments, which showed that aluminum is very strongly adsorbed by coal[3]. Hence, any Al^{+3} swept out from the burn zone into the coal bed would be expected to be quickly adsorbed.

Arsenic showed an increase in concentration inside the burn zone (8 mg/l) and 2 ft outside (DW-4, 21 mg/l); all other wells remained at baseline levels.

Barium was observed at above-baseline concentrations in well DW-4 immediately following gasification (i.e., during the 3-day post-gasification sampling). It was not detected, however, during the post-gasification sampling 83 days later. This is quite reasonable, since the SO_4^{-2} concentration had increased approximately 5 - 20 fold and Ba^{+2} is probably precipitated as $BaSO_4$ (Ksp = 1.0×10^{-10} moles ^{2}/liter^2 at 18°C). Post-gasification analyses showed no significant increase in heavy metals as a result of gasification. In particular, no large increase in lead or mercury was detected[10].

Anion Species

The anions included in the analyses are listed in Table 1. Large increases in concentration were observed for SO_4^{-2} and CN^- (Fig. 6). Bromide ion also increased and in general showed the same behavior as SO_4^{-2}.

The ash bed is the major source of increased SO_4^{-2} and Br^-. The observed increase in SO_4^{-2} concentration between 3 days and 83 days following gasification (Fig. 6) probably also results from the mixing induced by convection shortly following the process.

CN^- was observed in very high concentrations immediately following gasification (3 days). However, by 83 days after gasification, the concentration had dropped approximately three orders of magnitude, reaching background levels at 100 ft from the burn zone. Subsequent analyses (182 and 280 days) have shown a continuing drop in CN^- concentration. It is probable that CN^- is being adsorbed by the coal. Laboratory experiments are currently under way to examine the magnitude of CN^- sorption by coal.

Increased concentrations of nitrates and nitrites were not observed during the post-gasification sampling.

Phenols and other Organic Materials

The measured post-gasification distribution of phenolic materials is plotted in Figure 7. The highest concentration observed was 450 mg/l, three days following gasification at a distance of 2 ft from the burn boundary (well DW-4). The concentration falls off very sharply with radius. Inside the burn zone, the phenolic concentration is only 0.041 mg/l (Table 1).

Also plotted in Figure 7, are data from the 83, 182, and 280-day post-gasification sampling periods. The concentration of phenols has decreased approximately one order of magnitude over the 182 days since gasification. The drop in concentration of phenolic materials is probably the result of sorption by the coal[3,9]. The dissolved organic carbon analyses showed the same general trend observed for the phenolic material — wells close to the burn boundary had much higher DOC levels. Fractionation of the DOC into hydrophobic and hydrophilic groups of acids, bases and neutrals is discussed in more detail in refs. 4 and 10.

Many of the water samples obtained at Hoe Creek were analyzed for volatile and semi-volatile organics using GCMS. Analysis for volatile organics in post-gasification water samples shows an abundance of lower molecular weight polyaromatic and substituted aromatic compounds. As many as 200 different

Table 2. Comparison of laboratory and field measurements of various contaminants originating from ash.

Characteristic	Field measurements (83d) (sampling well in ash bed)	Laboratory Leaching Expts 1000°C	1100°C	1200°C
Ca^{+2} (ppm)	570	645	630	411
Na^{+} (ppm)	320	207	196	193
K^{+} (ppm)	57	9.7	8.9	7.7
Fe^{+3} (ppm)	.030	<.5	—	—
Al^{+3} (ppm)	.220	33	3.9	<.50
Mg^{+2} [a] (ppm)	19.0	(26.0)	(35)	62
Ba^{+2} (ppm)	0	<2.0	—	—
SO_4^{-2} (ppm)	2200	2193	2010	1667
pH	10-10.5	10-11	10.5	7.5-8.0
Conductivity (μmho/cm)	3500	3450	3100	2850

[a]See discussion in text concerning Mg^{+2} solubility at high pH.

species (not detected in the pre-gasification samples) have been quantitatively identified in the water wells close to the gasification zone.

A comparison of the volatile species in the product tar with those found in the water show some similarities. These similarities are best demonstrated when the chromatograms of two water samples- one approximately 45 feet from the burn, and another 5 feet from the burn — are compared with a chromatogram of the product tar. The results show the marked decrease in high-boiling, high-molecular-weight material at points further from the gasification zone. In particular, the concentration of xylenes, other substituted benzenes, indenes indans, and napthalenes is observed to decrease significantly at the greater distance from the gasification zone. The reader is refered to references 4, 8 and 10 for more details on the GCMS analysis of these water samples.

B. Laboratory Ash Leaching and Phenol Transport Experiments

Details of a series of experiments dealing with coal ash leaching and transport of pollutants near an in-situ gasifier are given in Ref. 9. In this paper we summarize some of the important results of that work which relate to the above field measurements.

Ash Leaching

Subbutuminous coal ash samples heat treated to 1000, 1100 and 1200°C were water leached and the leachate analyzed for Ca^{+2}, SO_4^{-2}, Al^{+3}, Fe^{+3}, Ba^{+2}, Mg^{+2}, K^{+}, Na^{+} and OH^{-}. The laboratory results are compared with the cation and anion concentration data from the field measurements in Table 2. Except for K^{+} and Al^{+3} the agreement between the laboratory and field data is excellent. This good correlation suggests that plume dispersion calculations(3) carried out using laboratory leaching data for input may be able to accurately predict

pollutant transport from an underground gasification site. Currently experiments are in progress to generate further laboratory data that can be used in modeling post-gasification plume development.

Phenol Transport Through Coal

Phenolic materials are one of the major organic pollutants associated with in-situ coal gasification. Maximum levels of near 500 ppm have been measured in the groundwater (Fig. 7). Transport of these material away from the gasification site pose a potential long term pollution hazard (Fig. 2).

We have studied the transport of a 600 ppm phenol solution through a column of subituminous coal and measured the absorption of the material on the coal matrix (Fig. 8). The flow rate was 101 m/yr and the distribution coefficient (K_d) was calculated to be approximately 40. This very strong adsorption of phenol on coal is in agreement with static experiments (K_d = 30-40) and with field observations (See Fig. 7). It was also found that the movement of the phenolic solution through the coal column is accurately predicted using a one-dimensional transport model. Results from these and other transport experiments are given in ref. 9.

Acknowledgments

The authors gratefully acknowledge the GCMS work of Dr. E. Pellizzari of Research Triangle Institute and the assistance of S. Santor, W. Mead, B. Suderland and B. Lim of LLL.

NOTICE

"This report was prepared as an account of work sponsored by the United States Government. Neither the United States nor the United States Energy Research & Development Administration, nor any of their employees, nor any of their contractors, subcontractors, or their employees, makes any warranty, express or implied, or assumes any legal liability or responsibility for the accuracy, completeness or usefulness of any information, apparatus, product or process disclosed, or represents that its use would not infringe privately-owned rights."

REFERENCES

1. R. W. Hill and C. B. Thorsness, "Results from an In Situ Coal Gasification Experiment Involving Explosive Fracturing: Hoe Creek Experiment No. 1", Lawrence Livermore Laboratory, Rept. UCRL-52229, (1977).

2. C. Thorsness, R. Hill and D. Stephens, "Preliminary Results from an In-Situ Coal Gasification Experiment Using Explosive Fracturing", Division of Fuel Chemistry, American Chem. Soc. Preprints, 22, 1 (1977).

3. J. H. Campbell and H. Washington "Preliminary Laboratory and Modeling Studies on the Environmental Impact of In-Situ coal Gasification" Proceedings of the Second Underground Coal Gasification Symposium, Morgantown Energy Research Center, Morgantown, West Virginia, (1976) p. 119.

4. S. Warren Mead, John H. Campbell, and Douglas R. Stephens "Ground-Water Quality Effects of an Underground Coal Gasification Experiment" 3rd Annual Underground Coal Conversion Symposium, Lawrence Livermore Laboratory, Livermore, California, (1977), Rept. UCRL-79867.

5. E. Brown, M. W. Skougstad, and M. J. Fishman, "Methods for Collection and Analysis of Water Samples for Dissolved Minerals and Gases", Techniques of Water-Resources Investigation of the U. S. Geological Survey, Chapter A-1, U. S. Department of Interior, 1970.

6. D. R. Goerlitz and E. Brown, "Methods for Analysis of Organic Substances in Water", Techniques of Water-Resources Investigation of the U. S. Geological Survey, Chapter A-3, U. S. Department of Interior, 1972.

7. "Water Analysis Handbook" Hach Chemical Company, Ames, Iowa, 1976 edition.

8. E. D. Pellizzari, "Identification of Components of Energy-Related Wastes and Effluents", Research Triangle Institute Rept., Research Triangle Park, North Carolina (1977).

9. V. A. Dalton and J. H. Campbell "Laboratory Measurements of Groundwater Leaching and Transport of Pollutants Produced During Underground Coal Gasification", Lawrence Livermore Laboratory, Rept. UCRL (in press) 1977.

10. J. H. Campbell, J. Busby, S. Santor and W. Mead "Effects of the Hoe Creek I Underground Coal Gasification Experiment on Ground Water Quality", Lawrence Livermore Laboratory, Livermore, CA, Rept. UCRL (in press) 1977.

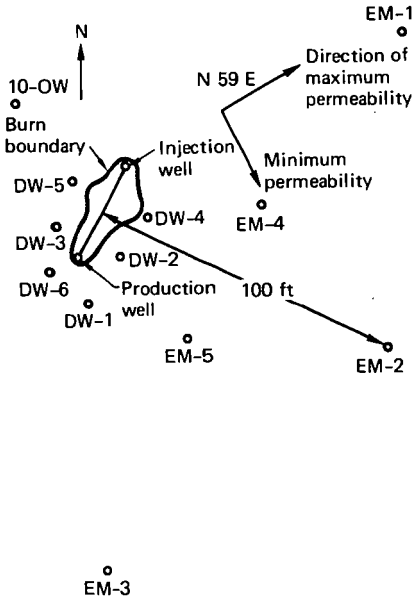

Fig. 1. Wells used for water sampling at the Hoe Creek Site.

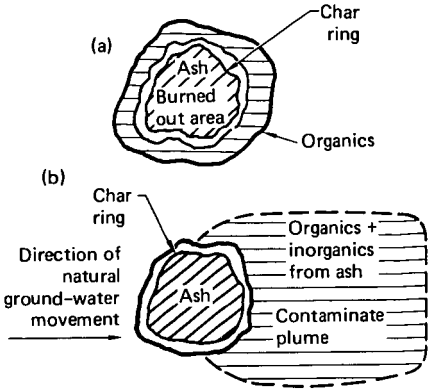

Fig. 2. Plan view of post-gasification burn region (a) and the plume that develops as a result of ground-water flow (b).

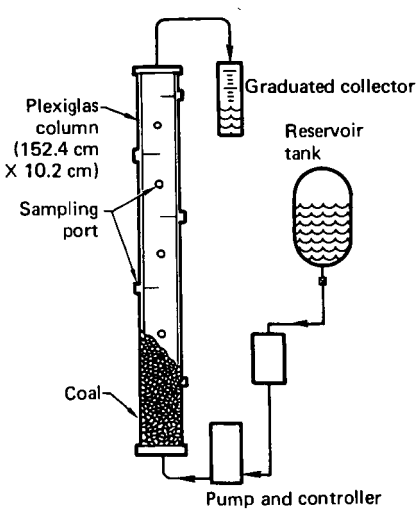

Fig. 3. Schematic of coal column apparatus used to simulate flow of contaminated water through coal.

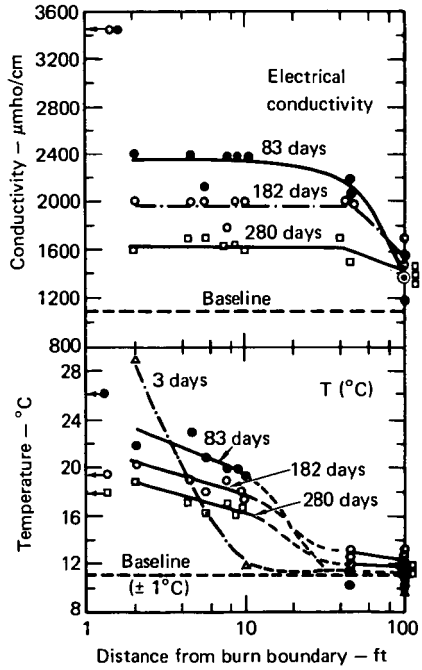

Fig. 4. Electrical conductivity and temperature as a function of distance from the gasification burn boundary. The arrows near the ordinate indicate values measured inside the burn boundary.

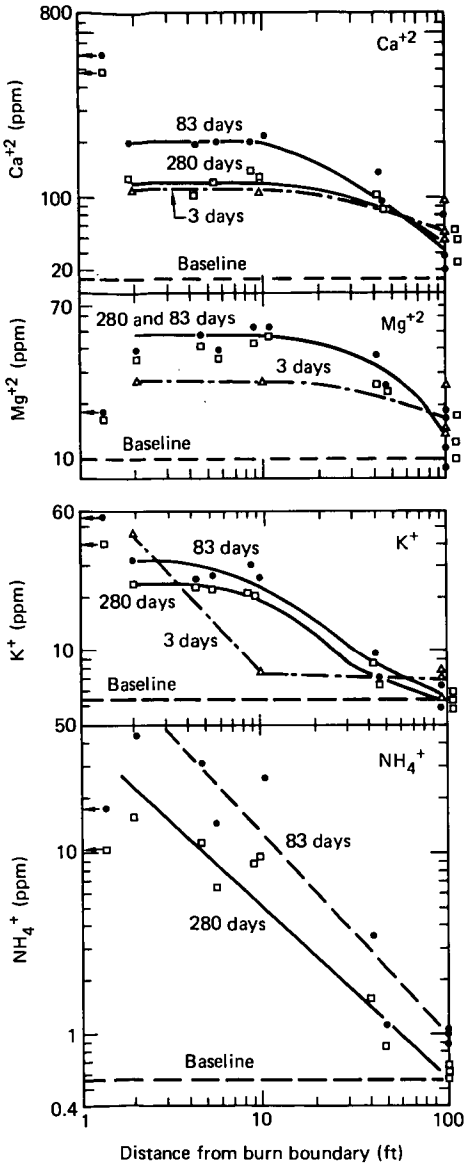

Fig. 5. Concentration of Ca^{+2}, Mg^{+2}, NH_4^+ and K^+ as a function of distance from the gasification burn boundary. The arrows near the ordinate represent values inside the burn boundary.

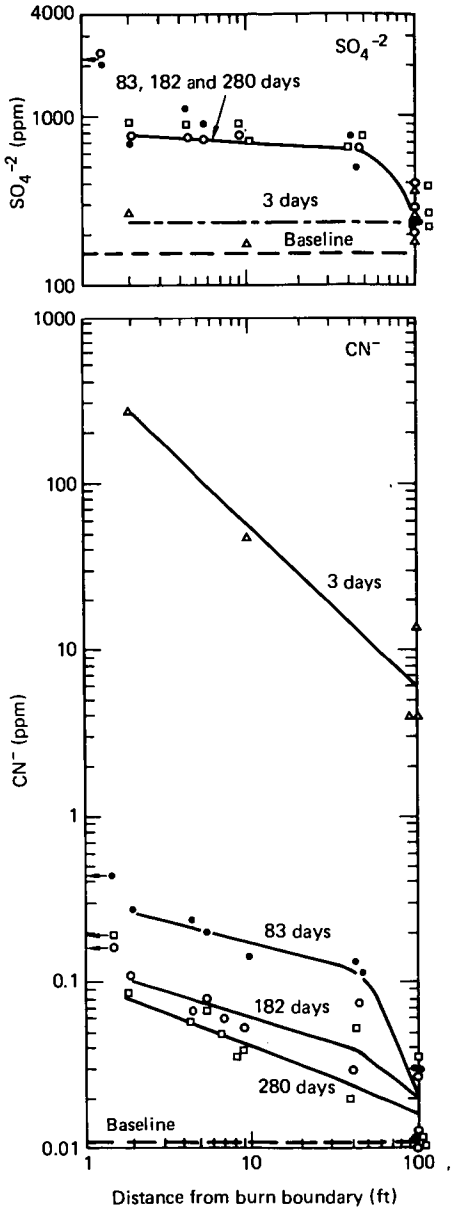

Fig. 6. Cyanide and sulfate concentration as a function of distance from the gasification burn boundary. The arrows near the ordinate represent values inside the burn boundary.

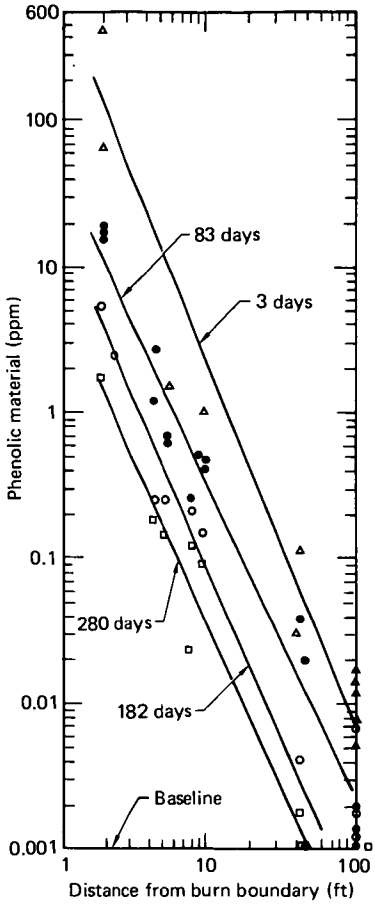

Fig. 7. Concentration of phenolic material as a function of distance from the burn boundary.

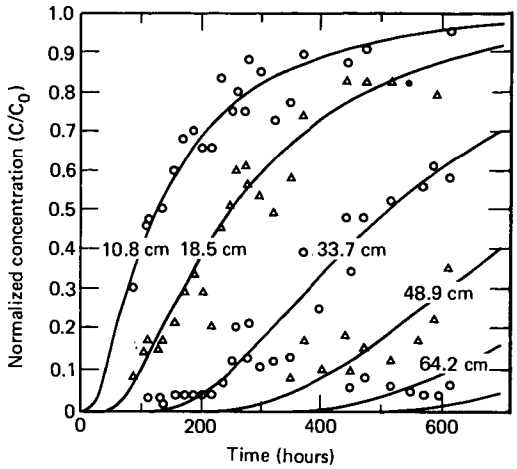

Fig. 8. Phenol breakthrough curves calculated (–) and measured at various distances (shown on figure) along a 1.5 m packed column of sub-bituminous coal. The coal column is shown in Fig. 3. The concentration of the phenol solution was 600 ppm; the solution was pumped through the column at a linear velocity of 101 m/yr. The average particle size of the coal was 0.71 cm. Further details are given in the text and in ref 9.

Sampling, Analysis and Characterization of Effluents from the Grand Forks Energy Research Center's Slagging Fixed-Bed Gasifier

Leland E. Paulson, Harold H. Schobert, and Robert C. Ellman

Grand Forks Energy Research Center
Grand Forks, North Dakota 58202

INTRODUCTION

The Grand Forks Energy Research Center is operating a slagging fixed-bed coal gasification pilot plant. The pilot plant was previously operated from 1958 to 1965 to establish operability of the slagging method of ash discharge and to evaluate process parameters (1, 2). Operation was resumed in April 1976 with the major objectives being to study the effluents produced in gasification. In this report, methods currently used at GFERC to sample and analyze effluents are presented and results are related to gasifier operation.

GFERC GASIFIER

A flowsheet of the GFERC pilot plant is given in Figure 1. Recent publications (3-6) have discussed the test equipment and procedures in detail. A brief summary will be provided here.

The test coal is introduced into the gasifier through a lock hopper. As the coal descends through the shaft, it is heated by the countercurrent flow of hot gases coming from the reaction zone. Drying, devolatilization, and gasification occur in distinct zones in the coal bed (7). The coal is reacted with a steam-oxygen mixture which is injected into the hearth. Gasification occurs at temperatures of 2800-3100° F, completely consuming the coal and leaving only slag. The molten slag drains continuously into a water quench bath. The gas enters a recycled liquor spray washer where water vapor, tars, oils, and dust are removed. The accumulating liquids are periodically drained into an atmospheric holding tank. The gas is further cooled, sampled, depressurized, demisted, metered, and flared. A typical gas composition is 58% CO, 29% H_2, 5% CH_4, and 7% CO_2, with small amounts of C_2-C_4 hydrocarbons.

COAL TESTED

All tests described in this report were performed with Indian Head lignite obtained from the North American Coal Company mine in Mercer County, ND. The moisture content of the coal as mined ranged from 35 to 37%. Due to moisture loss during handling and storage, the moisture content of the coal tested ranged from 23 to 30%. Table 1 shows a typical analysis for as-gasified coal and the range of observed analyses.

SAMPLING METHODS

Collecting representative and reproducible samples of effluents produced by the gasifier presents special problems because the system is under pressure and the streams that are sampled contain a multiphase combination of gas, water and organic vapors and/or aerosols, and entrained fuel particles. At GFERC several sampling methods and procedures are being developed to address these problems. These include; collecting a composite of the total liquor generated during a run, periodically collecting samples of recycle liquor circulated through the spray washer system, and by using sampling trains attached to product gas stream. Figure 1 shows the location of the sampling points.

Composite samples of tar and water produced during the entire test are collected from the liquor accumulated in the holding tank after phase separation and weighing. Component concentrations and quantities of water collected are corrected for system start-up water.

The recycled condensate liquor is sampled at each coal charge which represents a timed data period. The mass production rate and concentration of each component generated are determined by differences in liquid analysis and inventory between samplings.

Schematics of three sampling trains are shown in Figure 2. Each of these units operate slightly above atmospheric pressure and remove condensibles from a side stream of raw gas produced by the gasifier. Sampler I is a four staged heat exchanger. Tar is collected in Stage 1 (maintained at 212° F), Stages 2, 3, and 4 cool the gas progressively to 32° F and condense and collect water and light oil. Gas flow rate to the sampler is less than 1 pct of the total gas produced. The first stage of sampler II is a cyclone which removes tar. In Stage 2 and 3 water and oil are removed by heat exchange which cools the gas to 40° F. This sampling system will be fully described in a separate publication in the near future. Sampler III consists of four steel impingers in series immersed in an ice bath. A fourth system using on-line gas chromatographs to measure mass rates of water and tar in product gas is under development, and will also be described in a separate publication.

ANALYTICAL METHODS

The dissolved solids, specific gravity, pH, alkalinity, ammonia, and sulfide content are determined by wet chemical methods described in the literature (8). Instrumentation includes a Hach model 16500 reactor for chemical oxygen demand (COD), a Beckman model 915A total organic carbon (TOC) analyzer, and a Leco model 532 total sulfur analyzer. Organic species are identified using a DuPont 491B mass spectrometer (MS).

Although a large body of literature exists regarding the preparation, preservation, and analytical methods for liquor samples, it appears that, at least to an extent, the effluent generated by each gasifier is unique, requiring slight modifications to existing analytical procedures. For example, experience at GFERC has shown that wet chemistry procedures for sulfide and cyanide as reported in the literature have not given satisfactory precision. The modified analytical procedures developed at GFERC will be detailed in future publications. A cooperative program with Carnegie Mellon University is in progress in which the accuracy and precision of most of the procedures used at GFERC will be studied.

The reproducibility of the procedures for analyzing tar-free liquor is shown in Table 2. Each test is run on aliquots, treated identically before analysis. Table 2 shows the replicate values, the average, standard deviation, and coefficient of variation (9). Coefficient of variation is 10% or less, indicative of good reproducibility, for all tests except COD, for which the value is 13.6%. The reproducibility of MS analysis for tar has been reported previously (6).

EFFLUENT PRODUCTION

The mass rates of water, tar, ammonia, and TOC produced during seven gasification runs are shown in Table 3. These runs represent a range of operating pressures from 100 to 400 psi, oxygen rates of 4000 and 6000 scfh, and coal moisture contents from 22 to 30%. The oxygen/steam molar ratio was 1.0. Mass rates were separately calculated from data from the composite samples, recycle liquor samples, and side stream samplers I and II. For each run the composite consists of a single sample representing the entire run. Depending on run

organic material, while the remaining fraction consisted of heavier organic components. If a sample is filtered with a .45 micron millipore filter, most of the material of mass greater than xylenol will be removed.

Tar Composition

The MS analysis of tar from RA-21 is shown in Table 6. Shown in the table is the analysis of tars from side stream samplers I, II, and III and from the composite. Results indicate that the MS analysis of the tars collected in the various samplers was similar and that the composition of tar does not greatly change during the run. Additional analytical data of the tars can be found in reference (6).

FUTURE PLANS

The pilot plant facilities are being upgraded with the objective of achieving 5 day continuous operation and the capability of gasifying caking bituminous coal. If a higher gas offtake temperature occurs in bituminous coal gasification as expected, revision of sampling methods will be required.

The use of dedicated samplers to collect a specific effluent constituent will provide improved characterization. For example, future installation of an isokinetic sampling system incorporating filter and impinger trains will allow collection and characterization of the dust in the gas stream. Similarly an impinger train containing an appropriate acidic collector and a preservative will be used for sampling ammonia.

The development of methods for measuring trace element constituents in gas, liquor, and tar is an area in which future work is planned. The trace constituents consist of metallic elements such as mercury, arsenic, and antimony; sulfur compounds such as carbonyl sulfide, carbon disulfide, and mercaptans; and non-metallics such as selenium, chlorine, fluorine, and phosphorous. As sample preparation methods are developed, it will become possible to calculate material balances for the various trace elements and to determine the fate of those compounds in the gasification process.

Proper design of downstream gas-liquor-tar separation and treatment systems will require knowledge of the physical properties of the effluent streams as well as their chemical composition. Thus determination of viscosity, density, and other scalable physical properties represents another area in which work is needed.

REFERENCES

1. Gronhovd, G.H., A.E. Harak, W.R. Kube, and W.H. Oppelt. Design and Initial Operation of a Slagging, Fixed-Bed, Pressure Gasification Pilot Plant. BuMines RI 6085, 1962.

2. Gronhovd, G.H., A.E. Harak, M.M. Fegley, and D.F. Severson. Slagging Fixed-Bed Gasification of North Dakota Lignite at Pressures to 400 psig. BuMines RI 7408, 1970.

3. Ellman, R.C. and B.C. Johnson. Slagging Fixed-Bed Gasification at the Grand Forks Energy Research Center. Eighth Synthetic Pipeline Gas Symposium, Chicago, IL, 1976.

4. Ellman, R.C. and H.H. Schobert. Pilot Plant Operation of a Fixed-Bed Slagging Gasifier. American Chemical Society 173rd National Meeting, New Orleans, LA, 1977.

duration, the recycle liquor data is derived from up to seven data periods, each representing the time interval between coal charges. The data from each side stream sampler represents up to three samples, each collected over three data periods.

The results are influenced by inaccuracies of analytical procedures, limitations in duration of gasifier operating time, and difficulties in accounting for system water inventory during the test period.

A comparison of mass rates calculated for a given run from data for the composite, recycle, and side stream samples generally shows consistency between the sampling methods. For example, for run RA-12 the mass rates in lbs/ton maf coal gasified range from 988 to 1059 for water, 6.9 to 7.1 for ammonia, 9.4 to 10.4 for TOC, and 70 to 80 for tar.

Replication between tests run at the same conditions is shown by comparing RA-11 and -12, both run at 200 psi, and by comparing RA-14 and -16, both run at 400 psi. All of these tests were run on lignite with moisture that ranged from 24 to 26% and at an oxygen rate of 4000 scfh. The pounds of ammonia produced per ton maf coal ranged from 6.1 to 7.6 in RA-11 and from 6.9 to 7.7 in RA-12. The pounds of tar produced per ton maf coal was 70.6 for RA-11 and ranged from 69.6 to 79.4 for RA-12.

Side stream sampler II was first tested in RA-16. Results obtained using this system in RA-16, -17, and -21 (all at 400 lbs pressure) are consistent. RA-16 and -21 were performed at an oxygen rate of 4000 scfh on coal of 23.9 and 30.5 pct moisture respectively while RA-17 was run at an oxygen rate of 6000 scfh and a coal moisture of 22.8 pct. Water production rate in lbs/ton maf coal was 831 and 844 for tests RA-16 and -17, and 913 for the higher moisture coal gasified in RA-21. Ammonia production rate in lbs/ton maf coal was 9.8 for RA-16, 8.2 for RA-21, and 9.7 for RA-17. Dissolved organics (TOC) production rate in lbs/ton maf coal was 8.2, 9.0, and 7.5 for the three tests and tar production on the same basis was 58.1, 52.0, and 55, respectively.

EFFLUENT COMPOSITION

The composition of the effluent generated in the seven gasifier runs previously described is shown in Table 4. Results are based on composite samples and are corrected for water introduced in start up and shutdown.

Of special interest is the fact that approximately 3 to 6 pct of the carbon and 27 to 50 pct of the nitrogen from the coal is present in the effluent. The carbon in the effluents includes carbon particles, dissolved organics and tar. The nitrogen in the effluent includes ammonia in the liquor and nitrogen in the tar.

The relationship between gasifier operating pressure and ammonia concentration in the effluent is shown in Figure 3. The results were based on runs RA-11, -12, -14, -16, and -18 using the four sampling methods previously described. Results indicate that the ammonia concentration in the liquor increases with pressure. There appears to be no similar relationship between gasifier operating pressure and dissolved organic concentration in the liquor.

The aqueous fraction of gas liquor contains a variety of water soluble and semi-soluble organics. Table 5 shows an MS analysis of the organic material in this fraction from the composite sample of RA-14. This sample was cleanly skimmed of all apparent tar, but was not filtered. This sample would be expected to be typical of the liquor in a waste water treatment plant before phenol extraction. The phenolic grouping (phenol, cresol and xylenol) accounted for approximately 80 pct of the

5. Ellman, R.C., B.C. Johnson, H.H. Schobert, L.E. Paulson, and M.M. Fegley. Current Status of Studies in Slagging Fixed-Bed Gasification at the Grand Forks Energy Research Center. Ninth Biennial Lignite Symposium, Grand Forks, ND, 1977.

6. Ellman, R.C., M.M. Fegley, B.C. Johnson, L.E. Paulson, and H.H. Schobert. Slagging Fixed-Bed Gasification. 4th Annual International Conference on Coal Gasification, Liquefaction, and Conversion to Electricity, Pittsburgh, PA, 1977.

7. Johnson, B.C., H.H. Schobert, and M.M. Fegley. The Grand Forks Slagging Gasifier: Gas-Solid Reactions in the Real World. American Institute of Chemical Engineers, Symposium on Theory and Practice of Gas-Solids Contactors in Fossil Fuel Processing, New York, NY, 1977.

8. Rand, M.C., A.E. Greenberg, and M.J. Taras (eds.). Standard Methods for the Examination of Water and Wastewater. American Public Health Association, Washington, DC, 1976.

9. Belz, M.H. Statistical Methods in the Process Industries. John Wiley & Sons, New York, NY, 1973.

TABLE 1. - Analyses of lignites tested, percent

	Typical analysis	Range for lignite as tested			Typical analysis	Range for lignite as tested	
Proximate analysis, pct:				Ultimate analysis, pct:			
Moisture	25.8	23.9	30.5	Hydrogen	6.0	5.8	6.5
Volatile matter	31.1	29.2	32.1	Carbon	47.1	43.9	49.5
Fixed carbon	34.5	32.3	36.9	Nitrogen	.6	.6	.8
Ash	8.6	6.2	10.9	Oxygen	37.0	34.9	40.5
				Sulfur	.7	.5	.8
				Ash	8.6	6.2	10.9
				Heating value, Btu/lb, as received	7790	7290	8232

TABLE 2. - Comparison of the reproducibility of specific analytical tests

Tests	Replicates				Average	Standard deviation	Relative standard deviation
Ignited dissolved solids.....ppm..	105	87	91		94	9.4	10
Dissolved solids.....ppm..	1,499	1,296	1,396		1,384	82.2	6
Total organic carbon.....ppm..	4,650	4,550	4,700		4,633	76.4	1.6
Specific gravity.....	1.0073	1.0079	1.0075		1.0076	.0003	.03
pH.....	8.33	8.27	8.21		8.27	.067	.7
Alkalinity $CaCO_3$.....ppm..	12,235	12,974	13,012		12,740	438	3.4
Ammonia.....ppm..	4,065	4,298	4,266		4,210	126	3.0
Sulfur.....ppm..	881	876	877	864	875	7	0.8
Sulfide.....ppm..	136	144	160	152	148	10	7.0
COD.....ppm..	11,040	11,040	9,200	12,880	11,040	1,500	13.6

TABLE 3. - Comparison of mass rate of effluents produced by different sampling methods, RA-11 through -21[a/]

Test run number	RA-18	RA-11	RA-12	RA-14	RA-16	RA-21	RA-17
Operating conditions:							
Gasifier operating pressure ....psig..	100	200	200	400	400	400	400
Oxygen rate....scfh..	4,000	4,000	4,000	4,000	4,000	4,000	6,000
Steam-oxygen rate....	1.0	1.0	1.0	1.0	1.0	1.0	1.0
Coal moisture....pct..	22.8	25.3	26.3	24.2	23.9	30.5	22.8
Gas production....scfh..	20,108	20,125	20,460	20,006	20,079	19,765	29,637
EFFLUENT PRODUCTION:							
Water Production lb/Ton MAF Coal:							
End of run composite....	990	822	1,059	624	849	1,190	871
Recycle water....	874 ± 109	899 ± 156	1013 ± 57	1009 ± 30	1001 ± 72	1080 ± 177	821 ± 129
Side stream sampler I....	886 ± 93	b/	988 ± 32	b/	838 ± 71	1340 ± 86	807 ± 90
Side stream sampler II....	1044 ± 11	b/	b/	b/	831	913 ± 12	844 ± 26
Ammonia Production lb/Ton MAF Coal:							
End of run composite....	6.5	6.1	7.1	6.0	7.2	9.2	8.7
Recycle water....	5.7 ± 0.5	7.6 ± 0.1	6.9 ± 2.6	9.9 ± 2.0	9.3 ± 1.2	8.3 ± 0.8	8.7 ± 2.0
Side stream sampler I....	5.7 ± 0.9	b/	7.7 ± 0.5	b/	7.7 ± 0.6	9.2 ± 0.2	7.5 ± 0.5
Side stream sampler II....	7.8 ± 0.6	b/	b/	b/	9.8	8.2 ± 0.8	9.7 ± 0.5
Dissolved Organic Production lb/ Ton MAF Coal:							
End of run composite....	9.7	17.3	10.4	6.3	10.4	12.9	8.2
Recycle water....	8.0 ± 0.9	13.0 ± 4.6	9.4 ± 1.9	11.2 ± 3.4	10.0 ± 0.8	9.2 ± 2.4	8.3 ± 2.8
Side stream sampler I....	8.4 ± 0.8	b/	9.7 ± 0.7	b/	7.7 ± 1.0	13.5 ± 1.25	6.2 ± 0.1
Side stream sampler II....	10 ± 1.0	b/	b/	b/	8.2	9.0 ± 0.5	7.5 ± 0.2
Tar Production lb/Ton MAF Coal:							
End of run composite....	92.4	70.6	69.6	50.6	60.4	70.4	71.9
Recycle water....	b/	b/	b/	b/	b/	b/	b/
Side stream sampler I....	105 ± 4	68.5 ± 10.9	79.4 ± 10.9	87.9	55.6 ± 6	98 ± 23	87 ± 11
Side stream sampler II....	95 ± 6	b/	b/	b/	58.1	52 ± 2	55 ± 10

a/ Data expressed as x ± y indicates an average of several values and the standard deviation.
b/ Not determined.

TABLE 4. - Effluent data from composite spray washer samples

Test run number	RA-18	RA-11	RA-12	RA-14	RA-16	RA-21	RA-17
Test run condition:							
Gasifier operating pressure.....psig..	100	200	200	400	400	400	400
Oxygen rate.....scfh..	4,000	4,000	4,000	4,000	4,000	4,000	6,000
Coal moisture.....pct..	22.8	25.8	26.3	24.2	23.9	30.5	22.8
Liquor analysis:							
pH.....	8.7	8.56	8.54	8.9	9.0	8.6	9.6
Alkalinity, ppm as $CaCO_3$.....	13,786	b/	14,516	13,500	19,470	14,800	20,873
Turbidity, JTU.....	b/	b/	62	43	66	b/	b/
Conductivity, MHO.....	18,000	b/	21,500	b/	b/	b/	19,000
TOC, concentration a/.....ppm..	9,747	21,040	9,847	10,015	12,205	10,800	9,204
NH_3, concentration a/.....ppm..	6,544	7,420	6,704	9,605	8,500	7,721	9,953
Total dissolved solids a/.....ppm..	8,025	5,261	3,579	2,924	4,840	3,743	9,190
Inorganic dissolved solids a/.....ppm..	321	352	397	418	291	293	465
Sulfur, concentration a/.....ppm..	b/	b/	b/	b/	b/	593	413
Sulfide, concentration a/.....ppm..	b/	b/	b/	b/	b/	415	210
Elemental production rate and mass balance:							
Carbon in effluent.....lb/ton MAF coal..	86.1	78.6	71.8	49.3	61.8	71.1	74.6
Nitrogen in effluent...lb/ton MAF coal..	7.1	6.6	7.5	6.4	7.9	9.6	9.3
Sulfur in effluent.....lb/ton MAF coal..	b/	b/	b/	b/	b/	1.1	.7
Pct of coal carbon in effluent.....	6.1	5.7	5.2	3.6	4.4	5.0	5.3
Pct of coal nitrogen in effluent.....	40.6	28.6	35.1	27.6	33.4	36.9	48.3
Pct of coal sulfur in effluent.....	b/	b/	b/	b/	b/	4.6	3.8

a/ All concentrations are corrected for start up water.
b/ Not determined.

TABLE 5. - Mass spectrometer analysis of organics liquor in aqueous fraction from composite sample RA-14

Component	ppm	Percent
Phenol	5,647	56.4
Cresol	1,965	19.6
Xylenol	453	4.5
Methylnaphthalene	34	0.3
Biphenyl	19	0.2
Dimethylnaphthalene	26	0.3
Fluorene	17	0.2
Carbazole	9	0.1
Dibenzofuran	74	0.7
Phenanthrene	318	3.2
Methyloibenzofuran	101	1.0
Methylphenanthrene	76	0.7
Pyrene/Fluoranthene	100	1.0
Methylpyrene	178	1.8
Benzonaphthofuran	68	0.7
Chrysene	12	0.1
Benzopyrene	71	0.7

TABLE 6. - Mass spec analysis of tars from gasifier run RA-21, percent

Sampling method	Sampler I			Sampler II			Sampler III	End of run Composite
Test period	2 & 3	4 & 5	6 & 7	2 & 3	4 & 5	6 & 7	2 thru 7	1 thru shutdown
Phenols	24.3	22.8	26.7	23.2	32.6	29.0	33.0	23.1
Napthols	3.3	4.1	4.4	3.9	3.7	4.5	4.6	4.8
Dihydroxybenzenes	2.3	2.9	3.5	2.1	3.4	3.4	4.0	2.7
Naphthalenes	11.0	10.9	11.2	11.1	12.5	11.3	14.4	9.5
Aromatic Hydrocarbons with 3 to 5 rings	8.2	11.2	9.4	9.6	5.4	6.6	9.3	5.7
Saturated Hydrocarbons	3.3	4.3	5.5	6.9	4.0	4.5	2.7	6.6
Non Volatile at 300° C and .1 torr.	6.8	8.4	6.2	5.0	3.8	6.2	8.7	10.7
Average Mol wt of Volatile Compounds	147	154	150	151	140	145	145	139

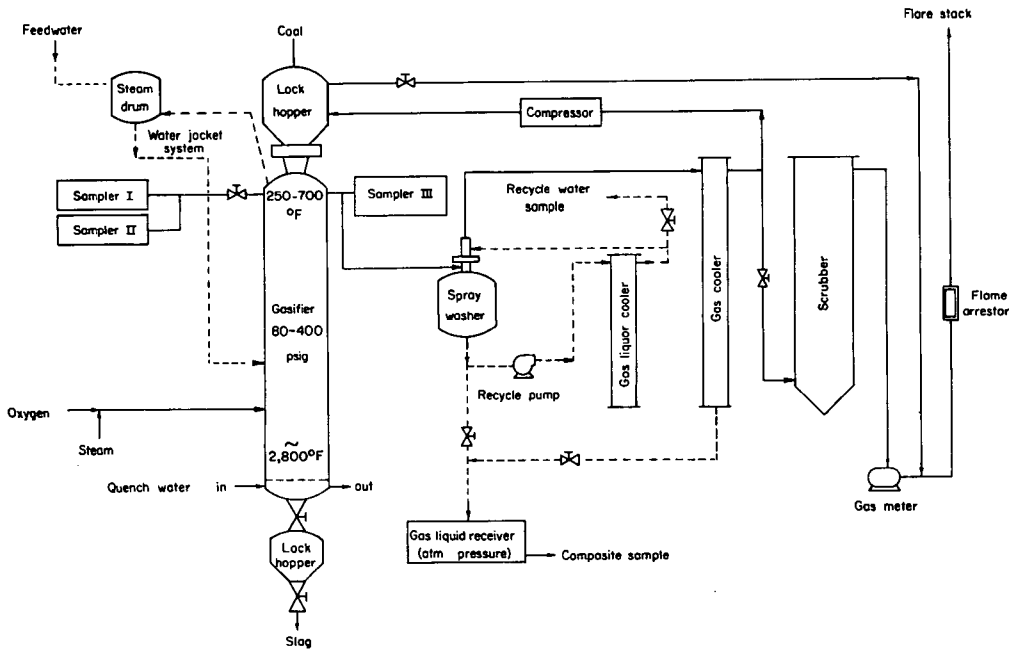

Figure 1. - Schematic of Grand Forks Energy Research Center slagging gasifier pilot plant.

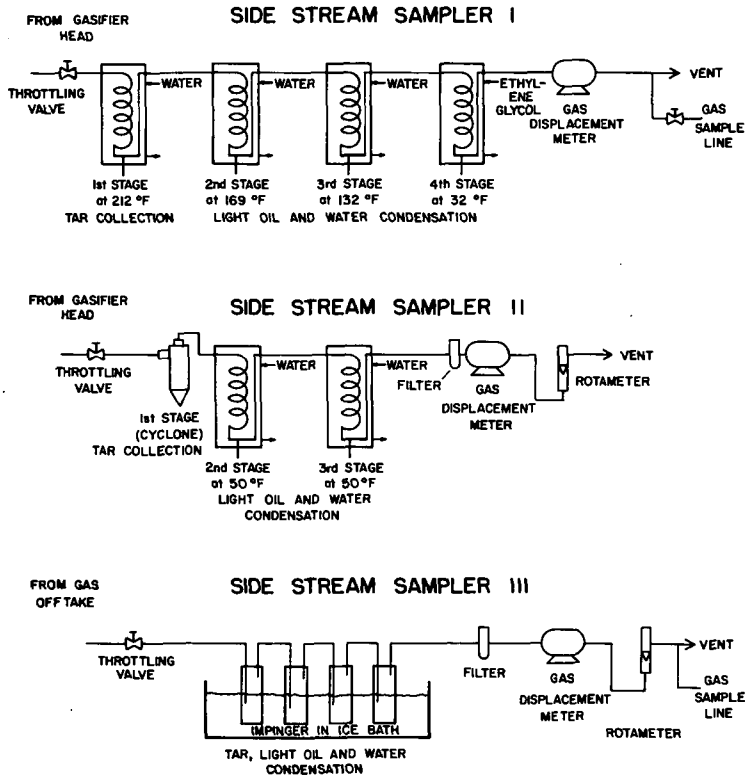

Figure 2. - Sampling trains used to condense effluents from gas stream.

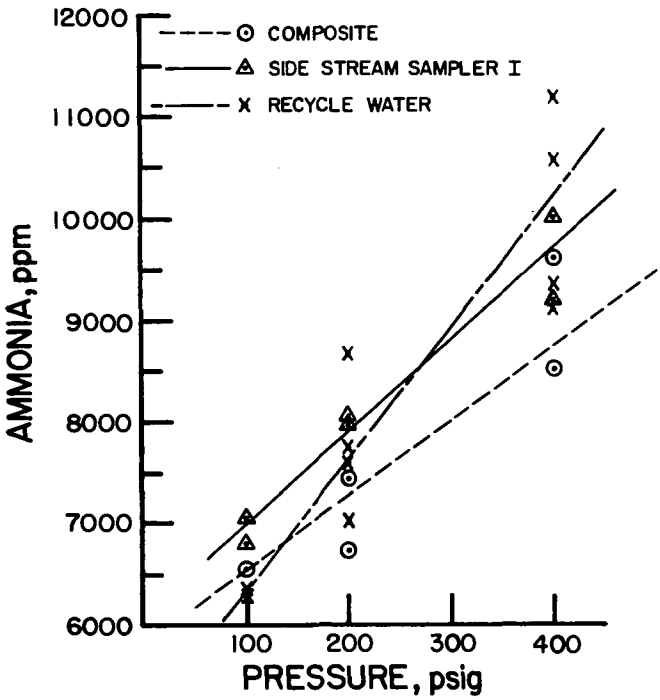

Figure 3. - Ammonia concentration in liquor as a function of gasifier pressure.

ANALYTICAL STUDY OF THE EFFLUENTS FROM A HIGH TEMPERATURE ENTRAINED FLOW GASIFIER

Milton L. Lee, Ralph Ahlgren, Lee R. Phillips,
Nolan F. Mangelson, and Lee D. Hansen

Chemistry Department and Thermochemical Institute
Brigham Young University
Provo, Utah 84602

Ralph L. Coates

Mountain Fuel
180 East 100 South
Salt Lake City, Utah 84139

INTRODUCTION

The toxic and carcinogenic potentials of various coal conversion products and by-products have led to detailed studies of effluents including trace contaminants produced by coal gasifiers. A wide variety of coal gasification schemes have been proposed, and many are presently under development to meet the immediate and future demands for clean gaseous fuels.

High temperature entrained flow coal gasifiers have a well-known advantage over lower temperature fixed-bed or stirred-bed gasifiers. This advantage is the marked reduction in tars, phenols, and other condensible hydrocarbons as gasifier by-products. For example, the Lurgi fixed-bed gasifiers produce from 50-100 pounds of tar, 30-70 pounds of tar oil and naptha, and 8-12 pounds of phenols per ton of coal (1,2). Similar by-product compounds and yields have been reported for a fluidized bed gasifier operated by the Pittsburgh Energy Research Center (3). On the other hand, the Koppers-Totzek and Texaco High temperature entrained flow gasifiers are claimed to produce negligible amounts of tars or oils as by-products. The gas and water purification equipment is, therefore, less complicated and less expensive than that required for the Lurgi process. It was anticipated that advanced high temperature entrained flow gasifiers would also have this advantage.

The experimental gasifier studied in this report is a pressurized, entrained-flow gasifier that has a capacity of 100 pounds of coal per hour. This gasifier has a downflow configuration with some similarity to an entrained flow gasifier operated by the Bureau of Mines during the period 1952-1962. It also has some similarity to the Texaco entrained flow gasifier configuration. Throughput rates of over 1,000 pounds of coal per hour per cubic foot of gasifier volume have been demonstrated with cold gas conversion efficiencies in excess of 75 percent.

A diagram of the laboratory gasifier and the necessary coal feeding, gas cooling and cleaning, and ash handling equipment is presented in Figure 1. Major equipment is noted in this figure.

Pulverized coal is fed to the gasifier from a pressurized feed hopper entrained in a stream of air or recycled product gas. The coal is rapidly mixed and reacted with a mixture of superheated steam and oxygen. The reaction is carried out at pressures of 50 to 300 psig and gasifier outlet temperatures 2300-2800°F. Residence times for gasification reactions are of the order of 0.1 second.

The gasifier products pass downward into a quench section where they are partially cooled by mixing with a feed stream of water and/or saturated steam or simply by heat transfer to monotube boiler coils which form the walls of this section. Sufficient cooling occurs in this section to solidify the molten ash droplets.

The products then pass into a slag removal section where the slag droplets and larger fly-ash particles are separated by gravity, dropping into the lower section of this vessel that is partially filled with water. The slag is periodically discharged through a lock hopper and transported to a settling pond. The gasification products then pass through a heat exchanger and into a scrubber column.

Cleaning of soot and fly-ash particles from the gas is accomplished in the water scrubber column. Unreacted steam is also condensed in this column. A recycle water stream is pumped through a heat exchanger to remove the heat of condensation, and a feed stream of cooled water is introduced at the top of this column to provide final cooling and washing, and to suppress foaming. Approximately six pounds of cooled water is required per pound of coal fed.

The overflow from the scrubber passes through a fabric filter to remove the solids and the filtered liquor is discharged through a pressure reduction valve into a flash tank where dissolved gases are released and separated from the water.

In this study, a detailed characterization of pollutants associated with the previously described gasifier has been performed.

EXPERIMENTAL

Samples were taken from the cooled and water-scrubbed product gas stream, the scrubber effluent water, the gas evolved on depressurization of the scrubber water, and the particulate matter filtered from the scrubber water during gasification of a high-volatile, non-caking, Utah bituminous coal. Four process parameters were varied; coal feed rate, reactor pressure, oxygen to coal ratio, and steam to coal ratio. The compositions of these samples were determined using the analytical techniques of gas chromatographic mass spectrometry, proton-induced x-ray emmission spectroscopy, thermometric titrimetry, ion chromatography, and atomic absorption spectroscopy. The scrubber water analysis scheme is shown in Figure 2.

RESULTS AND DISCUSSION

The gasifier test matrix is given in Table 1. Individual runs were made under each set of conditions, and only one condition was varied in consecutive runs. The constituents found in the product gas, filtered scrubber water, organic extract of

Table 1. GASIFIER TEST MATRIX

Run Number	Coal Feed Rate (lbs. coal/hr.)	Reactor Pressure (PSIA)	Oxygen to Coal Ratio	Steam to Coal Ratio
1	40	150	0.9	0.1
2	40	150	0.9	0.3
3	40	150	0.9	0.5
4	40	150	0.8	0.3
5	40	150	1.0	0.3
6	40	300	0.9	0.3
7	40	75	0.9	0.3
8	20	150	0.9	0.3
9	60	150	0.9	0.3

particulate matter, and gas obtained during depressurization of the scrubber water are given in Tables 2 through 5. The variation from run to run was found to be insignificant and, therefore, the values reported are averages of all runs. These data emphasize the low levels of contamination produced by this particular gasifier. The comparison between the scrubber water and the uncontaminated water before entry

into the scrubber tank (Table 3) demonstrates the cleanliness of the gasifier operation. Even the organic compound levels are extremely low (Table 4). The presence of phthalates in the scrubber water is due to a ramming mix used in the reactor.

Table 2. PRODUCT GAS COMPOSITION

Species[a]	Average Volume Percent	Analytical Technique Used[b]
CO	42.4	GC
H_2	31.2	GC
CO_2	12.3	GC
N_2	6.3	GC
CH_4	7.2	GC
	Average Concentration (ppm)	
H_2S	590	DT
HCN	1.7	DT

[a] SO_2, COS, NH_3, CS_2 and hydrocarbon gases were not detected.

[b] GC = Gas Chromatography, DT = Dräger Tube

Table 3. ANALYSIS OF FILTERED SCRUBBER WATER

Species	Average Concentration (ppm) Before Scrubber	After Scrubber	Analytical[a] Technique Used
Elemental			
S	10.0	17.8	PIXE
Cl	19.2	18.4	PIXE
K	0.5	1.4	PIXE
Ca	28.7	75.4	PIXE
Fe	0.3	11.6	PIXE
Cu	0.2	0.2	PIXE
Zn	0.3	1.2	PIXE
Sr	0.0	1.0	PIXE
Inorganic			
F^-	0.1	1.4	IC
Cl^-	11.7	13.7	IC
NO_2^-	0.1	0.3	IT
SO_3^-	4.4	3.9	IC
NO_3^-	1.9	2.5	IC
SO_4^{2-}	41.4	43.4	IC
HCO_3^-	219.0	390.1	TT
Organic			
Tributylphosphate	0.0	2.7×10^{-3}	GC
Dibutylphthalate	0.0	2.8×10^{-3}	GC

[a] PIXE = Proton-Induced X-Ray Emission Spectroscopy
IC = Ion Chromatography
TT = Thermometric Titrimetry

Table 4. GAS CHROMATOGRAPHIC ANALYSIS OF ORGANIC EXTRACT OF PARTICULATE MATTER FROM SCRUBBER WATER

Compound[a]	Average Concentration[b] (expressed as ppb in scrubber water)
Naphthalene	25.0
1-Methylnaphthalene	1.4
2-Methylnaphthalene	1.3
Biphenyl	1.2
Acenaphthylene	5.8
Acenaphthene	5.3
Methylacenaphthylene	3.1
Phenanthrene	3.7
Fluoranthene	2.9
Pyrene	3.3
dibutylphthalate	6.1
diamylphthalate	7.0

[a]A number of additional unidentified compounds were present in concentrations less than 0.5 ppb

[b]All quantitation of organic compounds was done with respect to a naphthalene standard

Table 5. ANALYSIS OF GAS OBTAINED DURING DEPRESSURIZATION OF SCRUBBER WATER

Species[a]	Average Concentration (expressed as ppm in scrubber water)	Analytical Technique Used[b]
CO	87.7	GC
H_2	2.3	GC
CO_2	160.1	GC
N_2	80.5	GC
CH_4	8.5	GC
H_2S	1.6	DT
HCN	0.02	DT
SO_2	1.7	DT

[a]COS, CS_2, NH_3 and hydrocarbon gases were not detected

[b]GC = Gas Chromatography, DT = Dräger Tube

REFERENCES

1. "El Paso Natural Gas Company Burnham I Coal Gasification Complex Plant Description and Cost Estimates", Sterns-Roger, Inc., Denver, Colorado, October 1973.

2. "Trials of American Coals in a Lurgi Gasifier At Westfield, Scotland", Woodall-Duckham, Ltd., Sussix, England, ERDA Report No. FE-105.

3. Nakles, D. V., et. al., "Influence of Synthane Gasifier Conditions on Effluent and Produce Gas Production", Pittsburgh Energy Research Center, ERC/RI-75/6, December 1975.

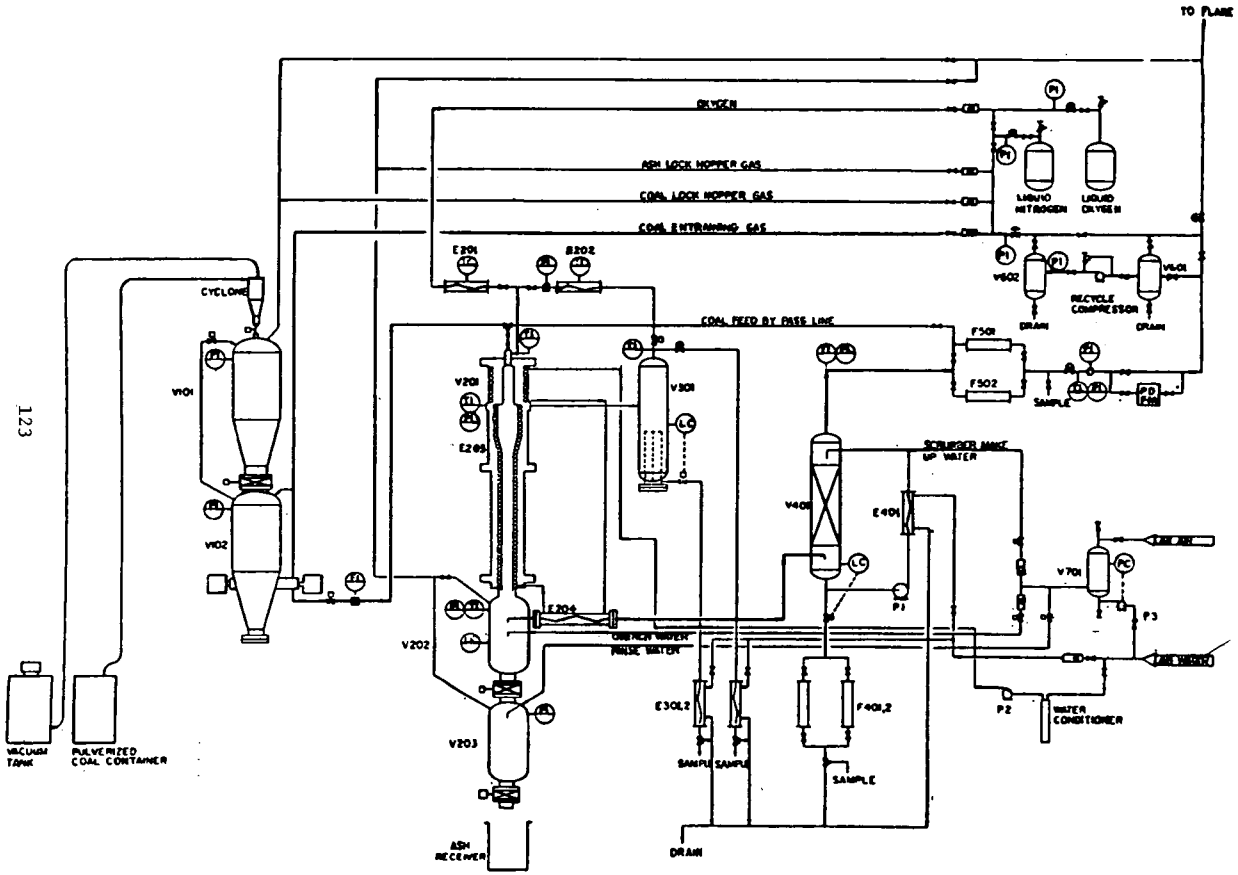

Figure 1. Flow diagram of Laboratory Scale Gasifier

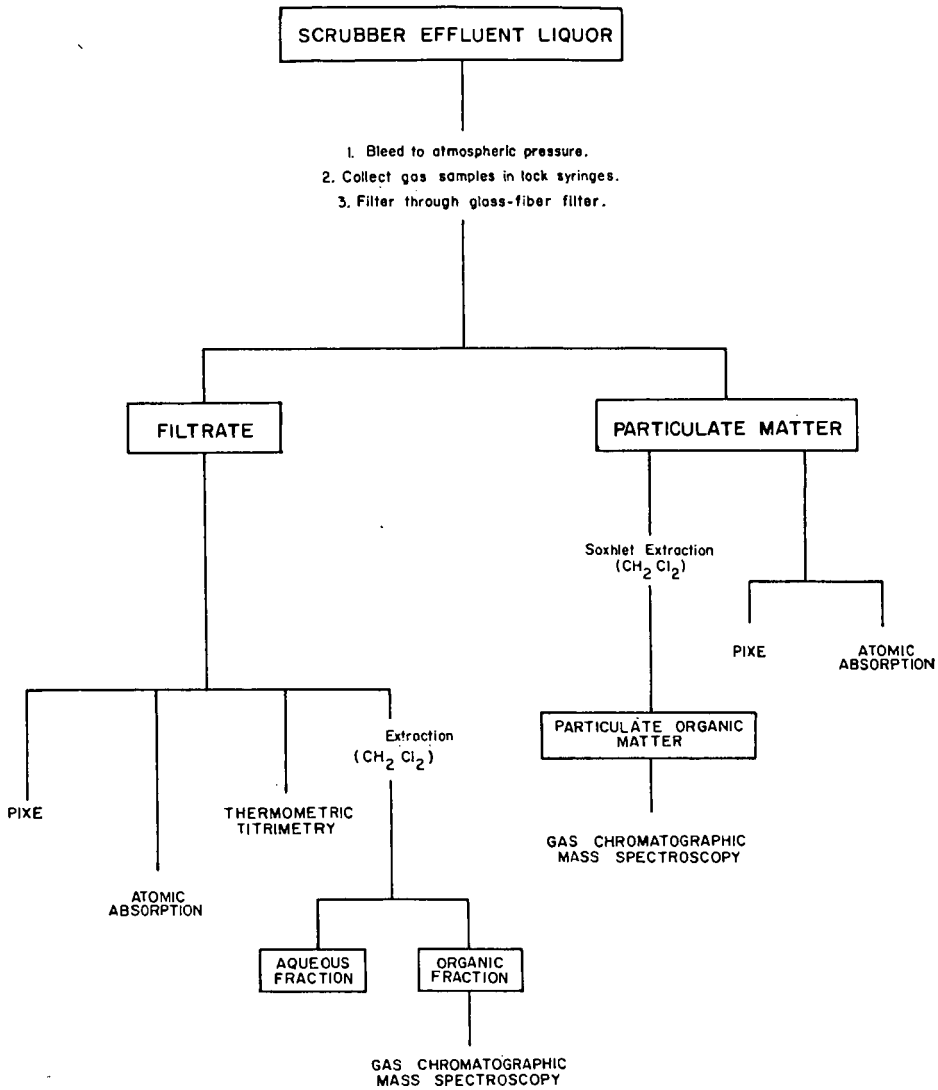

Figure 2. Scrubber water analysis flow diagram

LEACHING OF ORGANIC RESIDUALS FROM SIMULATED IN SITU RETORTED OIL SHALE

G. L. Amy,[1] J. F. Thomas,[1] and A. L. Hines[2]

[1]Sanitary Engineering, University of California, Berkeley, CA 94720
[2]Chemical and Petroleum-Refining Engineering,
Colorado School of Mines, Golden, CO 80401

Introduction

Various economic and environmental constraints have thus far inhibited development of oil shale resources by surface-retorting technologies. In an attempt to overcome these constraints, recent attention has focused on in situ methods of retorting oil shale.

In certain geographical areas, oil shale occurs as a continuous, relatively impermeable layer situated between two groundwater aquifers. An example of this situation is the Piceance Basin in Colorado where a rich layer of oil shale known as the Mahogany Zone persists throughout most of the basin. In areas such as the Piceance Basin, a major environmental hazard associated with in situ development is that it may potentially contaminate groundwater from adjacent aquifers. This potential contamination may evolve as a consequence of various organic and inorganic species being leached from the spent shale by groundwater migration into an abandoned underground retort (1),(2). During retorting, oil shale is transformed from a relatively inert substance into an unstable material containing various water soluble organic and inorganic components. The purpose of this paper is to assess the potential for contamination of groundwater by various organic residuals leached from in situ type spent shale.

Leaching Experiments

Two types of laboratory experiments were conducted to assess the potential for contamination of groundwater by organic leachants. These included (1) preliminary batch experiments and (2) equilibrium batch experiments. Both of these leaching experiments examined a series of unique spent shale samples under various experimental conditions. The analytical parameter selected for monitoring the quality of leachate was Total Organic Carbon (TOC).

Spent Shale Samples

Spent shale samples examined during this study were obtained from Lawrence Livermore Laboratory's (LLL) pilot-scale 125-Kg simulated in situ retort. The raw oil shale used by LLL was mined from the Anvil Points area in Colorado. The Fischer Assay of the raw oil shale was 24 gallons per ton while the organic carbon content of the raw oil shale was 10.8% by weight.

The retorting conditions employed during the production of spent shale are summarized in Table 1. As shown in Table 1, these samples represent a wide cross-section of the types of spent shale that may be produced under various retorting conditions.

The physical characteristics (i.e., particle size range, density, and porosity) of the spent shale samples examined in the leaching experiments were generally similar. However, a major difference observed was their solid-phase organic carbon content. The solid-phase organic carbon content of Types 1, 2, 3, and 4 spent shales was 0.2%, 1.8%, 2.1%, and 3.9% by weight, respectively.

As anticipated, the Type 1 spent shale contained the least organic carbon since it was produced during combustion retorting. In contrast, the Types 2 and 4 spent

shales contained higher levels of organic carbon as a result of retorting in an inert gas atmosphere. The Type 3 spent shale is perhaps the most interesting with respect to organic carbon content. Since the Type 3 spent shale was produced during combustion retorting, it was initially anticipated that very little residual organic material would remain on the shale matrix. However, for this particular type of spent shale, it is important to note that recycle gas was employed as part of the input gas. Since recycle gas contains significant amounts of volatile organics (3), it is hypothesized that the high organic carbon content of the Type 3 spent shale may be due to either the adsorption of certain volatile organics originally present in recycle gas or the condensation of hydrocarbons onto the shale behind the flame front.

Table 1. Retorting Conditions Employed in Production of Spent Shale Samples.

	Spent Shale Samples			
Retorting Parameter	Type 1	Type 2	Type 3	Type 4
Type of Retorting Run	Combustion	Inert Gas	Combustion	Inert Gas
Input Gas	Air + N_2 (7.6% O_2)	N_2	Air + Recycle Gas (10.5% O_2)	N_2
Maximum Retorting Temperature (^oC)	750	510	935	-
Retorting Rate (meters/day)	0.69	1.40	1.34	-

Source; W. Sandholtz, Lawrence Livermore Laboratory, letters dated 11/4/76 and 12/20/76.

Preliminary Batch Experiments

The preliminary batch experiments consisted of placing a small mass of spent shale (50 grams) and a small volume of water (50 milliliters) into a series of flasks. After sealing, each flask was allowed to quiescently sit for a designated time period, ranging up to 30 days. At the end of the designated time period, the leachate was decanted, filtered, and analyzed for Total Organic Carbon (TOC). For each type of spent shale examined, leachate samples from a series of these flasks were allowed to sit for time periods ranging from 0.5 to 30 days and were subsequently analyzed for TOC. In most cases, "pseude-equilibrium" conditions were attained after 30 days of leaching.

The major impetus behind the preliminary batch experiments was to identify factors that influence the leaching of organic material. Several experimental variables were examined, including: (1) retorting conditions, (2) temperature of the leach water, and (3) the initial quality of leach water.

The two water temperatures examined were 20^oC and 80^oC. The lower of these temperatures, 20^oC, represents the room temperature of the laboratory in which the experiments were conducted and is considered to be approximately representative of ambient groundwater temperature. The higher temperature, 80^oC, is considered to be approximately representative of anticipated water temperatures within an abandoned retort which has not cooled. Groundwater migrating into an abandoned retort may initially be converted to steam which will condense at temperatures slightly less than 100^oC.

The two general categories of leach water examined were distilled water and synthetic groundwater. The distilled water was considered to be approximately representative of good quality groundwater. The synthetic groundwater was produced in the laboratory by adding specified amounts of $NaHCO_3$, Na_2CO_3, NaCl, and Na_2SO_4 to distilled water. The specific conductivity of the synthetic groundwater was 12,000 μmhos/cm and its pH was 9.0. The synthetic groundwater was considered to be approximately representative of groundwater found in the lower aquifer of the Piceance Basin; groundwater from this aquifer is characterized by high levels of sodium and the carbonates.

The results of the preliminary batch experiments conducted for a leaching time period of thirty days are summarized in Table 2. As shown, retorting conditions, water temperature, and initial quality of leach water significantly influenced the leaching of organic material.

Employing distilled water at a temperature of 20°C, the highest level of organic carbon was observed in leachate derived from the Type 3 spent shale. It is hypothesized that most of the water soluble organic compounds associated with the Type 3 spent shale were originally components of recycle gas that adsorbed onto the spent shale matrix. These were held by weak physical forces and were readily leachable. The lowest organic carbon level was detected in leachate derived from the Type 1 spent shale. This may be attributed to its low solid-phase organic carbon content. The levels of organic carbon in leachate derived from spent shale samples produced during inert gas retorting were intermediate to values found in leachate derived from Types 1 and 3 spent shales.

Table 2. Preliminary Batch Experiments

	Total organic carbon (TOC) leached, mg/100 g of spent shale			
Experiment type	Type 1	Type 2	Type 3	Type 4
30-day distilled water batch exps. @ 20°C	1.1	1.9	3.5	1.7
30-day distilled water batch exps. @ 80°C	1.3	3.1	2.9	3.1
30-day groundwater batch exps. @ 20°C	1.0	2.3	3.8	2.0
30-day groundwater batch exps. @ 80°C	1.0	5.8	3.4	4.7

Employing distilled water at a temperature of 80°C, the highest levels of organic carbon were observed in the leachate obtained from samples produced during inert gas retorting. A comparison of experiments conducted with distilled water at temperatures of 20°C and 80°C reveals that the leaching of organic material from Types 2 and 4 spent shales was significantly enhanced at the higher temperature. This was attributed to the increased solubility of organic compounds at the higher water temperature. An elevated temperature appeared to have little overall effect on the leaching of organic material from Types 1 and 3 spent shales.

Employing groundwater at 20°C, the highest level of organic carbon was detected in leachate derived from the Type 3 spent shale while the lowest level was detected in leachate derived from the Type 1 spent shale. The results of the groundwater experiments conducted at 20°C were generally similar to the results of the corresponding

distilled water experiments. This implies that, at 20°C, the initial quality of leach water had little overall effect on the leaching of organic material.

Using groundwater at 80°C, higher levels of organic carbon were found in the leachate obtained from spent shale produced by inert gas retorting than in other samples. A comparison of groundwater experiments conducted at 20°C and 80°C reveals that a higher temperature significantly enhanced the leaching of organic material from Types 2 and 4 spent shales. The above observations are similar to those made when using distilled water. For Types 2 and 4 spent shales, significantly greater quantities of organic carbon were found in leachates obtained when using groundwater at 80°C than in the distilled water experiments conducted at the same temperature. This implies that some kind of synergistic mechanism, involving both water temperature and initial quality, resulted in more organic material being leached from Types 2 and 4 spent shales during the high-temperature groundwater experiments than during the high-temperature distilled water experiments.

Equilibrium Batch Experiments

The equilibrium batch experiments consisted of placing a small mass of spent shale (50 grams) and a variable volume of water, ranging from 30 to 200 milliliters, into a series of flasks. Each flask was sealed and allowed to quiescently sit for a period of 30 days. After this period, the leachate was decanted, filtered, and analyzed for TOC.

The major impetus behind the equilibrium batch experiments was to generate data enabling the development of equilibrium isotherms. The results of the preliminary batch experiments suggested that 30 days was, in most cases, an adequate time period for the establishment of "psuedo-equilibrium" conditions. Consequently, a leaching time of 30 days was used.

The experimental variables examined during the equilibrium batch experiments were identical to those considered during the preliminary batch studies with the following exceptions: (1) only Types 1 and 2 spent shales were used and (2) a series of shale to water ratios were evaluated.

The results derived from the equilibrium batch experiments are presented in Table 3. As shown, the concentration of organic carbon in all leachates increased for greater shale to water ratios.

An attempt was made to model the data derived from the equilibrium batch experiments by employing both the Freundlich and Langmuir equations. The Freundlich model is defined by;

$$q = KC^{1/n} \qquad (1)$$

where q = mass of solute adsorbed per unit mass of adsorbant
C = equilibrium concentration of solute
K & n = constants

Transforming the above equation into logarithmic form yields;

$$\log q = \log K + 1/n \log C \qquad (2)$$

In contrast to the Freundlich model, the Langmuir equation is defined by;

$$q = \frac{abC}{1 + aC} \qquad (3)$$

where a & b = constants

The Langmuir equation is often expressed in linear form as;

$$\frac{1}{q} = \frac{1}{b} + \frac{1}{ab} \frac{1}{C} \qquad (4)$$

Table 3. Equilibrium Batch Experiments

Type of Experiment	Concentration of Organic Carbon (mg/l)							
	Type 1				Type 2			
	50 g + 30ml	50 g + 50ml	50 g + 100ml	50 g + 200ml	50 g + 30ml	50 g + 50ml	50 g + 100ml	50 g + 200ml
Distilled Water at 20°C	18	11	5.0	3.9	25	19	11	5.4
Distilled Water at 80°C	16	13	6.9	4.9	36	31	24	15
Groundwater at 20°C	19	10	6.9	3.6	25	23	10	6.7
Groundwater at 80°C	16	10	7.7	4.4	67	58	38	17

	Mass Leached Per Unit Mass (mg/100 g)							
	Type 1				Type 2			
	50 g + 30ml	50 g + 50ml	50 g + 100ml	50 g + 200ml	50 g + 30ml	50 g + 50ml	50 g + 100ml	50 g + 200ml
Distilled Water at 20°C	1.1	1.1	1.0	1.6	1.5	1.9	2.2	2.2
Distilled Water at 80°C	1.0	1.3	1.4	2.0	2.2	3.1	4.8	6.0
Groundwater at 20°C	1.1	1.0	1.4	1.4	1.5	2.3	2.0	2.7
Groundwater at 80°C	1.0	1.0	1.5	1.8	4.0	5.8	7.6	6.8

The Freundlich and Langmuir models were originally developed to describe the adsorption phenomenon. In some cases, experimental data will fit one model better than the other. If experimental data conform to the Freundlich model then a plot of log q versus log C should be linear. Correspondingly, if experimental data conform to the Langmuir model, then a plot of 1/q versus 1/C should be linear.

In order to apply the above adsorption models to a leaching/desorption phenomenon, it is necessary to redefine the parameters C and q. The parameter C is defined as the equilibrium TOC contration in the leachate, expressed in terms of mg/l. The parameter q is defined as the mass of organic carbon remaining on the spent shale per unit mass of spent shale (expressed in terms of mg TOC/g spent shale). The parameter q can be estimated by subtracting the mass of organic carbon leached, as defined by measurements of C, from the initial solid-phase organic carbon content of the spent shale sample.

A least squares computer subroutine was used to estimate constants for both the Freundlich and Langmuir models. Estimates of constants for each equation are presented in Table 4. Employing these constants, either model can be used to predict the equilibrium TOC concentration resulting from a particular shale to water ratio.

Table 4. Constants for Freundlich and Langmuir Models.

	Type 1 Spent Shale				Type 2 Spent Shale			
	Freundlich		Langmuir		Freundlich		Langmuir	
	K	n	a	b	K	n	a	b
Distilled Water at 20°C	1.98032	615.433	81.1577	1.99075	17.9688	3850.47	433.849	17.9846
Distilled Water at 80°C	1.97197	318.766	36.4383	1.99237	17.8187	408.520	19.1234	17.9995
Groundwater at 20°C	1.98256	816.308	111.354	1.99027	17.9638	3116.45	241.323	17.9852
Groundwater at 80°C	1.97152	274.904	36.5797	1.99405	17.7054	298.471	6.18471	17.9989

All data derived from the equilibrium batch experiments were plotted as log q versus log C and 1/q versus 1/C. The purpose of this graphical exercise was to examine the plots for linearity and thus, to ascertain whether a particular model was appropriate for various groups of data.

Experimental data obtained from the Type 2 spent shale are plotted according to the logarithmic form of the Freundlich Model in Figures 1 and 2 and according to the linear form of the Langmuir Model in Figures 3 and 4. Both the Freundlich and Langmuir equations appear to be fairly appropriate for modelling experimental data for the Type 2 spent shale.

In contrast to the Type 2 spent shale, the Freundlich and Langmuir equations appear to be less appropriate for modelling experimental data derived from the Type 1 spent shale. Although plots of log q versus log C and 1/q versus 1/C appeared to roughly follow a linear trend, they were not as linear as corresponding plots for the Type 2 spent shale. It appears that another isotherm model may be more appropriate.

Conclusions

Based on the results of the preliminary batch experiments, it is apparent that there exists a significant potential for contamination of groundwater by organic residuals leached from in situ spent shale, particularly spent shale produced during inert gas retorting or combustion retorting employing recycle gas. This contamination may preclude certain beneficial uses of groundwater in the immediate vicinity of abandoned in situ retorts.

Both the Freundlich and Langmuir equations appear to be fairly appropriate for modelling the leaching of organic material from spent shale samples produced during inert gas retorting.

Acknowledgements

The research described in this paper was jointly sponsored by ERDA and the Department of the Interior. Sincere appreciation is given to Lawrence Livermore Laboratory, in particular W. Sandholtz, for supplying samples of spent shale.

References

(1) G. Amy and J. Thomas, "Factors that Influence the Leaching of Organic Material from In Situ Spent Shale", Proceedings of Second Pacific Chemical Engineering Congress, 1977.

(2) H.W. Parker, "Simulated Groundwater Leaching of In Situ Retorted or Burned Oil Shale", 1976 (Quarterly Progress Report for Grant #G0254011 funded by ERDA for Texas Tech University.)

(3) Engineering Science, Inc., "Air Quality Assessment of the Oil Shale Development Program in the Piceance Creek Basin", 1974.

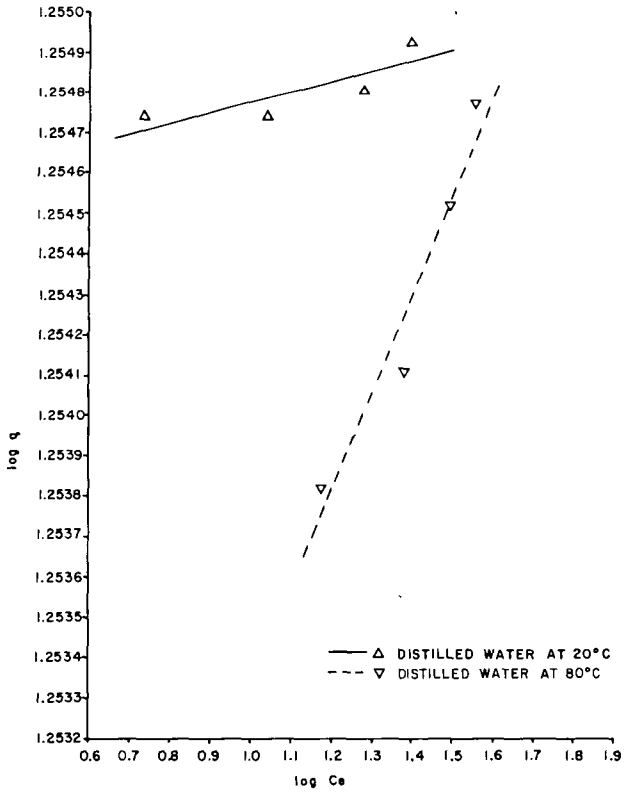

FIGURE 1. LOGARITHMIC FORM OF FREUNDLICH ISOTHERM FOR TYPE 2 SPENT SHALE/ DISTILLED WATER.

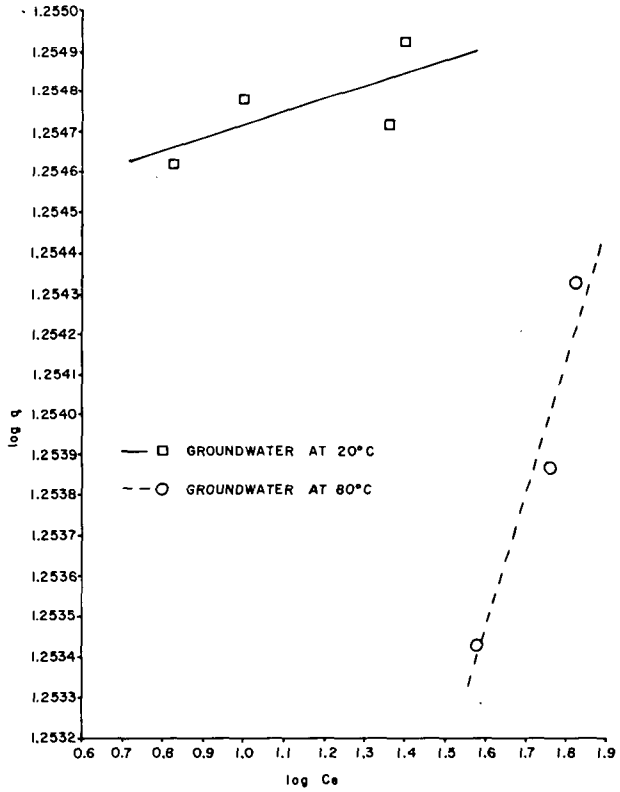

FIGURE 2. LOGARITHMIC FORM OF FREUNDLICH ISOTHERM FOR TYPE 2 SPENT SHALE/ GROUNDWATER.

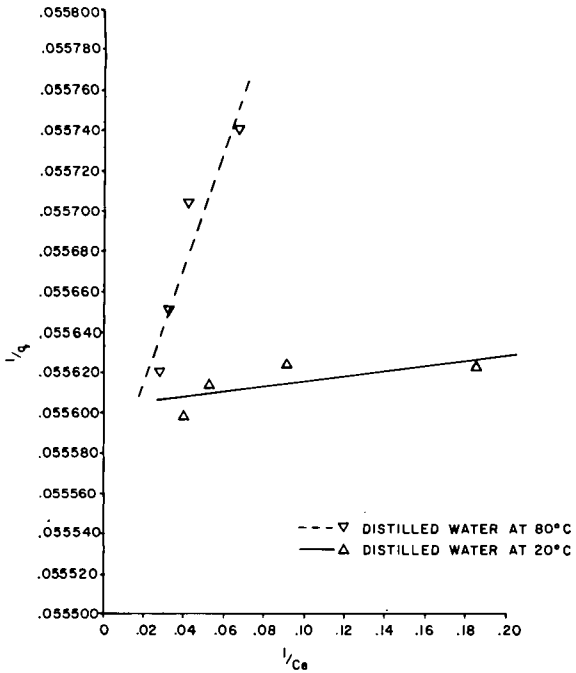

FIGURE 3. LINEAR FORM OF LANGMUIR ISOTHERM FOR TYPE 2 SPENT SHALE/DISTILLED WATER.

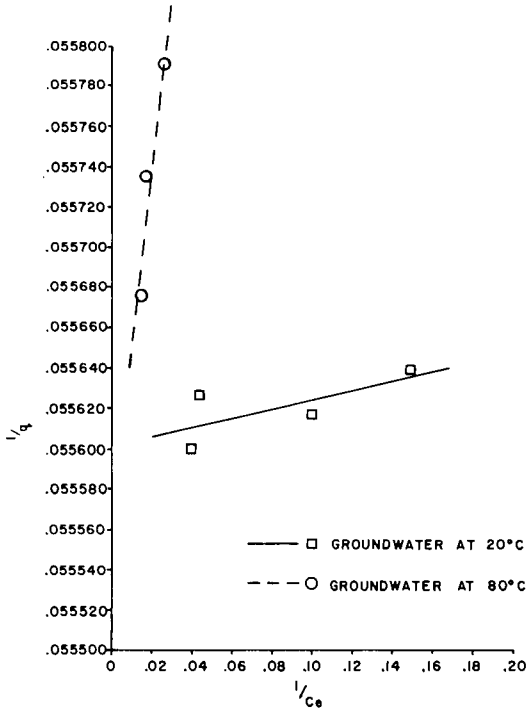

FIGURE 4. LINEAR FORM OF LANGMUIR ISOTHERM FOR TYPE 2 SPENT SHALE/GROUNDWATER.

ANALYSIS OF VOLATILE POLAR ORGANICS IN UNTREATED BY-PRODUCT WATERS FROM COAL CONVERSION PROCESSES

Curt M. White and Charles E. Schmidt

U. S. Department of Energy, Pittsburgh Energy Research Center
4800 Forbes Avenue, Pittsburgh, PA 15213

INTRODUCTION

Analysis of by-product waters from coal conversion processes is important because the need for constructing large-scale coal liquefaction and gasification plants is increasing. Coal liquefaction and gasification technologies will use or produce water which must be made environmentally acceptable before discharge from the plant. However, some gasification processes plan to recirculate a major portion of the process water within the plant. It is therefore necessary to obtain qualitative and quantitative data concerning the trace organic constituents present in these process waters in order that effective water treatment technologies can be developed and evaluated. This knowledge would also provide insight into the potential environmental impact of coal conversion processes.

Interest in trace organic constituents present in waters from coal conversion processes is not new. Schmidt, Sharkey and Friedel (1) identified a large number of organic components in SYNTHANE (2) gasifier condensate waters, using extraction techniques followed by analysis via combined gas chromatography-mass spectrometry (GC-MS) and high resolution mass spectrometry (HRMS). Ho, Clark and Guerin (3) have used direct aqueous injection gas chromatography to quantitate sixteen organic compounds present in by-product waters from two coal conversion processes. Ellman, Johnson, Schoubert, Paulson and Fegley (4) have recently used mass spectrometry to investigate the nature of water-soluble organics in water from a modified Lurgi slagging fixed-bed gasification process. Kavan and Basyrova (5) have determined by gas chromatography (GC) the ketone content of waste water from the "pressure gasification" of coal.

The present investigation was undertaken to more fully define the nature of the trace volatile polar organics in by-product waters from four coal conversion process development units, in order to provide input for water treatment process design and to develop rapid analytical techniques to monitor the effectiveness of various water treatments. The samples investigated included by-product waters from two gasification processes, SYNTHANE (2) and a modified Lurgi slagging fixed-bed gasification process (4), and two liquefaction processes, SYNTHOIL (6) and Project Lignite (7). A variety of analytical techniques were used, including direct aqueous injection GC-MS, GC-MS of extracts from these waters, and direct aqueous injection GC employing flame ionization and flame photometric detection.

EXPERIMENTAL

The combined GC-MS analyses were performed using a Varian* 1700 gas chromatograph equipped with a flame ionization detector interfaced to a DuPont 490 mass spectrometer. Mass spectrometric data reduction and storage was accomplished by a Hewlett-Packard 2100A computer. The mass spectrometer was operated at a resolution of one part in 600 and an ionizing voltage of 70 eV. The ion source, jet separator and glass line connecting the chromatograph to the spectrometer were held at 275° C.

*Use of brand names facilitates understanding and does not necessarily imply endorsement by the Department of Energy.

The chromatographic effluent was continuously scanned at a rate of four seconds per decade of mass by the mass spectrometer.

In most cases, the gas chromatographic separations were effected using a 20 ft. x 1/8 in. glass column packed with 60/80 mesh Tenax GC with a helium flow rate of 15 cc per minute. The column was held at 30° C for 6 minutes and then temperature programmed at 2 C^{o} per minute to 300° C.

Where possible the combined GC-MS analyses were performed by direct injection of the aqueous samples (8). In cases where the amounts of individual components present were insufficient to obtain usable mass spectrometric data, the waters were extracted using methylene chloride (1) and the resulting extracts were subjected to GC-MS analysis using conditions identical to those used during direct aqueous injection.

In general, identification of specific compounds was made on the basis of mass spectral data and in most cases was subsequently confirmed by co-chromatographic experiments in which pure compounds were spiked into the by-product waters. In a few cases, this was not done because standard compounds, such as certain alkyl furans and C_3-phenols, were not available.

Gas chromatographic analysis of the volatile sulfur constituents of SYNTHANE condensate water was performed using a Tracor 550 gas chromatograph equipped with a dual flame ionization detector and a flame photometric detector specific for sulfur. The sulfur components were chromatographed using a 10 ft. x 1/8 in. glass column packed with 60/80 mesh Tenax GC.

Identification of specific sulfur compounds using flame photometric detection was achieved solely on the basis of co-chromatographic experiments using by-product water spiked with authentic sulfur compounds. In addition, the mass spectrum of carbon disulfide was observed in a number of GC-MS experiments where the untreated by-product waters were injected directly into the GC-MS system.

Gas chromatographic results were quantitated by determining peak areas from chromatographic profiles obtained from direct aqueous injection of the by-product waters. In order to obtain specific response factors for individual compounds, a standard solution was injected and separated using chromatographic conditions identical to those under which the sample was analyzed.

RESULTS AND DISCUSSIONS

Figure 1 shows gas chromatographic profiles obtained by direct aqueous injection of by-product waters from four different coal conversion processes: 1. end-of-run liquor from a slagging fixed-bed gasifier (4); 2. by-product water from Project Lignite (7); 3. SYNTHANE (2) gasifier condensate water; and 4. SYNTHOIL (6) process development unit scrubber water. The numbered chromatographic peaks are identified in Table 1. The chromatographic profile of SYNTHANE condensate water, obtained using sulfur specific flame photometric detection, appears in Figure 2, and the numbered peaks are identified in Table 2.

The data presented in Table 2, obtained with the use of a flame photometric detector, are preliminary but illustrate the potential applicability of element-specific gas chromatographic detectors to the analysis of coal conversion products. The sulfur compounds identified in Table 2 have not been quantitated.

Table 1. Organic constituents in untreated by-product waters from coal conversion process development units.[a]

Peak #	Compound	Concentration in mg. per liter			
		Slagging gasifier	Project Lignite	SYNTHANE	SYNTHOIL
1	methanol	900	5000	140	80
2	ethanol	<10	320	<10	10
3	acetonitrile	500	320	210	40
4	isopropanol	--	5600	--	30
5	acetone	540		950	200
6	carbon disulfide	400	10,200	1400	40
7	acetic acid				--
8	propionitrile	60	30	40	<10
9	2-butanone	100	1100	230	100
10	propionic acid	30	3400	30	--
11	3-methyl-2-butanone	30	50	80	<10
12	butyronitrile	10	<10	<10	<10
13	2-pentanone	30	130	20	20
14	i-butyric acid	--			
15	n-butyric acid	<10	630	<10	--
16	valeronitrile	10	20	<10	<10
17	cyclopentanone	30	160	40	20
18	i-valeric acid				--
19	n-valeric acid	20	200	<10	--
20	methylcyclopentanone	20	50	10	20
21	n-caproic acid	50	60	70	--
22	phenol	2700	4700	3100	3300
23	C_2-furan[b]	80	100	70	--
24	aniline	40	--	30	140
25	o-cresol	550	980	560	1300
26	m- and p-cresols	1100	1800	1100	1900
27	C_4-furan[b]	90	--	40	--
28	2,6-xylenol	30	30	30	110
29	o-ethylphenol	40	80	50	160
30	2,4- and 2,5-xylenols	130	210	130	280
31	3,5-xylenol and p-ethylphenol	140	280	160	300
32	2,3-xylenol	50	60	50	<10
33	3,4-xylenol	[c]			
34	2-isopropylphenol	60	90	50	<10
35	C_5-furan[b]		--	--	--
36	C_3-phenol[b]	10	--	--	20

Table 1. Organic constituents in untreated by-product waters from coal conversion process development units.[a] (Continued)

Peak #	Compound	Concentration in mg. per liter			
		Slagging gasifier	Project Lignite	SYNTHANE	SYNTHOIL
37	C_3-phenol*	10	--	--	10
38	C_3-phenol and naphthalene	--	70	20	--
39	3-ethyl-5-methylphenol	<10	30	10	20
40	catechol				
41	2,3,5-trimethylphenol	<10	20	10	<10
42	resorcinol, C_3-phenol[b] and C_4-phenol[b]	--	50	10	30

[a]The data obtained on SYNTHANE and SYNTHOIL by-product waters are similar to results obtained on many other water samples from these processes. The results obtained on Project Lignite and fixed-bed slagging gasification by-product waters represent the analysis of a single sample from each process.

[b]Refers to the number of alkyl carbons. These compounds were identified on the basis of mass spectrometric data only. All other compounds listed were identified on the basis of mass spectrometric data and confirmed by co-chromatographic expriments.

[c]Includes 3, 4-xylenol and C_5-furan, while 2-isopropylphenol was not detected.

Table 2. Organic sulfur constituents identified in an untreated by-product water from the SYNTHANE process development unit.

Peak No.	Compound
1	carbon disulfide[a]
2	thiophene
3	2-methylthiophene
4	benzothiophene

[a]Compounds were identified on the basis of co-chromatographic experiments.

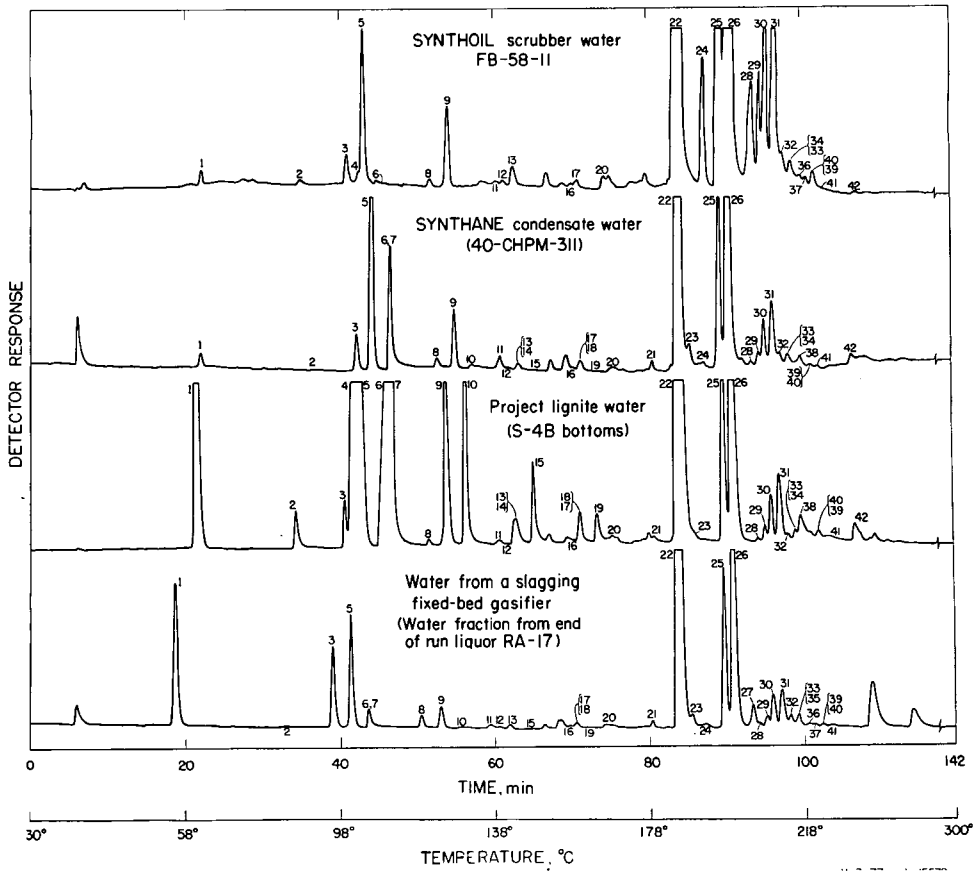

Figure 1. Chromatographic profile of by-product waters from coal conversion processes. The numbered compounds are identified in Table 1.

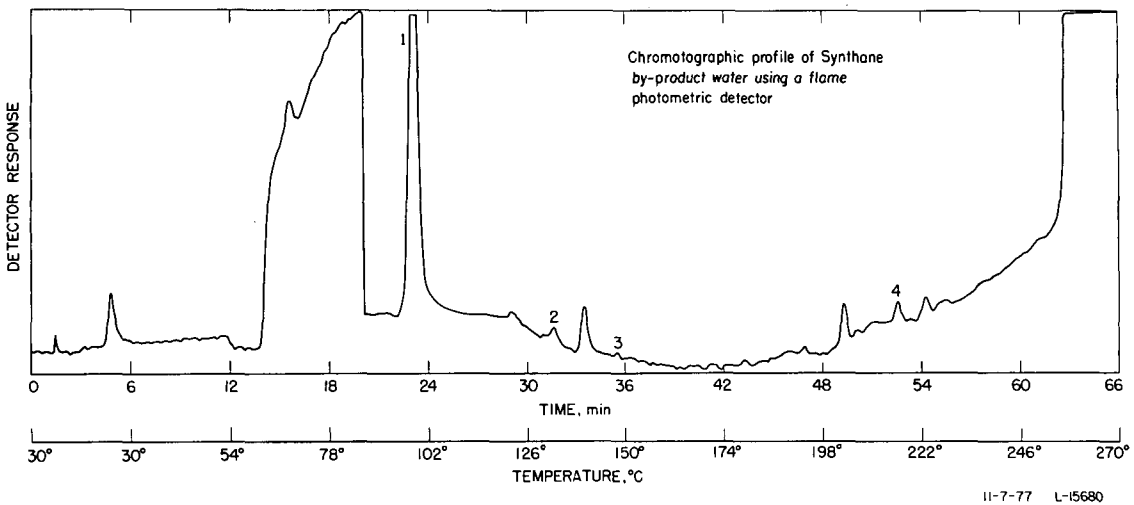

Figure 2. Chromatographic profile of a SYNTHANE by-product water using a sulfur specific flame photometric detector. The numbered compounds are identified in Table 2. These compounds were identified on the basis of co-chromatographic experiments only.

While monitoring the trace volatile polar organics in SYNTHOIL and SYNTHANE by-product waters, it was determined that the same compounds are present irrespective of minor changes in process conditions; however, the concentrations in which components are present can change significantly with changes in plant operating conditions.

The results of this study agree reasonably well with those reported by other investigators. In particular the chromatographic profile of SYNTHANE condensate water and overall results obtained by Ho, et al. (3) are very similar to that shown here. Many of the compounds identified earlier by Schmidt (1) have also been observed in this investigation. Although the mass spectrometric data obtained by Ellman (4) and co-workers on the organic content of by-product water from a fixed-bed slagging gasifier indicated many relatively non-volatile compounds, the results of that investigation support our findings that phenol and cresols are the major components. Further, Kavan and Basyrova (5) have identified ketones and an alcohol in by-product water from the "pressure gasification" of coal and these results are in agreement with those reported here.

The detection of alcohols and nitriles in these by-product waters is interesting. To our knowledge, this is the first report in which nitriles have been positively identified and quantitated in products formed during the hydroliquefaction or gasification of coal. Although alcohols have been previously reported in gasification products (5), they have not, to our knowledge, been positively identified and quantitated in products formed during the hydroliquefaction of coal. The origin of alcohols in the by-product waters is unknown; however, three routes to their formation are reasonable. Alcohols could be: 1. the pyrolysis or hydrogenolysis products of coal or lignite; 2. formed by catalytic reaction of synthesis gas (CO and H_2); or 3. formed by secondary reactions occurring in the aqueous phase. Alcohols are present in highest concentration in the by-product water from Project Lignite. In this process, lignite is solvent-refined in the presence of CO and H_2, using the naturally occurring mineral constituents of lignite as catalysts. CO and H_2 are known to react in the presence of some catalysts to form methanol as well as other products (9, 10). Alcohols are known to be products formed during the Fischer-Tropsch reaction. It is conceivable that at least some of the alcohols detected in by-product water from Project Lignite were formed by catalytic conversion. The SYNTHOIL process does not use CO, and therefore the small amounts of alcohols in SYNTHOIL by-product water were probably formed by routes 1 and/or 3. The alcohols detected in by-product waters from SYNTHANE and the slagging fixed-bed gasification process may have been formed from any one or a combination of the three suggested routes.

The presence of naphthalene, which was found in some of these by-product waters, is significant and indicates that higher homologs of polynuclear aromatic hydrocarbons (PAH's) may be present. This is particularly true in light of the recent mass spectrometric results of Ellman, et al. (4) who detected PAH's in by-product water from the slagging fixed-bed gasifier. Because many PAH's are known or suspected carcinogens, it is important to determine their exact nature and level in these waters. The analytical techniques used in this investigation employing Tenax GC are not effective in the analysis of higher homologs of PAH's.

Several homologous series of organic compounds have been detected, including alcohols, nitriles, ketones, carboxylic acids, furans, and phenols. In general, the first member of each homologous series is present in highest concentration. This is probably due to the higher water solubility of the lower homologs.

Gas chromatography using direct aqueous injection on Tenax GC is an excellent technique for rapidly and reproducibly monitoring the trace volatile polar organics in by-product waters from coal conversion processes. The gas chromatographic analysis can be completed in less than two hours and may be entirely automated and computerized using an autosampler and chromatographic data system. Further, little sample preparation time is required, and no prior concentration of components is needed. These characteristics of the analysis suggest that the gas chromatographic techniques employed in this research could be used online within a coal conversion plant to monitor trace volatile polar organic constituents of by-product waters.

The overall trace volatile polar organic contents of the four by-product waters investigated are very similar although a few significant differences exist. This study implies that, since the volatile polar organic contents of the waters from four different coal conversion processes are very similar, it may be possible to develop a single waste water treatment technology that is effective in treating the by-product waters from more than one coal conversion process.

It should be emphasized that the by-product waters investigated were untreated. The present investigation not only provides detailed quantitative analytical data for by-product waters from selected coal conversion process development units, but also provides an indication of the types of materials that may be present in waters from larger scale-up units.

ACKNOWLEDGEMENT

We are indebted to S. Akhtar and N. Mazzocco for providing the necessary samples from the one-half ton per day SYNTHOIL unit at the Pittsburgh Energy Research Center a to S. Gasior and R. Kornosky for providing samples from the one-half ton per day SYNTHANE unit. Further we appreciate the cooperation of J. Schiller and Everett Sondreal from the Grand Forks Energy Research Center and R. Baltisberger of the University of North Dakota for generously providing samples of by-product waters from the fixed-bed slagging gasifier and Project Lignite, respectively.

REFERENCES

1. Schmidt, C. E., Sharkey, A. G., Jr., and Friedel, R. A., Bureau of Mines Technical Progress Report 86, 1974.

2. Forney, A. J., Gasior, S. J., Haynes, W. P., and Katell, S., Bureau of Mines Technical Progress Report 24, 1970.

3. Ho, C. H., Clark, B. R., and Guerin, M. R., J. Environ, Sci. Health, 7, 481 (1976).

4. Ellman, R. C., Johnson, B. C., Schobert, H. H., Paulson, L. E., and Fegley, M. M., 9th Biennial Lignite Symposium, Grand Forks, North Dakota, May 18-19, 1977.

5. Kavan, I, and Basyrova, Z. V., Sb. Pr. UVP (Ustav Vyzk. Vyuziti Paliv) 12, 252, 1968. (CA:72:82739W).

6. Akhtar, S., Mazzocco, N. J., Weintraub, M., and Yavorsky, P. M., Energy Communications, 1, 21 (1975).

7. Severson, D. E., Souby, A. M., and Baker, G. G., Preprints, Div. of Fuel Chemistry, Amer. Chem. Soc., 22 (6), 161 (1972).

8. Harris, L. E., Budde, W. L., and Eichelberger, J. W., Anal. Chem., 46, 1912 (1974).

9. Natta, G., "Synthesis of Methanol," in Catalysis Vol. III, Hydrogenation and Dehydrogenation (P. H. Emmett, ed.), Reinhold, New York, 1955, Chap. 8.

10. C. L. Thomas, Catalytic Process and Proven Catalysts, Academic, New York, 1970, Chap. 14.

IDENTIFICATION OF ORGANIC CONSTITUENTS IN AQUEOUS EFFLUENTS FROM ENERGY-RELATED PROCESSES

E. D. Pellizzari, N. P. Castillo, S. Willis, D. Smith and J. T. Bursey

Research Triangle Institute, P. O. Box 12194
Research Triangle Park, North Carolina 27709

The emphasis on and drive toward national energy self-sufficiency implies a very real possibility for large scale environmental degradation. There is great concern on the one hand that unabated growth in energy production and utilization will cause irreparable harm to the environment and on the otherhand that measures to protect the environment may further exacerbate the current supply problems faced by the energy industry. It is generally recognized that the nation must use coal and oil-shale over the next few decades at a rate of activity which will double or triple our current levels (1).

Prior to this report a paucity of information was available on the individual volatile organic species and their quantities in aqueous samples from energy-related processes. Characterization of energy-related effluents for volatile and semi-volatile organic components is necessary if we are to understand the energy recovery process itself as well as its environmental impact.

The development and application of capillary gas-liquid chromatography/mass spectrometry/computer (glc/ms/comp) and gas chromatography/Fourier Transform-infrared/computer (gc/ft-ir/comp) methods for characterizing and quantifying volatile and semi-volatile organics in aqueous samples from energy-related processes is described here.

EXPERIMENTAL PROCEDURES

Sampling Methods--One-liter glass amber containers were cleaned with dilute HCl, deionized-distilled water and then heated to 450°C for 2 hr. Teflon® -lined screw caps were used.

Product water from an *in situ* coal gasification experiment in Hanna, WY (Hanna II, Phase II, Laramie Energy Research Center, Laramie, WY) was obtained from a high temperature product stream using an ethylene glycol-cooled stainless steel condenser system. A 24 hr composite was collected in a sump, the product water and tar separated, and shipped to the laboratory. Samples were chilled to 4°C until processed.

Sample Preparation--Volatile organics were recovered from aqueous samples using previously developed methods (2-9). A 3-100 ml aqueous sample was diluted to 100 ml with deionized-distilled water, and purged with Helium in an all glass vessel (Fig. 1). The He was passed through a short glass condensor to remove water vapor and the volatiles were trapped on a 1.5 x 8.0 cm bed of Tenax GC (2,6-diphenyl-*p*-phenylene oxide, Applied Sci. Lab., State College, PA, 35/60 mesh). Tenax GC cartridges were prepared as previously described (10,11). Organic volatiles were purged from the sample at 60°C with a 25 ml/min He flow for 90 min. After purging, the Tenax GC cartridge was dried over 1 g $CaSO_4$ for 2 hr in a sealed Kimax® culture tube. Samples were stored at -20°C until analysis time.

Semi-volatile organics not quantitatively recovered by the above procedure were extracted from aqueous samples using Freon-TF® (Ashland Chem. Co., Raleigh, NC). Freon-TF® was purified through a florisil column prior to its use. For extraction of neutral and basic compounds, the pH was adjusted to >11 and the aqueous sample (100 ml) was partitioned four times with 100 of Freon-TF. Organic phases were combined and the organic bases extracted with 100 ml 1N HCl (F-2). The organic phase was concentrated to 2.0 ml in a Kuderna-Danish (K-D) apparatus and then to 300 µl under a slow N_2 stream. The fraction containing neutral compounds (NE) was submitted directly to instrumental analysis. The aqueous acid layer (F-2) was adjusted to pH 12 with 5N NaOH and extracted four times with 100 ml of Freon-TF®.

Freon-TF® fractions were combined, concentrated to a 2 ml in a K-D apparatus and then to 300 µl under a slow N_2 stream (B).

The original alkaline solution (F-1) was adjusted to pH 4 with 5N HCl and partitioned four times with 100 ml Freon-TF®. Organic phases were combined and concentrated to 300 µl as above (A).

Fractions containing organic acids (A) were treated with 200 µl of CH_2N_2 in diethyl ether (12) and analyzed directly by glc/ms/comp and gc/ft-ir/comp. Organic bases (B) were treated with 100 µl perfluoroproprionic anhydride (PFPA, Pierce Chem., Rockford, IL) for 1 hr @ 45°C. The PFPA was neutralized with 100 µl 5% $NaHCO_3$ and the organic layer was examined by glc/ms/comp.

Instrumental Methods--Volatile organics were thermally recovered and analyzed by gc/ms/comp using a previously described inlet manifold (8-11) shown in Figure 2. Table 1 presents the instrumental parameters employed. In a typical thermal desorption cycle, a Tenax GC cartridge was placed in the preheated chamber (270°C) and the helium passed through the cartridge (∿20 ml/min) to purge the desorbed vapors into the liquid N_2 cooled Ni capillary trap. This operation was conducted with the valve in position "A" (Fig. 2). After 4 min of thermal desorption, the six-port valve (Valco Inst. Inc., Houston, TX) was rotated to position "B" (Fig. 2). The capillary trap temperature was raised from -196° to 220°C in 3 sec and the He carrier gas carried the vapors onto an OV-101 support coated open tubular column (SCOT). The SCOT's were prepared by a previously reported method (11).

Table 1. Operating Parameters for GLC-MS-COMP System

Parameter	Setting	Parameter	Setting
Inlet-manifold		MS	
desorption	270°C	scan range	m/e 20 → 300
valve	220°C	scan rate,	
capillary trap - min.	-195°C	automatic-cyclic	1 sec/decade
max.	220°C	filament current	300 µA
desorption time	4 min	multiplier	6.0
		ion source vacuum	∿4 x 10^{-6} torr
GLC			
100 m SCOT OV-101	20-240°C, 4/C° min		
50 m SCOT Carbowax 20 M	80-240°C		
carrier (He)	∿3 ml/min		
separator	240°C		

Semi-volatile organic compounds (3-5 µl) as neutrals, methylated acids and derivatized bases were also analyzed using the inlet manifold in the splitless injection mode (13). A Carbowax 20 M SCOT was employed.

Mass cracking patterns were automatically and continuously acquired throughout the chromatographic run using a Varian MAT CH-7 mass spectrometer/620L computer system (i.e., 30 eV) equipped with a Diablo Dual Disk system, Statos 3185 recorder, and a Magnetic Tape Deck.

Nicolet 7091 (Nicolet Inst., Madison, WI) and Digilab FTS-20 (Digilab Inc., Cambridge, MA) gc/ft-ir/comp systems were used for acquiring infra-red spectra (0.5 sec/scan, 8 cm^{-1}) of semi-volatile organic acids. Gas chromatography was performed on a 1/8 in x 9 ft S.S. column packed with 10% Carbowax 20 M on 80/100 mesh Chromosorb W(HP).

Radiolabeled Recovery Studies--To determine the percent recovery for the volatile and semi-volatile purification procedures, radiolabeled compounds were employed. Toluene[Ring-^{14}C, 4.0 µC/mM], benzene [^{14}C, 13.6 µC/mM], phenol [^{14}C (U), 10.7 µC/mM], acetone [2-^{14}C, 6.5 µC/mM], dimethylbenzanthracene-^{14}C, phenyl ethyl amine·HCl-^{14}C, and 3-amino-1,2,4-triazole were purchased from New England Corporation, Boston, MA. Acetonitrile [1-^{14}C, 14.9 µC/mM] and n-hexanoic acid [1-^{14}C, 58 µC/mM] were purchased from Amersham Searle, Corp. Plains, IL.

Radioisotopes were diluted in distilled-deionized water to a few μC/ml. Samples were spiked with radiolabeled compounds prior to purification. The radioactivity on the solid sorbent Tenax and in liquid fractions from the liquid-liquid (LL) fractionation scheme was determined with a Packard Tricarb 3375 liquid scintillation spectrometer. To the fraction was added 15 ml of scintillation fluid and the sample was counted until a standard error of 2.5 was obtained. The scintillation fluid contained 18 g of Omnifluor®, 1 ℓ of Triton-X® and 2 ℓ of toluene. Observed radioactivity was corrected for quenching by the external standard ratio method and by adding known quantities of radiolabeled compounds to each of the fractions to be counted. All counts were converted to disintegrations, per minute.

Data Interpretation--Identification of resolved components was achieved by comparing the mass cracking pattern of the unknown to an eight major peak index of mass spectra (14). Individual difficult unknowns were submitted to the Cornell University STIRS and PBM systems and/or the EPA MSSS System (Cyphernetics) for identification. When available, authentic compounds of the tentatively identified components were obtained and chromatographed under identical conditions on the OV-101 or Carbowax 20 M glass capillary column. The elution time and temperature for the authentic compounds was compared to the unknown in order to establish further the identity of the component.

Identities were assigned on a graded scale. When observed mass spectra matched library spectra and/or indexes of tabulated spectra and the elution time and temperature corresponded with that of an authentic compound identification was positive. Confirmation was also provided by infra-red spectra, particularly for isomeric forms. When the isomeric form could not be distinguished, the name of the compound as an isomer was indicated. In other cases, only an empirical formula could be assigned since the mass cracking patterns of isomers were very similar and the retention index could not be determined for all of the isomers since all the authentic compounds were not available. In some cases, a tentative identification was assigned when the mass cracking pattern yielded a "similar" match, and no retention index was available for that compound.

Quantification of Volatiles and Semi-volatiles--The volatile and semi-volatile compounds were quantitated by glc/ms/comp utilizing the total ion monitor and, when necessary, mass fragmentography. In order to eliminate the need to obtain complete calibration curves for each compound for which quantitative information was desired, we used the method of relative molar response (RMR) factors. This method required information on the exact amount of reference standard added and the relationship of the RMR for the unknown to the RMR of the standard. The method of calculation was as follows:

$$RMR_{unknown/standard} = \frac{A_{unk}/Moles_{unk}}{A_{std}/Moles_{std}} \quad 1) \qquad \text{or} \qquad RMR_{unk/std} = \frac{A_{unk}/g_{unk}/GMW_{unk}}{A_{std}/g_{std}/GMW_{std}} \quad 2)$$

A = Peak area
g = number of grams present
GMW = gram molecular weight

Thus, in the sample analyzed:

$$g_{unk} = \frac{A_{unk} \cdot GMW_{unk} \cdot g_{std}}{A_{std} \cdot GMW_{std} \cdot RMR_{unk/std}} \quad 3)$$

The value of RMR is determined from at least five independent analyses.

Reference standards, hexafluorobenzene (HFB) and perfluorotoluene (PFT), were added (200 ng) after the volatile organics were trapped on the Tenax GC cartridge. On an OV-101 glass capillary they did not interfere with the analysis of unknown compounds. Nitrobenzene-d_5 (200 ng) was used for quantification of semi-volatile organic compounds.

Quality Control Procedures--To monitor the possible introduction of impurities from the materials used in the purification procedures, we used a reagent and glassware

control that incorporated blanks. High quality commercial reagents and solvents were available, but the quality was somewhat variable. Freon-TF® which was used for extraction of semi-volatiles was concentrated by a factor of 100 to determine the potential contaminants. This procedure was repeated with each new lot of Freon-TF®. Deionized-distilled water was obtained by passing tap water through an ion exchange bed (No. 3508B, Corning Glass, Corning, NY), and a carbon adsorption cartridge (Hydro•Purge, Durham, NC) to remove trace elements and organic constituents, respectively, prior to its distillation. Water which was used for the dilution of the liquid samples was independently assessed for background contamination by subjecting it to the entire analytical procedure including gc/ms analysis. All glassware was cleaned with Isoclean (Isolab, Akron, OH), rinsed with deionized-distilled water, HCl, deionized water and then heated to 450°-500°C to remove traces of organic compounds.

Instrumental control was employed to insure that the entire system was calibrated and properly working. A 12 component reference mixture was used to evaluate the performance of the entire high resolution gc/ms/comp system. The mixture contained non-polar, semi-polar and polar substances.

RESULTS AND DISCUSSION

Radiolabeled Recovery Studies--(Volatiles)--Recovery of ^{14}C-acetone, acetonitrile, benzene and toluene from energy-related samples (*in situ* coal gasification) was determined. For compounds which are highly soluble in water, *e.g.*, acetonitrile, the recovery by this method was very low (∿10%). Recovery of ^{14}C-labeled acetone was ∿50%. On the other hand, the recovery of hydrocarbons, aromatics (benzene and toluene) and alkyl-aromatics was ≥80%. These observations were consistent with previously reported data (2-4).

In general, the purging of volatile organics from an aqueous medium utilizing an inert gas was quantitative for compounds with boiling points ≤210° and <2% solubility and for compounds with boiling points of <150° with a solubility of <10% in water. The percentage recoveries which were determined for ketones, aliphatic and aromatic hydrocarbons, thiophenes and aldehydes, was used for calculating concentrations of sample components.

(Semi-Volatiles)--Percent recovery for selected radiolabeled compounds added to aqueous samples was also determined for the LL extraction method (Table 2). The observed percentage recovery represents an overall average prior to instrumental analysis. For toluene and dimethylbenzanthracene, essentially quantitative recovery was observed for the LL extraction method and the K-D concentration steps. Quantitative recoveries for palmitic, hexanoic, and benzoic acids and phenol were also obtained. However, the highly water soluble butyric acid was not recovered. It was concluded that, for quantification of acids utilizing this LL extraction method, reliable data could be obtained for acids containing four or more methylene units.

Two bases were also subjected to the LL extraction method to determine its efficiency. A recovery of ∿68% was observed for phenyl ethyl amine in the basic fraction with only minor amounts remaining in several other fractions. In contrast, the water soluble amine, 3-amino-1,2,4-triazole, could not be quantitatively extracted.

From these data, it was concluded that moderately water soluble and/or moderately volatile compounds could be recovered by this LL extraction technique and retained in the receiver of the K-D apparatus. These data were used for calculating the quantities of the individual semi-volatile acids, bases, and neutral compounds in the energy samples.

Quantification by GC/MS/COMP Using Relative Molar Response (RMR) Factors--The RMR of several aliphatic and aromatic compounds based upon the total ion current monitor are presented in Table 3. As can be seen from these data, similar RMR's for the aliphatic hydrocarbons allow calculation of an "average RMR" for this chemical class. Thus, other compounds in the same chemical class for which authentic standards were not available could be quantified.

Table 2. Percent Recovery of Selected Radiolabeled Compounds Using Liquid/Liquid Extraction Method

Radiolabeled Compound	Fraction					
	Neutral (NE)	Acid (A)	Base (B)	H_2O/H^+ [a]	H_2O/OH^- [b]	Total (Organic Phase)
Toluene	76 ± 9%	0.8 ± 0.4%	1.2 ± 0.6%	1.5 ± 1.0%	0%	79.5%
Dimethylbenzanthracene	83 ±12%	3.0 ± 1.0%	0%	0%	0%	86.0%
Palmitic acid	31 ± 4%	80 ± 8%	0%	0%	0%	111.0%
Hexanoic acid	0%	75 ± 5%	0%	24 ± 3%	0%	75.0%
Benzoic acid	0%	54%	1.5%	45%	0%	55.5%
Butyric acid	0%	0%	0%	87 ± 13%	0%	0%
Phenol	0%	53 ± 3%	0%	46 ± 4%	0%	53%
Phenylethylamine	3 ± 2%	2 ± 1%	68 + 7%	11 ± 3%	4 ± 2%	73.0%
3-Amino-1,2,4-triazole	0%	0%	0%	85 ± 14%	0%	0%

[a] Remaining after extraction of acidic solution.
[b] Remaining after extraction of basic solution.

Table 3. Examples of Relative Molar Response (RMR) Factors for Several Compounds Based Upon Total Ion Current Monitor

Compound	PFB[a]			PFT[a]		
	RMR	Var.[b]	S.D.[b]	RMR	Var.	S.D.
n-Heptane	1.39	0.150	0.39	1.66	0.080	0.29
n-Nonane	1.85	0.020	0.14	2.04	0.008	0.09
n-Undecane	1.71	0.048	0.22	1.94	0.016	0.12
n-Tridecane	1.31	0.130	0.36	1.44	0.110	0.34
2-Pentanone	2.84	0.260	0.41	2.94	0.060	0.240
2-Ethylfuran	2.59	0.230	0.48	2.68	0.100	0.320
Toluene	2.38	0.020	0.15	2.48	0.110	0.33
Cumene	1.56	0.050	0.22	1.76	0.026	0.16
1,3,5-Trimethylbenzene	1.48	0.050	0.22	1.63	0.037	0.19
1,2,4-Trimethylbenzene	1.47	0.025	0.16	1.47	0.006	0.08
1,2,3-Trimethylbenzene	1.26	0.040	0.19	1.45	0.013	0.11
o-Xylene	2.90	0.170	0.42	2.33	0.200	0.41
Anisole	1.77	0.290	0.54	2.14	0.040	0.20
Acetophenone	1.48	0.040	0.20	1.79	0.007	0.08
2-Methylbenzofuran	1.46	0.003	0.06	1.32	0.030	0.18
Indan	1.54	0.024	0.16	1.76	0.027	0.16
m-Tolualdehyde	1.56	0.020	0.15	1.54	0.003	0.06
o-Ethylaniline	1.62	0.170	0.41	1.28	0.060	0.25

[a] PFB = perfluorobenzene, PFT = perfluorotoluene which were external standards.
[b] Var. = statistical variance, S.D. = standard deviation.

Many additional RMR's not presented in this table were also determined and calculated. The RMR factors for ketones, aldehydes, thiophenes, ethers, amines, anilines, acids, etc. were determined for those compounds which were commercially available and an "average RMR" value for each chemical class was used for estimating the concentrations of compounds appearing in the energy samples for which authentic standards were not available.

Table 4 presents selected examples of RMR factors based upon fragment ions. The RMR factors were determined for two ions utilizing mass fragmentography, and the concentration of each compound in the unknown sample was calculated. As for the RMR's based upon the total ion current monitor, the RMR factors for selected fragment ions were determined for those authentic compounds which were commercially available and in those cases where authentic compounds were not available, an "average RMR' value was calculated for each homologous series.

Table 4. Examples of Relative Molar Response Factors for Several Compounds Based Upon Selected Fragment Ions[a]

		1st Ion		2nd Ion	
Compound	MW	m/e (I)	RMR	m/e (I)	RMR
Toluene	92	91 (100)	2.37	64 (13)	0.66
o-Xylene	106	105 (27)	3.46	51 (10)	0.39
Anisole	108	108 (100)	1.19	65 (76)	1.30
Acetophenone	120	105 (100)	1.97	120 (29)	1.27
Naphthalene	128	128 (100)	1.92	51 (12)	0.18
2-Pentanone	86	43 (100)	1.98	57 (26)	0.14

[a]RMR values were calculated relative to m/e 186 (100) for the external standard, HFB.

Mass Fragmentography--The technique of mass fragmentography was utilized for the quantification of volatile and semi-volatile organics when inadequate resolution existed for the total ion current monitor. Additional specificity was obtained with ion chromatograms for the individual components. Even though high resolution glass capillary columns (SCOT's) were used for effecting the resolution of the components in each mixture, the separation efficiency of the capillaries was inadequate for obtaining baseline resolution for every constituent in the sample. Since it was impractical to utilize very high resolution capillaries, e.g. wall-coated open tubular (capacity too low) or very long SCOT capillaries, we chose the mass fragmentographic technique to obtain sufficient resolution for quantification of the individual species.

Figure 3 depicts a mass fragmentogram for several selected ions for the volatile organics in product water (13L) from an in situ coal gasification experiment. Peaks labeled 1 (m/e 67), 2 and 3 (m/e 114), 4 (m/e 71) and 5 (m/e 186) represent the compounds pyrrole, n-octane, 2-heptanone and PFT, respectively. Additional ion chromatograms were also obtained for this and other samples which allowed the quantitation of essentially all of the components that were identified.

GC/FT-IR/COMP--The acid fraction of an aqueous sample was also analyzed by gc/ft-ir/comp. The flame ionization chromatogram obtained simultaneously with ir spectra is shown in Figure 4. Infra-red spectra for peaks 6, 8, 10, 12 and 14 in Figure 4 confirmed these compounds as methyl benzoate, methyl hexanoate (Fig. 5), methyl heptanoate, methyl octanoate and methyl nonanoate, respectively (15,16). Figure 6 is an ir spectrum of phenol which had been also identified by gc/ms/comp. The broad peak from 300-3500 cm^{-1} due to molecular hydrogen bonding observed in condensed phase spectra (15) is absent in this gas phase system. The two peaks between 1175-1300 cm^{-1} represent symmetric and asymmetric CO stretching bands. In condensed phase spectra, this is a broad single band (15). Peaks 18, 22, and 23 were identified as methyl-m-toluate, 3,5-dimethylphenol and o-cresol, respectively after examining their ir spectra.

Sample Composition--Tables 5 and 6 present the volatile and semi-volatile organics characterized and quantified in an aqueous sample from in situ coal gasification

Table 5. Volatile Organics in Produced Water (-13L) From Well 5-6 In Situ Coal Gasification (LERC, ERDA)

Chromatographic Peak No.	Elution Temp. (°C)	Compound	ppb
1	42	CO_2	NQ
2	45	carbonyl sulfide	NQ
2A	48	1-butene	NQ
3	49	n-butane	NQ
6	61-3	acetone	1243±0
7	61-4	acetonitrile	620±60
9	70	carbon disulfide	NQ
11	77	propionitrile	382±47
13	82	methyl ethyl ketone	645±33
15	88	isobutyronitrile	53±16
16	92	perfluorotoluene (eS)	-
16A	96	methyl isopropyl ketone	55±5
17	98	benzene	607±6
18	100	n-butyronitrile	267±13
18A	101	thiophene	620±6
19	104	2-pentanone	124±111
20	106	3-pentanone	55±0
21	112	α-methylbutyronitrile	32±9
22	115	N-methylpyrrole	2±0
23	116	4-methyl-2-pentanone	148±80
24	118	pyrrole	208±21
25	121	n-pentylnitrile	53±0
26	123	toluene + methylthiophene	556±200
		+ pyridine	2222±4
27	124	3-hexanone	27±8
28	125	cyclopentanone	32±9
29	127	n-octane	1±0
31	133	sulfur compound (?)	NQ
32	135	3-methylpyrrole	46±4
33	138	2-methylcyclopentanone	101±10
		+ 2-methylpyrrole	24±2
34	140	methylpyridine isomer	120±11
35	141	C_9H_{20} isomer	17±7
36	143	ethylbenzene	222±27
36A	144	C_8H_{16} isomer	4±0.3
37	146	p-xylene	561±60
38	148	2,4-dimethylthiophene	15±0
39	149	2-heptanone	5±0
40A	151	2,3-dimethylthiophene	52±3
40	152	styrene + C_9H_{18} isomer	118±11
41	153	o-xylene	472±37
42	155	n-nonane +	39±12
		dimethylpyridine isomer	74±15
43	157	dimethylpyridine +	417±7
		C_9H_{18} isomers	
44	158	dimethylpyrrole isomer	7±1
45	160	isopropylbenzene	11±0
	160	$C_{10}H_{20}$ isomer	209±7
46	161	$C_{10}H_{18}$ isomer	5±0
47	163	C_3-alkyl cyclohexane isomer	57±2
48	165	$C_{10}H_{22}$ isomer	27±8
49A	167	$C_{10}H_{20}$ isomer	11±5
49	168	n-propylbenzene	28±3
	169	$C_{10}H_{20}$ + trimethylcyclohexane isomers	96±14
50	170	m-ethyltoluene	184±16
51	170	p-ethyltoluene	61±7
52	171	2-isopropylthiophene	38±16
52A	172	$C_{10}H_{20}$ + $C_{10}H_{22}$ isomers	21±0.3
53	172	trimethylpyridine isomer	40±2
53A	173	cyanobenzene	44±5
54	175	o-ethyltoluene	67±17
56	177	$C_{10}H_{20}$ isomer	30±2
57A	178	α-methylstyrene + $C_{10}H_{20}$	349±42
57	180	1,2,4-trimethylbenzene +	267±27
		n-decane + benzofuran	111±16
58	182	$C_{10}H_{20}$ +	11±0.6
		trimethylthiophene isomers	15±0
58A	184	C_4-alkyl benzene isomer	6±2
59	186	C_4-alkyl benzene isomer	9±3
60	187	C_3-alkyl pyridine isomer	15±3
61	189	indan	334±33
61A	190	phenol	NQ
62	181	indene	272±32
63	192	C_4-alkyl benzene isomer	71±20
63A	193	C_4-alkyl benzene isomer	20±7
64	193	$C_{11}H_{24}$ isomer	57±5
65	195	C_4-alkyl benzene isomer	22±11
66	197	C_4-alkyl benzene isomer	NQ
		+ o-cresol	
67	198	$C_{11}H_{22}$ + C_4-alkyl benzene isomers	95±32
68A	201	C_5-alkyl benzene isomer	139±21
69	203	methylbenzofuran isomer	28±4
70	205	p-cresol	NQ
71	206	C_4-alkyl benzene isomer	12±6
71	207	dimethylindan isomer	47±3
72	208	C_5-alkyl benzene isomer	69±13
73A	209	C_5-alkyl benzene isomer	12±1
73	210	methylindan isomer	126±15

(continued)

Table 5 (cont'd)

Chromatographic Peak No.	Elution Temp. (°C)	Compound	ppb
73B	211	$C_{12}H_{26}$ + methylindene isomers	184±164
74A	212	C_5-alkyl benzene isomer	12±1
74	212	$C_{10}H_{12}$ + C_4-alkyl benzene isomers	63±15
75	213	methylindene isomer	196±31
76	215	dimethylphenol + C_5-alkyl benzene isomers	NQ
76A	216	C_5-alkyl benzene isomer	T
	217	dimethylindan isomer	T
77	218	1-dodecene	13±5
78	200	n-dodecene	86±8
79	221	naphthalene	640±32
79A	222	dimethylindan + C_6-alkyl benzene isomers	162±15
		benzothiophene	42±5
80	224	dimethylbenzofuran isomer	118±6
81	225	$C_{12}H_{16}$ + C_6-alkyl benzene isomers	148±22
82	227	$C_{11}H_{14}$ isomer	56±4
83	228	dimethylindene + C_6-alkyl benzene isomers	11±0
	229	trimethylindan isomer	17±7
84	230	$C_{13}H_{28}$ isomer	22±0
85	231	$C_{11}H_{14}$ + C_6-alkyl benzene isomers	NQ
86	232	dimethylindene + $C_{14}H_{30}$ isomers	50±10
87	233	dimethylindan + dimethylindene isomers	128±11
88	235	1-tridecene + trimethylindan isomer	12±0.7 94±7
89	237	n-tridecane	222±11
90	238	trimethylindan isomer	115±15
92	240	α-methylnaphthalene	162±16
93	isothermal	β-methylnaphthalene	345±7
94		2-isopropylbenzimidazole (tent.)	25±2
95		$C_{13}H_{18}$ isomer	11±0
96		$C_{14}H_{30}$ isomer	19±4
97		n-heptylbenzene	26±5
98		$C_{15}H_{32}$ isomer	21±6
99		1-tetradecene	47±4
99A		biphenyl	114±12
100		n-tetradecane	129±14
101		$C_{13}H_{18}$ isomer	16±7
102		ethylnaphthalene isomer	39±9
103		dimethylnaphthalene isomer	195±17
104		dimethylnaphthalene isomer	100±12
105		dimethylnaphthalene isomer	135±52
106		$C_{16}H_{32}$ isomer	26±11
107		dimethylnaphthalene isomer	47±14
108		ethylnaphthalene isomer	69±21
109		n-pentadecane	T
111		acenaphthene	612±9
112		isopropylnaphthalene isomer	
113		$C_{18}H_{28}$ isomer (tent.)	T
114		$C_{14}H_{20}$ isomer	31±5
115		trimethylnaphthalene isomer	7±1
117		C_3-alkyl naphthalene isomer	5±1
119		C_3-alkyl naphthalene isomer	7±0
119A		methyl acenaphthene isomer	15±3
120		C_3-alkyl naphthalene isomer	T

Table 6. Semi-Volatile Organics in Produced Water (-13L) From Well 5-6 *In Situ* Coal Gasification (LERC, ERDA)

Elution Temperature (°C)	Compound	ppb	Elution Temperature (°C)	Compound	ppb
97	C_5H_{12} isomer	NQ	107	2-hexanone	140
98	methyl ethyl ketone	NQ	107	n-pentanoic acid	1060
99	methyl isopropyl ketone	NQ	107	2-methylpentanoic acid	260
99	propanal	NQ	108	α-methylbutyronitrile	T
100	benzene	156	109	n-butyronitrile	84
101	n-butanal	NQ	110	$C_7H_{14}O$ isomer	T
101	2-pentanone	1170	111	ethylbenzene	T
101	n-butyric acid	90	112	p-xylene	140
102	4-methyl-2-pentanone	80	112	isohexanoic acid	190
103	isopentanoic acid	170	113	C_2-alkyl benzene isomer	T
103	3-methyl-2-pentanone	110	114	unknown	NQ
104	n-propionitrile (tent.)	130	116	n-hexanoic acid	1470
104	$C_5H_{10}O_2$ carboxylic acid	42	117	o-xylene	66
105	toluene	90	118	n-pentylnitrile	T
105	3-hexanone	T	119	cyclopentanone	48
106	$C_5H_{10}O_2$ carboxylic acid	T	119	methylcyclopentanone + n-propylbenzene	T
106	2-methyl-1,3-dioxane	T			

(continued)

Table 6 (cont'd)

Elution Temperature (°C)	Compound	ppb	Elution Temperature (°C)	Compound	ppb
120	$C_8H_{16}O_2$ carboxylic acid	T	158	benzofuran	90
121	2-n-pentylfuran	T	189	d_5-nitrobenzene (eI)	
122	$C_6H_{10}O$ isomer	48	201	aniline	3460
123	$C_8H_{16}O_2$ carboxylic acid	78	204	dimethylphenol isomer	990
124	isoheptanoic acid	30	215	phenol + cresol isomer	270000
128	n-heptanoic acid	870	217	dimethylphenol isomer	600
132	n-butylbenzene	18	220	ethylphenol isomer	18
136	anisole	100	221	dimethylphenol isomer	60
141	n-octanoic acid	110	222	cresol isomer	850
145	n-pentylbenzene	T	223	cresol isomer	10200
149	p-cresyl methyl ether	18	227	C_3-alkyl phenol isomer	170
153	dimethylpyridine + methylethyl-		227	C_3-alkyl phenol isomer	180
	pyridine isomer	12	229	C_3-alkyl phenol isomer	830
156	$C_{10}H_{12}$ isomer	T	231	dimethylphenol isomer	7800
156	indene	96	235	C_3-alkyl phenol isomer	6
157	pyrrole	270	237	C_2-alkyl phenol isomer	8100

(Hanna, WY). Many compounds containing sulfur (thiophenes, mercaptans, sulfides, etc.), nitrogen (nitriles, pyridines, aniline, etc.), oxygen (aldehydes, ketones, acids, phenols, etc.) were present. Many hydrocarbons and aromatic compounds were also identified.

The techniques of glass capillary gc/ms/comp and gc/ft-ir/comp were found to be powerful complementary tools for the characterization of energy samples when used with the described sample preparation procedures.

REFERENCES

1. Ayer, F. A., Symposium Proceedings: Environmental Aspects of Fuel Conversion Technology (May 1974, St. Louis, Missouri). Publication No. EPA-650/2-74-118, October 1974.
2. Bellar, T. A. and J. J. Lichtenberg. "The Determination of Volatile Organic Compounds at the μg/ℓ Level in Water by Gas Chromatograph", EPA Rept. No. 650/4-74-009, November, 1974.
3. Zlatkis, A., H. A. Lichenstein and A. Tishbee, Chromatographia, 6, 67 (1973).
4. Dowty, B., D. Carlisle, J. L. Laseter and J. Storer, Science, 187, 75 (1975).
5. Pellizzari, E. D., EPA Quarterly No. 2, Contract No. 68-03-2368, July, 1976.
6. Pellizzari, E. D., J. E. Bunch, B. H. Carpenter and E. Sawicki, Environ. Sci. Tech., 9, 552 (1975).
7. Pellizzari, E. D., B. H. Carpenter, J. E. Bunch and E. Sawicki, Environ. Sci. Tech., 9, 556 (1975).
8. Pellizzari, E. D. "Development of Method for Carcinogenic Vapor Analysis in Ambient Atmospheres". Publication No. EPA-650/2-74-121, Contract No. 68-02-1228, July, 1974.
9. Pellizzari, E. D. "Development of Analytical Techniques for Measuring Ambient Carcinogenic Vapors". Publication No. EPA-600/2-75-076, Contract No. 68-02-1228, 187 pp., November, 1975.
10. Pellizzari, E. D. "The Measurement of Carcinogenic Vapors in Ambient Atmospheres". Publication No. EPA-600/7-77-055, Contract No. 68-02-1228, 228 pp., June, 1977.
11. Pellizzari, E. D. "Analysis of Organic Air Pollutants by Gas Chromatography and Mass Spectroscopy". Publication No. EPA-600/2-77-100, June, 1977.
12. Fales, H. M., T. M. Jaouni and J. F. Babashale, Anal. Chem., 45, 2302 (1973).
13. Pellizzari, E. D. "Identification of Components of Energy-Related Wastes and Effluents". EPA Contract No. 68-03-2368, 500 pp., October, 1977.

14. Eight Peak Index of Mass Spectra. Vol. I (Tables 1 and 2) and II (Table 3) Mass Spectrometry Data Centre, AWRE, Aldermaston, Reading, RG74PR, UK, 1970.
15. Silverstein, R. M., G. C. Bassler and T. C. Morrill, "Spectrometric Identification of Organic Compounds, 3rd Ed., John Wiley & Sons, New York, NY, 1974, 339 pp.
16. Sadtler Research Laboratories, "Catalog of Infrared Spectra", Philadelphia, PA.

ACKNOWLEDGEMENT

The authors wish to thank Ms. A. Alford of the Environmental Research Laboratory, U. S. Environmental Protection Agency, Athens, GA for her helpful assistance and encouragement throughout the program.

This research was supported by EPA Contract No. 68-03-2368 of HEW.

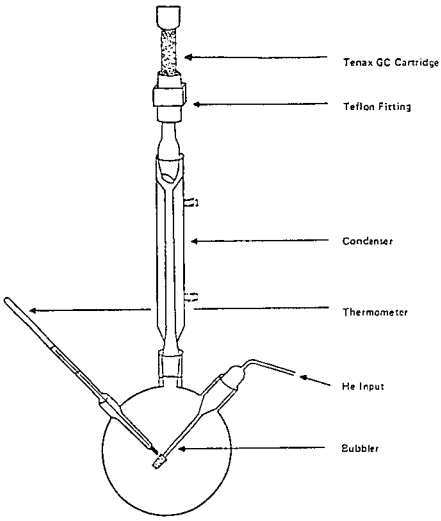

Figure 1. Purge apparatus for volatile organics.

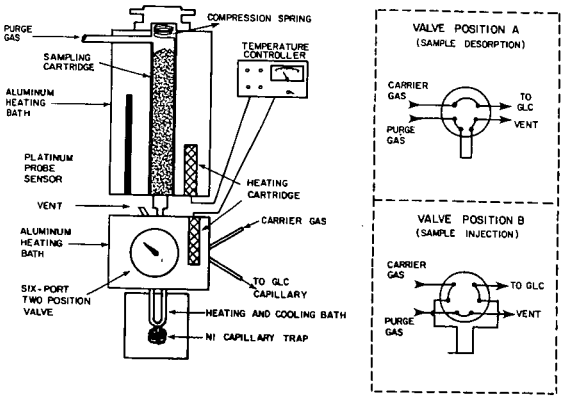

Figure 2. Inlet manifold for recovery of volatile organics from Tenax GC® cartridges.

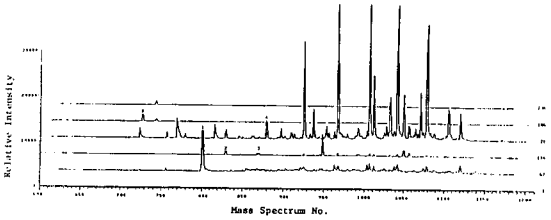

Figure 3. Mass fragmentograms of aqueous sample from in situ coal gasification.

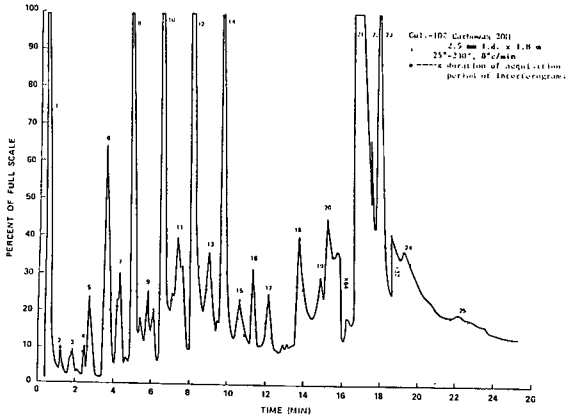

Figure 4. Flame ionization chromatogram for organic acid fraction obtained during ir spectral acquisition.

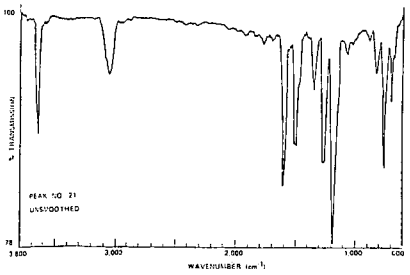

Figure 5. Ir spectrum of peak No. 8 in Figure 4.

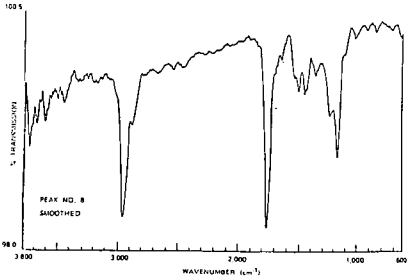

Figure 6. Ir spectrum of peak No. 21 in Figure 4.

Aqueous Effluents From the SYNTHOIL Process

Sayeed Akhtar, Nestor J. Mazzocco and Paul M. Yavorsky

Department of Energy
Pittsburgh Energy Research Center
4800 Forbes Avenue
Pittsburgh, PA 15213

INTRODUCTION

Conversion of coal to an environmentally acceptable utility fuel is a high priority objective of the Department of Energy. Work on several processes designed to convert coal to a low-sulfur, low-ash liquid or solid fuel is in progress. One such process under development is the SYNTHOIL process using direct hydroliquefaction. A unit of 1/2 ton of coal slurry per day capacity has been in operation for over three years, and a larger process development unit of 10 tons of coal per day capacity is under construction. The aqueous effluents from a conceptually integrated commercial SYNTHOIL plant are reviewed in this presentation and the analytical results for the one aqueous effluent available from the existing 1/2 ton per day SYNTHOIL unit are presented.

PROCESS DESCRIPTION

Figure 1 is a flow sheet of the SYNTHOIL process. Hydrogen and a slurry of pulverized coal in a recycle oil are preheated and passed through a turbulent-flow, fixed-bed reactor packed with pellets of Co-Mo/SiO_2-Al_2O_3 catalyst. The turbulence provides vigorous contacting of the gas-slurry mixture which leads to high conversion in short residence time. The reactor is operated at 2,000 to 4,000 psi and 450° C, at which condition coal is converted to liquid hydrocarbons while sulfur, nitrogen and oxygen are eliminated as H_2S, NH_3 and H_2O respectively. The product stream from the reactor is cooled to 250° F and led to a gas disengager where liquids and unreacted solids are separated from gases and vapors. The liquid stream is passed through a centrifuge to remove the unreacted solids consisting of mineral matter and unconverted coal. The centrifuged liquid is a low-sulfur, low-ash fuel oil. A portion of the whole centrifuged liquid is recycled to convey more coal into the plant while the rest of it is available as the net product. An additional quantity of fuel oil is obtained by pyrolyzing the solids from the centrifuge. The residue, or char, from pyrolysis is gasified to produce hydrogen for the process.

The gases from the gas disengager are contacted with water at plant pressure to dissolve ammonium sulfide, cooled and led to a second gas disengager where the scrub water and any organic condensates are separated from gases. The layer of organic condensates is combined with the liquid products from the first gas disengager while the aqueous layer is a waste stream. In addition to the scrub water, this waste stream will also contain any water going in with coal or formed chemically during liquefaction. The gas from the second disengager is further purified by washing with an oil to remove hydrocarbon vapors, and then with an amine to remove acid gases. The purified gas is combined with make-up hydrogen and is recycled to the reactor. The gas purification is conducted at the plant pressure to minimize the cost of recycling the purified gas. The H_2S recovered by amine wash is converted to elemental sulfur in a conventional Claus plant.

Results from operation of a 1/2 ton per day SYNTHOIL unit are reported in (1,2,3).

AQUEOUS EFFLUENTS

The aqueous effluents from a commercial SYNTHOIL plant will consist of the following:

1. Rain run-off from the coal storage and handling area;
2. Water evolved from coal during drying and pulverization;
3. A combined stream of reactor gas scrub water, the residual water in the pulverized coal introduced into the reactor, and the water produced chemically during coal hydrogenation;
4. Gas scrub water and chemically produced water from the pyrolyzer for the centrifuged solid;
5. Aqueous effluents from the char gasifier for hydrogen production;
6. A waste water stream from the Claus reactor.

Effluent 1 will be obviously intermittent while effluents 2 to 6 will be continuous.

Effluents from maintenance operations, e.g. boiler blowdowns, demineralizer discharges, cooling tower blowdowns and sewage treatment facility discharges are not included in this discussion.

Rain Run-Off

Effluent 1, the rain run-off, will be similar to mine drainage which has been a subject of considerable research (4,5,6). The run-off will contain suspended coal particles, leachates from coal's mineral matter, and sulfuric acid. Iron pyrite, a mineral almost always present in coal, reacts with atmospheric oxygen in the presence of water to form ferrous sulfate and sulfuric acid according to the following reaction:

$$2FeS_2 + 7O_2 + 2H_2O \rightarrow 2FeSO_4 + 2H_2SO_4 \qquad 1)$$

Ferrous sulfate is not a stable product. It oxidizes to ferric sulfate by reacting with oxygen and sulfuric acid as follows:

$$4FeSO_4 + 2H_2SO_4 + O_2 \rightarrow 2Fe_2(SO_4)_3 + 2H_2O \qquad 2)$$

Reaction 2 will appear to be welcome inasmuch as sulfuric acid is consumed therein but the relief is short-lived: ferric sulfate hydrolyzes to ferric hydroxide and sulfuric acid, the former precipitating out as "yellow boy".

$$Fe_2(SO_4)_3 + 6H_2O \rightarrow 2Fe(OH)_3 + 3H_2SO_4 \qquad 3)$$

The sequence of reactions 1, 2 and 3 is not the only mechanism for the formation of sulfuric acid. Iron pyrite may react with oxygen, in the absence of water, as follows:

$$FeS_2 + 3O_2 \rightarrow FeSO_4 + SO_2 \qquad 4)$$

The ferrous sulfate produced in reaction 4 may contribute to the formation of sulfuric acid by way of reactions 2 and 3. Ferrous sulfate may also be formed by a reaction of ferric sulfate and iron pyrite. It has been claimed that microorganisms may have a role in the formation of sulfuric acid from iron pyrite by catalyzing one or more of the above reactions (6,7).

An obvious solution to the problem of the rain run-off from the coal storage and handling area of a SYNTHOIL plant will be to store and handle coal under a shed. This solution, however, may be too costly in which case the run-off will be treated in the same manner as acid mine drainage. The most developed process for treating acid mine drainage consists of neutralization with lime, or limestone, followed by aeration to facilitate oxidation of Fe^{++} to Fe^{+++}. The water is then impounded in a lagoon for "yellow boy" to settle out. Al and Mg, frequently present as dissolved salts in mine drainage, also settle out as hydroxides. The hydroxides of Fe, Al, and Mg are very gelatinous and bring down with them suspended particles of coal or any other insoluble matter. The clean water, although free from the contaminants originally present in it, is now saturated with calcium sulfate which has a solubility of about 0.3 g/100 ml of cold water. It is therefore released only intermittently in natural waterways and preferably during periods of high flow to facilitate rapid dilution of the calcium sulfate. The water may be rendered suitable for industrial use by secondary treatment, e.g. reverse osmosis or ion-exchange, but at a considerable cost as of now. Reverse osmosis and ion-exchange have been investigated also directly with acid mine drainage (8).

Water From Coal Drying

The feed to a SYNTHOIL reactor is a slurry of coal in recycle oil. For a stable slurry, coal is pulverized to approximately 70 pct through 200 mesh and 100 pct through 50 mesh, U.S. standard sieves. Efficient pulverization to this fineness is not practicable if coal contains more than 3 pct moisture. Since most coals contain more than this, they must be dried for pulverization. In industrial practice, drying and pulverization are conducted simultaneously by passing a hot gas through the pulverizer. The gas also lifts the pulverized coal from the milling chamber to a classifier from where the oversize particles are returned to the mill while the coal of desired particle size range is conveyed, by the gas, to a cyclone separator. The cyclone separates the entrained coal from the gas, after which a portion of the gas is vented to purge moisture while the balance is mixed with a supply of hot make-up gas and returned to the pulverizer. In establishments of good housekeeping, the gas is filtered through a baghouse before venting.

The SYNTHOIL process is designed primarily for high-sulfur coals from the eastern parts of the United States, which contain 6 to 12 pct moisture. Assuming average moisture contents of 8 pct and 3 pct in the coal before and after pulverization respectively, approximately 12,500 gph of water will be released from the coal in a SYNTHOIL plant processing 25,000 tons of coal per day. Although at present no effort is made in pulverized-coal-consuming plants to condense and collect the water released by coal during the combined drying and pulverization operation, in the coal liquefaction plants of the future it may be necessary to collect this water to conserve the resource. Information on the contaminants to be expected in this water is not available but it may be surmised that the condensed stream will contain particulate contaminants and, possibly, traces of organic compounds released from the coal at the temperature of drying.

Reactor Gas Scrub Water (Sour Water)

The origin of this effluent is explained in the section on process description. In addition to the water injected into the gas stream to dissolve out ammonium sulfide, the effluent will also contain the process make water, organic condensates, and the entrained contaminants in the reactor gas. An analysis of this effluent from the 1/2 TPD SYNTHOIL unit is given in table 1. For purposes of comparison, analysis of the influent water is also included in the table. Two sets of data are presented, one where the gas was scrubbed with distilled water and the other where the gas was scrubbed with a dilute solution of NaOH in distilled water. In each case, the effluent was an emulsion which underwent a rapid but partial clarification in 2 to 4 hours,

TABLE 1.- Analysis of SYNTHOIL reactor gas scrub water (sour water)

	Gas Scrubbed With Distilled Water		Gas Scrubbed With a Solution of NaOH in Distilled Water	
Group A Analyses	Influent	Effluent	Influent	Effluent
Total carbon, mg/l	4	900	12	7,500
Total inorganic carbon, mg/l	≤2	150	6	140
Total organic carbon, mg/l	4	750	6	7,270
Chemical oxygen demand (COD), mg/l	-	8,200	≤10	27,200
Phenol, mg/l	-	250	-	5,100
SCN^-, mg/l	-	29	-	90
CN^-, mg/l	-	0.03	-	0.03
Suspended solids, mg/l	-	≤4	-	≤2
pH	5.7	8.4	10.1	8.7
Cl^-, mg/l	≤1	5	6	15
NH_3, mg/l	≤2	2,500	≤10	3,000
Biochemical oxygen demand (BOD), 5-day, ppm	-	630	-	13,500
S, mg/l	2	3,800	≤10	4,300
Group B Analysis				
Oil and grease, mg/l	-	85	-	1,150

after which no further clarification was visually detectable. The group A analyses of table 1, which extended over a period of about a week, were conducted on aliquots drawn from the water layer after the initial period of rapid clarification. For the group B analysis, samples of the effluent were collected directly in quart jars and the entire content of a jar was later analyzed as a single aliquot. Thus, the oily layer which had separated from water was included in the analysis of this group. The analyses were performed by the methods recommended by the American Public Health Association (9). The limits of detection and precision for these methods, where available, are also given in reference (9). Since NH_3 and H_2S interfere with BOD determination, the sample was acidified to remove H_2S and then made alkaline to remove NH_3 before BOD determination. A comparison of the results obtained by scrubbing the gas with distilled water and with a solution of NaOH in distilled water shows that significantly more phenols and other organic compounds were scrubbed out of the gas by the solution of NaOH than by pure water.

A survey of the metals in the influent and effluent is given in table 2. The survey was conducted by spark source mass spectrometry. Sufficient sample was evaporated onto the electrode material (graphite) to give a detection limit near 1 mg/l for most elements. The analysis is semiquantitative and reproducible to about a factor of three. The concentrations of metals in the influent and effluent are comparable, indicating that no significant amounts of metal compounds were scrubbed from the gas stream. The nature and concentration of the contaminants in the gas scrub water will of course depend on the coal being processed and the plant operating conditions. The effluent whose analysis is reported in tables 1 and 2 was obtained from the processing of a high-sulfur, hvBb coal from Homestead mine, Kentucky, at 450° C and 4,000 psi. The influent injection rate was 1 lb per lb of coal feed. Thus, 250,000 gph of this injected water will be released from a plant processing 25,000 tons of coal per day.

TABLE 2.-Survey of metals in the SYNTHOIL reactor gas scrub water (sour water)

Metal	Concentration, mg/l	
	Distilled Water Influent	Effluent
Na	11	12
K	0.2	0.1
Rb	≤ 0.002	-
Cs	0.0004	0.0003
Mg	≤ 1	≤ 7
Ca	0.1	0.1
Sr	0.007	0.01
Ba	0.007	0.01
Ti	-	≤ 0.1
Zr	≤ 0.03	≤ 0.01
V	0.01	0.01
Cr	0.006	0.01
Mo	≤ 0.004	≤ 0.005
Mn	0.01	0.01
Fe	1	2
Co	0.02	0.002
Ni	0.006	0.005
Cu	0.1	0.1
Zn	0.4	0.2
Cd	≤ 0.02	≤ 0.006
B	0.03	0.4
Al	0.2	0.4
Ga	≤ 0.009	≤ 0.001
In	≤ 0.003	≤ 0.001
Si	6	2
Ge	≤ 0.007	≤ 0.002
Sn	≤ 0.01	≤ 0.006
Pb	≤ 0.1	≤ 0.07
P	1	2
As	0.005	0.005
Sb	≤ 0.03	≤ 0.002

In addition to the injected water, the residual moisture left in the feed coal after drying will emerge with this stream. Since the average moisture content of the dried and pulverized coal was assumed to be 3 pct, approximately 8,000 gph of water will come from this source. The stream will also contain the water formed by the reaction of hydrogen with the oxygen in coal. The eastern coals that are likely to be processed in a SYNTHOIL plant contain about 8 to 12 pct oxygen. However, not all of this oxygen is eliminated as water during hydrogenation. Assuming an average oxygen content of 10 pct in the coal and 3 pct in the product oil, approximately 18,000 gph of chemically formed water will be released. Thus, the reactor gas scrub water effluent stream will add up to a total of about 276,000 gph. The treatment facility for this effluent must be designed to accommodate changes in the type and concentration of contaminants with changes in feed coal.

Pyrolyzer Gas Scrub Water

An analysis of the centrifuged solids obtained from the processing of Homestead mine, Kentucky, coal in the 1/2 TPD unit is given in table 3. Pyrolysis data for this

TABLE 3.- Analysis of centrifuged solids

Solvent analysis, wt pct	
Organic benzene insolubles	14.9
Asphaltenes	3.1
Oil	29.2
Ash	52.8
Ultimate analysis, wt pct	
Carbon	36.4
Hydrogen	3.7
Nitrogen	0.4
Sulfur	4.6
Oxygen, by difference	2.1
Ash	52.8

solid are not yet available, but the analysis suggests that considerable quantities of NH_3 and H_2S will be formed during pyrolysis, and the pyrolyzer off-gas will have to be scrubbed with water to remove ammonium sulfide. The water will also remove tar and entrained impurities in the gas.

A SYNTHOIL plant processing 25,000 tons of coal per day will generate approximately 6,000 tons of centrifuged solids in the same time. We estimate the scrub water requirement for the pyrolyzer processing these solids at 1 lb per lb of solids pyrolyzed (c.f. scrub water requirement of 1 lb per lb of coal for the reactor gas). Thus approximately 62,500 gph of effluent will be released. More information is needed to determine if this effluent can be combined with the reactor gas effluent for treatment.

The char from pyrolysis of the centrifuge solids will be gasified to produce hydrogen for the process requirement. The mixture of CO and H_2 from the gasifier will be washed with water to remove impurities before converting the gas to pure H_2 by the classical water-gas shift reaction. At present, no information is available on the composition of the char or its gasification properties. Consequently, no comment is possible on the contaminants in the aqueous effluent from scrubbing of the gasification products.

Water From Claus Reactor

The H_2S recovered from the amine scrubber, sour water stripper, solids pyrolyzer and the hydrogen plant will be converted to sulfur in a Claus plant. The reactions involved in the conversion of H_2S to S by the Claus process are the following:

$$H_2S + \frac{3}{2} O_2 \rightarrow SO_2 + H_2O \qquad 5)$$

$$2H_2S + SO_2 \rightarrow 3S + 2H_2O \quad . \qquad 6)$$

Reaction 6 -- known as the "Claus reaction" -- is catalyzed by bauxite.

For stoichiometric calculations, reactions 5 and 6 may be added to give the following equation:

$$3H_2S + \frac{3}{2} O_2 = 3H_2O \quad . \qquad 7)$$

H_2S and the stoichiometric quantity of air determined from equation 7 are introduced into a furnace. One-third of the H_2S is thus converted to SO_2, which then reacts with the remaining two-thirds of the H_2S to give elemental S. Although the combustion of one-third of the H_2S to SO_2 is complete in the furnace, the formation of S by the reaction of SO_2 with H_2S proceeds to only partial completion in the furnace. The product stream from the furnace is cooled in a waste heat boiler and then in a condenser where the product S separates out as a liquid. The gases containing SO_2 and H_2S are reheated and passed through a series of three or four catalytic Claus reactors with interstage cooling of the product stream to condense S and reheating of the unreacted gases. Overall conversion efficiencies as high as 98 pct have been claimed.

It will be seen from equation 7 that for each mole of S a mole of water is formed. Thus, if a coal containing 4 pct S is being processed to an oil containing 0.5 pct S and the ash rejected from the hydrogen plant contains negligible S, the Claus unit of a SYNTHOIL plant processing 25,000 tons of coal per day will produce approximately 5,500 gph of water. In addition to H_2S, SO_2 and S, the water may contain other sulfur compounds as contaminants (10). Furthermore, impurities in the feed to the Claus plant may give rise to other contaminants in the effluent (11).

CONCLUSIONS

Aside from the maintenance discharges, there will be six aqueous effluents from a commercial SYNTHOIL plant. A review of these effluents shows gaps in knowledge which must be filled in order to design treatment facilities for the effluents. Several of these effluents, however, are not yet available. The analysis of a sour water effluent, obtained from a 1/2 TPD SYNTHOIL unit, is presented.

REFERENCES

1. Akhtar, S., et. al. SYNTHOIL Process for Converting Coal to Nonpolluting Fuel Oil. Energy Communications, 1, No. 1, pp. 21-36 (1975).

2. Akhtar, S., et. al. The SYNTHOIL Process - Material Balance and Thermal Efficiency. Sixtyseventh Annual AIChE Meeting, Paper No. 35b, Wash., D.C., Dec. 1974.

3. Sternberg, H. W., et. al. SYNTHOIL Process and Product Analysis. ACS Symp. Ser. No. 20: Hydrocracking and Hydrotreating, pp. 111-112 (1975).

4. Processes, Procedures, and Methods to Control Pollution From Mining Activities. EPA-430/9-73-011. Supt. of Documents, U.S. Government Printing Office, Wash., D.C. 20402, 1973.

5. Acid Mine Drainage in Appalachia. Appalachian Regional Commission, 1666 Connecticut Ave., Wash., D.C. 20235, 1969.

6. Brant, R. A. and E. Q. Moullon. Acid Mine Drainage Manual, Bull. No. 179, Engineering Experiment Sta., College of Engineering, The Ohio State University, Columbus, Ohio, 1960.

7. Coal for Energy Self-Sufficiency. Environ. Sci. & Tech. 10, No. 13, pp. 1200-1202 (1976).

8. Akers, D. J., Jr. and W. F. Lawrence. Acid Mine Drainage Control Methods, Soc. of Mining Engineers of AIME Meeting, Rept. No. 86, Chicago, Ill., 1973.

9. Standard Methods for the Examination of Water and Waste Water. Prepared and published jointly by American Public Health Assn., American Waterworks Assns. and Water Pollution Control Federation, 143rd Ed., 1975.

10. Meisen, A. and H. A. Bennett. Consider all Claus Reactions. Hydrocarbon Proc., 53, No. 11, pp. 171-174, (1974).

11. Foar, B. G. Impure Feeds Cause Claus Plant Problems. Hydrocarbon Proc., 53, No. 7, pp. 129-132, (1974).

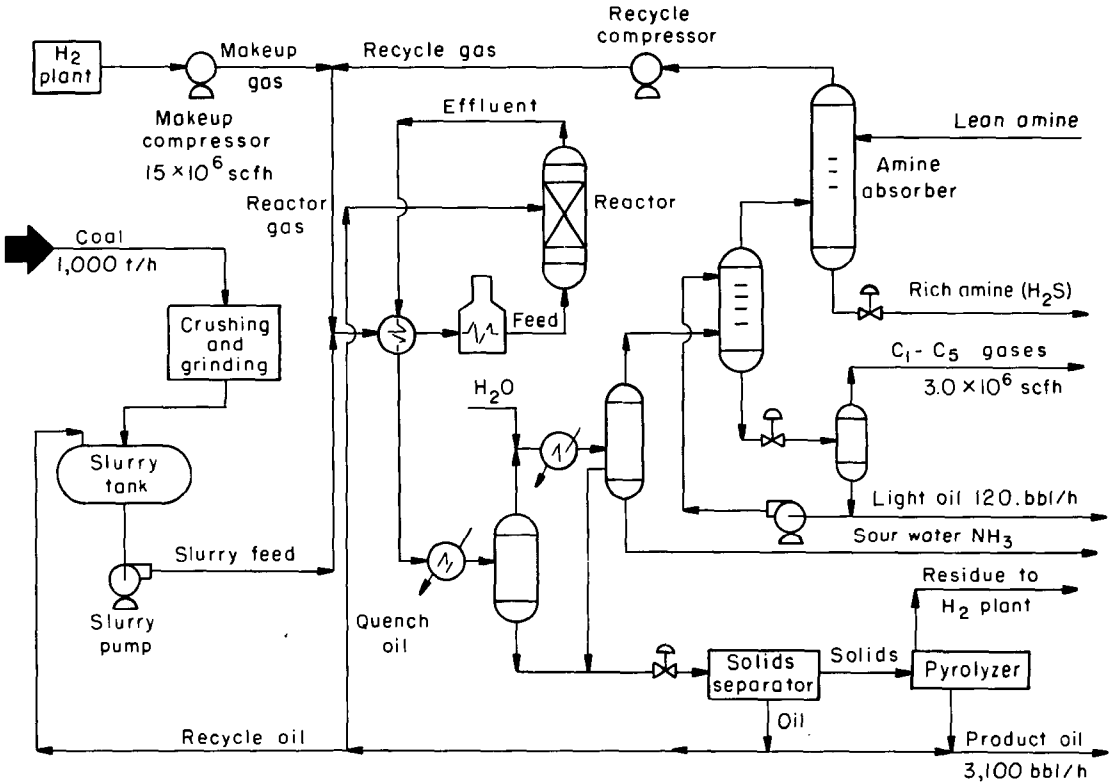

Figure 1. Flow diagram for a future commercial SYNTHOIL plant

L-14647

FRACTIONATION OF ORGANIC SOLUTES IN OIL SHALE RETORT WATERS FOR SORPTION STUDIES ON PROCESSED SHALE

H. A. Stuber and J. A. Leenheer

U.S. Geological Survey
Federal Center
Denver, Colorado 80225

A frequently proposed method for disposing of aqueous effluents from oil shale processing is the use of these waters for moistening processed shale (1). This method of disposal is part of the recently approved development plan for leased oil shale tract C-a (2). Retort waters produced with the oil are a major component of shale processing waste water. Retort waters contain high concentrations of organic and inorganic solutes which present serious disposal and purification problems (3-7). Many studies have focussed on solutes which might leach from processed shale (8-10), but little attention has been paid to the fate and transport of retort water solutes incorporated into processed shale or present in in situ retorts. Of particular interest are the organic solutes because of their potential toxicity.

Studies of organic solute transport are complicated by the complex and variable natures of both the retort waters and the processed shales which result from many diverse retorting methods. The use of surface-retorted processed shale has been proposed for the disposal of waste waters from both surface and in situ retorting (2). Organic solutes found in retort waters have been determined by many different methods (3, 11-13). This study will present a unique organic solute characterization based on sorption of both a true in situ and a simulated in situ retort water. This characterization data is then applied to solute sorption studies on TOSCO-II processed shale.

TOSCO-II[1] processed shale was selected as the sorbent in this investigation because its small particle size and high surface area facilitated laboratory studies and because it was considered most likely to give the high sorptive capacities (as compared to other processed shales) needed for disposal of retort water. Retort waters were obtained from both the 150-ton simulated in situ retort and the Rock Springs site 9 in situ retort of the Laramie Energy Research Center.

An organic solute fractionation scheme (DOC fractionation analysis) based upon adsorption was developed specifically for this study (14). Natural organic solutes in surface and ground waters in the area of the Green River formation were characterized by DOC fractionation analysis to assess the impact of possible inputs of waste water from oil shale processing. The purpose of this report is to relate DOC fractionation analyses of retort waters to sorptive interactions with processed shale so that predictions can be made about the movement of organic solutes from processed shale to adjacent soils and waters.

EXPERIMENTAL

Retort Water and Shale Samples. TOSCO-II processed shale was obtained from the TOSCO Corp. Research Center in Golden, Colorado. Site 9 in situ retort water, designated OMEGA-9 (15), and 150-ton retort water (barrel 66, run 13) were obtained from the Laramie Energy Research Center. Previously filtered OMEGA-9 water was stored at 4°C in a plastic lined, sealed drum. 150-ton retort water samples were aliquoted from an oil-and water-containing drum stored at room temperature. Filtration of 150-ton water through glass fiber filters removed suspended oil. Production wells 3, 4, 8, and 9 at the Laramie Energy Research Center's Site 9 in situ retort were sampled in May 1977. The warm oil and water mixture pumped from the wells was chilled to 4°C and stored in glass bottles. Glass fiber filtration removed suspended oil before fractionation and analysis.

Water Analysis. The major inorganic solutes in the retort waters were determined by the U.S. Geological Survey Denver Central Laboratory (16). Most of these

[1] The use of brand names in this report is for identification purposes only and does not imply endorsement by the U.S. Geological Survey.

data are available elsewhere, but the sulfur speciation of these waters has not been previously reported. Total sulfur was determined by a standard bromine in carbon tetrachloride digestion procedure (17). Sulfate was determined by a barium sulfate turbidimetric procedure (16). Thiosulfate was determined by iodimetric titrations. Raw waters as well as carbon filtered (to remove organic solutes) and zinc acetate treated (to precipitate any sulfide) water were titrated with standardized sodium triiodide. Sulfite was determined by the difference in equivalents of iodine consumed before and after addition of formaldehyde to complex any sulfite.

DOC Fractionations. DOC fractionation using macroreticular resins (5) was used to determine the distribution of organic solutes in the water samples. Analytical scale DOC fractionations were performed by Huffman Laboratories, Wheat Ridge, Colorado. Preparative scale fractionations of 150-ton and OMEGA-9 retort waters were conducted by a modification of the analytical scale method. In the modified procedure the acidification of the sample is accomplished on the H^+ form cation exchange column rather than by HCl addition. This eliminates CO_3 and HCO_3^- as CO_2, whereas HCl addition introduces Cl^- ions which require later removal on a large anion exchange column. The procedure is outlined in figure 1. Samples of the retort waters were diluted to a concentration of 500 mg/L DOC with distilled water and fractionated. Ten liters of diluted OMEGA-9 water and 36 liters of 150-ton retort water were fractionated. Hydrophobic solutes were concentrated and fractionated on a 3,200 mL bed of Amberlite XAD-8, a nonionic macroreticular acrylic ester resin. Hydrophobic bases (HPO-B) were eluted with 0.1 *N* HCl, hydrophobic acids (HPO-A) with 0.5 *N* NH_4OH and hydrophobic neutrals (HPO-N) with methanol. Hydrophilic bases (HPI-B) were concentrated on a 2,300 mL column of H^+ form AG MP-50 (BioRad Laboratories) cation exchange resin and eluted in 0.5 *N* NH_4OH. Hydrophilic acids (HPI-A) were concentrated on a 1,000 mL bed of OH^- form AG MP-1 anion exchange resin and eluted with 0.5 *N* HCl. Hydrophilic neutrals (HPI-N) passed through all columns and were collected.

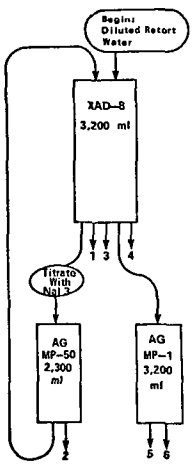

Figure 1.--Flow diagram of the fractionation of organic solutes in retort waters. 1. Hydrophobic bases, 2. Hydrophilic bases, 3. Hydrophobic acids, 4. Hydrophobic neutrals, 5. Hydrophilic neutrals, 6. Hydrophilic acids.

The procedure developed to fractionate retort waters on a large scale involves the addition of concentrated NaI_3 to the first XAD-8 eluate to destroy thiosulfate present. Thiosulfate dissociation to elemental sulfur and sulfite resulted in fouling of the cation exchange resin if this step was not included. The DOC concentrations of solutions derived from preparative fractionations were determined on a Beckman Model 915 carbon analyzer.

Sorption Studies. 150-ton retort water was diluted 1:10 (DOC≈500 mg/L) with distilled water. Weighed variable amounts of TOSCO-II processed shale were added to 200 mL volumes of the diluted retort water and the suspensions stirred for one week at 25°C in a water bath. After centrifugation aliquots of the supernatant solution were analyzed for DOC. Fractions of 150-ton retort water were diluted to a concentration (C_f) of organic solutes (as carbon) equal to 1/10 the concentration of that solute fraction in the original retort water. These solutions were brought to pH 8.65 and a specific conductance of 7,400 μmho/cm at 20°C by the addition of $NH_4(CO_3)_2$ and HCl to provide an inorganic solute composition similar to that in ten-fold diluted 150-ton retort water. Aliquots (200 mL) of these diluted fractions were equilibrated by stirring for 1 week at 25°C with varying amounts of TOSCO-II processed shale. After centrifugation, the DOC concentration of the supernatant solutions were determined. The hydrophobic neutral fraction was not studied because these solutes are obtained from the fractionation in methanol and are insoluble in water.

Amounts of activated carbon (Calgon Filtrasorb 400) varying from 10 mg to 10 g were added to 200 mL volumes of 150-ton retort water diluted 1:10 with distilled water. The suspensions were stirred for 1 week at 25°C, centrifuged, and DOC determinations were run on the supernatant solutions.

RESULTS AND DISCUSSION

Retort Water Inorganic Solute Analysis. The major inorganic constituents of the retort waters are presented in table 1. It was necessary to determine these species to devise a workable fractionation procedure and to properly design adsorption experiments. OMEGA-9, the in situ retort water, differs from the 150-ton simulated in situ retort water mainly in having lower concentrations of ammonia, carbonate species and organic solutes, and in having a far larger concentration of sodium. 150-ton water displays the character of a distillate in containing no appreciable concentrations of nonvolatile cations. 150-ton water also has a higher total ionic solute concentration (1,200 meq/L vs 500 meq/L) than the OMEGA-9 water. The differences in Na concentration and in total solute content probably are a result of the dilution of OMEGA-9 by native saline ground water. Analytical data on the native ground waters at the site (3) support this hypothesis.

The presence of thiosulfate in these waters has not been previously reported and the authors feel there has been some confusion about the sulfur speciation in OMEGA-9. We were led to study the sulfur chemistry of the waters because the application of OMEGA-9 to H^+ form cation exchange columns in the DOC fractionation scheme resulted in the formation of a sulfur precipitate which fouled the resin. Acidification of the waters also causes this same sulfur yielding dissociation of thiosulfate:

$$S_2O_3^{2-} + 2H^+ \rightleftharpoons SO_{2(g)} + S_{(s)} + H_2O. \qquad 1)$$

Several qualitative and quantitative tests were used to verify the sulfur chemistry of OMEGA-9 water. The presence of thiosulfate was indicated by the formation of elemental sulfur upon acidification, by the characteristic behavior of thiosulfate solutions upon addition of silver ions, and by the ability of OMEGA-9 water to dissolve silver chloride after all ammonia has been removed. No sulfide was detectable in the water by lead acetate paper tests of steam from acidified retort water. Sulfide was undetectable by the addition of $AgNO_3$ solution to retort water (Ag_2S forms if sulfide is present). The total sulfur content (2,300 mg/L) of OMEGA-9 matches the sum of the SO_4^{2-} (620 mg/L S as SO_4^{2-}) and $S_2O_3^{2-}$ (1,700 mg/L S as $S_2O_3^{2-}$) sulfur concentrations so that other S species must be at low levels

Table 1. Retort water solute analysis

Constituent	Barrel 66, run 13 150-ton retort	OMEGA 9 In situ retort
pH	8.6	8.5
Specific Conductance (micromhos at 20°C)	48,000	25,800
	Milligrams per liter	
Calcium (Ca)	4	8
Magnesium (Mg)	16	12
Sodium (Na)	188	4,100
Potassium (K)	24	43
Bicarbonate (HCO_3)	33,400	15,100
Carbonate (CO_3)	14,900	2,100
Chloride (Cl)	2,800	3,900
Fluoride (F)	12	56
Sulfate (SO_4)	1,340	1,400
Thiosulfate (S_2O_3)	2,050	3,000
Total Sulfur (S)	------	2,300
Ammonium (NH_4 as N)	------	3,800
Total Kjeldahl Nitrogen (TKN)	18,000	4,000
Dissolved Organic Carbon (DOC)	5,000	1,000
	Milliequivalents per liter	
NH_4	1,280*	271
Ca	0.2	0.4
Mg	1.3	1.0
K	0.6	1.1
Na	8.2	178
Cation Sum	1,290.3	451.5
HCO_3	547	247
CO_3	498	70
Cl	79	110
F	0.6	2.9
SO_4	27.9	29.1
S_2O_3	36.6	53
Anion Sum	1,189.1	512.0

* NH_4 estimated from TKN

relative to $S_2O_3^{2-}$ and SO_4^{2-}. Results of iodimetric determinations of $S_2O_3^{2-}$ were identical for raw samples, for carbon filtered (70 percent of DOC removed) and zinc acetate treated (to precipitate any sulfide which could also have oxidized NaI_3) samples. Sulfite was not present at detectable levels by iodimetry because consumption of iodine was identical before and after addition of formaldehyde which complexes any SO_3^{2-} present.

We can speculate on the origin of thiosulfate in retort water. Heated gasses containing SO_2 and steam probably contacted sulfides, H_2S or perhaps even elemental sulfur derived from the roasting of pyrite. These known aqueous solution reactions are perhaps clues to the sulfur chemistry in the retort:

$$SO_3^{2-} + S_{(s)} \longrightarrow S_2O_3^{2-}{}_{(aq)} \text{ alkaline pH,}$$

$$SO_{2(aq)} + H_2S_{(aq)} \longrightarrow S_2O_3^{2-}{}_{(aq)} + \text{other polythionates (Wackenroder's solution)} \qquad 2)$$

Organic Solute Fractionation. DOC fractionation analysis was developed to serve as a compound classification based on sorption that fills the gap in organic solute characterization between organic solute concentration (DOC) and specific compound identification. Hydrophobic solutes are first isolated and fractionated into acid, base, and neutral components by physical adsorption and desorption on a macroreticular, acrylic ester resin. After removal of hydrophobic solutes from water, hydrophilic base and acid solutes are isolated by ion-exchange sorption on cation and anion exchange resins, respectively. Hydrophilic neutral solutes remain dissolved in the deionized water sample at the end of the fractionation sequence. Because DOC fractionation analysis is based on various sorptive interactions, it is a useful method for studying and defining the sorptive interactions which occur between retort water organic solutes and processed shale. In addition, the sorption studies have been simplified to six compound classes which are relatively homogeneous with respect to their sorptive interactions, as opposed to the impossible task of defining the sorptive interactions of each compound in retort water. Additional uses and interpretations of data from DOC fractionation analysis have been previously discussed (14), and table 2 lists the types of compounds likely to be found in each fraction.

Table 2. Compound classes in organic solute fractions

HPO-B:	Aromatic amines except pyridine,
HPO-A:	Aliphatic carboxylic acids > five carbons; aromatic carboxylic acids, phenols.
HPO-N:	Hydrocarbons, aliphatic alcohols, amides esters, ketones, and aldehydes of < five carbons, pyrroles, and indoles.
HPI-B:	Aliphatic amines, pyridine, amino acids.
HPI-A:	Aliphatic acids of ≤ five carbons, polyfunctional acids.
HPI-N:	Aliphatic amides, alcohols, aldehydes esters, and ketones ≤ five carbons. Polyfunctional alcohols, carbohydrates.

The analytical DOC fractionation data from 150-ton and OMEGA-9 retort water and a natural surface water are shown in table 3.

Table 3. Dissolved organic carbon fractionation analyses as percent of initial DOC

Fraction	150-ton retort Water (5,000 mg/L DOC)	OMEGA-9 Retort Water (1,000 mg/L DOC)	Piceance Creek at White River (9.1 mg/L DOC)
Hydrophobic solutes	65	49	51
Hydrophilic solutes	35	51	49
Hydrophobic bases	9	13	1
Hydrophobic acids	28	19	23
Hydrophobic neutrals	28	17	27
Hydrophilic bases	8	12	2
Hydrophilic acids	17	29	44
Hydrophilic neutrals	10	10	3

In the preparative scale fractionations the overall yield of organic solutes (based on DOC) obtained in the fractions was 85 percent for 150-ton retort water and 90 percent for OMEGA-9 water. The 150-ton retort water contains a higher concentration of hydrophobic solutes, with most of the difference appearing in

hydrophobic acids and neutrals. Hydrophobic acids can act as anionic detergents which would tend to increase the solubility of hydrophobic neutral species in water. The higher concentration of hydrophobic neutrals in 150-ton water is probably due to solubilization by hydrophobic acids.

The presence of significant concentrations of basic solutes distinguishes the solute distribution in these retort waters from that in most natural waters. Natural waters normally contain a hydrophilic base concentration of 1-10 percent of the total DOC, but hydrophobic bases are usually nearly undetectable (18). The data from the DOC fractionation of the Piceance Creek sample is typical of a natural surface water. Hydrophobic organic base concentrations in natural waters are generally low because such solutes are strongly adsorbed by cation exchange processes on most soils and sediments, and by hydrophobic interactions (19). Also, there are not as many natural sources for organic bases as there are for organic acids. The contamination of a natural water by retort water might be readily detectable by an increase in the level of hydrophobic base solutes.

Sorption Studies. The sorption isotherms presented in this study were generated by allowing solutions of identical initial organic solute concentration (C_i) to equilibrate with varying weights of sorbent, then measuring the equilibrium organic solute concentrations (C_{eq}). The sorptive capacity of the sorbent (mg organic carbon/g sorbent) is plotted as a function of C_{eq}. This experimental approach makes it possible to observe differences in the affinity of the sorbent for different components in a complex mixture of solutes. The data generated in this manner also provides better insight into the transport of a mixture of solutes through processed shale than the alternate experimental design in which the sorbent weight is held constant while C_i is varied. This experimental design is important because one of the goals of this study was to determine which types of organic solutes are strongly sorbed by the processed shale and which are not. All retort waters were diluted with distilled water to a C_i = 500 mg/L DOC to reduce organic solute-solute interactions so that the varied affinities of the different solute fractions might be better observed. Above C_i = 500 mg/L DOC, the DOC fractionation changed with increasing DOC, whereas below C_i = 500 DOC, the DOC fractionation remained essentially constant as DOC decreased.

TOSCO-II processed shale was compared with activated carbon to better evaluate its potential as a sorbent for the organic solutes in retort water. Sorption isotherms based on DOC for unfractionated 150-ton retort water on TOSCO-II processed shale and on Calgon Filtrasorb 400 activated carbon are shown in figure 2. The most significant result is that, on an equivalent weight basis, activated carbon has a far greater sorptive capacity for retort water organic solutes than processed shale, despite similarities in surface appearance. On an equivalent carbon basis using five percent non-carbonate carbon remaining in TOSCO-II processed shale, the shale has approximately half the sorptive capacities of activated carbon. An interesting feature of the processed shale sorption isotherms is the sudden increase in the slope of the curve at C_{eq} = 400 mg/L DOC (C_{eq} = 80 percent of C_i). This indicates that about 20 percent of the retort water DOC has a much higher affinity for TOSCO-II processed shale than the remaining 80 percent.

Sorption isotherms of the individual organic solute fractions derived from 150-ton retort water on TOSCO-II processed shale (figure 3) provide insight into specific sorptive processes. The most important aspect of the solute fraction isotherm data is the greater sorptive capacity of the shale for acid fractions than for base fractions, an unexpected result. Cation exchange properties of most natural soils and sediments normally results in higher sorptive capacities for bases than acids (7). The processed shale does not seem to exhibit this sorptive capacity for the bases in retort water. As expected, hydrophobic solute fractions are more strongly sorbed than hydrophilic fractions. The rapid increase in the slope of the unfractionated sorption isotherm (fig. 2) at C_{eq} = 400 mg/L DOC (C_{eq} = 80 percent of C_i) is probably due to the expected high affinity of the water insoluble hydrophobic neutral fraction for the processed shale. The individual fraction isotherms in figure 3 have been added to yield a fraction composite isotherm.

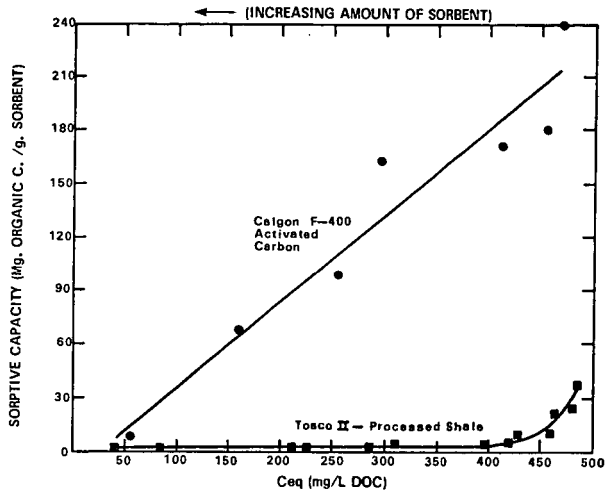

Figure 2.--Sorption of 150-ton retort water on Calgon F-400 and TOSCO II-processed shale.

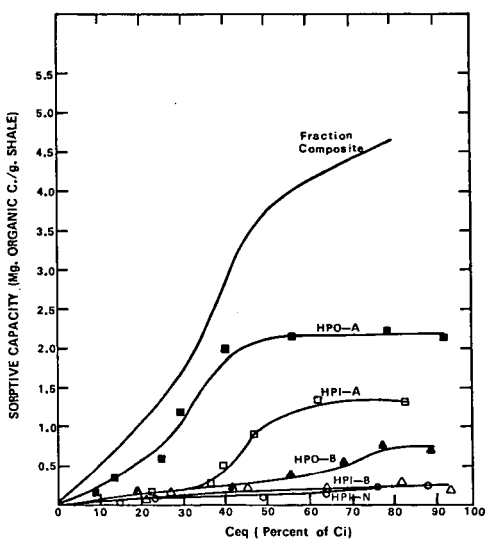

Figure 3.--Sorption of 150-ton retort water organic solute fractions on TOSCO II-processed shale.

Figure 4 compares the fraction composite isotherm with the unfractionated sorption isotherm. Below C_{eq} = 80 percent of C_i the two isotherms represent sorptive capacities of the same magnitude but do not exactly coincide and the difference is very likely due to the absence of any contribution from the hydrophobic neutral fraction to the composite fraction isotherm. In the unfractionated sorption isotherm experiment the sorption of high affinity hydrophobic neutrals could result in a modified sorbent surface, different from that present in experiments on separate fractions. Differences between the composite and unfractionated data could also arise from solute-solute interactions. Above C_{eq} = 80 percent of C_i the unfractioned sorption isotherm diverges greatly from the composite isotherm because of the high capacity of the shale for hydrophobic neutral solutes.

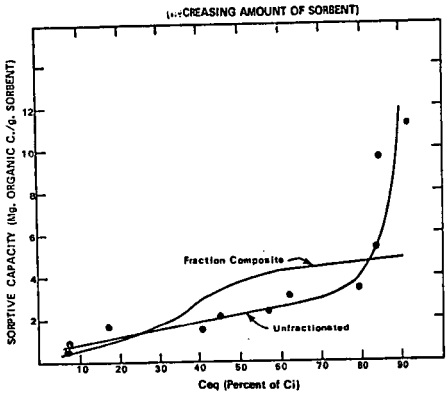

Figure 4.--Comparison of unfractionated versus fraction composite sorption isotherms of 150-ton retort water on TOSCO-II processed shale.

Rock Springs Site 9 Studies. Production wells 3, 4, 8, and 9 at the Rock Springs site 9 in situ retort were sampled for water in May 1977, approximately seven months after OMEGA-9 water was collected. The primary objective was to determine changes in organic solute composition with time. Table 4 presents the data from this study arranged in order of decreasing organic solute concentration (based on DOC) from left to right. The decrease in DOC and the shift in the hydrophobic-hydrophilic ratio seem to indicate that extensive dilution of the Site 9 retort water by native ground water has occurred in the seven months since collection of OMEGA-9. The most significant result here is that the hydrophobic base fraction has not been removed by sorption on the processed shale in the retort. This finding is in accord with the laboratory sorption data. Meaningful interpretations of other organic solute changes cannot be made because the system is complicated by inputs from the native ground water.

Thiosulfate was not detectable in water from any of the four wells. Sulfide and sulfite were also undetectable by iodimetry. A determination of sulfate and total sulfur content in water from one of the wells (no. 9) shows that essentially all sulfur present is in the form of sulfate. It is not known whether all thiosulfate containing water has been effectively displaced by ground water, or whether an oxidative, microbial, or sorptive process is the cause of the disappearance.

Table 4. DOC Fractionation Analyses of Site 9 Ground Water as percent of initial DOC

Fraction	OMEGA-9 (1,000 mg/L DOC)	Well 3 (500 mg/L DOC)	Well 8 (140 mg/L DOC)	Well 4 (80 mg/L DOC)	Well 9 (120 mg/L DOC)	Ground-water composite collected before retorting
Hydrophobic solutes	49	62	63	66	65	71
Hydrophilic solutes	51	38	37	34	35	29
Hydrophobic bases	13	14	10	13	4	1
Hydrophobic acids	19	29	32	34	39	38
Hydrophobic neutrals	17	19	21	19	22	32
Hydrophilic bases	12	12	9	11	9	8
Hydrophilic acids	29	19	18	17	22	17
Hydrophilic neutrals	10	7	10	6	5	5

CONCLUSIONS

This study has presented a characterization of the organic solutes in retort water based on sorption processes and has identified some important features of the sorptive properties of TOSCO-II processed shale. Retort waters contain high concentrations of ammonia, organic bases, and thiosulfate, that are normally very low in natural waters. TOSCO-II processed shale sorbs organic acids preferentially to organic bases whereas the reverse is true in most soil systems.

TOSCO-II processed shale has a low overall sorptive capacity for retort water organic solutes when compared on an equal weight basis to activated carbon, despite similarities in appearance. The organic solute fractions most likely to pass through or run off TOSCO-II processed shale are the hydrophilic neutral, hydrophilic base and hydrophobic base fractions. Of most obvious environmental concern is the hydrophobic base fraction that is at low levels in natural waters. TOSCO-II processed shale is an effective sorbent for hydrophobic neutral species and thus will better retain hydrocarbonlike solutes. Polyaromatic hydrocarbons and neutral polynuclear heterocycles, refractory compounds of great environmental importance, would very likely be removed from oil shale waste waters by contact with TOSCO-II processed shale. This kind of information should be utilized in the design of waste-water disposal methods.

It appears that DOC fractionation analysis can provide useful information about the transport of retort water organic solutes from in situ retorts and about the migration of organic solutes from surface-disposed retort waters. The results of this work have led to other investigations into the surface chemistry of retorted oil shale and into the sorptive interactions of retort water solutes with soils and sediments. It is hoped that the research presented here will be the first step in developing a conceptual model of the transport organic solutes derived from retort water through processed shales, and later of their transport through soil systems.

ACKNOWLEDGMENTS

The authors thank R. E. Poulson, D. S. Farrier, and L. P. Jackson of the Laramie Energy Research Center for furnishing support, advice, and supplying all retort water samples. We also wish to thank M. T. Atwood and R. M. Coomes of TOSCO Corp. for supplying the TOSCO-II processed shale.

REFERENCES

(1) Cameron Engineers, Inc., Synthetic Fuels Data Handbook; compiled by J. A. Hendrickson, p. 102, (1975).

(2) Gulf Oil Corporation and Standard Oil (Indiana), Revised Detailed Development Plan for Tract C-A, Submitted to Area Oil Shale Supervisor, U.S. Geological Survey, (1977).

(3) Harding, B. L., K. D. Linstedt, E. R. Bennett, and R. E. Poulson, Removal of ammonia and alkalinity from oil shale retort waters by the use of weak acid cation exchange resins. Proceedings of the Second Pacific Area Chemical Engineering Congress, Denver, Colorado, 1, p. 442-449, (1977).

(4) Jackson, L. P., R. E. Poulson, T. J. Spedding, T. E. Phillips, and H. B. Jensen, H. B., Characteristics and possible roles of various waters significant to in situ oil shale processing, Quar. Colorado School of Mines, 70, no. 4, p. 105, (1975).

(5) Murphy, C. L., A. L. Hines, and R. E. Poulson, Hot gas stripping of simulated in situ oil shale retort water: This symposium. (1975).

(6) Neal, L. G., J. Cotter, R. D. Sung, and C. Prien, An evaluation of the pollution abatement technologies available for treatment of wastewater from oil shale processing, Proceedings of the 68th Annual Meeting of the American Institute of Chemical Engineers, Los Angeles, California, 32 pp., (1975).

(7) Ossio, E., P. Fox, J. F. Thomas, and R. E. Poulson, Anaerobic fermentation of simulated in situ oil shale retort water, This symposium, (1975).

(8) Amy, G., J. Thomas, and A. L. Hines, Leaching of organic residuals from simulated in situ retorted oil shale: This symposium, (1977).

(9) Parker, H. W., R. M. Bethea, N. Guren, M. N. Gaydor, and J. C. Watts, Interactions between ground water in in situ retorted oil shale. Proceedings of the Second Pacific Area Chemical Engineering Congress, Denver, Colorado, 1, p. 450-454, (1977).

(10) Ward, J. C., Water pollution potential of spent oil shale residues from above ground retorting: Colorado State University, (1972).

(11) Ho, C. H., B. R. Clark, and M. R. Guerin, Direct analysis of organic compounds in aqueous by-products from fossil fuel conversion processes. Oil shale retorting, Synthane coal gasification, and COED coal liquefaction. J. Environ. Sci. and Health, 11, p. 481, (1976).

(12) Pellizzari, E. D., N. P. Castillo, S. Willis, D. Smith, and J. T. Bursey, Identification of organic constituents in aqueous effluents from energy-related processes: This symposium, (1978).

(13) Wen, C. S., Electrolytic processes of oil shale and its derivatives: Doctoral Dissertation, University of Southern Californis, 239 p., (1976).

(14) Leenheer, J. A., and E. W. D. Huffman, Jr., Classification of organic solutes in water by using macroreticular resins. Jour. Res. U.S. Geol. Survey, 4, no. 6, p. 737-751, (1976).

(15) Farrier, D. S., R. E. Poulson, Q. D. Skinner, and J. C. Adams, Aquisition, processing, and storage for environmental research of aqueous effluents derived from in situ oil shale processing, Proceedings of the Second Pacific Chemical Engineering Congress, Denver, Colorado, 2, p. 1031-5, (1977).

(16) Techniques of Water Resources Investigations of the U.S. Geological Survey, Methods for the analysis of inorganic substances in water and fluvial sediments, In preparation, (1977).

(17) Official Methods of Analysis of the Association of Official Analytical Chemists, 11th Ed., AOAC, p. 31, (1970).

(18) Leenheer, J. A., Unpublished data. (1977).

(19) Stevenson, F. J., Organic matter reactions involving pesticides in soil, Ch. 15 in ACS Symposium Series, no. 29, Bound and Conjugated Pesticide Residues, p. 180-207 (1975).

Biokinetics of Activated Sludge Treatment of SYNTHANE Fluidized Bed Gasification Wastewaters

Ronald D. Neufeld*, Charles J. Drummond, Glenn E. Johnson

U. S. Department of Energy
Pittsburgh Energy Research Center
4800 Forbes Avenue
Pittsburgh, PA 15213

*Also Associate Professor of Civil Engineering
University of Pittsburgh
Pittsburgh, PA 15261

Introduction

The SYNTHANE process, developed at the Pittsburgh Energy Research Center, is a second generation fluidized bed gasification process capable of producing a high-Btu substitute natural gas product. This process differs from fixed bed or slagging processes in that the coal is kept in a fluidized state, the fluidizing media consisting of steam and pyrolysis gases. Ground coal, which may be pretreated to destroy its agglomerating properties, is fed to the gasifier where it reacts with steam and oxygen. Bed temperatures and product gas composition may be varied within limits by the steam to coal and oxygen to coal ratios employed. Due to overall thermal balance considerations, about 70% of the carbon in the coal is gasified, while the remaining carbon and an inorganic residue is removed from the gasifier bottom as a char product which will be burned in a commercial plant. While much of the coal carbon is converted to CO, CO_2, and CH_4, a small fraction, amounting to about 4% to 6% of the feed carbon, appears as liquid effluent tars and potential water pollutants from the scrubbed product gas. This value as found for SYNTHANE is similar in magnitude to that reported by Ellman et al. (1) for the slagging fixed bed gasification at the Grand Forks Energy Research Center. It further appears that, for fluidized bed gasification, this fraction of liquid phase carbon may be further reduced via alteration in coal injection geometry (2) and via alterations in gasification conditions (3). However, such alterations extract an economic toll in terms of thermal efficiency and have not been fully evaluated.

While characterization of components and concentrations of coal gasification wastewater has been reported (4,5,6), little published data exists regarding normalization of components of pollutants produced per unit coal gasified. Table 1 presents effluent production data for the SYNTHANE gasification of Montana Rosebud coal (37 gasification runs), Illinois #6 coal (27 gasification runs), and North Dakota lignite (9 gasification runs) in terms of pounds of pollutants produced per ton of coal gasified, moisture and ash free (MAF). These data were collected from the 40 lb coal per hour SYNTHANE PDU gasifier located at the Pittsburgh Energy Research Center. All environmental analyses were conducted in accord with Standard Methods (7). Data on the same basis from the literature for fixed bed Lurgi, slagging fixed bed, and Hygas gasifier effluents are also presented in Table 1.

This table shows that the effluent pollutant component production is of a consistent order of magnitude for the SYNTHANE gasification of Montana Rosebud, Illinois #6, and North Dakota lignite coals with the exception of thiocyanate and cyanide production. These components appear to be about one order of magnitude greater for the gasification of the Illinois #6 coal than for the other coals considered.

Comparison of published data for the Lurgi, Hygas, and GFERC gasification facilities indicates that the Lurgi gasification of Rosebud coals in the existing Lurgi first generation facility at Westfield, Scotland produced more of each pollution

Table 1. - Normalized Production of Gasifier Wastewater Pollutants (lb/ton of coal (MAF) + coefficient of variation if available)

Parameter	SYNTHANE			LURGI(8)	GFERC(1)		HYGAS (9)
	Montana Rosebud	Illinois #6	North Dakota Lignite	Montana Rosebud	Lignite 200 psi	Lignite 400 psi	Lignite Run #37
BOD	27.1 ± 34%			66.5	7		
TOC	22.1 ± 69%	21.1 ± 23%	40.7 ± 24%		13.9	8.3	39.1
COD	55.5 ± 64%	64.2 ± 12%	70.6 ± 33%	103			
PHENOL	8.72 ± 79%	9.12 ± 22%	10.8 ± 36%	21.8		6.8	11.4
OIL & TAR	1.77 ± 44%	1.96 ± 34%		3.2	2.8	0.78	
ACETONE SOL.[a/]	1.98 ± 62%	2.26 ± 36%					
THIOCYANATE	0.067 ± 105%	0.67 ± 40%	0.053 ± 71%	0.08			2.5
CYANIDE ($x10^{-4}$)	2 ± 225%	7.8 ± 89%	2.1 ± 110%	200			0.287
H_2S	0.033 ± 95%			0.57			
TOTAL SULFUR	0.449 ± 22%			1.31			0.2
FREE + FIXED NH_3	14.0 ± 29%			72.1	6.6	6.6	13.1
ALKALINITY	3.95 ± 33%			219	13.3	12.1	
TOTAL TAR + OIL PRODUCTION[b/]	30.4 ± 83%	77.6 ± 50%		210	70.1	55.5	
WASTEWATER PRODUCTION	2740 ± 46%	3920 ± 19%	3300 ± 42%	2976	916	736	

a/ Acetone Soluble Tars: A measure of high molecular weight organics precipitated from pretreated gasifier water by pH depression, an analytical technique developed at PERC

b/ Measured prior to settling and hence is not part of the wastewater.

component than did each of the improved or second generation domestic experimental gasification facilities. Comparison of the data for SYNTHANE and Hygas indicates a degree of similarity; however, the SYNTHANE data is an averaged composite of many runs while the data collected to date for Hygas is from one specific run. Thus, such comparisons, at this time, must be considered as preliminary.

Results and Discussion

Initial evaluation of raw gasifier water indicated a need for partial removal of ammonia and floating oily materials prior to biological processing. An overview of linkages of suitable SYNTHANE wastewater processing steps with preliminary process proof of principle data is discussed by Johnson, et al. (4). In this experimental approach, ammonia is reduced from 10,000 mg/l to about 500 mg/l via batchwise air stripping at an elevated pH. This treatment also results in an 80% reduction of the alkalinity of the wastewater reducing the chemical requirements of future pH manipulations.

The removal of trace suspended oils and tars is accomplished by pH depression with sulfuric acid and alum coagulation. About 20% of the influent soluble TOC and about 50% of the wastewater oils, grease and tars are removed in this step. Filtration of the treated effluent assures no particulate carry-over to the biological reactor. In larger scale installations, this filtration step would be replaced by sedimentation, sand bed filtration or dissolved air flotation.

Experimental Protocol

Continuously operated 7-liter biological reactors were designed with adjustable internal clarifiers to provide recirculation of settled bio-sludge. Pumping was accomplished via micro-bellows pumps. The prepared feed for each reactor was kept at about 4°C via a large chilled water bath. Appropriate levels of mono and dibasic potassium phosphate were then added as nutrients to the feed so that the influent TOC/N/P ratios were about 60/6/1 with a buffered pH of about 7.5. However, both phosphate and nitrogen were periodically monitored to assure ample supply. Influent and effluent samples of each bioreactor were monitored for pH, suspended solids, volatile suspended solids (used as a monitor of biomass level), phenolics, biochemical oxygen demand (BOD), chemical oxygen demand (COD), and total organic carbon (TOC). Both sludge volume index and specific oxygen consumption were monitored once steady state was achieved. Prepared feed to the biological reactors was diluted with tap water for appropriate kinetic determinations. In most cases, the hydraulic detention time was kept at about 1 day while the sludge age and applied organic loading varied as independent parameters.

Biological growth kinetic analysis indicates that the net growth rate of biomass follows the relationship:

$$\frac{dX}{dt} = uX - bX \qquad 1)$$

where: u = specific growth rate (day^{-1})

X = volatile suspended solids (mg/l, a measure of concentration of biological solids)

b = endogenous decay coefficient (day^{-1})

t = time

The specific growth rate (u) is a kinetic function, and is therefore related to the nature of the organic substrate, pH, temperature, toxicant levels, limiting nutrients, etc. Thus, for conditions where only the organic substrate (S) ambient to the organisms is allowed to vary, with all other parameters essentially constant, we may write:

$$u = \frac{dX}{dt} \cdot \frac{1}{X} = f\ (S) \qquad 2)$$

where f(S) is a derived kinetic equation expressing the rate of biomass growth as a function of substrate concentration.

The growth of organisms (dX/dt) is also related to the rate of substrate utilization (dS/dt) by the relationship:

$$dX/dt = a(dS/dt) - b\ X \qquad 3)$$

where a = yield coefficient (wt biomass/wt substrate used)

Equation 2 may be written in terms of the specific utilization rate of substrate as:

$$\frac{dS}{dt}\frac{1}{X} = f'(S) \qquad 2a)$$

For aerobic systems such as those utilized in this research, the utilization of oxygen is related to the oxygen required for substrate bio-oxidation, and to the oxygen required for maintenance of the cellular biomass. Thus, an oxygen utilization equation may be written of the form:

$$\frac{dO_2}{dt} = a'\frac{dS}{dt} + b'X \qquad 4)$$

where: a' = oxygen utilization coefficient (wt O_2/wt substrate)

b' = endogenous constant (wt O_2 used/wt biomass-day)

The approach used in this research is to evaluate the constants of Equations 3 and 4, and determine the functional form of Equation 2a, the governing kinetic equation, for several measures or bases of organic substrate in SYNTHANE gasifier wastewater.

Test Results

Each "run" for the continuous biological reactors lasted a period of several weeks to months, during which time steady state was achieved and sustained.

During each run, the feed to the majority of the reactors was diluted with tap water to 15% $\pm$ 5% concentration of gasifier condensate, the exact value depending on the TOC level of the specific wastewater sample. Thus, each data point on Figures 1 and 2 represents a sustained steady state condition with influent feed being composed of effluent from a series of Montana coal gasification runs, the overall influent TOC being held constant. Three experimental runs, however, were conducted with undiluted gasifier water in order to determine potential deviations from developed bio-kinetics and to illustrate "worst case" conditions for effluent quality stability. These points are also identified on Figures 1 and 2.

Analysis of data from the diluted gasifier feeds indicated that a first order relationship of the form:

$$\frac{\Delta TOC}{\Delta t}\frac{1}{X} = K\ (TOC) \qquad 5)$$

did not go through the origin. This indicated the existence of a non-degradable fraction of TOC in gasifier water. For the 15% concentrations used, this value

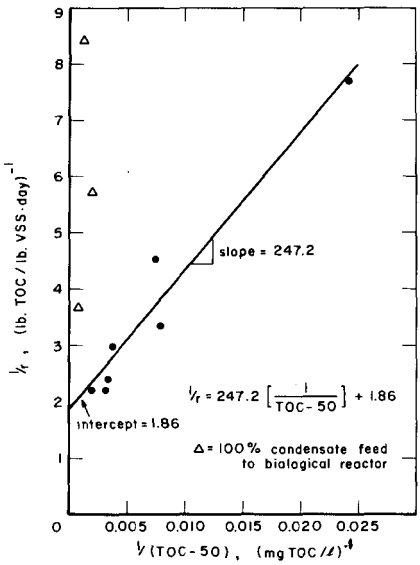

Figure 1 - Lineweaver - Burk plot of TOC data corrected for non - degradable TOC. SYNTHANE gasifier water, Montana Coals.

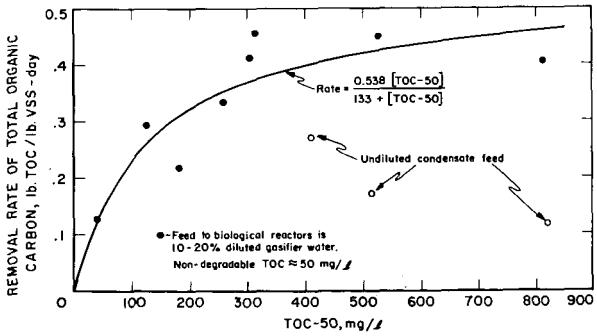

Figure 2 - Biokinetics of TOC removal. SYNTHANE gasifier water, Montana Coals.

11-22-77 L-15698

appeared to be on the order of about 50 mg/l. The set of observed data was found to fit a classical Monod relationship (10), modified to reflect the non-degradable TOC fraction, of the form:

$$r = \frac{\Delta\ TOC}{\Delta\ t}\frac{1}{X} = \frac{r'\ (TOC-50)}{k + (TOC-50)} \qquad 6)$$

where: r' = maximum specific rate of TOC utilization (lb TOC/lb VSS-day)

r = measured specific rate of TOC utilization (lb TOC/lb VSS-day)

(TOC-50) = biodegradable level of soluble TOC ambient to biomass (mg/l)

k = constant (mg/l)

The values of r' and k may be graphically determined, using linear regression techniques, by noting the inverted or Lineweaver-Burk (10) linear form of the equation as:

$$1/r = \frac{k}{r'}\frac{1}{(TOC-50)} + \frac{1}{r'} \qquad 7)$$

A plot of 1/r against 1/(TOC-50) should yield a straight line if the functional form of the kinetic equation fits Monod type kinetics. Figure 1 illustrates the graphical determination of such constants from slope and intercept analysis, yielding the result:

$$\frac{\Delta\ TOC}{\Delta\ t}\frac{1}{X} = \frac{0.538\ (TOC-50)}{133 + (TOC-50)} \qquad 8)$$

This equation is plotted on Figure 2 with data points for comparison. It should be noted that the three steady state values for TOC utilization for the reactors with undiluted condensate feed do not fit the overall kinetics obtained. One possible explanation for these phenomena is that some toxic inhibitor exists in SYNTHANE plant wastes in concentrations which become significant only at SYNTHANE condensate concentrations stronger than the 15% value used for kinetic determinations. Also, one should note that the nonbiodegradable portion of the undiluted condensate would be larger than the 50 mg/l value cited. Investigations are underway to quantify the non-biodegradable TOC concentration of the wastewater and to determine if toxic inhibition does exist.

The functional form of the kinetic equation for BOD utilization did <u>not</u> similarly correlate in accord with Monod kinetics. Figure 3 indicates that, for the range of BOD from 2 mg/l to 130 mg/l, the BOD utilization data best fit the relationship:

$$\frac{\Delta\ BOD}{\Delta\ t}\frac{1}{X} = 0.182\ (BOD)^{0.186} \quad \text{(lb BOD used/lb VSS-day)} \qquad 9)$$

Some scatter exists in this correlation, however, it should be noted that BOD measurements are, by nature of the test, subject to considerable error and scatter (7).

Development of a suitable correlation for specific <u>phenol</u> utilization rates from gasifier water is difficult since phenol, as measured by <u>Standard Methods</u> (7), is a colorimetric test sensitive to phenol, cresols, and other aromatic hydrocarbons to various degrees. For phenol levels of less than 5 mg/l, Figure 4 shows that the specific utilization rate best appears to fit the relationship:

$$\frac{\Delta\ (Phenol)}{\Delta\ t}\frac{1}{X} = 0.423\ (Phenol)^{0.58} \quad \text{(lb phenol used/lbVSS-day)} \qquad 10)$$

This relationship does <u>not</u> appear to properly model phenol utilization over an expanded range of phenol concentrations as shown on Figure 5. A better fit was found

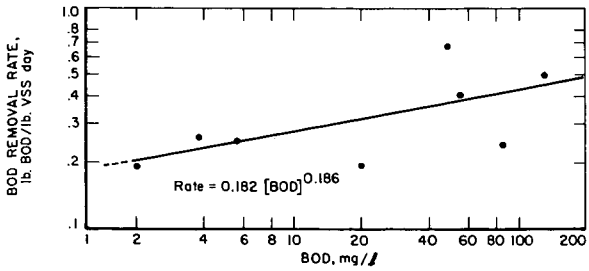

Figure 3 – Biokinetics of BOD removal from SYNTHANE gasifier condensate, Montana Rosebud Coal.

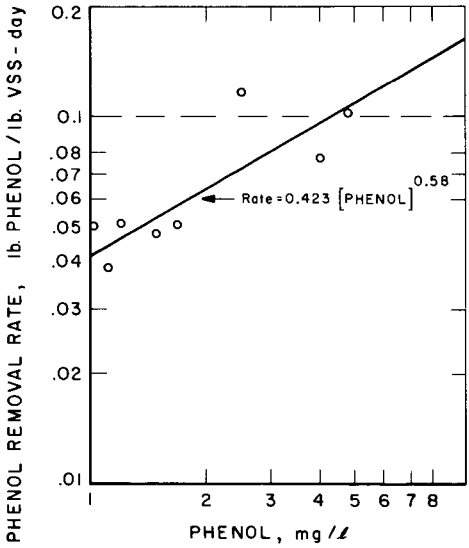

Figure 4 - Biokinetics of phenol removal in SYNTHANE gasifier condensate. Montana Rosebud Coal, low phenol concentrations.

11-22-77 L-15699

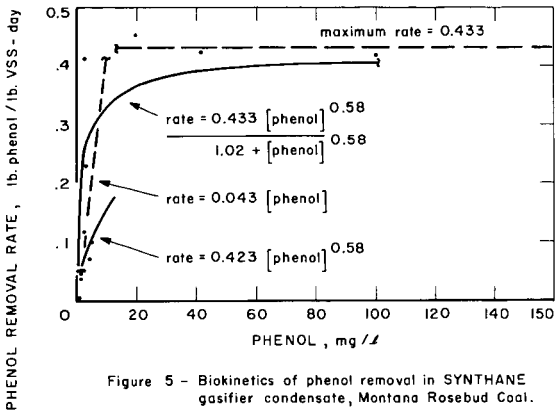

Figure 5 - Biokinetics of phenol removal in SYNTHANE gasifier condensate, Montana Rosebud Coal.

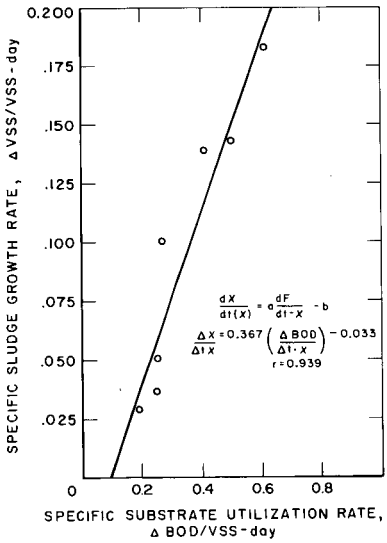

Figure 6 - Biomass production parameter determinations.

11-22-77 L-15700

using a continuous equation of the form of modified Monod kinetics:

$$\frac{\Delta\ (\text{Phenol})}{\Delta\ \ t}\ \frac{1}{X} = \frac{0.433\ (\text{Phenol})^{0.58}}{1.02 + (\text{Phenol})^{0.58}} \qquad 11)$$

Figure 5, however, also indicates that over the wider range of phenol levels, the governing kinetic equation for specific rates of phenol utilization may be best approximated by a zero order relationship of the form:

$$\frac{\Delta\ (\text{Phenol})}{\Delta\ \ t}\ \frac{1}{X} = 0.433 \quad (\text{lb phenol used/lb VSS-day}) \qquad 12)$$

for phenol levels ambient to the organisms greater than 10 mg/l, and a first order relationship for lower phenol levels. As indicated above, due to the non-specificity of the Standard Methods (7) phenol test, a mixed model for phenol utilization may be expected. It should also be anticipated that similar models based on pure phenol bio-degradation would give different numerical results.

Parameters fitting the biomass production equation (Equation 3) are developed as shown in Figure 6. From this figure, it may be seen that: a = 0.367 lb biomass produced/lb BOD removed; and the decay coefficient is: b = 0.033/day.

Similar curves shown on Figure 7 were developed for oxygen consumption in accord with Equation 4, yielding the following results for "a'" and "b'".

Substrate Basis	a' lb O_2 used/lb substrate removed	b' endogenous respiration coefficient lb O_2/lb VSS-day
BOD	0.747	0.110
TOC	1.680	0.090
COD	0.562	0.093

With biokinetic parameters for substrate utilization rates and necessary sludge production and respiration parameters for the degradation of SYNTHANE wastes, process design computations for a suspended film biological reactor of the activated sludge type become rote (11).

Process Stability Observations

While kinetic and stochiometric data obtained from laboratory-size reactors are applicable to larger-size facilities, similar extrapolations regarding process stability should not be made. Laboratory-size reactors demonstrate both effluent quality and quantity fluctuations due to slight deviations in pumping rates, minor laboratory temperature variations, etc. Such unavoidable deviations in small equipment is of a relatively greater magnitude than that found in larger-scale operations. As a "worst case" example of the process stability that might be found in a large-scale treatment plant, Figure 8 illustrates a probability plot of effluent TOC for a one-stage biological reactor with undiluted Montana condensate as feed. For example, the effluent TOC from this reactor was less than 448 mg/l 50% of the time, while the influent TOC was 3979 mg/l, indicating a process efficiency of 89% or better 50% of the time.

An asymptote of about 415 mg/l is evident in this figure, indicating that this is the approximate level of non-biodegradable TOC in these samples of SYNTHANE Montana condensate. This value is in fair agreement with the data shown in Figure 2, indicating about 50 mg/l in a 10% to 20% concentration of gasifier wastewater as being the non-biodegradable fraction.

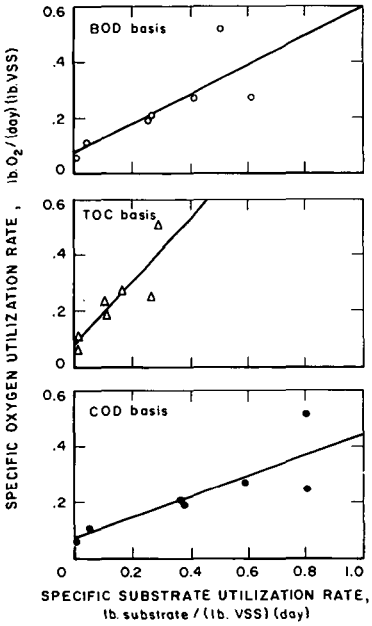

$$\frac{do_2}{dt(x)} = a' \frac{d(TOC)}{dt(x)} + b'$$

Calculated values		
Substrate basis	a' $\left(\frac{lb.\,O_2}{lb.\,substrate\ removed}\right)$	b' $\left(\frac{lb.\,O_2}{lb.\,VSS\ day}\right)$
BOD	0.747	0.110
TOC	1.680	0.090
COD	0.562	0.093

Figure 7 - Oxygen consumption as a function of biological substrate utilization.

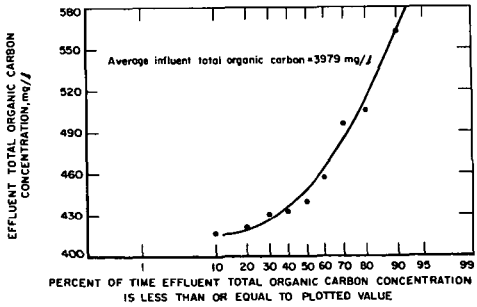

Figure 8 - Effluent quality - probability plot.

11-22-77 L-15701

Summary and Conclusions

1) Data is presented on a normalized basis for key pollutant parameters from the SYNTHANE gasification of Montana Rosebud, Illinois #6, and North Dakota lignite coals. These values are of the same order of magnitude as existing limited published data from other second generation gasification facilities, and less than that from the Westfield, Scotland Lurgi gasification of Rosebud coals.

2) Biological kinetic parameters, sludge production parameters, and oxygen utilization parameters are established for the activated sludge treatment of wastewater from the SYNTHANE gasification of Montana Rosebud coal. The following represent equations of best fit for the biokinetics of activated sludge treatment of diluted wastewaters from the SYNTHANE gasification of Rosebud coal:

a)

Basis for Specific Utilization (r)	Equation	Comments
lb TOC/lb-VSS-day	$r = \frac{0.538(TOC-50)}{133 + (TOC-50)}$	TOC < 800 mg/l
lb BOD/lb-VSS-day	$r = 0.182\ (BOD)^{0.186}$	BOD < 130 mg/l
lb Phenol/lb-VSS-day	$r = \frac{0.433\ (Phenol)^{0.58}}{1.02 + (Phenol)^{0.58}}$	Phenol < 80 mg/l

b) BOD sludge yield coefficient of 0.37 lb VSS/lb BOD and decay coefficient of 0.033/day.

c) Oxygen utilization coefficients are: 1.68 lb O_2/lb TOC, 0.747 lb O_2/lb BOD, and 0.562 lb O_2/lb COD with an endogenous respiration coefficient of 0.093 lb O_2/lb VSS-day.

3) About 12% of the TOC in the feed to biological reactors from Montana gasifier condensate is not biologically degradable. This may correspond to about 400 $\pm$ 100 mg/l TOC for such wastewaters.

4) Based on experimental observations from the biological treatment of Montana Rosebud condensates, a one-stage aerobic biological reactor with sludge age of 10 days and hydraulic detention time of about 1 day is capable of treating SYNTHANE by-product wastewater.

5) Biological processing should have a major role in the water pollution abatement of SYNTHANE gasifier water, and is probably applicable to other first and second generation gasification wastewaters. Biological processing cannot, however, completely remove all organics from gasifier wastewater. Research seeking answers to questions of the chemical nature and potential processes for further treatment of the biologically treated effluent is an area of high priority.

References

1. Ellman, R. C., B. C. Johnson, H. H. Schobert, L. E. Paulson, and M. M. Fegley. "Current Status of Studies in Slagging Fixed-Bed Gasification at the Grand Forks Energy Research Center", Presented at the 9th Biennial Lignite Symposium, May 18-19, 1977, Grand Forks, ND.

2. Nakles, D. V., M. J. Massey, A. J. Forney, and W. P. Haynes. "Influence of SYNTHANE Gasifier Conditions on Effluent and Product Gas Production", ERDA/PERC/RI-75/6, December, 1975.

3. Energy Research and Development Administration, Internal Quarterly Technical Progress Report, ERDA/PERC/QTR-76/4, Oct.-Dec., 1976, pp. 70-72.

4. Johnson, G. E., R. D. Neufeld, C. J. Drummond, J. P. Strakey, W. P. Haynes, J. D. Mack, and T. J. Valiknac. "Treatability Studies of Condensate Water from SYNTHANE Coal Gasification", DOE/PERC/RI-77/13, November, 1977.

5. Singer, P. C., et al, "Composition and Biodegradability of Organics in Coal Conversion Wastewaters", Presented at the Symposium on Environmental Aspects of Fuel Conversion Technology III, EPA, Hollywood, FL, Sept., 1977.

6. Neufeld, R. D. and A. A. Spinola, "Ozonation of Coal Gasification Plant Wastewater", to appear in Environmental Science and Technology.

7. APHA, AWWA, WPCF, "Standard Methods for the Examination of Water and Wastewater", 14 ed., American Public Health Association, Washington, D.C., 1976.

8. "Trials of American Coals in a Lurgi Gasifier at Westfield, Scotland", ERDA R & D Report, FE-105, Dec., 1972-Nov., 1976.

9. Massey, M.J., R. W. Dunlap, F. C. McMichael, and D. V. Nakles, "Characterization of Effluents from the Hygas and CO_2-Acceptor Pilot Plant", FE-2496-1, Interim Report July-September 1976, November 1976.

10. Bailey, J. E. and D. F. Ollis, "Biochemical Engineering Fundamentals", McGraw-Hill, NY, 1977.

11. Metcalf & Eddy Inc., "Wastewater Engineering: Collection, Treatment, Disposal", McGraw-Hill, NY, 1972.

Coal Humic Substances for Pollution Control in the Synthetic Fuels Industry

Stanley E. Manahan

Department of Chemistry, 123 Chemistry Bldg., University of Missouri, Columbia, Missouri 65201

Richard E. Poulson and David S. Farrier

Laramie Energy Research Center, U. S. Department of Energy, P. O. Box 3395, University Station, Laramie, Wyoming 82071

John B. Green

Bartlesville Energy Research Center, U. S. Department of Energy, P. O. Box 1398, Bartlesville, Oklahoma 74003

INTRODUCTION

Large quantities of by-product wastewater are associated with many of the major processes employed for synthetic fuels manufacture (1). Typical examples are water used to scrub dust, tar, and soluble organic compounds from the product of coal gasification and by-product water from the retorting of oil shale. Depending upon the source, these waters may contain substantial quantities of phenols, dissolved nitrogenous organic compounds, polycyclic aromatic hydrocarbons, biodegradable organics exerting a biological oxygen demand, heavy metals, ammonia, and other solutes. As both potentially valuable by-products and pollutants, the removal of these substances from by-product water is required.

It is imperative that economics and practicality be given the utmost consideration in the development of processes for the treatment of large quantities of by-product water from synthetic fuels manufacture because of the enormous quantities of water involved in a commercial synthetic fuels industry. Water treatment systems requiring expensive synthetic chemicals, elaborate apparatus, and intricate operations cannot be employed economically on a commercial scale. These considerations tend to exclude processes depending upon the use of large quantities of synthetic ion exchange resins, synthetic flocculents, and similarly expensive chemicals. Furthermore, for economic reasons and to avoid disposal of excessive amounts of waste chemicals, recyclable chemicals or those with a fuel value must be employed wherever possible.

This research has examined the uses of coal humic substances (CHS) for the treatment of by-product water. These materials meet the criteria of ready availability, low cost, and processing simplicity. In addition, similar substances can be isolated from oil shale, and it is possible that these materials may find uses in pollution control. The preparation, properties, and selected applications of these materials to pollution control are discussed in this report.

PREPARATION AND PROPERTIES OF COAL HUMIC SUBSTANCES

Humic substances are degradation resistant organic compounds derived from vegetable matter. These materials participate significantly in the environmental chemistry of water and soil (2). Humic substances are divided into three main categories based upon extraction with base and subsequent treatment of the extract with mineral acid: (a) a non-extractable residue called *humin*, (b) *humic acid* precipitated when the extract is acidified, and (c) *fulvic acid* remaining in the acidified solution. Additional details regarding the significance and properties of these fractions are to be found in the literature (3).

Humic substances may be prepared by the partial oxidation and base extraction of coal. In this work the general term, *coal humic substances* (CHS) is employed to describe these materials. The major categories of coal humic substances considered herein are *coal humic acids* (CHA), water-soluble coal humates (*e.g.*, the sodium salt of coal humic acid), and water-insoluble coal humates (particularly the calcium salt of coal humic acid). Numerous works have been published dealing with coal humic substances. These are summarized in two publications (4,5) dealing with the subject.

Coal humic substances are formed as intermediate steps in the partial oxidation of coal under moist conditions. This occurs by way of the general sequence shown in Figure 1. Figure 2 shows a hypothetical "molecule" of coal humic acid. It should not be taken as an exact, or even typical structure, but rather to illustrate the main structural and functional characteristics of this material.

Coal humic acids and their humate salts have a number of properties which make them potentially useful for wastewater treatment. These properties, and their potential applications to wastewater treatment, are the following:

1. Coal humates react with H^+ ion in solution. Therefore, solutions of soluble coal humates or suspensions of insoluble coal humates may be employed to neutralize mineral acid in excessively acidic wastewaters, or to sorb acid gases, such as SO_2, from gas streams.
2. Coal humic acids and most coal humates (other than alkali metal, magnesium, and ammonium humates) are water-insoluble. This provides a solid phase into which impurities may be partitioned and removed from wastewater and enables removal of humic substances from water that has been treated with these materials. Suspended solids in wastewater are entrained and removed by the precipitation of humates.
3. Heavy metal ions strongly chelated by coal humic substances may be removed by precipitation of the chelates or sorption of the chelates by a solid sorbent.
4. Some classes of organic compounds are sorbed by humic acids and insoluble coal humates enabling their removal from water.

5. Coal humic acids behave as flocculents in the precipitation of inorganic compounds, such as metal hydroxides or carbonates, produced in water treatment.

6. Solutions of coal humates foam strongly, leading to potential applications in froth flotation treatment of water.

EXPERIMENTAL

Coal humic acid used in these studies was prepared by nitric acid oxidation of Wyoming Wodak Amax sub-bituminous coal. Each batch consisted of 100 g of pulverized coal slurried to a thick paste with water. A volume of con. nitric acid equal to the volume of the coal slurry was added in 10 small batches, with stirring, over a 1-hour period. *Because of the evolution of NO_2 gas and the possibility of violent ejection of the material from the container, this operation must be performed cautiously in a hood with proper shielding.* The mixture was allowed to stand for 2 hours after the addition of all nitric acid. It was then washed with approximately 3 times the volume of residual solid by each of the following in sequence: (1) 3 separate batches of distilled water, (2) 1 batch of con. HCl for iron extraction, and (3) 3 separate batches of distilled water. The humic and fulvic acid fractions were then dissolved in 500 ml of 1.0 M NaOH, the solid residues were removed by centrifugation, and coal humic acid precipitated at pH 3 with con. HCl. After settling overnight, the humic acids were removed by centrifugation and washed twice with 1×10^{-3} M HCl, followed by centrifugation after each washing.

The removal of organic compounds labeled with radioactive carbon-14 from oil shale retort water was followed with a Beckman Instruments Model LS-9000 liquid scintillation spectrometer. Aqueous samples (0.5 - 1.0 ml) were counted in 12 ml of Dimilume-30 (Packard Inst. Corp.). All samples were counted for a sufficient time to achieve a 2-sigma statistical counting error of 1% or less.

The predominant cation in the oil shale retort water studied is NH_4^+ ion (271 meq/*l*) and the predominant anion is HCO_3^- (247 meq/*l*). Approximately 75-ml quantities of this water were dosed with less than 1 mg/*l* of ^{14}C-labeled compound whose removal was to be studied. A 50-ml portion of the spiked retort water was removed and 1.0 g of coal humic acid gel added to this portion, dissolving to form a black coal humate solution in the basic medium. Three 8-ml portions of labeled retort water (without added humic acid) and three 8-ml portions containing added humic acid were measured into 15-ml centrifuge tubes. Exactly 206 mg of solid $Ca(OH)_2$, 10 percent greater than that required stoichiometrically to remove all HCO_3^- and CO_3^{2-}, was added to each tube followed by thorough mechanical agitation. A voluminous precipitate of $CaCO_3$, darkened by the presence of calcium humate in those samples containing dissolved coal humic substance, formed immediately. The samples were centrifuged for 20 minutes at 2000 rpm, 0.5 or 1.0 ml aliquots of supernatant were withdrawn, and these were subjected to radioassay by liquid scintillation counting. Comparison of the supernatant to the untreated solution enabled calculation of the degree of removal of the spiked compound.

RESULTS AND DISCUSSION

When coal humic acid is added to shale oil retort water, the reaction,

$$H(CHS) + OH^- \rightarrow (CHS)^- + H_2O \qquad 1)$$

occurs in which the insoluble coal humic acid, H(CHS), dissolves in the basic medium, producing coal humate anion, $(CHS)^-$, and turning the water an opaque black color. Addition of $Ca(OH)_2$ (lime) to the medium containing ammonium, bicarbonate, carbonate, and CHS^- ions causes the following reactions to occur:

$$Ca(OH)_2 + 2NH_4^+ + CO_3^{2-} \rightarrow CaCO_3\downarrow + 2NH_3\uparrow + 2H_2O \qquad 2)$$

$$Ca(OH)_2 + 2HCO_3^- \rightarrow CaCO_3\downarrow + 2H_2O + CO_3^{2-} \qquad 3)$$

$$Ca(OH)_2 + 2(CHS)^- + 2HCO_3^- \rightarrow Ca(CHS)_2\downarrow + 2CO_3^{2-} + 2H_2O \qquad 4)$$

The solubility of calcium coal humate is comparable to that of $CaCO_3$ so that it is necessary to remove the greater part of the bicarbonate and carbonate to ensure essentially complete removal of dissolved $(CHS)^-$. When this is done and the suspension centrifuged, the supernatant liquid is again transparent and indistinguishable from the original retort water prior to the addition of coal humic acid. The precipitate is a heterogeneous dark gray mass consisting of a mixture of $Ca(CHS)_2$ and $CaCO_3$.

Impurities, including organic impurities, may be coprecipitated with $CaCO_3$ in oil shale retort water treated with lime, or with $Ca(CHS)_2$ if coal humic acid has been added. This phenomenon is shown in Table 1. Examination of this table shows a wide variation in removal efficiency with compound. Removal of the organic acids is almost certainly as the calcium salt, and removal efficiency should increase with increasing concentration because of solubility product considerations. In all cases the addition of a small quantity of coal humic acid significantly enhances removal. Increased removal of carcinogenic benz(a)pyrene by the addition of coal humic acid is quite significant. By taking out an additional 2/3 of the benz(a)pyrene that simple lime treatment did not remove, coal humic acid could well make the difference between a marginal treatment and adequate removal of this important compound.

It is noted that naphthalene is the second most efficiently removed compound, perhaps indicating that the removal of aromatics increases with increased condensation. Therefore, treatment with lime plus coal humic acid very likely yields efficient removal of polynuclear aromatic compounds and tars.

Coal humates, the salts of coal humic acids, have some uses for by-product water treatment as noted in the Introduction. Fly ash has been investigated as a source of base for the preparation of coal humates, yielding primarily calcium and magnesium humates. Details of this preparation and its potential uses are given in a reference dealing with the subject (5). In addition to providing a source of base, fly ash so treated is less susceptible to leaching and more amenable to disposal in a satisfactory manner.

TABLE 1. Removal of Carbon-14 Labeled Compounds from Oil Shale Retort Water by Treatment with Lime and Lime Plus Coal Humic Acid.

Compound	Percent removal with lime	Percent removal with lime plus coal humic acid
Benz(a)pyrene	97.5	99.2
Naphthalene	50.4	69.2
Phenol	1.28	5.61
Benzoic acid (benzoate anion)	0.00	3.99
Octanoic acid (octanoate anion	18.7	27.9
KCN (cyanide ion)	5.08	8.74
Carbonate species*	94.4	not measured

* Spiked with ^{14}C-labeled Na_2CO_3, largely converted to HCO_3^- ion by equilibria in the solution.

REFERENCES

1. "Environmental and Occupational Health Considerations in Coal Conversion Processes," Chap. 12 in *Fundamentals of Coal Chemistry*, Stanley E. Manahan, Wiley, New York, N.Y., in press.

2. "Complexation in Natural Waters," Chap. 4 in *Environmental Chemistry*, 2nd ed., Stanley E. Manahan, Willard Grant Press, Boston, Mass., 1975, pp. 71-104.

3. M. Schnitzer and S. U. Khan, *Humic Substances in the Environment*, Marcel Dekker, Inc., New York, N.Y., 1972.

4. W. W. Fowkes, *Some Characteristics of Natural and Coal-Derived Humates: With Bibliography*, GFERC/IC-75/1, United States Research and Development Administration Office of Public Affairs, Technical Information Center, Washington, D.C., 1975, 67 pages.

5. John B. Green, *Potential of Humic Acids as Stack Gas Scrubbing Media for Removal of Sulfur Dioxide and Fly Ash*, Ph.D. Thesis, University of Missouri Department of Chemistry, Columbia, Mo., 1977.

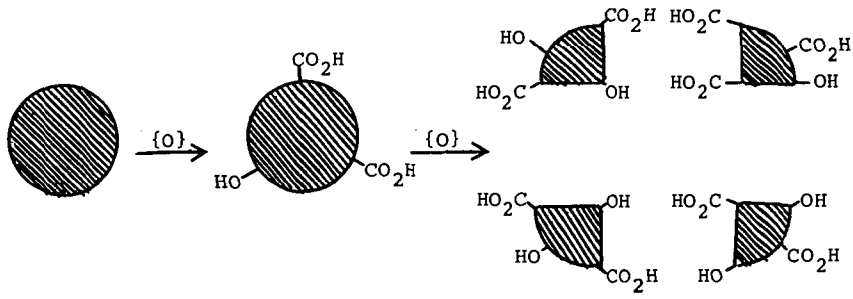

FIGURE 1. Partial oxidation of coal to form surface-oxidized coal and coal humic acid

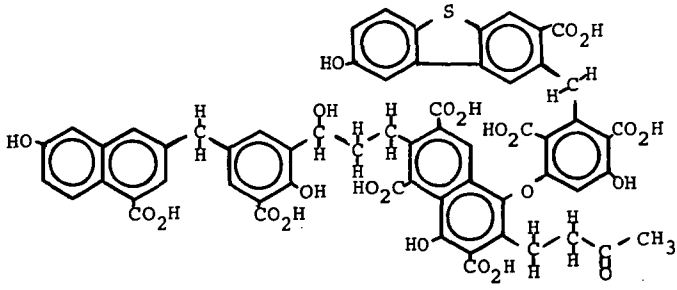

FIGURE 2. Representation of a coal humic acid molecule showing the predominant structural and functional features.

HOT GAS STRIPPING OF SIMULATED IN SITU OIL SHALE RETORT WATER

C. L. Murphy,[1] A. L. Hines,[1] R. E. Poulson,[2]

[1]Chemical and Petroleum-Refining Engineering,
Colorado School of Mines, Golden, CO 80401
[2]Department of Energy, Laramie Energy Research Center, Laramie, Wyoming 82071

Introduction

The large quantity of water produced by in situ oil shale retorting processes poses a potential pollution problem of significant magnitude. Waters collected from experiments conducted in the Laramie NTU type simulated in situ retorts have been examined (1) and have been shown to contain large concentrations of organic and inorganic species that could pollute the environment if not removed prior to disposal of the water. A study by Cook (2) of water produced from the Tosco II process revealed the presence of a variety of organic materials that could also harm the environment. Further, Hubbard (3) studied the process water produced by the Bureau of Mines gas combustion retort operated at Rifle, Colorado, and the water produced from the in situ retorting process near Rock Springs, Wyoming. He found that the waste water produced by both processes contained essentially the same components although in different quantities. Hubbard suggested two slightly different schemes to treat the waste water. One was to first contact the water with lime followed by: activated carbon, a cation exchange resin, and finally an ion exchange resin. In his second scheme he suggested that the waste water should first be contacted with activated carbon and then with lime and the ion exchange resins. He concluded that it may be possible to recover ammonia and ammonia salts in addition to purifying the water.

A number of other investigators have also studied various retort waters and have found essentially all the species identified in the work of Jackson et al. (1). Using the assumption Of Harak, Long, and Carpenter (4), that one barrel of water is produced with each barrel of oil, a 50,000 barrel per day in situ process would produce 2352 acre feet of water annually. Consequently, the study of methods to treat retort water is very important to the development of a viable shale oil industry.

The most prevalent species found in the retort water are the ammonium ions and the carbonates. Because they are present in large quantities, 13,000 ppm ammonia and 45,000 ppm carbonates, they must be dealt with prior to the treatment of retort water by either adsorptive or ion exchange techniques. A search of the literature (5-19) revealed that the petroleum industry routinely uses hot gases, particularly steam and flue gases, to strip sour water containing H_2S and NH_3. Because of the success of the petroleum industry in removing H_2S and NH_3, the removal of ammonium ions and carbonates from retort water appears feasible and will be addressed in this study.

Experimental

The equipment used in carrying out the experimental study consists of a stripping column equipped with fluid handling devices, heat transfer equipment, and temperature and pressure monitoring sensors; a schematic of the apparatus is shown in Figure 1. The liquid feed is introduced into the column with a variable speed diaphram type metering pump and the flow rate is measured with a rotameter. Prior to entering the column, the feed water flows through a three zone electrical resistance furnace where it is heated to the desired temperature.

The gas system is presently set up for two types of gases; one is steam supplied by a miniature steam generator, the second is a bottled gas, such as compressed nitrogen or air. The gas also flows through an electrical resistance furnace where

heat is transferred into a twenty foot long section of tightly coiled stainless steel tubing. From the furnace, the stripping gas passes through a rotameter and is injected into the bottom of the column where it flows upward, countercurrent to the downward flowing liquid feed. The gas exits from the top of the tower and passes through a small water cooled heat exchanger, then through two water traps and finally is vented to the atmosphere. The stripped water flows from the bottom of the column, through another small heat exchanger and is collected for subsequent analysis.

Temperature measurements are made by inline thermocouple connections at all inlet and outlet ports on the column as well as on the heat exchangers. Control of the inlet temperatures of the gas and liquid streams is made by two separate temperature controllers. The temperatures are read to ±2 degrees Farenheit from a digital readout device connected in parallel to a millivolt recorder. The absolute pressure is monitored with a pressure transducer connected to a digital millivolt output device.

The column itself is constructed of heavy wall, two inch NPS glass pipe made up in six sections of varying lengths for a total height of nine and one half feet; the sections are flanged together using a Teflon type gasket material. The packing height can be varied by using one of four different liquid injection ports along the column. The gas enters the bottom of the column just above the point at which the liquid exits. The gas passes upward through the irrigated packing and is removed from the top of the column. Connections from the 1/4 inch stainless steel tubing and the 3/8 inch glass column ports are made by a combination of flexible stainless steel hose and a special Teflon reducing union. In order to obtain representative data, it has been suggested that the column diameter be approximately eight times greater than the packing size. Consequently, the two inch column used in this study is packed with 1/4 inch Intalox saddles. To decrease water entrainment, four inches of Pyrex glass wool is packed into the top of the column. Because of the ineffectiveness of dry packing in distributing the liquid feed across the column, a flow distributor has been installed in all liquid inlets.

The effects of several key variables on the desorption rates of ammonia and carbon dioxide from a simulated retort water have been measured using the bench scale stripper column. In this study a number of parameters are evaluated: the effects of liquid and gas flow rates, the temperature of the stripping gas and retort water, and the packing height. The effects of pH, lime addition, and comparisons between actual and simulated retort water are presently underway, but as yet have not been completed.

Water flow rates varied over the range of 430 - 1,300 lb/hr ft^2 while gas rates were varied from 60 - 150 lb/hr ft^2. The liquid to gas ratios varied from 6 - 35 SCF/gal of feed, and are within the range used to strip comparable quantities of H_2S and NH_3 from sour water refinery streams. The column was maintained at a constant temperature for each run; the stripping temperatures were varied from 160 - 200 ^oF. The packed height available for stripping can be set at: 0.98, 2.79, 4.35, or 7.21 feet by changing the position of the water feed. Flooding characteristics of the two inch column were such that the approach to flooding varied from 12 to 20 percent. These values were maintained to keep entrainment of retort water in the gas to a minimum.

The water used to date has been a simulated retort water containing only ammonium bicarbonate. The pH of this water was that of the natural pH of the solution, 7.8 - 8.0 and the average concentrations of NH_3 and HCO_3^- were 11,000 ppm and 43,000 ppm respectively.

Results

Several operating parameters such as: temperature, liquid and gas flow rates,

and column height, were evaluated to determine their effect on the stripping of a simulated retort water. Equilibrium data for the ternary system NH_3, CO_2, and H_2O presented by Van Krevelin, et al., (20) and Badger and Pexton (21), show that CO_2 has a partial pressure higher than NH_3 in the vapor phase above the aqueous solution containing these compounds. The conclusion that may be drawn by examining this equilibrium data is that it is much more difficult to strip NH_3 from solution than CO_2. When compared to CO_2, the removal of NH_3 requires: higher temperatures, larger gas to liquid flow rates, and/or taller columns.

The relative effects of the liquid flow rate on the removal of bicarbonate ions, HCO_3^-, are shown in Figure 2 and the corresponding graph for the removal of NH_3 is given in Figure 3. For this set of runs, the temperature was held constant at 200°F and the average gas flow was 165 lb/hr ft^2. This gas rate corresponded to about 11, 20, and 40 SCF/gal of solution feed. As can be seen, the smallest liquid flow of 431 lb/hr ft^2 corresponded to the lowest solution concentration. The gas to liquid ratio of 40 SCF/gal corresponds to the maximum gas flow used by the petroleum industry to strip H_2S and NH_3 from sour water. For a flow rate of 20 SCF/gal, the concentrations of both NH_3 and HCO_3^- are higher than at the highest flow ratios. From the figure, it is seen that the HCO_3^- concentration initially ranges from 35,000 to 47,000 ppm by weight and rapidly decreases to 250 - 1,300 ppm. The NH_3 has an initial concentration of 15,000 ppm and drops to 3.7 ppm for the lowest liquid flow rate after passing through 7.2 feet of packing.

A situation similar to the one above can be seen in Figures 3 and 4. In these graphs the effects of a 40 percent gas rate increase at the constant liquid flow rate of 431 lb/hr ft^2 are illustrated; the gas to liquid ratios are 29 and 41 SCF/gal. Note that a 40 percent gas rate increase does not affect the concentrations as much as a change in the column height. At a packed height of only 0.98 feet, the HCO_3^- concentration is reduced from 45,000 ppm to approximately 21,500 ppm. The HCO_3^- concentration is further reduced to about 9,000 ppm after 2.69 feet of packing and to about 4,000 ppm after 4.35 feet of packing. The final bicarbonate concentration leaving the bottom of the column is about 1,000 - 2,000 ppm. These data indicate bicarbonate removal in the range of 98 percent at only 180°F with a corresponding ammonia removal of 97 percent. At the same gas to liquid ratio of about 40 SCF/gal, an increase in the temperature to 200°F permits removal of greater than 99.5 percent HCO_3^- and 99.9 percent NH_3. Figure 6 illustrates the effects of temperature on the quantity of HCO_3^- that remains in solution at a fixed gas to liquid rate of 11 SCF/gal. At this gas to liquid ratio the chemical equilibrium shifts with the increase in temperature from 180° to 200°F to provide a larger driving force for mass transfer. The equilibrium change with increasing temperature results in higher gas partial pressures of NH_3 and CO_2 for a given liquid composition. At the higher temperature, a shorter column could be used to produce a given effluent composition.

Conclusions

This study demonstrates that NH_3 and CO_2 can be effectively removed from water by hot gas stripping. At a stripping temperature of 200°F and a stripping ratio of 40 SCF/gal, the ammonia concentration was reduced from 11,000 ppm to 3.7 ppm and the bicarbonate concentration was reduced from 47,000 ppm to 220 ppm. These values reflect a removal of about 99.5%.

The components introduced into the stripping gas could be removed by a number of methods including incineration and adsorption. Assuming an NH_3 concentration of 13,000 ppm in a process that produces 50,000 barrels of water per day, the potential ammonia recovery would be about 41,600 tons per year. Because of the value of ammonia to the fertilizer industry, its recovery should be economically feasible.

References

1. Jackson, L. P., Poulson, R. E., Spedding, T. J., Phillips, T. E., and Jensen, H. B., "Characteristics and Possible Roles of Various Waters Significant to In Situ Oil-Shale Processing," Proc. of Colo. Sch. of Mines Environmental Oil Shale Symp. (Oct. 1975).

2. Cook, E. W., "Organic Acids in Process Water from Green River Oil Shale," Chem. and Ind., No. 1, 485 (1971).

3. Hubbard, A. B., "Method for Reclaiming Waste Water from Oil Shale Processing," ACS Div. of Fuel Chemistry, Preprint 16, No. 1, 21 (1971).

4. Harak, A. E., Long, Jr., A., Carpenter, H. C., "Preliminary Design and Operation of a 150-Ton Oil-Shale Retort," Colorado School of Mines Quart., 64, No. 4, 41 (1970).

5. Peoples, R. F., Krishman, P., and Simonsen, R. N., "Nonbiological Treatment of Refinery Wastewater," J. Water Pol. Fed., 44, 2120 (Nov. 1972).

6. Kostenbader, P. D., and Flecksteiner, J. W., "Biological Oxidation of Coke Plant Weak Liquor," J. Water Pol. Fed., 2, Part 1 (Feb. 1969).

7. Hart, J. S., "An Improving Wastewater Quality," Water and Sewage Works, 1W20 (Sept. - Oct. 1970).

8. Annessen, R. J., and Gould, G. D., "Sour Water Processing Turns Problem into Paydirt," Chemical Engineering, 67 (March 22, 1971).

9. Klett, R. J., "Treat Sour Water for Profit," Hydrocarbon Processing, 97 (Oct. 1972).

10. Finneran, J. A., and Whelchel, P.H., "Recovery and Reuse of Aqueous Effluent from a Modern Ammonia Plant," Proc. Ind. Process Design Workshop, 109, AIChE (San Francisco, CA., March 31 - Feb. 2, 1970).

11. Mavrovic, I., "Recovery of Nitrogen Compounds from Effluents in Urea and Ammonia Plants," Proceedings Workshop on Industrial Process Design for Pollution Control, Vol. 7, 1 (New Orleans, LA., Oct. 15 - 17, 1974).

12. Suhr, L. G., and Kepple, L., "AWT Plant gets Tough with Ammonia," Water and Wastes Eng., 26 (March 1975).

13. Resen, L., "Sour-Water Stripping Unit," The Oil and Gas J., 138 (March 12, 1956).

14. Elkin, H. F., and Henderson, G. R., "Waste Treatment at Sun Oil's Sarnia Refinery," Can. J. Chem. Eng., 129 (Oct. 1957).

15. Hull, C. D., "How Conoco Treats Waste Water," Oil and Gas J., 73 (Dec. 8, 1958).

16. Ewing, R. C., "Shell Refinery uses Pollution-abatement Units," Oil and Gas J., 62 (March 8, 1971).

17. Brunet, M. J., and Parsons, R. H., "Mobil Solves Fouling Problems in Sour-Water Strippers," Oil and Gas J., 62 (Nov. 20, 1972).

18. Rodrigues, D. G., "Sour Water Strippers: Its Design and Application," AIChE Symp. Ser., 70, No. 136, 667 (1974).

19. Beychok, M. R., "The Design of Sour Water Strippers," Proc. of the 7th World Pet. Cong. 1967, 9, 313 (Pub. 1968).

20. Van Krevelin, D. W., Hoftijzer, P. J., and Huntjens, F. J., "Composition and Vapor Pressures of Aqueous Solutions of Ammonia, Carbon Dioxide, and Hydrogen Sulfide," Rec. Trav. Chim. Pays - bas, 68, 191 (1949).

21. Pexton, S., and Badger, E. H. M., "Vapor Pressures of Ammonia and Carbon Dioxide in Equilibrium with Aqueous Solutions," J. Soc. Chem. Ind., 57, 107 (1938).

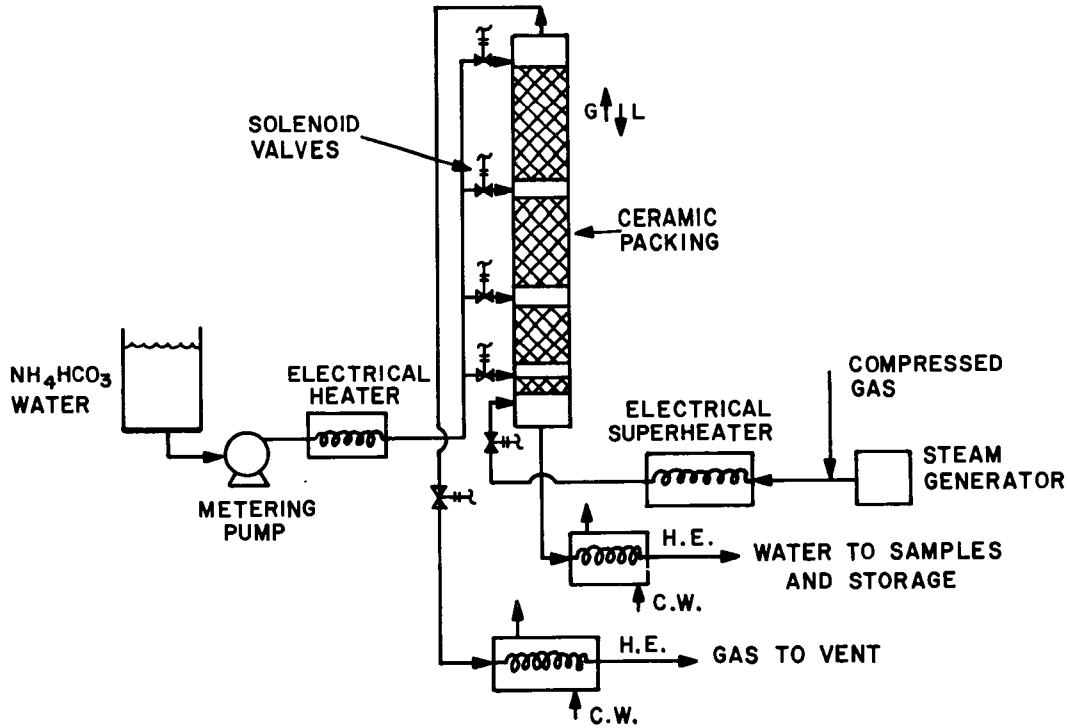

FIGURE I. EXPERIMENTAL EQUIPMENT

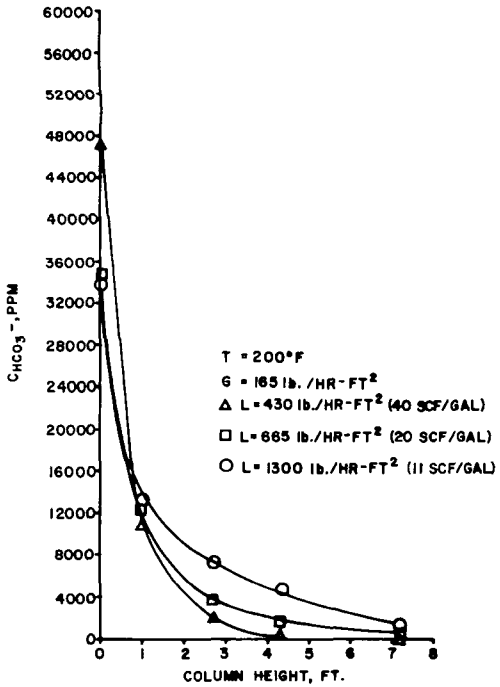

FIGURE 2. EFFECT OF WATER FLOW RATE ON BICARBONATE EFFLUENT CONCENTRATION AS A FUNCTION OF COLUMN HEIGHT.

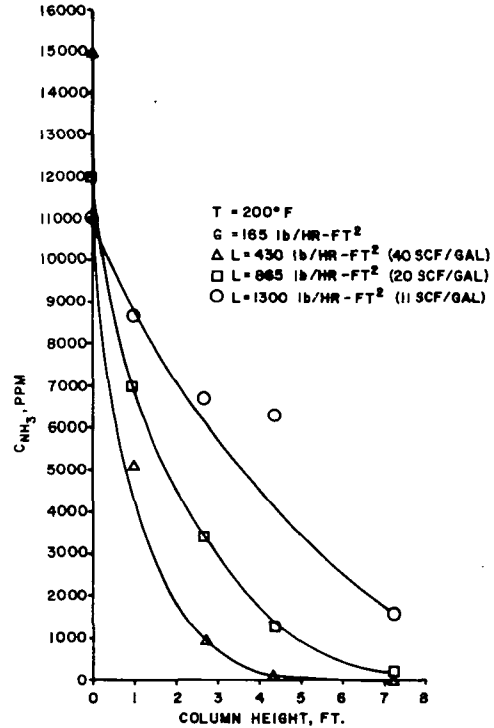

FIGURE 3. EFFECT OF WATER FLOW RATE ON AMMONIA EFFLUENT CONCENTRATION AS A FUNCTION OF COLUMN HEIGHT.

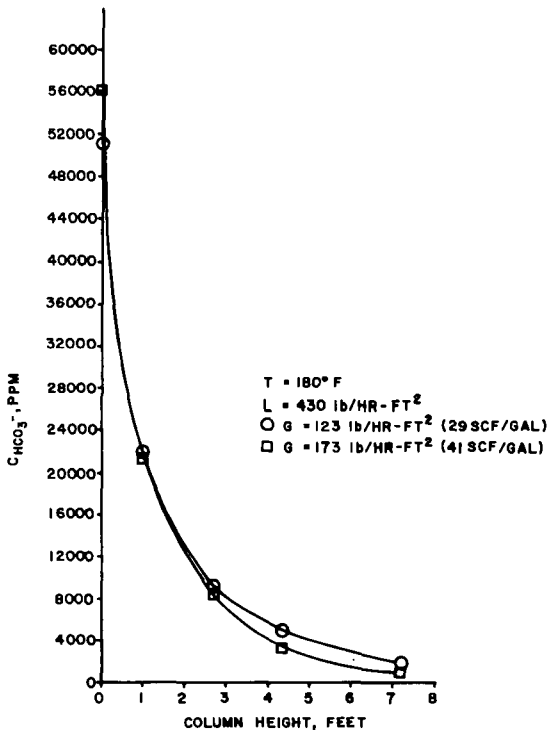

FIGURE 4. EFFECT OF GAS FLOW RATE ON BICARBONATE EFFLUENT CONCENTRATION AS A FUNCTION OF COLUMN HEIGHT.

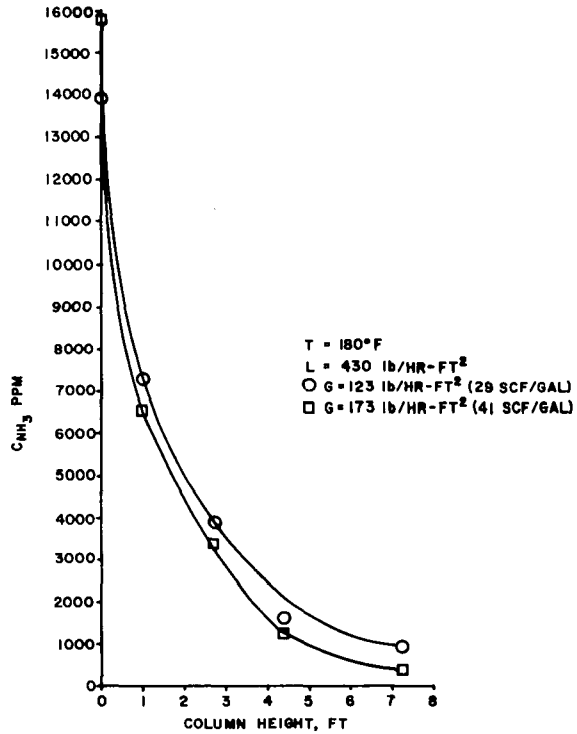

FIGURE 5. EFFECT OF GAS FLOW RATE ON AMMONIA EFFLUENT CONCENTRATION AS A FUNCTION OF COLUMN HEIGHT.

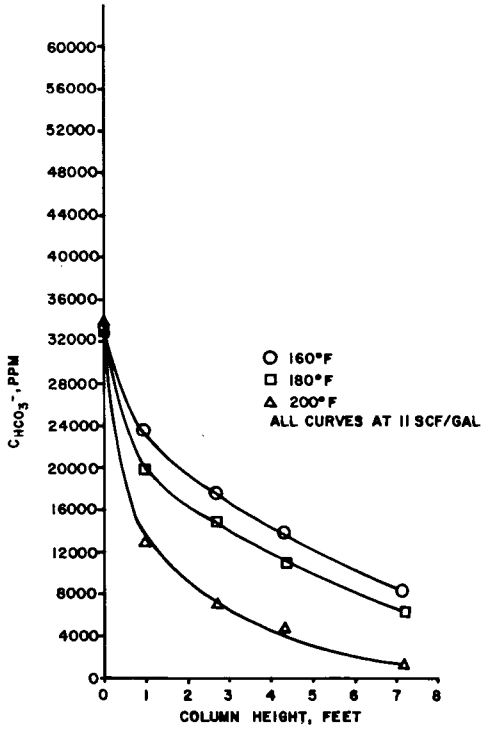

FIGURE 6. EFFECT OF TEMPERATURE ON BICARBONATE EFFLUENT CONCENTRATION AS A FUNCTION OF COLUMN HEIGHT.

ANAEROBIC FERMENTATION OF SIMULATED IN-SITU OIL SHALE RETORT WATER*

E. A. Ossio, J. P. Fox and J. F. Thomas

Lawrence Berkeley Laboratory
University of California
Berkeley, California 94720

R. E. Poulson

Laramie Energy Research Center
Department of Energy
Laramie, Wyoming 82071

INTRODUCTION

Water coproduced with shale oil and decanted from it is referred to as retort water. This water originates primarily from the combustion of organics and from the release of free and bound water present in the oil shale matrix. When retorting occurs in the presence of oxygen, the retort water to oil volume ratio is ~1. This is equivalent to 2.1 MGD for a 50,000 barrel per day oil shale plant and is comparable to the volume of wastewater produced by a town with a population of 14,000. The composition of retort water is characterized by a pH range from 8.5 - 9.6 and high levels of a number of inorganic and organic constituents. The principal inorganic constituents are ammonia, ammonium, and bicarbonate. The organic constituents are primarily polar, and carboxylic acids are often a major component.

Water management will be complex for the oil shale industry due to the scarcity of water in the region, the uncertain regulatory climate and the complex nature of retort water. Retort water will be required to meet the water needs of an oil shale complex and will be upgraded for on-site use. Potential uses, arranged in order of requisite quality, are spent shale compaction (poor quality water is suitable), dust control, mining, prerefining, agriculture and cooling tower makeup (good quality water is required). Any excess water will be stored for future use, evaporated or discharged to surface or ground waters. Stringent water quality regulations combined with the shortage of water in the region will limit direct discharge to surface or ground waters, and promote reuse combined with evaporation of residuals.

Each potential use of retort water will likely require the removal of some or all of the organic material which may be achieved by biological, physical or chemical processes. The purpose of this work was to investigate the removal of soluble organics from a retort water by anaerobic fermentation. Suspended solids, oils and grease, and ammonia removal were investigated as requisite pretreatment for anaerobic fermentation. Biological processes are typically more economical than physical or chemical processes for the removal of organics. The anaerobic fermentation process was chosen because the level of soluble organics in retort water is too high for direct treatment by an aerobic process and methane gas, a good fuel, is produced. Relative to aerobic processes, anaerobic fermentation stabilizes a larger portion of the organic material; has lower nutrient requirements; produces less sludge; handles toxic substances better; and is more suitable for seasonal loading.

PROCESS FUNDAMENTALS

Anaerobic fermentation is a biological treatment process conventionally employed for the treatment of municipal sludges and other concentrated wastes.(1) A schematic of the conventional process is shown in Fig. 1. The process consists of a heated digestion tank containing waste and bacteria. Raw waste is introduced either periodically or continuously and is preferably mixed with the digester contents. A two-stage biochemical process occurs within the digester. This process has been described in Refs. (1,2) and is summarized by the following equation:

$$(CH_2O)_n \xrightarrow[\text{formers}]{\text{acid}} RCOOH \xrightarrow[\text{formers}]{\text{methane}} CH_4 + CO_2 \,.$$

The waste, represented by $(CH_2O)_n$, is stabilized by conversion to CH_4 and CO_2, gases which are removed from the system and which may be collected and used. In the first stage, complex organics are converted largely to fatty acids by a group of facultative and anaerobic bacteria commonly called the "acid formers." No waste stabilization occurs during this stage. The waste stabilization occurs during the second stage of treatment. In this stage, the fatty acids are converted into CO_2 and CH_4 by a group of bacteria called the "methane formers." These bacteria are strictly anaerobic.

Successful use of the process depends on the proper maintenance of these two groups of organisms. Optimum conditions for anaerobic treatment include a pH range from 6.6 - 7.6, absence of certain toxic

*Work supported by U.S. Department of Energy and Department of Interior.

materials, sufficient nutrients, anaerobic conditions and a temperature range from 29 - 38°C. (3) Frequent causes for failure of the process are nutrient deficiencies and toxicity. Optimum and toxic levels for a number of constituents for the process are summarized in Table 1. These values should not be considered absolute because of the possibility of synergistic and antagonistic effects.

Table 1. Optimum and toxic levels for anaerobic fermentation. (4)

Parameter	Optimum Level (a) (mg/ℓ)	Toxic Level (b) (mg/ℓ)
Sodium	230	>4600
Potassium	390	>3900
Ammonium (as NH_4)	180	>1350
Calcium	200	>2000
Magnesium	120	>1200
Soluble sulfide (as S)	(c)	> 200
Nitrogen	(d)	–
Phosphorus	(d)	–

(a) Maximum efficiency from an anaerobic treatment system can be obtained by maintaining the major ions as close to their optimum values as possible.
(b) Toxic levels may vary considerably from the values shown due to synergistic or antagonistic effects of other ions.
(c) At levels lower than 200 mg-S/ℓ, sulfides can have a beneficial effect by precipitating certain toxic heavy metals, e.g., Cu, Zn, Ni, Fe.
(d) Optimum levels of nitrogen and phosphorus have been demonstrated to depend on the growth rate and concentration of organisms present in the system. They are ~11% of cell volatile solids weight for N and 2% of cell volatile solids weight for P. (3)

LITERATURE REVIEW

In preliminary experiments, Yen (5) seeded (10%) a 4.5-liter batch anaerobic digester with municipal sludge. Retort water from LERC's 10-ton oil shale retort was buffered at pH 7 with 1.0 g/ℓ KH_2PO_4, and the digester was loaded with 50 lb BOD_5/1000 ft^3. The COD in the influent was reduced from 3050 - 2500 mg/ℓ in 30 days and CH_4 was detected. Subsequently, Yen (6) loaded one digester with retort water and another with glucose. The nutrient solutions KH_2PO_4 and NH_4Cl were added to the glucose digester and KH_2PO_4 to the retort water digester. The COD in the glucose digester decreased from 550 - 350 mg/ℓ in 25 days while the COD of the retort water digester decreased from 550 - 400 mg/l in 55 days and CH_4 production steadily dropped. In another experiment (7), acclimation was accomplished by adding 75 mg/ml COD and a phosphate buffer solution incrementally to a digester containing a glucose substrate. The COD decreased from an initial value of around 600 - 300 mg/ℓ by the 42nd day of operation and thereafter, increased to a final value of 750 after 90 days. The CH_4:CO_2 ratio steadily decreased; no pH change was noted. Yen concluded that digester failure in the latter two experiments was due to the accumulation of a toxicant within the digester.

EXPERIMENTAL METHODS

Four Experiments (I - IV) were conducted to assess the treatability of a retort water by the anaerobic fermentation process and to identify toxic and deficient constituents in the water. These experiments are summarized in Table 2. In each experiment, a raw retort water was pretreated to remove oil and grease, suspended solids and ammonia, to adjust the pH and to alter any toxic or deficient constituents. An attempt was then made to acclimate a microbial population to the pretreated water. The raw, pretreated, and anaerobically treated waters and digester mixed liquor were chemically characterized to determine the cause for digester failure and/or the efficiency of organic removal.

The four experiments summarized in Table 2 resulted in the development of a method to successfully

Table 5. Summary of Experiments I - IV.

EXPERIMENT	PURPOSE	PRETREATMENT	DIGESTER	Acclimation Step % Organic Load: Retort Water	Acclimation Step % Organic Load: Artificial Substrate	INFLUENT: Total Ammonia (mg/ℓ)	INFLUENT: Organic Loading (lb Vm/ft^3-day)	INFLUENT: Hydraulic Residence Time (days)	INFLUENT: Mean Cell Residence Time (days)	MIXED LIQUOR: NH_4^+-N (mg/ℓ)	MIXED LIQUOR: $S^=$ (mg/ℓ)	RESULTS: BOD_5 Removal (%)	RESULTS: Failure Caused By
I	Assess affect of ammonia on digester performance	Retort Water A											Digester A
		pH elevation to 11 with 1N NaOH; 24 hr aeration; skimming; pH adjustment to 7.3 with 1N H_2SO_4	A	0%	100%	125	0.065	25	25			84%	Sulfide toxicity
			B			125	0.065	25	25			84%	
			A	25%	75%		0.013	58	58				
			B				0.020	58	58				Digester B
			A	50%	50%		0.013	38	38			38%	Ammonia toxicity
			B				0.026	38	38		122	11%	
		Retort Water B	A	66%	34%		0.014	30.5	30.5		335		
		pH adjustment to 7.3 with 1N H_2SO_4	B										
II	Resolve sulfide toxicity problem	pH elevation to 11 with $Ca(OH)_2$; skimming; pH adjustmnet to 7.3 with CO_2	C	8%	92%	125	0.065	25	25				Ammonia toxicity & nutrient deficient conditions
						1813	0.036	25	25	1565			
III	Residue ammonia toxicity problem and operate digester as cell recycle unit	pH evaluation to 11 with $Ca(OH)_2$; extensive aeration; skimming pH adjustment to 7.0 with CO_2	D	0%	100%	125	0.035	50	∞				Nutrient deficient conditions
				100%	0%	357	0.0087	15	∞				
IV	Solve nutrient deficient condition	Same as III; Ca, Mg and P added	D	100%	0%	357	0.0026	50	∞			78%	No failure occurred
	Control	None; 100% artificial substrate used	E	100%	0%	357	0.0026	50	50			80%	No failure occurred
			F	0%	100%		0.034	50	50			84%	

pretreat retort water, acclimate a microbial population to it and stabilize the organics present in the pretreated water. This methodology is presented in the "Results" section. The following sections discuss, in general terms, the experimental procedures used in Experiments I - IV.

Experimental Apparatus. A schematic of the batch laboratory-scale anaerobic digesters used in this study is shown in Fig. 2. These digesters were seeded with 750 ml of digested sludge from the City of Richmond Water Pollution Control Plant, Richmond, California. The characteristics of the digested sludge are summarized in the first column in Table 3. Retort water was added to the seeded digesters. On start up, the system was flushed with nitrogen gas to produce anaerobic conditions.

Retort Water. The retort water used in this study was from run 13 of LERC's 150-ton simulated in-situ oil shale retort. Retort operating conditions and shale characteristics for this run are summarized in Table 4.

Table 3. Characterization of Richmond's anaerobic digested sludge and artificial substrate used in acclimation procedure.

	Anaerobic Digested Sludge[a]	Artificial Substrate[b]
Total solids	29,000 mg/ℓ	29,500 mg/ℓ
Volatile matter	16,000 mg/ℓ	26,300 mg/ℓ
Percent volatile matter	–	89%
Suspended solids	–	nil
pH	7.0	7.05
Alkalinity as $CaCO_3$	3,600 mg/ℓ	1,710 mg/ℓ
Volatile acids as CH_3COOH	77 mg/ℓ	550 mg/ℓ
Organic nitrogen	–	3,960 mg/ℓ
NH_3-N	–	125 mg/ℓ
Total phosphate as $PO_4^{\equiv}$	–	1,020 mg/ℓ
Reactive (inorganic) phosphate as $PO_4^{\equiv}$	–	540 mg/ℓ
COD (dichromate)	–	38,340 mg/ℓ
BOD_5 (5 day, 20°C)	–	29,000 mg/ℓ
DNA	–	nil

(a) Source of Sludge – City of Richmond Water Pollution Control Plant, Richmond, California.

(b) Prepared from 20 gm/ℓ tryptone, 10 gm/ℓ dextrose and 6 gm/ℓ beef extract. (8)

Table 4. Retort operating conditions and shale characteristics for Run 13, LERC 150-ton simulated in-situ oil shale retort.

Shale Characteristics	
Shale Source	Anvil Points, Colorado
Shale Size	Mine run (fines – 72 in.)
Fischer Assay	24.6 gal/ton
Void Volume	37.8%
Operating Conditions	
Length of run	10.82 days
Atmosphere	21% O_2; recycle not used
Maximum Bed Temperature	1500°F
Retort Advance Rate	1.94 in./hr
Air Injection Rate	138.9 scf/min

The composition of a retort water depends on the process, retort operating conditions and the type of oil shale used. Wide variations in retort water composition occur due to these factors. Therefore, it is important to consider the results of this work in the framework of both of the process, the oil shale used and the retort operating conditions that produced the water.

Pretreatment. The raw retort water was pretreated using several different procedures. Each method used is briefly summarized in Table 2 in the pretreatment column. Pretreatment methods were designed to solve nutrient deficient or toxic conditions encountered during the acclimation procedure.

Acclimation. The microbial population in the digested sludge was acclimated to pretreated retort water by incremental additions of retort water to an artificial substrate. The composition of the artificial substrate is shown in the second column on Table 3. The incremental additions used in each experiment are summarized in Table 2 in the column entitled "step" in terms of percent organic load applied. After initiation of each step of the acclimation procedure, each digester was monitored until steady-state conditions were attained. The parameters used as indicators of steady state were volatile suspended solids, volatile acids, and volume and composition of digester gas. Digester performance was evaluated by monitoring BOD_5 and COD in the influent and effluent.

Analytical Procedures. Two types of parameters were measured in this work. They were those used to assess the operational behavior of the system (COD, BOD_5, volatile acids, volatile suspended solids, volume and composition of digester gas) and those used to identify toxic or deficient constituents (NH_3, S, Ca, Mg, P and others). The analytical methods used to measure these parameters are summarized in Table 5.

Table 5. Analytical methods for chemical characterization.

Parameter	Method
Al, Br, Cl,* Cu, Pb, Mn, Na,* V, Zn	Neutron activation analysis
As, Ba, B, Ca,* Cr, Co, F, I, Fe, Mg,* Ni, P,* K,* Se, Si,* S*	Spark source mass spectrometry
Ca,* Mg,* K,* Na,* Si,* P,* Cl,* S*	X-ray flourescense spectrometry on freeze-dried sample (9)
COD; BOD_5, Total Alkalinity, Solids, Volatile Acids, Hardness, pH, Kjeldahl N, oil & grease	Standard Methods, 13th Edition (10)
Sulfides	Standard Methods, 12th Edition (11)
Inorganic & Organic Carbon	Beckman Model 915 Total Carbon Analyzer with a Model 215A Infrared Detector. Organic carbon determined according to Standard Methods, 14th Edition (12)
Gas Analysis	Varian Aerograph Model 90-P gas chromotography unit with He carrier gas
Ammonia	Standard Methods, 13th Edition (10) modified to accommodate small sample size

*The asterisked (*) parameters were determined by neutron activation analysis or spark source mass spectrometry in the raw retort water and by x-ray fluorescense in the pretreated retort water.

RESULTS

Effluent Characterization. The characterization of the raw retort water used in this study is presented in Table 6. The water is well buffered at a pH of 8.6 by the ammonia and carbonate system. The most significant inorganic constituents (greater than 500 mg/ℓ) are ammonium, ammonia, bicarbonate, sodium and sulfate. Minor inorganic constituents include most trace elements, calcium, magnesium and phosphorus. Soluble organics, as measured by BOD_5 and COD, are considerably greater than found in conventional municipal wastes. Volatile acids are a major organic component and constitute 40% of the measured TOC. [This is an operational parameter (Ref. 10) for certain fatty acids. The volatile acids determination

Table 6. Characterization of raw, pretreated and anaerobically treated retort water.

	Raw Retort Water	Pretreated Retort Water (Digester Influent)	Anaerobically Treated Retort Water (Digester Effluent)
Alkalinity, Total (mg/ℓ $CaCO_3$)	38,000	1,800	–
Aluminum	16.6	–	–
Arsenic	1.4	–	–
Barium	0.17	–	–
Biochemical Oxygen Demand, 5-day (BOD_5)	5,325	2,695	580
Boron	3.4	–	–
Bromine	1.5	–	–
Calcium	3.3	67	–
Carbon, Inorganic	5,850	310	–
Carbon, Total Organic (TOC)	4,980	2,260	–
Chemical Oxygen Demand (COD)	8,800	9,440	2,250
Chlorine	57	21	–
Chromium	0.018	–	–
Cobalt	0.31	–	–
Copper	15.6	–	–
Fluorine	26	–	–
Hardness (as $CaCO_3$)	86	–	–
Iodine	0.11	–	–
Iron	4.7	–	–
Lead	0.3	–	–
Magnesium	24	–	–
Manganese	0.22	–	–
Nickel	0.014	–	–
Nitrogen, Total NH_3 (as NH_3)	10,150	357	–
Nitrogen, Kjeldahl (as N)	11,000	–	–
pH	8.6	7.0	–
Phosphorus (as P)	8.5	42	–
Potassium	37	24	–
Selenium	0.24	–	–
Silicon	25	28	–
Sodium	655	–	–
Solids, Total Dissolved	4,210	–	–
Solids, Total	–	780	–
Solids, Volatile	–	2,100	–
Solids, Suspended	–	nil	–
Sulfate (as SO_4)	1,100	–	–
Sulfur, Total (as S)	406	860	–
Vanadium	1.8	–	–
Volatile Acids (as CH_3COOH)	3,300	900	350
Zinc	6.4	–	–

measures water-soluble fatty acids that can be distilled at atmospheric pressure (up to six carbon atoms). When an analysis is referred to, the term volatile acids is used. Otherwise, the term fatty acids is used.] Wen (13), Yen (14) and Cook (15) found high levels of fatty acids in other retort waters.

Experiments I - IV. The four Experiments (I - IV) summarized in Table 2 led to the development of a method to pretreat and acclimate a microbial population to retort water and to stabilize 76 - 80% of the organics present in the pretreated retort water.

In Experiments I - III, gas production dropped to very low levels before the end of the acclimation procedure, indicating process failure. Typically, the onset of failure was indicated by a reduction in gas

production and an increase in volatile acids and COD concentrations. This is most likely due to improper functioning of the methane formers. The cause of the failures, based on chemical analyses of the pretreated influent and digester mixed liquor, was determined successively to be sulfide and ammonia toxicity and Ca, Mg and P deficiencies. Sulfide toxicity resulted from the use of H_2SO_4 for pH adjustment and not from the water itself. Pretreatment schemes were devised to resolve each problem as it was identified. Ultimately, in Experiment IV, all problems were resolved and the anaerobic fermentation process was used successfully to stabilize organics in pretreated retort water. The reproducibility of the results was verified by setting up a second digester, E (see Table 2 for designation in D, E), for which similar results were obtained. Digester performance was equivalent to that observed with more conventional wastes such as municipal sludge.

During these experiments, it was observed that a toxicity and a nutrient deficiency problem could be differentiated by comparing total gas production and gas composition. When toxicity was the the cause of failure, the gas composition changed significantly; CH_4 decreased and CO_2 and trace gases increased. When the system was nutrient limited, total gas production decreased while gas composition remained constant and comparable to that observed in a properly operating digester.

Pretreatment and acclimation procedures developed to stabilize organics in pretreated retort water are summarized in the sections on pretreatment and acclimation. The results presented correspond to those obtained during Experiment IV which was summarized in Table 2.

Pretreatment. The purpose of pretreatment was to make the raw retort water compatible with the anaerobic fermentation process. Each pretreatment step used would likely be required irrespective of whether biological treatment was part of the overall treatment system.

The pretreatment procedure was designed to reduce ammonia below the reported toxicity threshold of 1350 mg/ℓ NH_4^+, to reduce suspended solids, oils and grease and to adjust the pH to 7. This was achieved in the laboratory as follows:

(1) The pH was raised to 11 using $Ca(OH)_2$. This converts NH_4^+ to NH_3 gas which can then be stripped from solution by aerating.

(2) The pH 11 water was injected into an aeration basin with compressed air. Spraying the retort water with compressed air enhanced liquid-air contact, thereby improving stripping of the NH_3 from the water. The resulting mixture was aerated for 24 hr with a sparger.

(3) Floatables (suspended solids plus oils and grease) were removed by skimming, following aeration.

(4) The pH of the retort water was adjusted to a final pH of 7.0 using compressed CO_2.

(5) Nutrients were added directly to the digester. Nutrient addition is discussed subsequently.

This precise pretreatment sequence would not be used in a full-scale treatment system due to economic considerations. It was used for this bench-scale work because it is easy to carry out on a small scale with inexpensive, readily available laboratory equipment, and it produces a water with the necessary pH and ammonia concentrations.

In practice, dissolved solids and oil and grease would be removed by sedimentation and/or dissolved air flotation. Ammonia might be reduced by steam stripping. Nutrient addition might be achieved, in part, by blending retort water with other waste steams at an oil shale plant that are enriched in the required nutrients, e.g., municipal sludge.

Additional pretreatment may be required to reduce the volume of water to be treated. Table 2 indicates that the hydraulic residence times used in these studies ranged from 15 to 50 days. These large residence times would require a large volume digester to accommodate 2.1 MGD per 50,000 barrels/day of oil production capacity and would not be used in a full-scale plant. In practice, cell recycle, which increases the cell residence time and allows a reduction in hydraulic residence time, would be used. Kinetic studies are presently under way to determine if hydraulic residence times on the order of 2 to 3 days or less can be used with no significant reduction in organic removal.

The effect of pretreatment on the chemical composition of the retort water is shown in Table 6. By comparing the first column, raw retort water, and the second column, pretreated retort water, the effect of pretreatment on the measured parameters can be quantified. This comparison shows that BOD_5 is reduced by 49%, volatile acids by 73%, TOC by 55%, total NH_3 by 96%, Cl by 63% and alkalinity by 95%. The decrease in BOD_5, TOC and volatile acids is due to the conversion and removal of fatty acids during

pH adjustment. The BOD_5, TOC and volatile acids decreases are probably due to the reduction in solubility of high molecular weight fatty acids. At pH 7 many of these could drop out of solution. This is supported by visual observation of a white precipitate. The NH_3 alkalinity (CO_2, NH_3) and Cl are removed by stripping during aeration. In addition to these reductions, the Ca concentration was increased by a factor of 20 and the COD by a factor of 1.07. The increase in Ca was caused by the addition of $Ca(OH)_2$ for pH adjustment to 11. The cause of the increase in COD is not clear. Analytical error is not the source as results were checked by a second analyst. The reductions in TOC, BOD_5 and volatile acids are consistent and suggest that the increase in COD is due to an inorganic constituent and not an organic one. No significant change is noted in K or Si. The significant increase in total sulfur and phosphorus is believed to be due to analytical problems since the S and P levels were determined by different analytical methods in the raw and pretreated water. Significant discrepancies in the analysis of retort water by different methods have been noted (16) and is due to the complex and unusual nature of retort water. This problem is presently being studied by LERC and others. (16)

Acclimation. In Experiment IV, the system was operated with cell recycle to increase the cell residence time in the digester. This was achieved by removing a sample of the mixed liquor, centrifuging it at 2500 rpm for 3 min and returning the centrate (biological mass) to the digester with a volume of pretreated retort water such that the total volume removed was equal to the total volume added. This resulted in an infinitely large cell residence time and hydraulic residence time of 50 days.

The system was acclimated by first adding 100% artificial substrate described in Table 3 to the digester and operating it until steady-state conditions were reached. After steady state, 100% retort water, pretreated as indicated, was added in 50 ml increments. Results of Experiments I - III indicated intermediate additions of different mixtures of retort water and artificial substrate were not necessary. Immediately preceding or following the addition of retort water, nutrients were added directly to the digester. In this work, the nutrients Ca, Mg and P were used. The optimum combination and quantity of nutrients were not determined and are presently being studied experimentally. The nutrients were added as a calcium/magnesium versenate solution and as phosphate buffer. These solutions were prepared as follows:

phosphate buffer

8.5 g KH_2PO_4, 21.75 g K_2HPO_4, 33.4 g Na_2HPO_4 and 1.7 g NH_4Cl were dissolved in 500 ml distilled water and diluted to 1 liter.

calcium/magnesium versenate solution

10 ml versine (EDTA) were added to a solution of 0.1 g each of $CaCl_2$ and $MgSO_4$ and 2 ml distilled water. The amount of versine required to complex the Ca and Mg added was determined titrimetrically on three separate aliquots according to the hardness determination, Standard Methods, 13th Edition. (10)

The effect of nutrient addition on system performance is summarized in Fig. 3. This figure shows the time variation of total gas production in ml gas/day, gas composition, COD and volatile acids. Figure 3a indicates that each time nutrients were added, the total gas production increased. Figures 3a and 3c indicate that before the addition of nutrients on the 34th day of the experiment, volatile acids and COD concentrations were increasing and the total gas production was decreasing. This suggests that the methane formers, which are responsible for waste stabilization, and which convert fatty acids into CH_4 and CO_2, were not functioning properly. The increase in volatile acids indicates the acid formers were functioning. After the addition of 18 mg Ca and 10 mg Mg on the 34th day, the volatile acid concentration dropped, indicating the nutrients had a favorable effect on the methane formers. After five days, waste stabilization commenced. Approximately ten days after the first addition of nutrients, the system reached steady state. Gas volumes at steady state were approximately 11 ft^3 gas/lb volatile matter added. This is 92% of the theoretical possible production. (17) Gas composition was 55% CH_4, 25% CO_2 and 20% trace gases (N_2 was the predominant trace specie). The gas production and composition at steady state are comparable to those obtained with conventional waste types.

Treatability. The results presented in Fig. 3 were reproduced using a second digester, E. In addition, a control digester, F, was fed 15 ml/day artificial substrate during the duration of the study. The organic removal efficiencies of these three digesters as measured by BOD_5 and COD are summarized in Table 7 together with similar data for the pretreatment process and the total system consisting of pretreatment plus anaerobic fermentation. This table shows that the anaerobic fermentation process reduces both the BOD_5 and COD of pretreated retort water by 76 - 80%.

Table 7. Summary of retort water BOD_5 and COD removal efficiencies.

	Digester D (100% retort water)	Digester E (100% retort water)	Digester F (100% artificial substrate)
Pretreatment			
Influent COD	8,800	8,800	–
Effluent COD	9,440[a]	9,400(a)	–
Percent Removal	0%	0%	–
Influent BOD_5	5,325	5,325	–
Effluent BOD_5	2,695[a]	2,695(a)	–
Percent Removal	49%	49%	–
Anaerobic treatment			
Influent COD	9,440	9,440	38,340
Effluent COD	2,250	1,995	6,134
Percent Removal	76%	79%	84%
Influent BOD_5	2,695	2,695	29,000
Effluent BOD_5	580	530	5,220
Percent Removal	78%	80%	82%
Total system			
Influent COD	8,800	8,800	–
Effluent COD	2,250	1,995	–
Percent Removal	74%	77%	–
Influent BOD_5	5,325	5,325	–
Effluent BOD_5	580	530	–
Percent Removal	89%	90%	–

(a) Before nutrient addition

These removal efficiencies indicate that 76 - 80% of the soluble organics in the pretreated retort water are stabilized by the anaerobic fermentation process. The volatile acids data presented in Table 6 suggest that fatty acids are one of the components of retort water that are stabilized during anaerobic fermentation. Additional work is required to identify other organic components that are stabilized during the anaerobic fermentation process.

CONCLUSIONS

Based on the results of the four experiments summarized in Table 2, the following are concluded:

1) The retort water studied had to be pretreated to remove toxic and add deficient constituents before it could be successfully treated with the anaerobic fermentation process. Pretreatment included pH adjustment to 7, ammonia reduction and nutrient addition.

2) A digested sludge from a conventional municipal sewage treatment plant was successfully acclimated to the retort water studied.

3) A major fraction of the organics in the retort water studied was stabilized by conversion to CH_4 and CO_2 using the anaerobic fermentation process. BOD_5 and COD removal efficiences were 76 - 80%. Within the limits of experimental error, the same removal rate was obtained for both BOD_5 and COD.

4) The effluent from anaerobic fermentation of the retort water studied (BOD_5: 530 - 580 mg/ℓ) may be suitable for treatment by conventional aerobic processes. This process is presently being demonstrated experimentally.

5) The growth of the methane formers, which stabilize the organics, is nutrient limited in the retort water studied.

6) The pretreatment of the retort water studied removed 49% of the BOD_5. This was probably due to the reduction in solubility of high molecular weight fatty acids at neutral pHs; they drop out of solution and do not exert a BOD.

7) A major component removed from the retort water studied during anaerobic fermentation was fatty acids.

8) The long hydraulic residence time used in this study would not be used in practice. Cell recycle, which increases the cell residence and decreases the hydraulic residence time, would be exploited to achieve hydraulic residence times on the order of 2 - 3 days.

REFERENCES

(1) P. L. McCarty, Anaerobic Processes, presented at the Birmingham Short Course on Design Aspects of Biological Treatment, International Association of Water Pollution Research, Birmingham, England, September 18, 1974.

(2) P. L. McCarty, Anaerobic Waste Treatment Fundamentals, Part One, Chemistry and Microbiology, Public Works, September 1964.

(3) P. L. McCarty, Anaerobic Waste Treatment Fundamentals, Part Two, Environmental Requirements and Control, Public Works, October 1964.

(4) P. L. McCarty, I. J. Kugelman and A. W. Lawrence, Ion Effects in Anaerobic Digestion, Stanford University Technical Report No. 33, 1964.

(5) T. F. Yen and J. Findley, Progress Report on Retort Water Project, ERDA-LERC E(29-2)-3619, Quarter ending November 30, 1975, University of Southern California.

(6) T. F. Yen and J. Findley, Progress on Retort Water Project, ERDA-LERC E(29-2)-3619, Quarter ending February 29, 1976, University of Southern California.

(7) T. F. Yen and J. Findley, Progress Report on Retort Water Project, ERDA-LERC E(29-2)-3619, Quarter ending June 30, 1976, University of Southern California.

(8) H. H. Almgren, Physiological State and System Kinetics of Methane Fermentation, Ph.D. Thesis, University of California, Berkeley, 1958.

(9) A. J. Hebert and H. R. Bowman, Nondispersive Soft X-Ray Fluorescence Analyses of Rocks and Waters, in Proceedings of the Second U. N. Symposium on the Development and Use of Geothermal Resources, San Francisco, May 1, 1976, p. 751.

(10) Standard Methods for the Examination of Water and Wastewater, APHA, AWWA, WPCF, 13th ed., 1971.

(11) Standard Methods for the Examination of Water and Wastewater, APHA, AWWA, WPCF, 12th ed., 1965.

(12) Standard Methods for the Examination and Wastewater, APHA, AWWA, WPCF, 14th ed., 1976.

(13) C. S. Wen, T. F. Yen, J. B. Knight and R. E. Poulson, Studies of Soluble Organics in Simulated In-Situ Oil-Shale Retort Water by Electron Impact and Chemical Ionization from a Combined Gas Chromatograph-Mass Spectrometer System, 172nd National Meeting, American Chemical Society, Division of Fuel Chemistry, Vol. 21, No. 6, Preprints of papers presented at San Francisco, CA, August 29 - September 3, 1976.

(14) T. F. Yen, et al., Degradation of the Organic Compounds in Retort Water, Final Report, ERDA E(29-2)-3758, June 30, 1976 - June 29, 1977.

(15) E. W. Cook, Organic Acids in Process Water from Green River Oil Shale, Chemistry and Industry, May 1, 1971.

(16) D. S. Farrier, J. P. Fox and R. E. Poulson, Chemical Characterization and Analytical Considerations for an In-Situ Produced Oil-Shale Processing Water, LERC Report of Investigations, in press.

(17) Metcalf & Eddy Inc., Wastewater Engineering, McGraw-Hill, 1972.

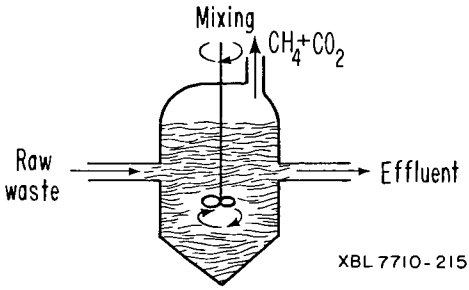

Fig. 1. Schematic of conventional anaerobic fermentation process.

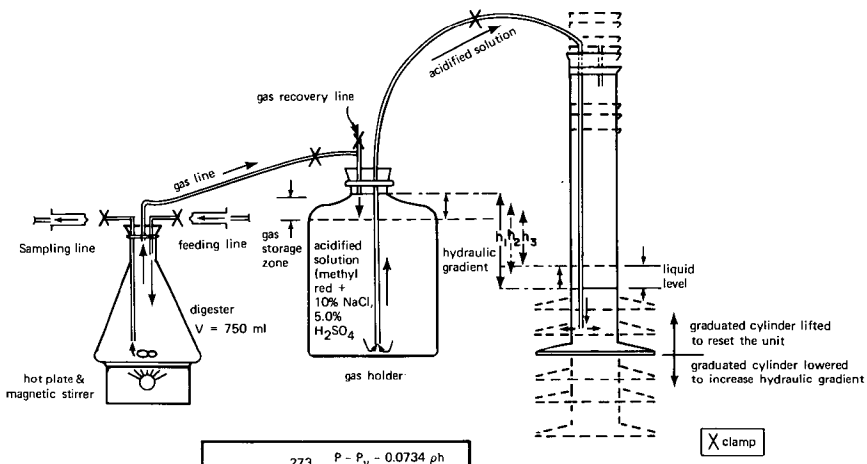

$$V_G = V_L \frac{273}{760} \frac{P - P_v - 0.0734\,\rho h}{T(^\circ K)}$$

V_G = Volume (liters) of fermentation gas at standard temperature & pressure

V_L = Volume (liters) of liquid displaced by fermentation gases

P = Atmospheric pressure, mm Hg

P_v = Vapor pressure (mm Hg) of water over the container liquid at temperature T

ρ = Density of container liquid

h = Height of the column of liquid suspended above the liquid outlet

XBL 7710-2163

Fig. 2. Schematic of anaerobic acclimation system. (a) Digester's contents are mixed and kept at constant temperature (35 ± 1°C) by means of a hotplate-magnetic stirrer. (b) Fermented gas is introduced into a gas holder unit by means of a slight negative pressure created by the water column differential (h). The gas holder unit contains an acidified solution to prevent the dissolution of CO_2. The gas, on entering the gas holder, displaces some of the acidified solution which is collected in the graduated cylinder. This volumn of acidified solution is used to calculate the volumn of gas produced using the formula for V_G. (c) The fermentation gas is recovered and the acidified solution level reset by lifting the graduated cylinder and properly operating the valves.

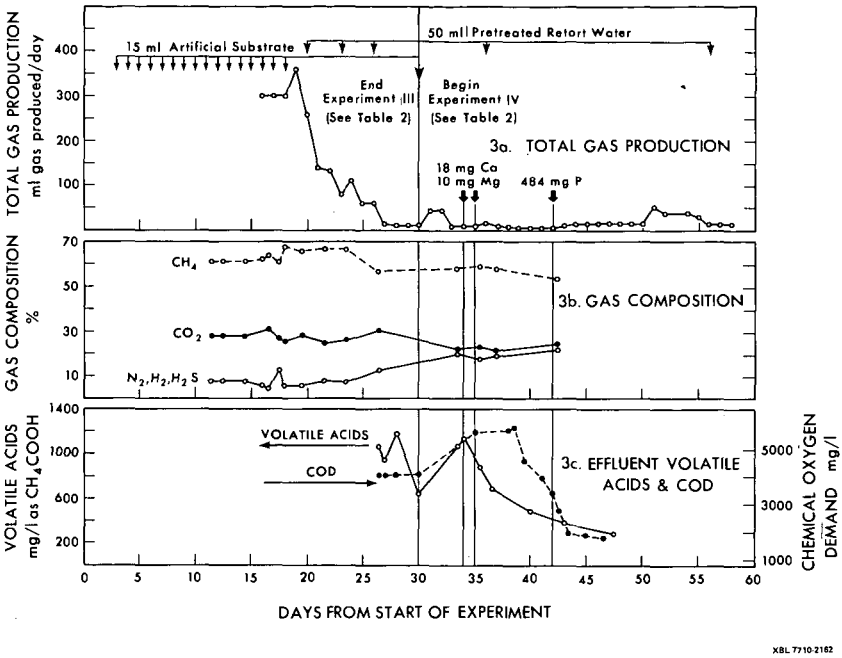

Fig. 3. Time variation of total gas production, gas composition, volatile acids and chemical oxygen demand for Experiments III and IV.

Capacity of Some California Alkaline Brines for Sulfur Dioxide

J.P. McKaveney and David Stivers
Occidental Research Corporation, La Verne, California 91750

INTRODUCTION

Following the 1973 fuel crisis, a national movement began to discover economical methods for either removing sulfur directly from coal, or to discover ways of burning the coal without the evolution of harmful, sulfur oxides. A number of proposals have been made for the absorption of sulfur oxides such as the use of sea water or the use of raw Trona ($Na_2CO_3 \cdot NaHCO_3 \cdot 2H_2O$) taken directly from Wyoming deposits and dissolved in water for the absorption.

California contains scattered natural reserves of highly alkaline brines which could also be used for the absorption of sulfur oxides. These alkaline dry lakes located primarily in desert areas have significant absorption capacities for the sulfur oxides and in addition contain valuable minerals, e.g., boron and tungsten. This report will show that as a result of the brine acidification with SO_2, tungsten can be recovered much easier, thus using a potential air pollutant to aid in natural resource recovery.

When high sulfur fuels are burned, two and possibly more acidic gases are produced, viz: carbon dioxide, sulfur dioxide and lesser amounts of sulfur trioxide and nitrogen oxides. As the acidic oxides pass into an alkaline salt solution, they are neutralized forming salts such as sulfite, sulfate, bicarbonate and nitrites. As the gases are absorbed, the pH will continue to decrease in solution. With decreasing pH, some of the less stable weaker acid salts will release their gases such as CO_2 from solution.

The chemisty of the brines is quite complex since a number of basic salts (carbonate, bicarbonate, borate and metaborate) are present as well as neutral salts such as NaCl, KCL, and Na_2SO_4. Because the brines are also quite concentrated (400 g/l), the usual stoichiometry and equilibria applicable in dilute systems do not always apply. In addition, salts such as borate and metaborate contribute a buffering capacity. With such a system, direct experimental measurement is the best approach.

The experiments in this study were performed using a brine from Searles Lake California. The lake is located about 185 miles northeast of Los Angeles and covers about 13 square miles of exposed surface. The salt body covers the whole 13 square miles of surface and a much larger subsurface area to a depth of 50 to 75 feet. During most of the year, the surface of the salt body is dry and hard but in winter after rains liquid may be two or three inches above the top of the salt body (1).

A typical brine analysis from Searles Lake is indicated in Table I (2). The brine contains about 35% dissolved solids. The composition varies somewhat at different locations; the lower structure brine contains more carbonate and borate than does the upper structure brine. It is apparent that this vast natural lake contains a ready sink for the sulfur dioxide.

TABLE I
TYPICAL BRINE ANALSYSES FROM SEARLES LAKE

Constituent	Upper Structure Brine, wt %	Lower Structure Brine, wt %
KCl	4.90	3.50
Na_2CO_3	4.75	6.50
$NaHCO_3$	0.15	
$Na_2B_4O_7$	1.58	1.55
$Na_2B_2O_4$		0.75
Na_2SO_4	6.75	6.00
Na_2S	0.12	0.30
Na_3AsO_4	0.05	0.05
Na_3PO_4	0.14	0.10
NaCl	16.10	15.50
H_2O (by difference)	65.46	65.72
WO_3	0.008	0.005
Br	0.085	0.071
I	0.003	0.002
F	0.002	0.001
Li_2O	0.018	0.009

EXPERIMENTAL

Apparatus and Reagents

1. Sulfur dioxide compressed gas containing in percent: 0.47 SO_2, 33.07 CO_2, 3.43 CO and the balance (approx. 63%) nitrogen.

2. Flow meter, Fischer and Porter No. 08F 1/16-12-5-36 set for 62 ml per minute gas flow by calibration.

3. Fischer-Milligan gas absorption bottles.

4. Hydrochloric acid (1:99), potassium iodate (0.2225 grams per liter) equivalent to 0.10 mg of sulfur per ml and starch indicator mixed appropriately to monitor sulfur dioxide absorption efficiency.

Absorption Train for SO_2 Bearing Gas

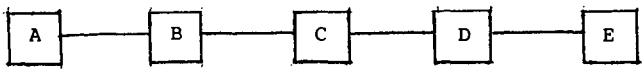

A - Tank of compressed SO_2 bearing gas and regulator.

B - Flow meter.

C - Searles Lake brine in Fischer Milligan bottle.

D - Sodium carbonate indicator solution with phenolphthalein used with 100% SO_2 gas when separating 50 ppm tungsten from 100 ml of brine.

E - 100 ml tall form beaker and gas bubbler used with 50 ml buret to deliver KIO_3 solution for titration of SO_2.

DISCUSSION OF RESULTS

The data on the absorption of the SO_2 bearing (0.47% SO_2) combustion gas indicates that about 71 grams of SO_2 can be absorbed per liter of raw Searles Lake brine. The efficiency of the single scrubber was 98% with an aliquot (2.5 ml to 100 ml) of the concentrated brine using the experimental apparatus at a gas flow of 62 ml per minute (8.6×10^{-4}g of SO_2 per minute). Sulfur dioxide break-through occurred after a total elapsed time of 4 hours and one minute. The net alkaline absorbance time (correcting for water absorbance) was 226 minutes. The break-through was detected by noting the continued fading of the blue iodine starch color from the exit gas bubbled into beaker E.

Because the data of Table I are analyses which can vary with location, the analyses of the actual brine used in the experiments is shown in Table II. It lists the principal sodium salts of the Searles brine and their calculated concentrations based on cation and anion analyses of the raw brine sample used. Not listed is approximately 65 grams per liter of KCL which is the principal potassium salt for a brine of specific gravity 1.30 at 21°C.

TABLE II
COMPOSITION BY ANALYSIS OF SELECTED COMPONENTS
OF SEARLES LAKE BRINE

Component	Concentration (g/l)	Calculated As	Concentration As (g/l)
Sodium	149.4		
Potassium	34.8		
Carbonate	35.2	Na_2CO_3	62.3
Chloride	151.0	NaCl	249.1
Bicarbonate	5.2	$NaHCO_3$	7.2
Sulfate	61.0	Na_2SO_4	90.3
Tetraborate	16.8	$Na_2B_4O_7 \cdot 10H_2O$	41.3

The SO_2 absorbing capacity of the selected sodium salts at the given concentration can be seen in the data of Table III for a 2.0 ml aliquot of each salt. The comparison of the total absorption

capacity for the sum of the synthetics was 165 minutes versus 168 minutes for a 2.0 ml aliquot of the actual brine with the 0.47% SO_2 combustion gas. This confirms that the synthetic data is giving a true absorption capacity for all the salts tested. Surprisingly even Na_2SO_4 is contributing slightly. The principal SO_2 absorbers appear to be sodium carbonate (76%) followed by sodium tetraborate (15%), sodium bicarbonate (6%) and sodium sulfate (3%).

Table III
SULFUR DIOXIDE ABSORPTION CAPACITY OF SELECTED SALTS PRESENT IN SEARLES LAKE BRINE - 2.0 ML ALIQUOT

Salt Concentration (g/l)	pH (initial)	pH (after)	Absorbance, Time (min)	Net Absorb. Time (min)
41.3 $Na_2B_4O_7 \cdot 10H_2O$	9.20	3.12	39	24
7.2 $NaHCO_3$	7.97	3.35	25	10
62.3 Na_2CO_3	11.65	5.45	141	126
90.3 Na_2SO_4	8.01	3.10	20	5
Water Blank (100 ml)	6.70	2.98	15	-

Absorbance equals 8.6×10^{-4} grams of SO_2 per minute and net absorbance is corrected for the water blank.

The reserves of sodium carbonate in Searles Lake have been estimated to be in excess of 150 million tons (3). Hence this huge carbonate reserve plus the other alkaline salts could provide a source of alkaline neutralizing capacity for high sulfur coal or oil burning power plants located near Searles Lake or sufficiently close so that the brine could be pumped to the location. In the case of Na_2CO_3 the reaction with SO_2 follows:

$$Na_2CO_3 + 2SO_2 + H_2O \longrightarrow 2NaHSO_3 + CO_2$$

Based on the above equation and assuming complete reaction, a brine of 62.3 g/l Na_2CO_3 (Table II) should absorb 75.2 grams of SO_2 per liter. However as shown in Table III, only 76% of the absorbing capacity was due to sodium carbonate, i.e., 71 (total SO_2 absorbance) x 0.76 or 54 grams of SO_2 per liter. This implies an efficiency of 54/75 x 100 or 72% if the neutralization were to go completely to $NaHSO_3$ formation from Na_2CO_3. As the data of Table III indicate for pure Na_2CO_3, the final pH after SO_2 absorption was 5.45 which lies close to the value observed on SO_2 gassing of the raw Searles brine.

TUNGSTEN RECOVERY

As indicated earlier, tungsten is one of the more valuable mineral components in Searles Lake brine. Although present at only 50 ppm, the amount of brine in the lake is so great that the total amount of tungsten is estimated at 170 million pounds of WO_3, equaling the total of all other known U.S. reserves. Earlier workers (4) had indicated that the tungsten might be recovered with organic reagents if the brine could be acidified by carbonating the liquor with flue gas. The data of Table IV indicates that tungsten requires a low pH for recovery from brine. Evidently, the rather weak acid nature of carbonic acid makes CO_2 a poor choice to reduce the pH of alkaline brines. Obviously the borate salts served as a buffer to prevent sufficient CO_2 acidification.

TABLE IV
RECOVERY OF TUNGSTEN FROM SEARLES LAKE BRINE
WITH ORGANIC REAGENTS SELECTIVE FOR TUNGSTEN

Test	Pretreatment	Organic Reagent	% W Recovered
1	SO_2 to pH 5.5 H_2SO_4 to pH 2.0	8-Hydroxyquinoline	0
2	Same as above	Cinchonine	20
3	CO_2 to pH 9.0	Tannic acid 8-Hydroxyquinoline	0
4	SO_2 to pH 5.5	Tannic acid 8-Hydroxyquinoline	15
5	None	Tannic acid Cinchonine	0
6	SO_2 to pH 5.5	Tannic Acid Cinchonine	100

100 ml of brine were used which would yield about 7.0 mg of tungstic oxide (WO_3). Also pure SO_2 gas was used rather than the dilute combustion gas (0.47% SO_2) so that the acidification could be completed in a reasonable time. Upon SO_2 gassing a yellow precipitate of sulfur first formed in the brine. These studies with pure SO_2 gas contacting the raw brine implies first a possible Claus reaction between the SO_2 and the Na_2S present (500 ppm) in the raw brine, i.e.,

$$2H_2S + SO_2 \longrightarrow 3S^{\circ} + 2H_2O$$

After completion of the SO_2 gassing, the sulfur precipitate was filtered from the solution, washed, ignited and subject to spectrographic analysis.

The data of Table V show that very little tungsten is removed with the elemental sulfur but that nearly 6% of the residue is arsenic.

TABLE V

EMISSION SPECTROGRAPHIC[1] ANALYSIS OF SULFUR RESIDUE FROM SEARLES LAKE BRINE IGNITED TO OXIDE

Element	Percentage
Na	32.
K	5.7
As	5.8
B	0.24
W	0.12
Cu	0.057
Si	0.23
Ca	0.095
Li	0.0059
Ag	0.00082
Ni	0.0030
Cr	0.054
Fe	0.026
Mo	0.0079
Ti	0.0095

Sulfur residue ignited at 570°C for 1 1/2 hours to produce a gray residue weighing 0.1004 grams separated from 100 ml of brine with SO_2 gas.

[1] This procedure was by arc semiquantitative optical emission.

Following the sulfur filtration, the filtrate was treated by standard methods using the reagents of Table IV. It is evident that high molecular weight reagents (cinchonine 294 and tannic acid 1701) are necessary to precipitate tungsten from a highly saline solution.

The data of Table VI for the ignited tungsten residue were obtained by a semi-quantitative analysis for all elements except tungsten which was analyzed by a modification of the McKaveney (5) hydroquinone photometric procedure. The modification involved fusion of the ignited residue with potassium pyrosulfate followed by a leach with sulfuric acid and dilution to 50 ml. An aliquot was then added to the hydroquinone for color development. The principal impurities in the tungstic acid are sodium and potassium with lesser amounts of silicon, boron and probably occluded chloride and sulfate. A water or dilute nitric acid leach should solubilize most of these impurities out of the tungstic acid.

TABLE VI
EMISSION SPECTROGRAPHIC ANALYSIS OF IGNITED OXIDE RESIDUE FROM TANNIC ACID - CINCHONINE SEPARATION OF SO_2 TREATED SEARLES LAKE BRINE

Element	%	Element	%
Na	23.	Ba	0.22
K	5.8	Fe	0.048
W	25.0	Ti	0.084
Ca	0.069	Zr	0.16
Al	0.19	Mo	0.035
Si	1.3	Sn	0.014
B	2.1	Cr	0.064

TECHNICAL AND ECONOMIC CONSIDERATIONS

Kerr-McGee, is now expanding its operations at Searles Lake. It is constructing a 64 megawatt coal fired power plant (6). The purpose is to replace scarce natural gas and to supply processing steam and electricity for their chemical operations. The carbon dioxide from coal combustion will be used for brine carbonation to manufacture sodium bicarbonate. By using higher sulfur fuels, SO_2 absorption could be used for easier tungsten recovery while carbon dioxide could be diverted to present chemical operations.

The authors have cited the utility of alkaline brines for the useful application of a harmful pollutant (SO_2) from coal or oil combustion. Also, their specific application dealt with Searles Lake and some modifications would be necessary for deposits containing other ratios of carbonate, borax and bicarbonate which are present in other California brines. In the future, the use of pipeline transportation of coal in water slurries may make many of these remotely located alkaline deposits realistic for power plant siting. The water from the slurry may be useful for cooling purposes. Also, the use of pipelines for transportation of seawater to inland locations may make it possible to utilize excess power plant heat for flash distillation of needed water. Seawater is relatively dilute in salt compared to the salt content of the dry lake or subsurface brine waters.

REFERENCES

1. J.E. Teeple, The Industrial Development of Searles Lake Brines, pp. 11-12, 86 pages, A.C.S. Monograph No. 49, The Chemical Catalog Co. Inc., New York, 1929.

2. Kirk-Othmer, Encyclopedia of Chemical Technology, Vol. 3, pp. 631-632, 1964.

3. D.E. Garrett and J.F. Phillips, "Sodium Carbonate from Natural Sources in the United States," A.I.M.E., Industrial Minerals and Rocks, pp. 799-808, 3rd Ed. (1960).

4. L.G. Carpenter and D.E. Garrett, Mining Engineering, pp. 301-303, (March, 1959).

5. J.P. McKaveney, Anal. Chem. 33 (6), pp. 744-47, (1961).

6. Anonymous, Chemical Week, 121 (11), Sept. 14, 1977.

Trace Element Chemistry of Leonardite and Its Potential Effect on Soil Geochemistry and Plant Growth

Alden Kollman

Project Reclamation, Box 8122, University Station, Grand Forks, ND 58202

Leonardite, a low BTU, naturally oxidized lignitic material has been suggested as a possible amendment for reclamation of strip mine spoils, especially orphan spoils, which are low in organic matter. These materials have a relatively high humic acid content and would be expected to improve the growth potential of these materials. It was found that in germination and growth chamber studies (5, 6) legumes responded favorably to the addition of 10% leonardite while grass production was decreased. Trace element sorption by these materials was possible cause for this differential response. In an initial study (2) the sorption and subsequent extractability of Fe^{+3}, Al^{+3}, Cu^{+2}, Zn^{+2} and Mn^{+2} by water, hydrochloric acid, ammonium acetate, DTPA-TEA and EDTA were determined, as was phosphorus sorption by the trace element saturated leonardites. In a second study, preliminary results of which shall be reported here the sorption capacities of 6 lignite materials (3 leonardites and 3 slack coals) were investigated. The materials were quite different in terms of humic acid content, total cations and sorption capacity. Leonardite is generally considered to be a lignite which is oxidized in situ, whereas slack coal is the upper layer of exposed coal seams and is not as highly oxidized.

The methods and results of the two experiments will be treated separately, but since the experiments are closely related they will be discussed together.

EXPERIMENT 1

Methods and Materials

A 60-gm sample of "Enderlin leonardite" (obtained from Prairie States Fertilizer Co.) was placed in a buchner funnel and successive aliquots (100 ml, 100 ml, 150 ml) of 0.1N solutions of Fe^{+3}, Al^{+3}, Cu^{+2}, Zn^{+2} or Mn^{+2} (all adjusted to pH 2) were passed through the sample and collected by suction filtration. The samples were then washed with 3-100 ml aliquots of distilled-deionized water, and dried. Replicated 4-gm samples of each of the five "saturated leonardites" and an untreated control were extracted by shaking for 2 hours with 20 ml of each of five extractants (water, 1N ammonium acetate, 0.005 M DTPA-TEA and 0.02 M EDTA). Samples of each saturated leonardite and control were then digested with 5:1, nitric: perchloric acids to determine whether there were changes in elemental composition due to cation exchange by the saturating ion and solution of soluble components. Cation concentrations were determined by atomic absorption spectrophotometry.

Since several studies have shown possible interactions between phosphorus and leonardite (1, 4) samples (4-gm) of each saturated leonardite were also treated with 40 ml of 500 and 1000 ppm phosphorus (as $Ca(H_2PO_4)_2$). After 3 days the P remaining in solution was determined by the molybdophosphoric blue color method (3).

Results

It was found that Fe^{+3} had the highest sorption (56 me/100 g) followed in decreasing order by Cu^{+2}, Al^{+3}, Zn^{++} and Mn^{++} (53, 51, 45 and 35 me/100 g, respectively). These results agree with the studies of fulvic acid extracted from Podzol Bh horizons by Schnitzer (7) in which the stability constants of several cations with the fulvic acid decreased in the following order at pH 3.5: Fe^{+3}, Al^{+3}, Cu^{+2}, Fe^{+2}, Ni^{+2}, Pb^{+2}, Co^{+2}, Ca^{+2}, Zn^{+2}, Mn^{+2}, Mg^{+2}.

The major cations in the untreated control samples were Ca^{+2}, Al^{+3}, Fe^{+3}, Mg^{+2}, and Na^{+1}; the remaining cations contributed less than 1 me/100 g (Table 2). The total cation content was higher in all samples that had been saturated by any trace element than in control samples. The major and minor cations behaved differently in the saturation process. Calcium^{+2}, Mg^{+2}, Na^{+1} were higher in the control than in the saturated samples. The decrease was presumed to be primarily a result of solution of soluble salts. The average quantity of Ca^{+2}, Mg^{+2}, and Na^{+1} remaining (non-replaceable) after saturations ranged from about 5% to 40% of the control concentrations (Fig. 1). Iron and Al had the highest sorption and appeared to be most tightly bound, however, the control samples and those saturated by any other cation were nearly equal. Consequently the replaceable fraction is very low (Fig. 1). The minor components appeared to behave similarly, all were low in the control and decreased by about 50% in the saturated samples.

The water, HCl and ammonium acetate extractions of saturated samples indicate that Fe^{+3} is most tightly bound, followed by Al^{+3}, Cu^{+2}, Zn^{+2} and Mn^{+2}. Since EDTA, a relatively strong chelating agent, removed about 50% of each cation, it is probable that the complexes formed have a stability similar to EDTA-cation complexes (Fig. 2).

Phosphorus sorption was highest (more than 90% of added P) in those samples which were saturated by Fe^{+3} and Al^{+3}. Samples saturated with Cu^{+2}, Zn^{+2} and Mn^{+2} sorbed amounts similar to that of the control.

EXPERIMENT 2

Methods and Materials

Origin and humic acid content of the lignitic materials used in this study were as follows:

SYMBOL	CLASSIFICATION	HUMIC ACID CONTENT %	ORIGIN
GPY	Leonardite	89.27	Gascoyne mine, Adams Co., ND
RR	Leonardite	85.76	Gascoyne mine, Adams Co., ND
E	Leonardite	65.29	Prairie States Fert. Co., Ransom Co., ND[1]
SB	Slack Coal	2.35	South Beulah Mine, Mercer Co., ND
GH	Slack Coal	2.84	Glenharold Mine, Mercer Co., ND
PYR[2]	Slack Coal	11.91	South Beulah Mine, Mercer Co., ND

[1]Mined at undisclosed location in Adams Co., ND

[2]Contains pyritic inclusions.

Each of the above materials was saturated with 0.1 N salts of Fe^{+3}, Al^{+3}, Cu^{+2}, Zn^{+2}, Mn^{+2} (adjusted to pH 2) by shaking a 2-g sample with two successive 20 ml aliquots of the solution. After shaking for 2 hours they were allowed to stand overnight, centrifuged and the supernatant decanted. The samples were then washed with two 30 ml-water rinses and dried at 80°C gor storage.

Samples (100 mg) for total analysis were digested in 3 ml of 1:5 nitric: perchloric acid, made up to 50 ml volume, and filtered. Cation concentrations were determined with Perkin-Elmer Models 403 and 503 atomic absorption spectrophotometers using standard instrument methods.

Results

The sorption was determined by analysis of both the quantity lost from the saturating solution and by the difference between the content of the control and saturated samples. In general the estimates based on the total analysis gave higher sorption, and the correlation was highly significant (r=0.93) (Fig. 3). The GPY sample had the greatest sorption capacity followed in decreasing order by SB, GH, RR, E and PYR (Fig. 4). As in the first experiment, Fe^{+3}, Al^{+3} and Cu^{+2} had the highest sorptions for all samples followed by Zn^{+2} and Mn^{+2} (Fig. 4 and Table 1).

Table 1. Sorption of trace elements by lignitic materials, based on the difference between total content of saturated and control samples.

Source	Fe	Al	Cu	Zn	Mn
	Sorption, me/100 g				
GPY	189.1	251.3	175.6	130.9	123.4
SB	137.8	117.9	117.4	91.8	110.6
GH	87.0	84.5	96.0	68.2	39.3
RR	111.2	97.8	96.0	47.4	35.3
E	107.4	77.8	81.8	35.2	24.7
PYR	97.8	66.7	63.0	35.2	18.3

The Fe^{+3}, Al^{+3} or Cu^{+2} concentrations of samples saturated by any other cation (e.g. Fe^{+3} in Al^{+3}, Cu^{+3}, Mn^{+2} or Zn^{+2} saturated samples) were similar to those of the control (Table 2) for all the materials tested. Zinc was significantly decreased in the saturated SB and PYR samples, and Mn was decreased by 50 to 90 percent in the saturated RR, E and PYR samples as compared to control. Sodium loss was almost uniform regardless of the saturating ion (Table 3) and appears to be lost roughly in proportion to the quantity originally present. Calcium and magnesium loss during saturation was greatest for Fe^{+3} and Al^{+3} saturations, commonly resulting in decrease of more than 90% regardless of the material. Manganese, Zn^{+2} and Cu^{+2} saturation allowed about 30-40 me/100 g more Ca and about 1-5 me/100 g more Mg to be retained by the materials.

Discussion and Conclusions

These materials are probably very similar in their behavior to naturally occurring humic materials since their sorption of Fe^{+3}, Al^{+3}, Cu^{+2}, Zn^{+2}, Mn^{+2} shows no serious conflict with the stability constants for fulvic acid cation complexes. However, there is not a good correlation between the humic acid content as determined by alkali extraction and trace element sorption. This may be an indication of the formation of complexes with compounds very different than humic acids. Further research is needed to determine the active functional groups and their bonding mechanisms. Results of the EDTA extraction in the first experiment indicate that at least for the "Enderlin" leonardite the major mechanism is probably chelation.

Before these materials are used as amendments for soils deficient in organic matter they should be tested for humic acid content, Fe^{+3} and Al^{+3} sorption and Na^{+1}, Ca^{+2} and Mg concentrations. The ideal material should have high humate and low Fe^{+3} and Al^{+3} sorption, which as a consequence will result in less P fixation. Since in this study it was found that Na^{+1}, Ca^{+2} and Mg^{+2} were easily lost they may potentially add to existing salinity or sodicity problems. In addition the Ca^{+2}

released may further fix phosphorus in marginally deficient systems. Of the materials tested the RR sample fits these criteria best and holds the greatest promise. A growth chamber study to test its effect on plant growth is planned.

Table 2. Concentration of major elements and trace elements in digested control samples.

Sample	Ca	Mg	Na	Fe	Al	Cu	Zn	Mn
	me/100 g					ppm		
GPY	197.5	120.8	18.3	43.0	70.0	43	25	93
SB	142.5	52.5	7.0	115.5	86.7	60	113	250
GH	110.0	45.8	58.7	31.1	36.7	33	38	55
RR	225.0	58.3	15.7	56.4	44.5	33	18	175
E	137.5	58.3	8.7	55.3	70.0	28	33	300
PYR	66.5	41.7	39.1	88.6	55.6	110	130	140

Table 3. Comparison of quantity of Ca, Mg and Na removed by saturating cations.

		Saturating Cation				
		Fe	Al	Cu	Zn	Mn
Calcium me/100 g	GPY	182.7	185.6	136.3	91.3	106.8
	SB	140.8	141.2	136.7	107.5	105.3
	GH	101.9	103.3	99.8	77.5	82.0
	RR	207.6	218.6	203.8	183.8	198.0
	E	122.0	130.0	116.7	107.5	107.3
	PYR	65.4	65.1	64.2	63.2	65.8
Magnesium me/100 g	GPY	118.2	112.7	109.8	99.6	96.5
	SB	36.2	38.4	36.4	34.6	32.4
	GH	31.8	38.3	41.2	38.5	38.5
	RR	57.0	56.5	56.4	54.9	55.1
	E	56.8	55.4	56.3	59.4	55.7
	PYR	35.8	35.8	34.5	33.8	30.0
Sodium me/100 g	GPY	11.9	11.8	11.4	11.7	13.7
	SB	--	--	--	--	--
	GH	51.6	50.2	50.9	50.9	52.2
	RR	9.6	9.9	9.1	9.0	12.8
	E	2.6	2.0	2.2	2.5	3.6
	PYR	32.3	32.2	31.6	32.6	34.9

REFERENCES

1. Harrell, J.W., Jr. and M. Saeed. 1977. Effect of Leonardite on diffusion phosphorus in coal mine spoils. Soil Sci. (in press)

2. Kollman, A.L. and M. Saeed. 1977. Trace element exchange characteristics of leonardite. Proc. N.D. Acad. Sci. 31(1):19.

3. Murphy, J. and J.P. Riley. 1962. A modified single solution method for the determination of phosphate in the natural waters. Anal. Chem. Acta. 27:31-36.

4. Saeed, M. 1977. Use of sorption-isotherms for evaluating effect of leonardite on P availability in surface-mined spoil materials. Rec. Rev. (in Press).

5. Safaya, N.M. and M.K. Wali. 1977. Effects of leonardite on the germination of some prairie grass and legume species. Proc. N.D. Acad. Sci. 31(1):27.

6. Safaya, N.M. and M.K. Wali. 1977. Growth and nutrient relations of some grass and legume species on a sodic mine-spoil as affected by different amendment and nutrient applications. Agron. Abstr. p. 130.

7. Schnitzer, M. 1969. Reactions between fulvic acid, a soil humic compound and inorganic soil constituents. Soil Sci. Soc. Am. Proc. 33(1):75-81.

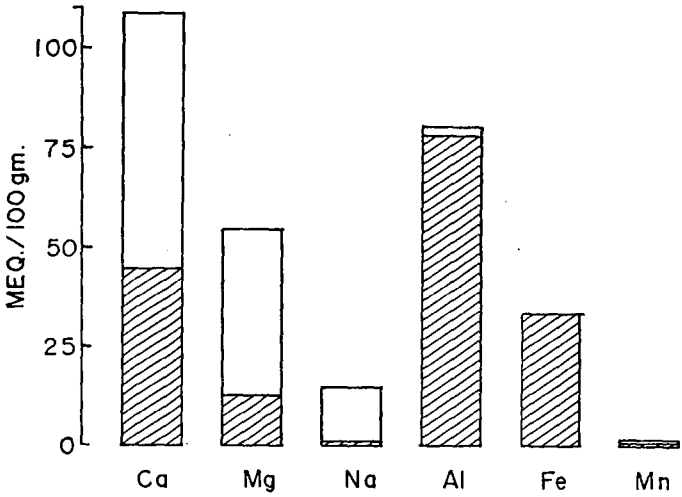

Fig. 1 Total and non-replaceable (shaded) concentrations of the dominant cations and manganese in E leonardite.

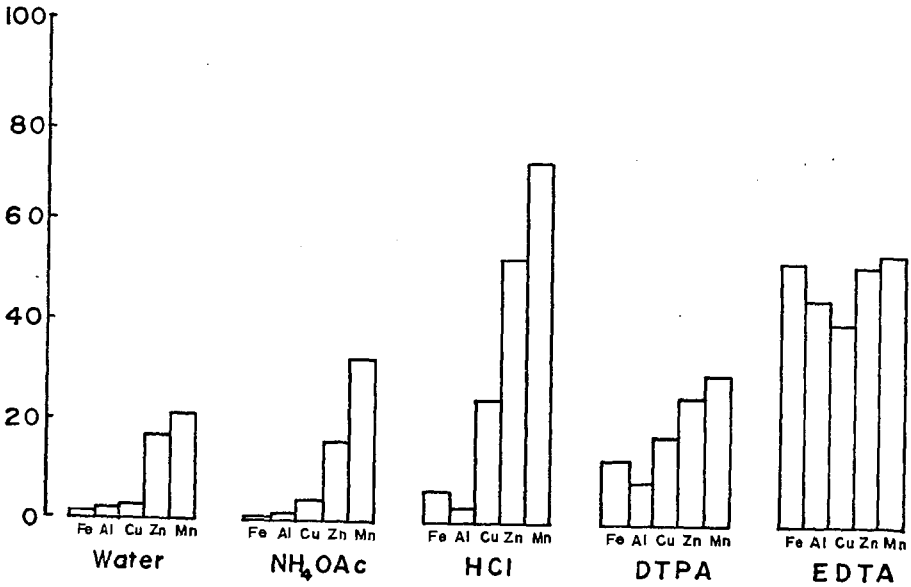

Fig. 2 Percentage of the sorbed cation that was extractable by several extracting solutions.

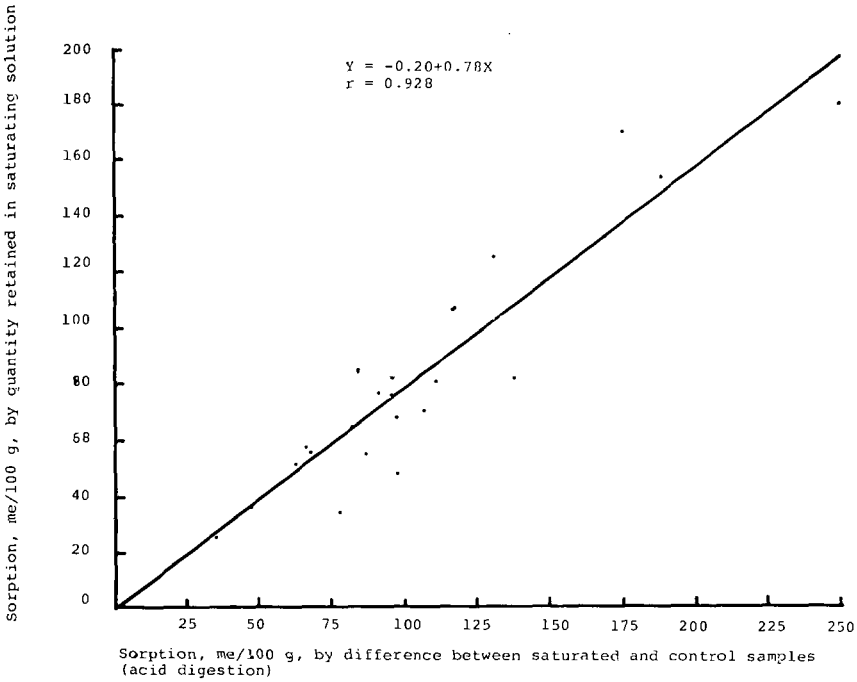

Figure 3. Comparison of sorption estimates by two methods.

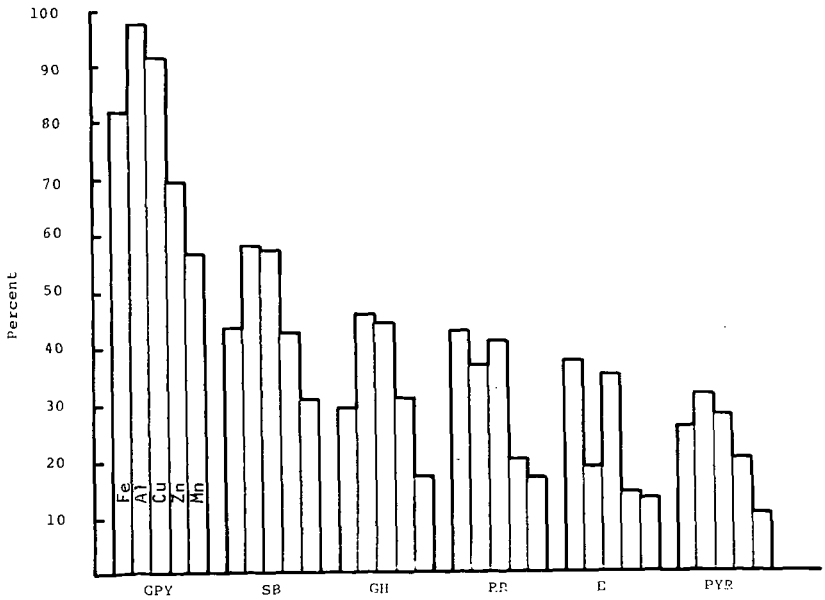

Figure 4. Quantity of trace element sorbed, as estimated by loss from the saturating solution, expressed as a percent of the total added.

TOPSOIL VERSUS SPOIL AS A PLANT GROWTH MEDIUM

Michal Harthill and Richard C. Barth

U.S. Bureau of Mines, DMRC, Denver Federal Center, Bldg. 20, Denver, Colorado, 80225; Colorado School of Mines Research Institute, P.O. Box 112, Golden, Colorado, 80401

Controversy generated by the actual depth of topsoil[1] required to adequately revegetate surface coal mined areas within the Northern Great Plains Coal Province (NGPCP) led the U.S. Bureau of Mines to fund the Colorado School of Mines Research Institute to research the problem. Results of the project should allow development of predictive models, useful within the NGPCP, for determining optimal topsoil depths for forage communities at minimal long-range costs.

EXPERIMENTAL METHODS AND RESULTS: Phase I of the study, initiated in 1976 consisted of canvassing the area's 17 existing mine sites for current reclamation practices. All of the mines apply topsoil, according to presiding state reclamation regulations, prior to seeding native and introduced plant species. Reclamation methods differ in the spoil treatments, depth of topsoil applied, time of year planted, species planted, use of cover crops, rate of seeding, use of fertilizers, use of mulch, and mowing or grazing of the revegetated areas(1).

Samples of regraded topsoil, and spoils, and undisturbed soil were collected from seven mine sites (2 in Wyoming, 1 in Montana, and 4 in North Dakota) and analyzed for a variety of physical and chemical characteristics (Table 1). Despite the varying climatic differences within the NGPCP and the geologic differences between the Powder River Basin and Williston Basin, all of the seven sites were generally similar to one another regarding existing plant growth media. Spoil salinity values were moderately high, and thus salinity is likely to inhibit salt intolerant plant species' growth. Soil and spoil pH for the Dave Johnston mine site was not included in the Table 1 averaged data because values were aberrantly acidic for the NGPCP. All values tend to fall within accepted state specifications. Because of known reclamation problem sites, the project sample number and design will be more inclusive in the future.

Phase II of the project consists of construction of 14 field wedge test plots (Figure 1) at existing surface coal mines in the NGPCP (Figure 2), and monitoring of plant growth on the plots. Plots were drill seeded at 30 seeds/0.1 m^2 during the spring of 1977 with a mixture of three of the following perennial grasses: Nordan crested wheatgrass (Agropyron cristatum), Luna pubescent wheatgrass (A. trichophorum), Critana thickspike wheatgrass (A. dasystachyum), Rosana western wheatgrass (A. smithii), and green needlegrass (Stipa viridula). Plant species were chosen for their ecological resilence and forage benefits. Fertilizer was applied at the rate of 30 ppm P as superphosphate and 50 ppm N as NH_4HO_3 over the entire plot.

(1) Topsoil is defined as the A (surface) horizon plus that portion of the underlying B and C horizons which is conducive to plant growth.

Vegetation characteristics measured after the first growing season were establishment and tillering of perennial grasses. These measurements do not necessitate plant harvesting, and the grasses were allowed to persevere. Volunteer species, primarily the annual Kochia, were harvested for above-ground biomass and for trace element accumulation. Percentage plant cover of both perennial grasses and annuals was estimated prior to plant harvest.

Perennial grass establishment on the wedge plots was 45.5% for topsoiled areas and 10.3% for spoils; differences were significant at the 1% level. Tillers, horizontal grass shoots, per plant average 2.8 for topsoil and 0.9 for spoils, significant at the 5% level. Above-ground biomass (Figure 3) of Kochia increased with increasing topsoil depth to approximately 35 cm, then leveled off. Although an empirical observation, the same trend occurred for percentage plant cover. Samples of annual plants are currently being analyzed for trace element accumulation; data will be correlated with substrate characteristics. Perennial grass samples will be assayed for trace element accumulation during the third, fourth, and fifth growing seasons, and uptake will be related to topsoil depth.

DISCUSSION: Although this study is in the preliminary stages, data indicate that topsoil allows for increased percentage plant cover and above-ground biomass, as well as increased plant establishment and tillering, over spoils treated in the same manner.

Future studies on this project will include increased soil/spoil sample design and number due to increased number of plots in various locations within the NGPCP. Soil/spoil studies will include percent organic matter, and seasonal changes in soil moisture and density. It is not intended that soil development will be detected within the longeveity of this project. However, significant differences between disturbed soil, which is essentially a secondary succession stage, and spoil, a primary succession stage, should be evident. Vegetative studies will include effective root depth correlated with suitable plant-growth medium depth, as well as physiological and morphological studies including plant susceptibility to drought, frost, and parasites.

Data collected over a five-year span should allow for development of predictive, perhaps site specific, models for determining optimum topsoil depth within the NGPCP at minimal reclamation costs.

REFERENCES:

(1) Barth, R.C., 1977, Reclamation practices in the Northern Great Plains Coal Province: Mining Congress Journal, May 1977, p. 60-64.

Site	Depth, cm From	Depth, cm To	pH in Water	pH in 0.01M $CaCl_2$	Soluble Salt Electrical Conductivity mmhos/cm	Sodium Water Soluble (milliequivalents/100 g)	Sodium NH_4 Acetate Soluble (milliequivalents/100 g)	Cation Exchange Capacity (milliequivalents/100 g)	Exchangeable Sodium Percentage	Ammonium ppm	Nitrate ppm	Phosphorus $NaHCO_3$ Extractable ppm
Reclaimed, Topsoil	0	19	8.0(1)	7.5(1)	5.6	0.31	0.50	24.7	0.8	8.5	35.2	15.6
Reclaimed, Spoils	19	50	7.7(1)	7.4(1)	10.1	0.87	1.23	23.7	1.5	8.9	29.1	12.1
Undisturbed	0	10	7.4	6.7	1.4	0.20	0.48	24.4	1.2	8.5	10.2	18.3
Undisturbed	10	50	7.9	7.2	4.9	1.30	1.91	24.9	2.4	7.9	5.0	10.5

Site	Depth, cm From	Depth, cm To	Potassium Available ppm	Water Soluble Sulfate ppm	Water Soluble Boron ppm	DTPA Extractable Copper ppm	DTPA Extractable Manganese ppm	DTPA Extractable Iron ppm	DTPA Extractable Zinc ppm	Molybdenum Anion Exchangeable ppm	Total Arsenic ppm	Total Cadmium ppm	Total Mercury ppm	NH_4 Acetate Extractable Nickel ppm	NH_4 Acetate Extractable Lead ppm
Reclaimed, Topsoil	0	19	294	422	1.45	1.8	24.5	90.3	1.0	0.3	1.9	<0.05	0.036	0.4	0.5
Reclaimed, Spoils	19	50	237	1375	1.26	4.9	29.1	156.0	1.4	0.4	1.7	<0.05	0.061	0.4	0.5
Undisturbed	0	10	413	74	1.16	1.9	28.0	73.7	1.9	0.2	1.7	<0.05	0.029	0.4	0.4
Undisturbed	10	50	294	495	1.21	2.6	34.4	81.9	1.0	0.2	1.7	<0.05	0.035	0.4	0.5

Site	Depth, cm From	Depth, cm To	Water-Holding Capacity, % (Dry Sample Wt. Basis) 1/3 Bar Suction	Water-Holding Capacity, % (Dry Sample Wt. Basis) 15 Bar Suction	Particle-Size Analysis, Wt. % Sand -2.0 +0.05 mm	Particle-Size Analysis, Wt. % Silt -0.05 +0.002 mm	Particle-Size Analysis, Wt. % Clay -0.002 mm	Textural Class
Reclaimed, Topsoil	0	19	17.3	9.0	58.3	23.8	18.0	Sandy loam
Reclaimed, Spoils	19	50	24.7	11.5	38.1	39.1	22.7	Loam
Undisturbed	0	10	22.4	11.7	47.6	36.6	15.8	Loam
Undisturbed	10	50	22.7	10.9	43.6	34.0	22.4	Loam

(1) Values from the Dave Johnston Mine site were not included.

TABLE 1. AVERAGED SOIL TRAITS OF RECLAIMED AND UNDISTURBED SITES.

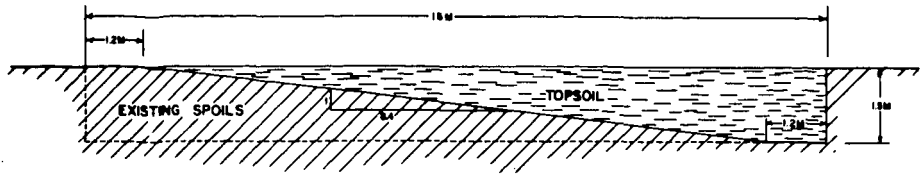

FIGURE 1. WEDGE TEST PLOT DESIGN.

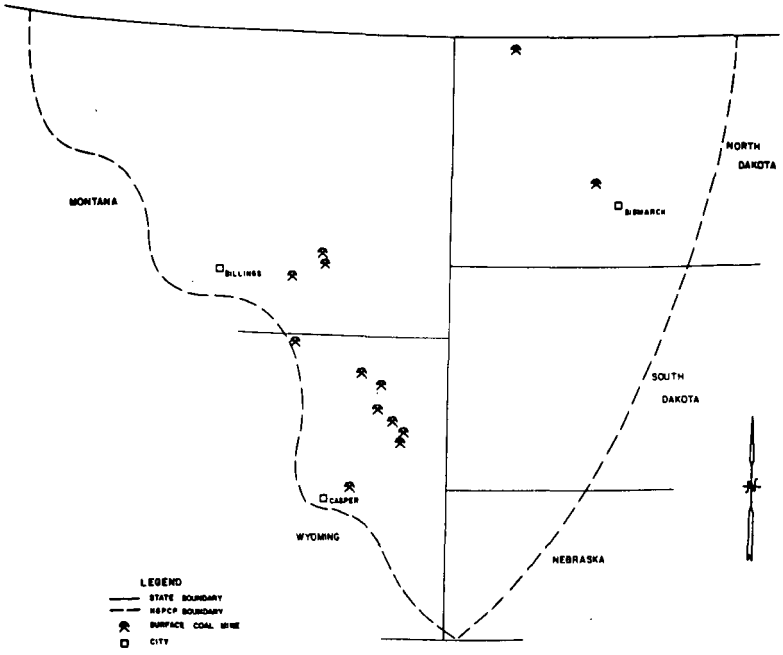

FIGURE 2. PHASE II WEDGE PLOT LOCATIONS.

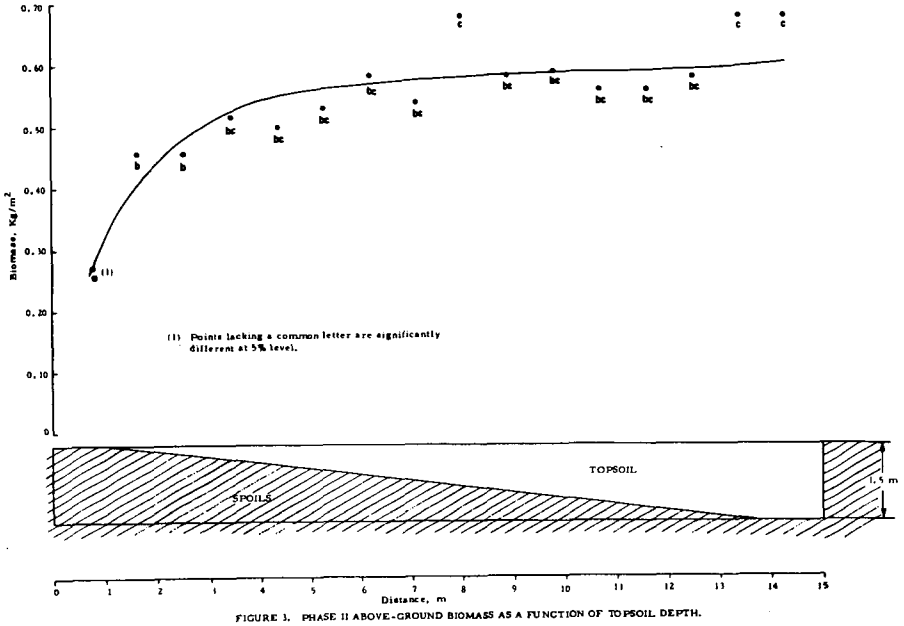

FIGURE 3. PHASE II ABOVE-GROUND BIOMASS AS A FUNCTION OF TOPSOIL DEPTH.

THE INFLUENCE OF BITUMINOUS COAL AND OVERBURDEN THERMO-MECHANICAL PROPERTIES ON SUBSIDENCE ASSOCIATED WITH UNDERGROUND COAL CONVERSION

Harold D. Shoemaker[1]
Sunder H. Advani[2]
Frank D. Gmeindl[2]
Yang-Tsi Lin[2]

[1]Morgantown Energy Research Center
Morgantown, West Virginia 26505

[2]West Virginia University
Morgantown, West Virginia 26505

INTRODUCTION

The in situ conversion of coal into combustible gas provides an attractive avenue for optimum utilization of the United States' principal fossil fuel resource. The primary benefits of underground coal gasification (UCG) over conventional mining methods are health, safety, controlled environmental subsidence, and maximum recovery of energy from coal deposits which are difficult to mine or are unminable. The success of UCG methods from environmental, technical, and economic considerations depends on a host of physical, chemical, and geological parameters. These factors have been extensively discussed in monographs detailing Soviet technology (1,2) and the recent British National Coal Board Status review of studies in the United Kingdom, Russia and United States (3). The major U.S. Department of Energy (DOE) sponsored projects in the United States are the Linked Vertical Well (LVW) programs at Hanna, Wyoming (4), and at Pricetown, West Virginia (5), in the medium thick western and thin eastern coal seams, respectively; and the Packed Bed Process (PBP) experiments near Gillette, Wyoming (6), also in the thick western coal seams.

The surface and subsurface environmental impact of in situ coal gasification may be predicted by utilizing the thermo-mechanical-structural properties of the in situ materials. The most serious structural mechanics related problems of UCG are those dealing with surface subsidence, roof stability, and coal permeability thermo-mechanical changes. The ensuing subsurface environmental consequences include possible gas leakage, water contamination, water influx into the combustion zone, and heat loss to the overburden. Control of the UCG process rate advancement, its stability, and surface and subsurface subsidence response is believed to be primarily due to the thermally induced strain and in situ stresses. In addition, coalbed permeabilities in the swelling bituminous coals are also influenced (7). Hence, the basic structural and constitutive properties of the in situ materials must be known in order to predict the effects of a gasification scheme with regard to roof collapse, coal fracturing, porosity, permeability, and surface subsidence.

This study represents an effort to provide somewhat more realistic and comprehensive experimental data of in situ gasification materials for utilization in subsidence comparisons from various empirical and phenomenological theories for the stratigraphy conforming to the Morgantown Energy Research Center (MERC) UCG experiments. An elastic finite element theory with specified failure criteria is used to identify the surface displacements, surface strains, and roof and surface failure zones.

PREVIOUS INVESTIGATIONS

Most of the research performed to determine the strength of coal has been from uniaxial compression tests on cubical, rectangular, or irregular shaped specimens (8,9,10). Coal has a greater ultimate compressive strength when loaded normal to the bedding planes than when loaded normal to either the face or butt cleats (8,9).

The ultimate strength increases when the stresses become representative of in situ tectonic stresses as shown from triaxial loading experiments (9,11,12,13). The ultimate compressive strength of coal whether loaded normal to the bedding planes or the cleat planes is test specimen size dependent (14,15,16), and increases exponentially with decreasing specimen size.

Similarly, there are many widely used shapes and sizes in determining the mechanical properties of rock; such as, cylinders, prisms and plates (17-25). The various studies on rock do not support the size dependence as shown in coal (22,23,26-31); that is, an increase in specimen size may or may not affect the ultimate strength of rock. However, under triaxial loading conditions the size effects are only present for low confining pressures (32).

There is evidence that coal and rock are viscoelastic materials and that coal behaves like a viscous fluid at elevated temperatures. Brewer (33) states that when bituminous coal is heated under appropriate conditions, it may exhibit plastic, viscous, or elastic flow, and often combinations of all three. Macrae and Mitchell (34) reported that the ultimate failure stress and deformation were notably time dependent. At room temperature, failure occurred after a high stress had been maintained on the specimen for an extended period of time. Sanada and Honda (35) have demonstrated that the time-temperature superposition principle can be applied to coal. Singh (36) demonstrated the three stages (primary, secondary, and tertiary) of the idealized creep curve in rock.

The utilization of thermo-mechanical properties of the involved materials in the application of subsidence and strata control theories, to underground mining, in the United States is relatively recent. The pioneering pre-World War II German experience and European efforts on pre-calculation of coal mine subsidence (37-41) have served as blueprint characterizations for sophisticated modeling. The techniques for predicting mine subsidence are based either on mathematical representations for the continuous trough profile or the influence function expressing the extraction of infinitisimal elements. A comprehensive survey of these methods and vertical subsidence S(x) computations for several profile or influence functions are given by Brauner (42). The empirical relations

$$V(x) = C_1 \ (dS/dx) \qquad 1)$$

and

$$E(x) = C_1 d^2S/dx^2 \qquad 2)$$

are employed for evaluation of the horizontal displacement V(x) and the horizontal surface strain E(x). Brauner (42) also presents considerations for time dependent and inclined strata subsidence behavior. The Subsidence Engineers' Handbook (43) furnishes extensive field results and design curves for predicting displacements, tilts, and strains. For critical or super critical widths, the maximum vertical subsidence S_{max} is generally from 0.50 to 0.90 of the seam thickness while the maximum horizontal displacement V_{max} is about one-third of S_{max}. The corresponding maximum tilt, compressive strain, and tensile strain values are approximately 2.5 S_{max}/depth, 0.5 S_{max}/depth, and 0.67 S_{max}/depth, respectively.

The mine subsidence representations discussed in the literature sited above are primarily semi-empirical and do not address local geo-mechanical variables. Various phenomenological model representations have been attempted to include geometric and material property effects. These investigations encompass two- and three-dimensional linear isotropic and anisotropic elasticity theory models (44-48), viscoelastic responses (49), experimental models (50), and elastic as well as elasto-plastic finite element model subsidence evaluations (51-53) utilizing experimental field data. Several roof stress response studies relating to underground opening design and mining operations have been conducted utilizing the finite element stress evaluations (54-56). Similar studies on the influence of stresses on roof rock fractures, block boundary weakening, and cavability have been conducted (57). Other investigators (1)

and reports (2) have also presented qualitative discussions relative to surface subsidence, roof collapse and the ensuing technical and environmental problems.

EXPERIMENTAL STUDIES

In examining structural property effects on subsidence, roof collapse, and various modes of failure, specific types of data are required. The basic properties required are directional (for coal) and temperature-dependent stress-strain relations and failure stresses in compression and shear.

The Pittsburgh bituminous coal and its adjacent overburden were evaluated in the experiments. All experiments were conducted in uniaxial compression and simple shear, in determining both the elastic and viscoelastic properties of the materials. Because of the size dependency of coal with regard to its ultimate strength, four different specimen sizes, ½" x ½" x 1", 1" x 1" x 2", 2" x 2" x 4", and 4" x 4" x 8" (1.27 x 1.27 x 2.54 cm, 2.54 x 2.54 x 5.08 cm, 5.08 x 5.08 x 10.16cm, and 10.16 x 10.16 x 20.32 cm), were used in the uniaxial compression tests and one in simple shear, ½" x 2" x 2" (1.27 x 5.08 x 5.08 cm) (figure 1). One specimen size was used in the overburden experiments in uniaxial compression, ½" x ½" x 1" (1.27 x 1.27 x 2.54 cm). The thermo-mechanical properties test apparatus and experimentation details are described elsewhere (58).

Elastic Experiments -- Temperature has a dramatic effect upon the ultimate strength and ultimate strain of coal and the overburden (figures 2-4). Regardless of specimen size, the ultimate strength of the coal is greatest at 200°F (93°C) (figure 2). The dark gray shale, which contains carbon, responds similarly to coal in that the largest ultimate strength is shifted to the right to approximately 350°F (177°C), while the light gray shale displays progressively increased strength as the temperature increases over the temperature range obtained (75°-700°F (24°-371°C)). The ultimate strain is relatively constant for the coal and dark gray shale until the temperature of the specimens exceed 500°F (260°C) and 575°F (302°C), respectively, where large finite strains occur; while for the light gray shale the ultimate strain remains relatively constant over the temperature range investigated (75°-700°F (24°-371°C)) (figures 2 and 3). Notice, figure 4, the characteristic S-shape of the stress-strain curves and the elasto-plastic response of the coal to uniaxial compressive loading.

Theory does not support the phenomen observed in the coal and dark gray shale that their strengths increase with temperature before a final decrease to very small values (figures 2-4). However, these characteristics have been observed in coal (34) and dark gray shale (59). Macrae and Mitchell (34) postulated that the increased strength at approximately 212°-248°F (100°-120°C) was due to the weaker secondary forces of the van der Waals-type between structural units being affected and that heating affects the mode of fracture from tension at ordinary temperatures to shear at temperatures above 212°F (100°C). These results were generally validated in the experiments.

The ultimate shearing strengths from the shear tests were, in general, independent of the orientation of loading (varied less than 200 psi (0.138×10^7 N/m^2) over the temperature range) (figure 5). The results for loadings normal to the face and butt cleats in uniaxial compression are also similar, but different from loadings normal to the bedding planes (figure 6). This similarity indicates that at least along these two directions the Pittsburgh coal behaves as a transversely isotropic material as also observed (9,35,60) for other coals.

Viscoelastic Experiments -- The viscoelastic properties of the coal and overburden also represent a large variety of linear and nonlinear rheological properties. The effect of orientation of the constant applied load on the creep compliance in coal is demonstrated in figure 7 at 500°F (260°C). Notice, the difference between the

curves, compressive loading normal to the bedding planes demonstrates failure in tertiary creep after approximately six minutes, while for loadings normal to the face and butt cleats failure did not occur until much later (35 minutes). This directional effect is apparently due to increased resistance to deformation in the face and butt cleat directions caused by the interlayering of the organic and inorganic materials when the loading is parallel to the bedding planes. The Pittsburgh coal can also be represented by the time-temperature superposition principle (figure 8).

ROOF RESPONSE EVALUATIONS AND SUBSIDENCE COMPUTATIONS

The presented experimental data is employed for the evaluation of UCG fractured roof zones, roof convergence, and surface subsidence. Figure 9a reveals the selected two-dimensional model corresponding to the planned Morgantown Energy Research Center line-drive experiments at Pricetown, West Virginia. Figure 9b illustrates the propagating cavity configuration at a specified time instant with the adjacent coke, softened layers, and overburden. The corresponding "steady state" constant temperature profiles, computed by the Alternating Direction Implicit Method (61) are shown in figure 9c.

The stress model simulations entail use of the NASTRAN finite element code for an initially selected cavity configuration at time t_1. The effects of temperature loading, in situ stresses, and internal pressure are superposed and temperature dependent mechanical properties are assumed for the Pittsburgh coal and overburden shale elements. On the basis of the computer principle stresses, failure criteria in terms of the tensile and compressive yield strengths are applied as follows.

Compression Failure -- This failure occurs when

$$C_o = \sigma_3 - \sigma_1 \left[\frac{(1 + \mu_f^2)^{\frac{1}{2}} + \mu_f}{(1 + \mu_f^2)^{\frac{1}{2}} - \mu_f} \right] \qquad 3)$$

where σ_1 and σ_3 are the major and minor principal stresses, respectively, C_o is the uniaxial compressive strength, and μ_f is the internal coefficient of friction.

Tension Failure -- For the case $3\sigma_1 + \sigma_3 > 0$, the limiting failure criterion is

$$\sigma_1 = T_o \qquad 4)$$

where T_o is the uniaxial strength in tension.

Shear Failure -- For the case $3\sigma_1 + \sigma_3 < 0$, failure is governed by

$$-(\sigma_1 - \sigma_3)^2(\sigma_1 + \sigma_3)^{-1} = 8T_o \qquad 5)$$

At the initial specified time instant, the elastic model is simulated and the failure zones are identified. The elastic properties of these failure regions are then reduced by a factor of 100 since the normal horizontal stresses are relieved. The resulting stress distributions, roof convergence, and surface subsidence values are determined. The procedure is continued until maximum roof convergence is obtained. For each subsequent time instant, this method is repeated and the new corresponding failure zones are obtained along with the roof convergence profile and surface subsidence.

The selected mechanical and thermal properties for the model simulation are presented in table 1 and figure 10. The roof and coal failure zones for different time instants computed from the NASTRAN model simulation and assigned failure criteria are illustrated in figure 11. The corresponding non-dimensionalized elastic and "fractured" roof convergence profiles are revealed in figure 12 with the vertical surface subsidence profiles shown in figure 13.

TABLE I. Selected Mechanical and Thermal Properties for the Master Model.

Property	Symbol	Units	Coal	Softened Coal Layer	Coke	Sandstone	Light Gray Shale	Dark Gray Shale
Young's Modulus	E	psi (N/m^2)	186×10^3 (128×10^7)	500 (0.345×10^7)	130×10^3 (89.6×10^7)	2.0×10^6 (1.38×10^{10})	800×10^3 (552×10^7)	See Figure 10
Poisson's Ratio	ν	---	0.44	0.47	0.25	0.12	0.15	0.45
Thermal Expansion Coefficient	α	$/^oF$ ($/^oC$)	2.78×10^{-6} (5.00×10^{-6})	5.40×10^{-6} (9.72×10^{-6})	4.50×10^{-6} (8.10×10^{-6})	4.50×10^{-6} (8.10×10^{-6})	4.50×10^{-6} (8.10×10^{-6})	4.50×10^{-6} (8.10×10^{-6})
Thermal Conductivity	K	Btu/^{o}F-in-sec (Kgcal/^{o}C-m-sec)	2.79×10^{-6} (4.98×10^{-5})	5.15×10^{-6} (9.20×10^{-5})	7.50×10^{-6} (13.4×10^{-5})	2.50×10^{-6} (4.47×10^{-5})	2.50×10^{-6} (4.47×10^{-5})	2.50×10^{-6} (4.47×10^{-5})
Mass Density	ρ	lbm/in^3 (Kg/m^3)	0.046 (1,273)	0.028 (775)	0.037 (1,024)	0.070 (1,938)	0.078 (2,159)	0.078 (2,159)
Compressive Strength	Small Specimen C_o	psi (N/m^2)	4,000 (2.76×10^7)	----	----	14,000 (9.65×10^7)	14,000 (9.65×10^7)	14,000 (9.65×10^7)
Compressive Strength	Scaled C_o	psi (N/m^2)	2,800 (1.93×10^7)	----	----	2,800 (1.93×10^7)	2,800 (1.93×10^7)	2,800 (1.93×10^7)
Tensile Strength	Small Specimen T_o	psi (N/m^2)	430 (0.3×10^7)	----	----	430 (0.3×10^7)	430 (0.3×10^7)	430 (0.3×10^7)
Tensile Strength	Scaled T_o	psi (N/m^2)	86 (0.06×10^7)	----	----	86 (0.06×10^7)	86 (0.06×10^7)	86 (0.06×10^7)

DISCUSSION AND CONCLUSIONS

The tests conducted on the Pittsburgh coal and adjacent overburden were conventional ones used for determining the properties identified for elastic or viscoelastic isotropic, homogeneous materials. The data from these tests represent a large variety of linear and nonlinear rheological properties including plasticity and creep, depending upon temperature. In reality, the Pittsburgh coal and dark gray shale behave as plastic, elasto-plastic viscoelastic materials under different conditions and none of the existing elasto-plastic or other known plastic theories are suitable for totally describing the stress-strain-time characteristics. Similar phenomena have been described by others (33-35).

These experimentally obtained Pittsburgh coal and overburden thermo-mechanical properties furnish basic data for the detailed structural simulation of the roof and surface subsidence responses during in situ gasification processes. A related study (62), utilizing an elasto-plastic finite element model with temperature independent overburden properties, has demonstrated that the maximum surface subsidence is 0.52 X seam thickness (for the two-dimensional plane strain model stratigraphy simulated here with a 500 foot (152 m) extraction width). The corresponding yielded zone extends to a distance of approximately 350 feet (107 m) immediately above the roof. This value apparently represents an upper bound since conservative overburden compressive and tensile structural strengths are used (C_o = 2800 psi (1.93×10^7 N/m^2) and T_o = 86 psi (0.06×10^7 N/m^2)). For the simulations presented here, the surface subsidence corresponding to an extracted width of 100 feet (30.5 m) is 0.14 X seam thickness (figure 13) with a vertical overburden fractured shear and tensile zone of approximately 36 feet (11 m) (figure 11). Related studies (61,62) have been conducted on crack propagation in the overburden roof rock. This thermal cracking of the roof block provides an avenue for water influx into the combustion zone to enhance the heating value of the produced gas. However, gas leakage to the surface, via the thermal cracks and the tensile and shear induced fissures in the roof, does not appear probable for this case. The magnitudes and slopes of the roof convergence profiles in figure 12 are important indicators of the intermittent roof fracturing process. The propagation of the combustion front is enhanced by the severe compressive stress concentrations induced at the cavity edge (figure 11, the Longwall Generator

underground gasification concept is here represented). Similar stress analysis considerations also apply to the Linked Vertical Well gasification concept with a tear drop shaped cavity. The corresponding sweep areas are limited for thin seam coal since the radial combustion velocities are limited and the resulting roof stress concentrations are considerably less severe than for the Longwall Generator case.

These thermo-mechanical data also become useful in understanding the basic mechanisms involved in mass and energy transport and mechanical-structural effects in gasification processes. For example, decreased permeability shortly after initiation of a burn in modeling coal gasification processes in the laboratory with the Pittsburgh coal and overburden is readily understood to be due to the swelling and effervescent nature (bubbling of tars into the fissures) of the Pittsburgh coal at elevated temperatures. The tars, along with the swelling of the Pittsburgh bituminous coal, tend to restrict the outward movement (reduce permeability) of the combustion front around a borehole or cavity as well as inhibit a forward burn along a borehole. However, the swelling, effervescent and coalescent nature of the Pittsburgh coal becomes an asset in control of channeling or short-circuiting in line-drive gasification processes (7) in that the fluidic coal will be forced into these channels by the pressure of the fractured roof (overburden) and the swelling of the coal.

Although water influx effects into the combustion zone are not explicitly considered in the subsidence analysis, the additional subsidence due to extraction of the neighboring fluids can be included by assigning the ratio of the depleted fluid volume during gasification to the caved block volume (62). The subsidence curve can then be accordingly modified.

REFERENCES

1. Skafa, P. V., "Underground Gasification of Coal," Gosudarstvenno Hauchno-Tekhnicheskoe Izdatel'stvo Literatury Po Gornomu Delu, Moscow (1960); also UCRL-TRANS-10880, September 1975, 324 pp.
2. Anon, "A Current Appraisal of Underground Coal Gasification," PB 209 274, Arthur D. Little, Inc., Cambridge, Mass., 1972.
3. Thompson, P. N., Mann, J. R., and F. Williams, "Underground Gasification of Coal," National Coal Board, UK, 1976.
4. Schrider, L. A. and D. D. Fisher, "In Situ Coal Gasification - A Unique Means for Energy Recovery," ASME Paper No. 75-PVP-44, 1975.
5. Strickland, L. D., "A Status Report on MERC's Program for In Situ Gasification of Bituminous Coals," presented at 3rd Annual Underground Coal Gasification Symposium, sponsored by Lawrence Livermore Laboratory at Fallen Leaf Lake, CA, June 6-10, 1977, 13 pp.
6. Stephens, D. R., "LLL In Situ Coal Gasification Program - Annual Report 1975," UCRL-50032-75, Lawrence Livermore Laboratory, Livermore, CA, 1975.
7. Advani, S. H., L. Z. Shuck, and K. Y. Lee, "Stress Response Investigations Related to In Situ Gasification of Coal," in press, ASME transactions, paper presented at the Energy Technology Conference and Exhibition, Houston, TX, September 18-22, 1977, Paper No. 77-Pet-25, 5 pp.
8. Evans, I. and C. D. Pomeroy, "The Compressive Strength of Rectangular Blocks of Coal," National Coal Board (England), Report 2077, October 1957, 15 pp.
9. Evans, I. and C. D. Pomeroy, "The Strength, Fracture, and Workability of Coal," Pergamon Press, New York, 1966, 277 pp.
10. Rad, P. F., "Mechanical Properties and Cutting Characteristics of Coal," BuMines Information Circular 8584, 1973, 46 pp.
11. Hobbs, D. W., "Strength and Stress-Strain Characteristics of Coal in Triaxial Compression," J. Geol., v. 72, March 1964, pp. 214-231.
12. Pomeroy, C. D. and D. W. Hobbs, "Fracture of Coal Specimens Subjected to Complex Stresses," Steel and Coal, v. 185, December 1962, pp. 1124-1133.

13. Ko, Hon-Yim and K. H. Gerstle, "Elastic Properties of Two Coals," Internat. Journal of Rock Mechanics, Mineral Science, and Geomechanics, v. 13, 1976, pp. 81-90.
14. Bieniawski, Z. T., "Effect of Specimen Size on Compressive Strength of Coal," Internat. Journal of Rock Mechanics and Mineral Science, v. 5, July 1968, pp. 325-335.
15. Evans, I., C. D. Pomeroy, and R. Berenbaum, "Compressive Strength of Coal," Coal, Eng., v. 38, 1961, pp. 75-87.
16. Gaddy, F. L., "Study of Ultimate Strength of Coal as Related to Absolute Size of Cubinal Specimens Tested," Va. Polytechnical Inst., Eng. Expr. Sta., Ser. 112, August 1956, 27 pp.
17. Narayanan R., "Some Factors which affect Concrete Strength," Cement and Concrete 2, 71-82, 1961.
18. Symons, I. F., "The Effect of Size and Shape of Specimen upon the Unconfined Compressive Strength of Cement-Stabilised Materials," Magazine of Concrete Research 22, 45-50, 1970.
19. Kadlecek, V. and Z. Spetla, "Effect of Size and Shape of Test Specimens on the Direct Tensile Strength of Concrete," RILEM Bulletin, No. 36, 175-184, 1967.
20. Bieniawski, Z. T., "The Compressive Strength of Hard Rock," CSIR Report MEG 272, Pretoria, 1968.
21. Gonnerman, H. F., "Effect of Size and Shape of Test Specimens on Compressive Strength of Concrete," Proc. ASTM 25, 237-250, 1925.
22. Hoskins, J. R. and F. G. Horino, "Influence of Spherical Head Size and Specimen Diameters on the Uniaxial Compressive Strength of Rocks," BuMines RI 7234, 1969.
23. Dhir, R. K., C. M. Sangha and J. G. L. Munday, "Influence of Specimen Size on Unconfined Rock Strength," Colliery Guardian 220, 75-80, 1972.
24. Robertson, E. C., "Experimental Study of the Strength of Rocks," Bull. Geol. Soc. Am. 66, 1275-1314, 1955.
25. Fumagalli, E., discussion on a paper by Iyenger et al—"Strength of Concrete under Biaxial Compression," Journal of the Am. Concrete Inst., Proc. 62, 1187-1189, 1965.
26. Obert L., S. L. Windes, and W. I. Duvall, "Standardized Tests for Determining the Physical Properties of Mine Rock," US BuMines RI 3891, 1946.
27. Skinner, W. J., "Experiments on the Compressive Strength of Anhydrite," The Engineer 207, 255-259 and 288-292, 1959.
28. Mogi, K., "The Influence of the Dimensions of Specimens on the Fracture Strength of Rocks," Bull. Earthquake Res. Inst., Tokyo Univ. 40, 1975-185, 1962.
29. Hodgson, K. and N. G. W. Cook, "The Effects of Size and Stress Gradient on the Strength of Rock," Proc. Second Congress Int. Soc. Rock Mech. Belgrade 2, 31-34, 1970.
30. Stamatiu, M. and C. C. Teodorescu, "Quelques Properties Physiques et Mecaniques du sel Gemme Roumain," Proc. Seventh Congr. Int. Min. Met. Geol. Appl., Paris 1, 317-320, 1935.
31. Ruhfus, B., "Investigation of the Influence of the Dimensions and Layering of Rock Specimens upon the Compressive Strength," M.S. Thesis, Colorado School of Mines, 1961.
32. Habib, P. and G. Vouille, "Sur la Disparition de l'Effect d'Echelle aux Hautes Pressions," Cr. hebd. Seanc. Acad. Sci., Paris, 1966.
33. Brewer, R. E., "Plastic and Swelling Properties of Bituminous Coking Coals," BuMines Bulletin 445, 1942, 260 pp.
34. Macrae, J. C. and A. R. Mitchell, "The Response of Bright Bituminous Coal to Undirectional Compression," Fuel, v. 36, October 1957, pp. 423-441.
35. Sanda, Y. and H. Honda, "Creep in Coal Over the Temperature Range 200 to 370°C," Fuel, v. 42, 1963, pp. 479-486.
36. Singh, D. P., "A Study of Creep of Rocks," Int. J. Rock Mech., Min. Sci., and Geomech. Abstr., v. 12, pp. 271-276, 1975.
37. Briggs, H., "Mining Subsidence," E. Arnold and Co., London, 215 pp., 1929.
38. Bals, R., "A Contribution to the Problem of Precalculating Mining Subsidences," Mitteilungen aus dem Markscheidewesen, v. 42/43, pp. 98-111, 1931/1932.

39. Knothe, S., "Observations of Surface Movements under Influence of Mining and Their Theoretical Interpretation," Proceedings of the European Congr. on Ground Movement, Univ. of Leeds, pp. 49-57, 1957.
40. Drent, S., "Some Considerations on the Connection Between Time-Curves and the Thickness of the Non-Carboniferous Overburden in the South Limburg Coalfield," Proc. of European Congr. on Ground Movement, Univ. of Leeds, pp. 49-57, 1957.
41. Zenc, M., "Comparison of Bals' and Knothe's Methods of Calculating Surface Movements Due to Underground Mining," Internat. J. of Rock Mech. & Min. Sci., v. 6, pp. 159-190, 1969.
42. Brauner, G., "Subsidence Due to Underground Mining," Part I: "Theory and Practices in Predicting Surface Deformation," Part II: "Ground Movements and Mining Damage," BuMines Info Circ. 8571, 8572, 1973.
43. "Subsidence Engineers' Handbook," Nat. Coal Board Mining Department, 1975.
44. Berry, D. A. and T. W. Sales, "An Elastic Treatment of Ground Movement due to Mining-II, Transversely Isotropic Ground," J. of Mech. & Phys. of Solids, v. 9, pp. 52-62, 1961.
45. Berry, D. A. and T. W. Sales, "An Elastic Treatment of Ground Movement Due to Mining-III, Three-Dimensional Problem, Transversely Isotropic Ground," J. of Mech. & Phs. of Solids, v. 10, pp. 73-83, 1962.
46. Berry, D. A., "The Ground Considered as a Transversely Isotropic Material," Internat. J. of Rock Mech. & Min. Sci., v. 1, pp. 159-167, 1964.
47. Salamon, M. D. G., "Elastic Analysis of Displacements and Stresses Induced by the Mining of Seam or Reef Deposits," J. of South African Inst. of Min. and Met., v. 64, pp. 128-129, pp. 197-218, pp. 468-500, 1963/1964.
48. Crouch, S. L. and C. Fairhurst, "Analysis of Rock Mass Deformations due to Excavations," Rock Mech. Symp., AMD-Vol. 3, ASME Pub., pp. 25-40, 1973.
49. Marshall, G. J., "A Visco-elastic Treatment of the Deformation of the Ground Caused by Mining Operations," J. of Mech. & Phy. of Solids, v. 17, pp. 151-162, 1969.
50. Pariseau, W. G. and H. D. Dahl, "Mine Subsidence and Model Analysis," Society of Mining Engineers, AIME, v. 241, pp. 488-494, 1968.
51. Brown, R. E., "A Multi-Layered Finite Element Model for Predicting Subsidence," PhD dissertation, Carnegie-Mellon Univ., Pittsburgh, PA, 1968.
52. Dahl, H. D., "A Finite Element Model for Anisotropic Yielding in Gravity Loaded Rock," PhD dissertation, the Penn. St. Univ., University Park, PA, 1969.
53. Mojumdar, B. K., "Mathematical Model of Ground Movement due to Underground Mining," PhD dissertation, the Penn. St. Univ., University Park, PA, 1974.
54. Kidybinski, A. and C. Babcock, "Stress Distribution and Rock Fracture Zones in the Roof of Longwall Face in a Coal Mine," Rock Mech., v. 5, pp. 1-19, 1973.
55. Kulhawy, F., "Finite Element Modeling Criteria for Underground Openings in Rock," Internat. J. of Rock Mech. & Min. Sci., v. 11, pp. 465-472, 1974.
56. Kulhawy, F., "Stress and Displacements Around Openings in Homogeneous Rock," Internat. J. of Rock Mech. & Min. Sci., v. 12, pp. 43-57, 1975.
57. Mahtab, M. and J. Dixon, "Influence of Rock Fractures and Block Boundary Weakening on Cavability," Soc. of Min. Engrs., AIME, v. 260, pp. 6-12, 1976.
58. Shoemaker, H. D., L. Z. Shuck, R. R. Haynes, and S. H. Advani," Directional Viscoelastic Properties of the Pittsburgh Coal at Elevated Temperatures in Compression and Shear," MERC/RI-76/5 (USERDA Rpt of Invest.), August 1976, 198 pp.
59. Baidyuk, B. V., "Mechanical Properties of Rocks at High Temperatures and Pressures," Gostoptekhizdat, Moscow, 1963 (translated by J. P. Fitzsimmons, Consultants Bureau, NY, 1967, 75 pp.).
60. Morgans, W. T. A. and N. B. Terry, "Measurement of Static and Dynamic Elastic Moduli of Coal," Fuel, v. 37, April 1958, pp. 201-219.
61. Advani, S. H., Y. T. Lin, V. Shah, and H. F. Wang, "Structural Mechanics and Model Simulations Associated with Underground Coal Gasification," proc. Am. Nuc. Soc. and ERDA Topical Mtg on Energy and Mineral Resource Recovery, 1977, in press.

62. Advani, S. H. and Y. T. Lin, "Subsidence and Roof Response Studies Related to Underground Coal Gasification," proc. 3rd Annual Underground Coal Conversion Symp., Fallen Leaf Lake, CA, June 1977, In press.

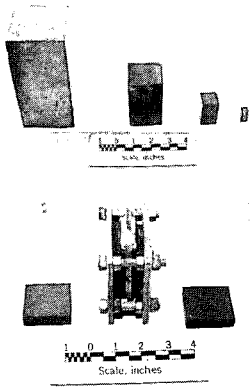

Figure 1. Pittsburgh Coal Specimens as Used in Uniaxial Compression and Shear Experiments.

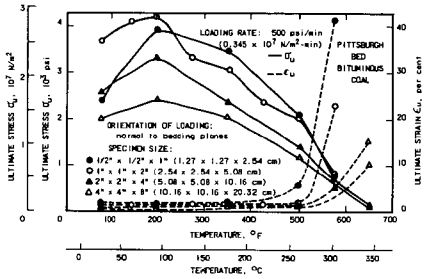

Figure 2. The Ultimate Stress and Strain-Temperature Curves Showing the Effect of Specimen Size of the Pittsburgh Coal When Loaded in Uniaxial Compression Normal to the Bedding Planes.

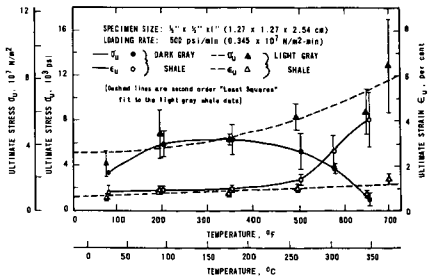

Figure 3. Ultimate Stress and Strain Curves as Functions of Temperature for Pittsburgh Seam Overburden When Loaded in Uniaxial Compression. The Bars on the Data Are ± One Standard Deviation.

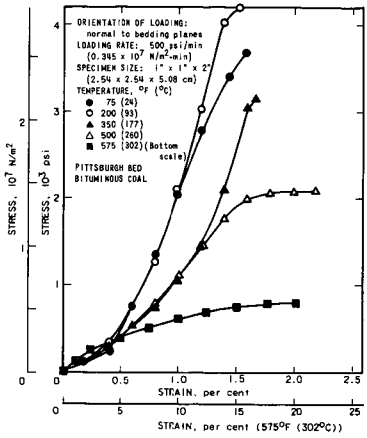

Figure 4. Stress-Strain Curves Loaded in Uniaxial Compression (Average Values) Showing the Effect of Temperature on the Pittsburgh Coal.

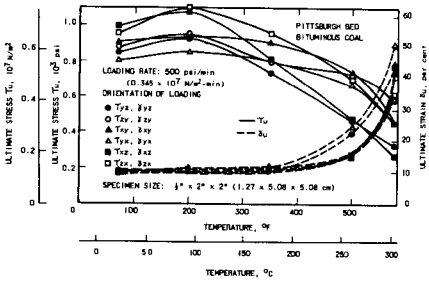

Figure 5. The Ultimate Stress and Strain-Temperature Curves Showing the Effect of Orientation of Loading in Shear on the Pittsburgh Coal.

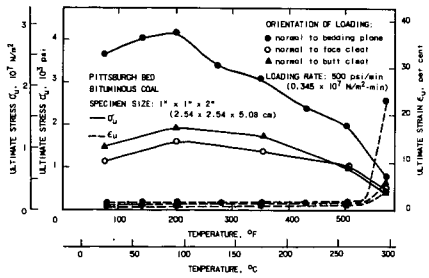

Figure 6. The Ultimate Stress and Strain-Temperature Curves Showing the Effect of Orientation of Loading on the Pittsburgh Coal When Loaded in Uniaxial Compression.

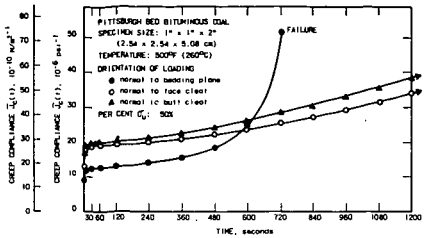

Figure 7. Creep Compliance-Time Curves Showing the Effect of the Orientation of Loading in Uniaxial Compression on the Pittsburgh Coal.

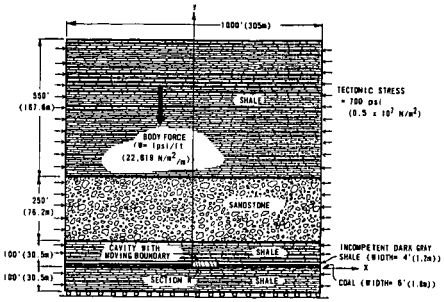

Figure 9a. The Master Model.

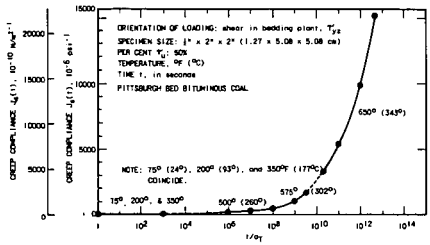

Figure 8. Time-Temperature Superposition Showing The Time Shift for the Pittsburgh Coal When Loaded in Shear.

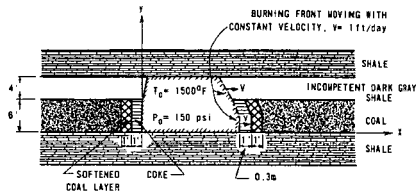

Figure 9b. Cavity with Moving Boundary (Section A) of the Master Model.

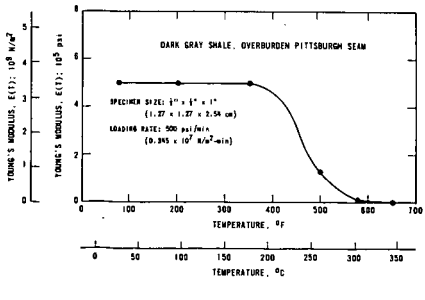

Figure 10. Young's Modulus for Dark Gray Shale as a Function of Temperature.

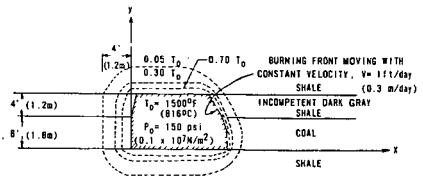

Figure 9c. Computed Steady State Temperature Distribution for the Master Model.

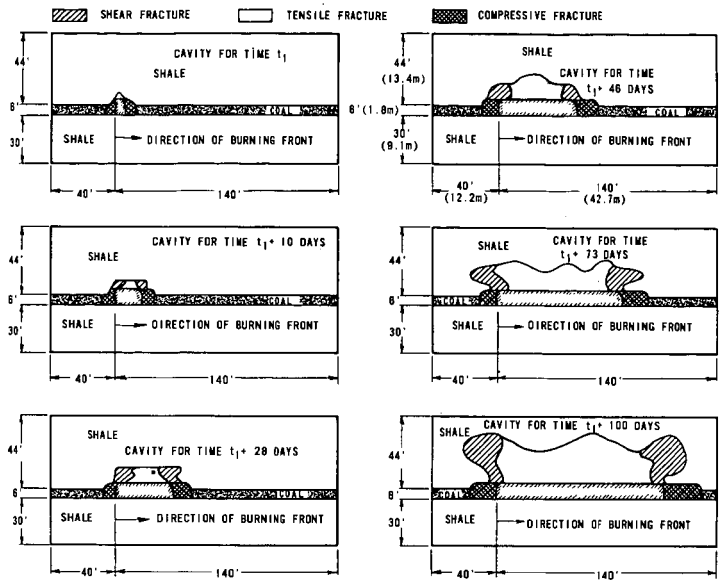

Figure 11. Failure Zones Adjacent to Cavity for Different Time Instants.

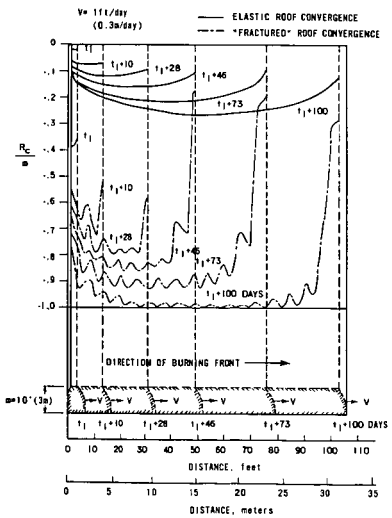

Figure 12. Roof Convergence Profiles for Different Burn Configurations.

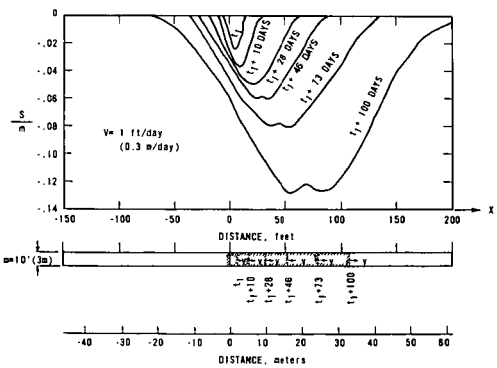

Figure 13. Surface Subsidence Profiles for Different Burn Configurations.

COMPARATIVE AUTO-OXIDATION STUDIES OF RAW AND RETORTED OIL SHALE AND WESTERN COALS

Schmidt-Collerus, J.J., W.A. Schmeling, and J.W. King, 2390 S. York, Denver, CO 80208.

The imminent commercial scale production of shale oil from the Green River Oil Shale Formation may apply some retorting processes which will produce large quantities of carbonaceous retorted shale and will also require large stockpiles of crushed raw shale for a continuous operation. From experiences in ongoing commercial shale oil production (e.g. Estonia) and previous commercial or pilot plant operations it is known that both the raw shale and the retorted carbonaceous shale are liable to auto-oxidation (similar to that of coals) which in some cases leads to self-ignition. In order to evaluate the self-heating liability of Green River Oil Shale and carbonaceous retorted shale therefrom, a comparative study between retorted oil shale from various above ground retorting operations, non-retorted oil shale and various Western coals was conducted utilizing some methods used in determining self-heating liabilities of coals. The results of this study will be presented and possible approaches for the prevention of self-heating will be discussed.

STUDIES FOR DESIGN OF A SOLID WASTE MANAGEMENT PROGRAM *

H. T. Jones

Division of Coal Conversion, Department of Energy
Washington, D.C.

H. M. Braunstein and W. J. Boegly, Jr.

Oak Ridge National Laboratory
Oak Ridge, Tennessee 37830

ABSTRACT

Passage of the Resource Conservation and Recovery Act (PL 94-580) in October 1976 will have far-reaching consequences for many solid-waste producing industries including future coal conversion facilities. Since little is known about the potential environmental problems from conversion wastes, a study is under way to evaluate landfill methods for disposal of these wastes. Residues from pilot plant and commercial processes are being characterized in a 3-tiered testing program which incorporates initial laboratory leaching studies, field-scale lysimeter testing and a full-scale landfill experiment. The information will lead to engineering design of safe economical solid-waste landfills for demonstration plants.

INTRODUCTION

In October 1976, the U.S. Congress passed the Resource Conservation and Recovery Act which provides for federal regulation of the treatment and disposal of solid wastes that represent a danger to the environment or to health. This Act is to solid wastes what the Clean Air Act Amendments of 1970 are to airborne wastes and the Federal Water Pollution Control Act Amendments of 1972 are to waterborne wastes. Compliance with this law may have far-reaching consequences for all coal-utilizing systems, especially those necessary for the demonstration of advanced fossil fuel technologies. Since near-commercial demonstration of coal conversion processes in the private sector is important for meeting our national energy objectives and since these technologies produce a voluminous solid waste with components that may possibly be classified as hazardous, a research program was undertaken to determine whether a problem exists. Management of the wastes from demonstration plants can be an important factor in demonstrating both the environmental acceptability and economic feasibility of a given alternative.

FOSSIL ENERGY DEMONSTRATION PROGRAM

In order to appreciate the role of environmental performance in the demonstration of advanced fossil energy technologies, it is helpful to understand the program's objectives, strategy, and structure. The objectives of the fossil energy demonstration program are shown in Fig. 1.

*Research sponsored by the Department of Energy under contract with the Union Carbide Corporation.

Environmentally, demonstration plants are unlike pilot plants. The latter are normally concerned only with process development whereas a demonstration plant has many areas of concern. The industrial partner in a demonstration project must show that his process is economically feasible, technically sound, and environmentally acceptable on a near-commercial scale. Not only is he challenged by an emerging technology, he must keep abreast of ever-changing environmental obligations. He must meet the NEPA requirement; he must address New Source Performance Standards; and he must remain alert to new regulations stemming from the Resource Conservation and Recovery Act. Figure 2 is a list of current planned demonstration plants.

In recognition of and to help alleviate the stresses, the government stands ready to support the early phases of demonstration with ample guidance to the industrial partner and with necessary research to develop information needed to respond quickly to crucial questions. The research discussed in this paper was an outgrowth of this information need.

THE SOLID WASTE PROBLEM

It was recognized even before enactment of the Resource Conservation and Recovery Act that solid wastes from coal conversion had the potential for causing adverse environmental impacts. What may not have been recognized was that virtually all wastes from coal conversion facilities will be solid wastes. Air and water quality are closely regulated. This means little if any waste will be allowed discharge into these media,. Consequently, air and water emissions will need to be converted into solids (Fig. 3). Thus, what would have been an air and water emissions problem becomes a solid-waste land-disposal problem.

Figure 4 shows the solid wastes associated with some of the unit operations in a gasification process stream. These cover a wide variety of materials, properties, and potentials for environmental effects. The studies to be discussed are presently directed at the wastes that are unique to coal conversion, those in the dashed circles. Our aim is to identify possible contaminants, to isolate the process parameters with which they are associated and to produce engineering designs that incorporate effective treatment or control schemes. By studying processes in operation, and by examining the wastes they produce, we plan to develop information about the environmental consequences of land disposal of coal conversion solid wastes.

LANDFILL DISPOSAL

Solid wastes from conversion processes must be disposed of. A plant processing 3000 tpd of coal with a 10% ash content will require disposal facilities for at least 300 tpd of solids. Landfilling is a readily available disposal technique. But little is known about landfilling of coal conversion wastes, and data from landfilling of other wastes indicate the possibilities for environmental disruption (Fig. 5).

Although surface runoff can transport contaminants, the primary environmental impact from a landfill would occur by transport of precipitation-generated waste leachate into groundwater through the subsoil. It is not yet known whether leachate from coal conversion wastes will be a problem, but in the event that it is, control of subsurface movement of the leachate will be the best means for protecting the groundwater. By studying the soils that comprise this subsurface environment, by identifying and utilizing their absorption and exchange properties, we hope to come up with an effective economical landfill design.

WASTE MANAGEMENT RESEARCH

The problem is being investigated at the Oak Ridge National Laboratory as part of an ongoing study now in its second year. The first segment of the program was to draw together a wide variety of relevant information, to assess that information and to provide an environmental source book on solid waste disposal as it bears on coal conversion.[1] The document addresses the environmental, ecological and biological aspects of coal conversion solid wastes. It was concluded that definitive studies were needed if the wastes were to be deposited safely, economically, and permanently by landfilling. The experimental study, which is the main subject of this paper, was undertaken to address this need.

OBJECTIVES

To meet the objective of the program, which is to develop engineering designs for safe economical disposal of conversion solid wastes from demonstration plants, the project is structured around a real-world situation. Process wastes will be obtained from pilot and commercial plants and they will be examined in a natural setting, in contact with normal soils especially those from demonstration sites. Process wastes to be studied include: (1) Slagging Lurgi, (2) COGAS, (3) HYGAS, (4) CO_2 Acceptor, (5) Synthane, (6) BI-GAS, (7) Battelle Agglomerating Burner, and (8) Westinghouse/Walz Mills.

SCOPE

The program incorporates three main levels of testing (Fig. 6). Each level of data collection will support the next such that as information accumulates it should be possible to evaluate and predict not only the short-term but also the long-term behavior of buried wastes.

METHODS

Laboratory studies

For coal conversion wastes, laboratory experiments are especially important. Not only is the composition of the wastes variable and process related, they contain an abundance and wide variety of trace element and organic materials. Also, since little is known about their leaching behavior, controlled laboratory leaching studies are needed to identify the effluents for the more comprehensive surrogate landfill studies.

Solids characterization. Each residue will be characterized physically and chemically and the properties will be compared with those of the feed coal from which it was derived. Properties such as solubility, density, porosity, compactibility and particle size distribution will be determined. Chemical analyses of the solids will include major components, trace elements and organic content, if any. Coals will be ashed under standard laboratory conditions to compare the physical and chemical properties with those of the process-derived residues.

Soils characterization. Soils can act as a large interactive medium for many toxic leachate effluents which can be either absorbed or precipitated by soil components. Like coal, the physical, chemical and mineralogical composition of soil varies widely and consequently its capacity to retain toxic effluents varies also. Soils will be characterized for their pH, buffer capacity, ion-exchange capacity,

lime equivalent, and mineralogical composition. The absorption — desorption behavior of soils will be examined with the aim of characterizing the persistence of leachate components in a landfill environment.

Batch leaching tests. Leaching under laboratory conditions will be conducted both in the batch mode and by use of leaching columns. Emphasis will be on eluting trace elements and organic compounds. Batch sampling is fast and simple. It simulates natural flooding conditions or submergence of landfill materials as when mounding of a shallow groundwater table occurs. Analyses of the batch effluents will indicate not only the inherent solubilities of trace substances in the wastes, but varying the pH of the effluent will provide data on waste behavior under neutral, dilute acidic or dilute alkali conditions. Batch leaching will be examined also for mixtures of residues with soils to determine the direct effect of soils of leachate quality.

Column leaching tests. Leaching in columns (Fig. 7) allows control of conditions to more closely simulate the natural movement of soluble constituents. The apparatus is simple, quickly assembled, and gives readily reproducible results. The leaching solution will be varied between weakly acidic and weakly alkaline, and fractions will be collected as functions of time and volume throughput. Samples, which will be compared with background-level blanks, will be analyzed by suitable methods to obtain accurate qualitative and quantitative characterization of the constituents. Multielement methods such as neutron activation analysis, atomic absorption spectrometry and isotope dilution mass spectrometry will be examined. If indicated, organic materials will be separated chromatographically and analyzed by mass spectrometry. As with the batch tests, column leaching will be performed using representative soil and residue combinations.

Standardization of procedures. Standard leaching procedures have not been established for coal conversion wastes. Therefore, while collecting leaching data, methods will be studied with the aim of recommending standard procedures. Since leaching behavior of waste materials depends not only on the nature of the wastes but also on soil type and constitution, these considerations will be incorporated in the recommended protocols.

Field-scale lysimeter studies

As soon as laboratory experiments are well under way, field studies will be initiated. Field-size lysimeters have been used in conventional sanitary landfill studies as well as for examining burial ground behavior of radioactive solid wastes. Figure 8 shows the typical lysimeter which will be exposed to natural weather conditions during field studies.

Use of field-scale lysimeters as a transition between laboratory and demonstration-size experiments has several advantages. They:

(1) require less waste

(2) prevent leachate escape

(3) eliminate wall effects, and

(4) cost less.

Whereas the lysimeters will be large enough to prevent wall effects, the amount of waste needed to simulate a loaded landfill is orders of magnitude less than a normal

burial site. Nonetheless, large volumes of leachate can be generated and collected without risking discharge of leachate to the environment. But the primary advantage is the small capital investment not only for the data obtained but for the experiential information needed to establish design criteria for the landfill burial studies.

The lysimeters will be loaded with soil and waste to simulate a vertical cross section of a landfill trench, and will be designed to prevent escape of leachate into the environment. Both soil and leachate will be sampled frequently and analyzed to determine the extent of trace element and organic compound attenuation. Analytical methods, developed during the laboratory phase, will be applied to both the solids and leachates.

As a first step toward predicting long-term effects, data gathered during the lysimeter phase will be used to test and modify in-house transport models for substrate behavior of trace contaminants. Results will be used in designing and establishing the field burial studies. Modeling studies are an ongoing activity at ORNL having been initiated to characterize movements of low-level radioactive wastes from burial grounds.

Landfill burial studies

Currently, disposal of coal conversion solid wastes is assumed to be performed using landfill methods similar to those used for conventional municipal or industrial solid wastes. Results of the laboratory- and field-scale lysimeter tests when completed, will indicate whether this conventional method of solid waste disposal will be environmentally acceptable or whether unconventional designs will be required for disposal at conversion facilities.

Burial studies will be conducted at the demonstration site. Landfill designs, developed during the lysimeter stage of the program, will be implemented in full-scale field studies after characterizing the subsurface hydrogeology of the proposed burial area. A monitoring plan will be established at the landfill site to sample both the landfill and subsurface soils, and to monitor groundwater movement and quality. Data obtained from the preliminary modeling studies will help establish both the site and the monitoring plan.

Full-scale modeling studies will be conducted concurrently with the burial work. The rationale for modeling comes from the need to predict possible long-term, long-distance environmental impacts. Most incidents of groundwater contamination are found to occur not only 20 to 30 years after burial but often long distances from the burial site. Mathematical models simulate both the spatial and temporal components of trace contaminant mobilization. The movement of contaminants will be described in terms of hydrogeologic parameters such as subsurface lithology, mineral constituents, texture and stratigraphic structure, and aquifer geometrical properties. Scenarios for transport will be developed and tested using data collected in the field monitoring operations.

As indicated by the experimental results, mitigating measures will be developed to be commensurate with both the probability of escape of contaminants and with the estimated risk associated with their possible escape.

Research on this program has been ongoing for the past year and a half. The status of the experimental studies will be discussed and results of data collected during this period will be presented.

REFERENCES

1. H. M. Braunstein, Ed., *Environmental and Health Aspects of Disposal of Solid Wastes from Coal Conversion: An Information Assessment*, ORNL-6157, Oak Ridge National Laboratory, Oak Ridge, Tenn., 1978.

By acceptance of this article, the publisher or recipient acknowledges the U.S. Government's right to retain a non-exclusive, royalty-free license in and to any copyright covering the article.

ORNL–DWG 77-21325

DEMONSTRATION PROGRAM OBJECTIVES

- TO INDICATE TECHNICAL AND ECONOMIC VIABILITY OF NEAR-COMMERCIAL SCALE PROCESSES
- TO SPREAD THE DEMONSTRATED TECHNOLOGY QUICKLY TO PRIVATE INDUSTRY
- TO ENCOURAGE INDUSTRY PARTICIPATION BY PROVIDING PARTIAL FUNDING TO MINIMIZE THE RISK
- TO VERIFY THE ENVIRONMENTAL ACCEPTABILITY OF PROCESSES PRIOR TO FULL-SCALE COMMERCIALIZATION

Fig. 1. Demonstration program objectives.

ORNL–DWG 77-21324

DEMONSTRATION PLANTS

PROCESS	INDUSTRY PARTNER
SLAGGING LURGI	CONOCO COAL DEVLOPMENT CO.
COGAS	ILLINOIS COAL GASIFICATION GROUP
TEXACO GASIFIER (FOR NH_3)	WR GRACE
U GAS	MEMPHIS, LIGHT, GAS, AND WATER
WOODAL-DUCKHAM	ERIE MINING
HYGAS	(DESIGN PHASE ONLY)
SOLVENT REFINED COAL	(PLANNING)

Fig. 2. Demonstration plants.

ORNL–DWG 77-21323

EXAMPLES OF EMISSIONS DISPOSITION

MEDIUM	EMISSION	CONVERTED TO	FINAL DISPOSITION
AIR	SO_2	FLUE GAS DESULFURIZATION SLUDGE	LANDFILL
	PARTICULATES	PRECIPITATES	
WATER	DISSOLVED MINERALS	PRECIPITATES OR SOLIDIFIED PRODUCTS	LANDFILL
	SUSPENDED PARTICLES	SETTLED SLUDGES	
LAND	FLY ASH SLURRY	ASH SOLIDS	LANDFILL
	SLAG OR BOTTOM ASH SLURRIES	SOLIDS	

Fig. 3. Examples of emissions disposition.

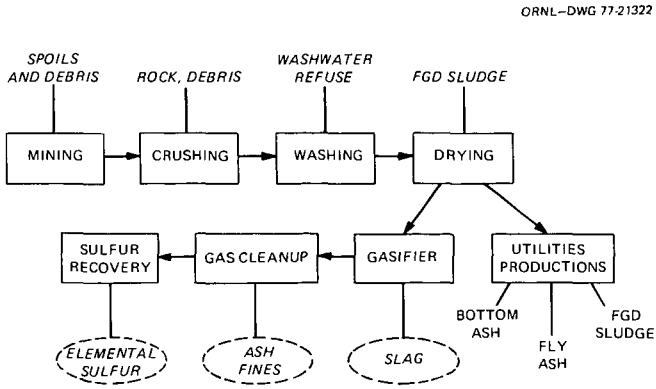

Fig. 4. Waste solids produced in a gasification facility.

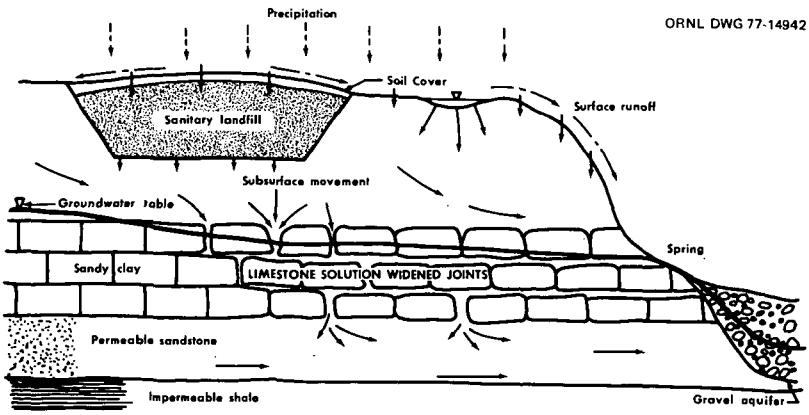

Fig. 5. Leachate formation and movement. Source: D. R. Brunner and D. S. Keller, "Sanitary landfill design and operation," EPA SW-65ts, 1972.

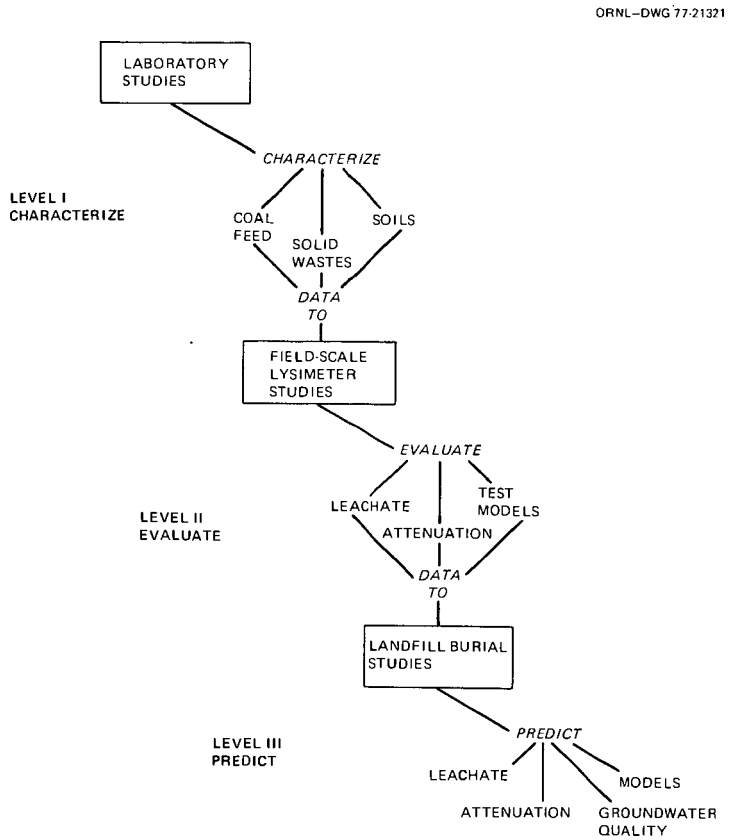

Fig. 6. Tiered approach of the ORNL Experimental Landfill Program.

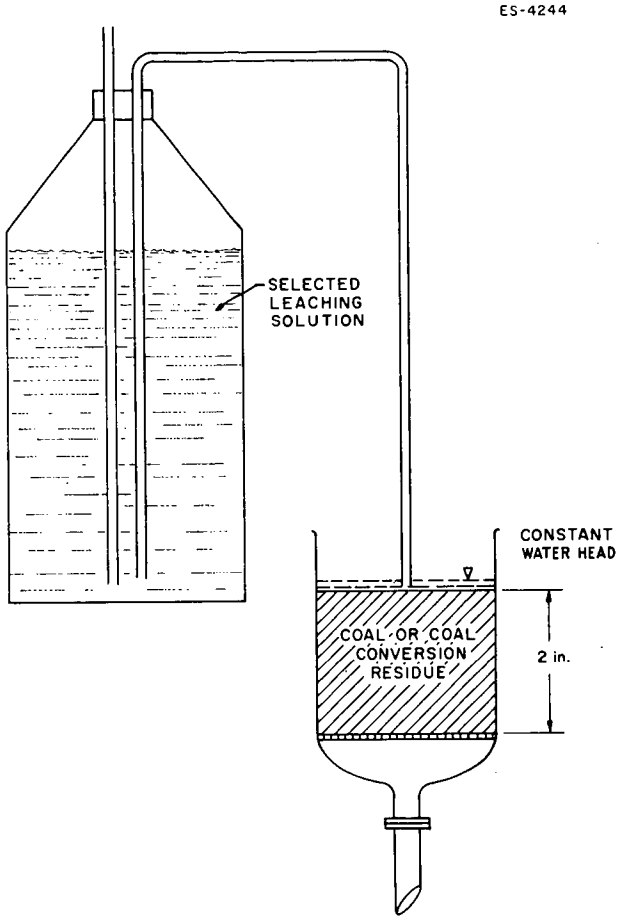

Fig. 7. Typical constant-water-head leaching column.

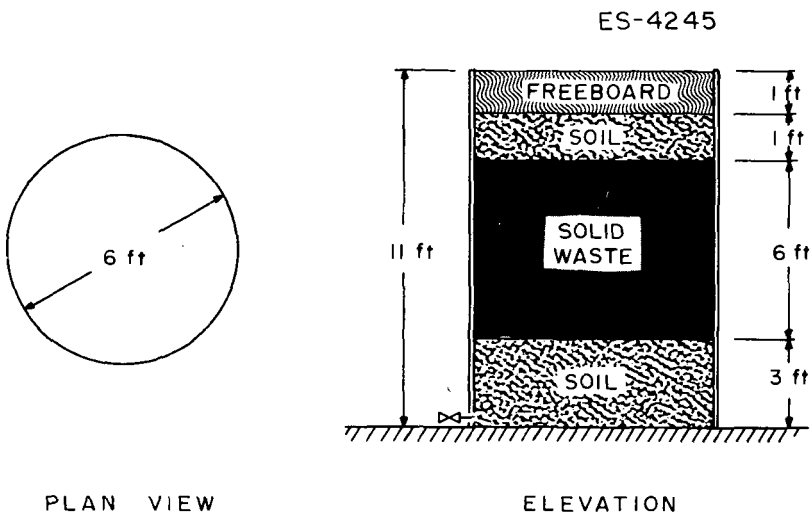

NOTES:
1. MATERIALS OF CONSTRUCTION – FIBERGLASS, PVC, OR ALUMINUM
2. SAMPLING MAINLY AT BOTTOM; SOME LYSIMETERS WITH SAMPLING POINTS AT VARIOUS DEPTHS
3. RELYING ON NATURAL RAINFALL WHEN POSSIBLE
4. PLACED ABOVEGROUND INSTEAD OF UNDERGROUND TO SIMPLIFY SAMPLING AND TO REDUCE COSTS

Fig. 8. Typical lysimeter.

EXPANDED COAL PRODUCTION
ENVIRONMENTAL IMPLICATIONS AND POLICY CONSIDERATIONS

M.T. El-Ashry

Environmental Defense Fund
1657 Pennsylvania Street, Denver, Colorado 80203

INTRODUCTION

Coal is considered one of the most valuable natural resources in the United States. Coal production in 1976 amounted to 665 million tons, and at such rate of production it could last for 300 years or more.

The earliest record of production in the U.S. was in 1820 when 3,000 tons of coal were produced. By comparison, total coal production in 1976 was 665 million tons, about 56% of which were produced by surface mining methods (Figure 1). During the period from 1939 to 1969, coal production from underground mines declined by about 3% from 357 million tons to 347 million tons, whereas coal from surface mines increased by 413%, from 38 million tons in 1939 to 195 million tons in 1969.

The electric utilities are the major users of coal in the U.S. The U.S. Bureau of Mines (1) reports that 390 million tons of coal (about 65% of the total production) were burned in electric power plants in 1974 and the trend for coal use by utilities is projected to increase to 800 million tons in 1985 (2).

In April 1977, President Carter announced his National Energy Plan with specific proposals aimed at solving the nation's energy problems. In order to reduce U.S. dependence on oil imports, one of the major proposals of the National Energy Plan is to increase coal production to 1,265 million tons in 1985, an increase of 90% over 1976 level. Long-range plans of the coal industry, without the new plan, call for an increase in coal production to about 1,040 million tons by 1985, about two-thirds of which would be mined in the East and about one-third in the West (Figure 2). Clearly, the major expansion in production will occur in the West, increasing by fourfold from 92 million tons in 1974 to about 380 million tons in 1985. The National Energy Plan, on the other hand, proposes to reduce the share of total production to be mined in the West and increase the share that will be mined in the East. In both plans, however, new developments for meeting production goals will be concentrated in surface mining operations, amounting to over 75% of the new facilities (3).

Coal mining and coal conversion have significant impacts on the environment of a region, some of them are irreversible and permanent. They include adverse impacts on: water quality and quantity, topography, soil erosion, surface subsidence, land use, landscape aesthetics, air pollution and associated health effects, as well as social and economic impacts. Some of these impacts are not presently regulated.

ENVIRONMENTAL IMPACTS OF SURFACE COAL MINING

Water Quality

Deterioration of water quality results mainly from acid mine drainage which affects water quality by lowering pH, increasing total

dissolved solids and adding undesirable amounts of heavy metals and sulfates (4, 5). Table 1 lists some examples of acid mine drainage from surface coal mines in four regions.

Table 1
Examples of Mine Drainage
From Surface Coal Mines (After: Hill (6))

	Southwestern Indiana	Western Pennsylvania	Southeastern Illinois	Northern West Virginia
pH	5.7	3.2	2.7	3.0
Acidity, mg/l	0	152	1,620	870
Alkalinity, mg/l	170	0	0	0
Hardness, mg/l	1,780	-	-	-
Iron, mg/l	0.4	9.4	130	75
Sulfate, mg/l	850	499	-	1,742
Chloride, mg/l	7	-	-	-
Manganese, mg/l	7.8	-	-	-
Calcium, mg/l	328	-	-	-
Aluminum, mg/l	-	-	-	60

Pollution by acid mine drainage increases the cost of water treatment, destroys aquatic life (7), inhibits the use of waterways for recreation and decreases aesthetic values. The major problems of acid mine drainage occur in the anthracite and bituminous coal regions in Appalachia. In 1964, the U.S. Fish and Wildlife Service reported that acid mine drainage adversely affected 5,890 miles of streams and 14,967 acres of impoundments in 20 states (7). Of the total affected waters, coal mining operations accounted for 97% of the AMD pollution reported for streams and 93% of that reported for impoundments. In 1970, more than 12,000 miles of streams in the U.S. were significantly degraded by mining related pollution (8). Of these, 10,516 miles or approximately 88% were located in Appalachia.

Western coal, generally, contains little pyrite and the stream waters and soils, in the West, are often highly alkaline resulting in that acid mine drainage is not as great a problem as it is in the East. However, high dissolved solids content and heavy metals remain a problem resulting in adverse impacts on the beneficial use of water in the West, specially on agriculture. In addition, shales overlying Paleocene coals in the Northern Great Plains may contain between 300-500 ppm total nitrogen which could cause a buildup of nitrate in surface and ground water around refuse piles (9).

Another aspect of stream pollution involves increased sediment loads resulting from destruction of vegetative covers, steep slopes, disruption of soil structure and compaction which increases erosion potential, and from refuse and coal storage piles. Sediment yields of as much as 1,000 times their former levels have been reported from surface mined regions in Kentucky (10).

Increased coal production, as proposed in the National Energy Plan, is expected to result in an increase of 107% for total dissolved solids in the nation's waters by the year 2000 over their 1975 levels (11). Runoff from coal mining operations is projected to account for 30% of dissolved solids releases in 2000. In the semi-arid West, total dissolved solids from coal extraction, cleaning and conversion are expected to increase fivefold in the same 25-year period.

Water Quantity

Surface streams are affected through decreased surface runoff through diversions and seepage. In the semi-arid West, most streams are intermittent or have very little flow during dry seasons. Accordingly, there is little stream flow available for dilution of mine drainage. Heavy sediment loads during periods of high flow can have adverse effects on important aquifers downstream from a stripping operation. Fine silt and clay from refuse piles can result in surface sealing and reduction of the infiltration capacity of the soils.

Surface mining operations may disrupt groundwater flow patterns as well as natural recharge areas. In some cases a coal seam acts as an aquifer that can be drained by the mining activity (12). Accordingly, groundwater supplies above and below the cut may be depleted temporarily or permanently (Figure 3). In the West, alluvial aquifers are an important source for irrigation water. In addition, shallow alluvial aquifers serve to buffer seasonal fluctuations in surface runoff and reduce flood peaks through bank storage.

Mine location relative to aquifers could play a major role in minimizing the impacts of a surface mine or ground water resources (13). Figure 4 shows that the mine located at the left will cause both local and regional effects on the water resource while locating the mine at the outcrop of an aquifer (mine location at the right) will have only local impacts on ground water.

In addition to the effects on surface and ground water resources, surface mining of western coal would also intensify existing demand and competition for scarce water resources. Potential problems include water depletion for surface reclamation and for rapid increase in population.

Topography

Topography is modified by the elimination of old landforms and the creation of new ones as well as by increased slope angles. Moisture-catching depressions and pits increase the potential of acid mine drainage production in the East and may cause surface accumulation of salt in the West. It should also be mentioned that actions which change the topography of an area also influence the surface and subsurface drainage patterns of that area. In the Wilkes-Barre area in the Northern Anthracite Field of northeastern Pennsylvania, surface mining along the ridges on both sides of the Wyoming Valley with its attendant unreclaimed pits that continually collect water from precipitation and from upward movement of ground water have resulted in a rise in the ground water table in the valley floor causing basement flooding in many homes.

Air Pollution

Air pollution as a result of surface mining is primarily in the form of airborne particulate matter from silt ponds and refuse banks, and gases from culm (refuse) bank fires. The most toxic gases are carbon monoxide (CO), carbon dioxide (CO_2), hydrogen sulfide (H_2S), sulfure dioxide (SO_2), and ammonia (14). These gases in addition to smoke and minute dust particles have in many instances proven fatal to vegetation, a health hazard to humans, and caused deterioration of surrounding buildings and structures.

In 1968, the U.S. Bureau of Mines reported 292 burning coal refuse banks throughout the United States covering over 3,200 acres (14). In comparison, 495 coal refuse banks were burning in 1963, in 15 out of the 26 coal-producing states.

Social and Economic Impacts

The influx of large numbers of people in a relatively short period of time into sparsely populated areas, attracted by mining activities and energy-related developments, results in significant social and economic impacts. The influx of money and jobs during the height of the mining operations and related activities brings along an economic boom and high inflation that only turns into a bust when the operation is completed. Many of the poverty stricken areas of Appalachia are living examples of such process. Gillette and Rock Springs, Wyoming, are good examples of present-day boom towns. The last examples are cause for concern when potential massive development of western coal is considered. The Northern Great Plains is a vast, rural, sparsely-settled region. The population of Campbell County, Wyoming, is expected to increase sixfold to 70,100 by the year 2000 if development proceeds as projected (15). Most of this growth will occur in Gillette which can be expected to reach a population of 65,000 by the year 2000 (Figure 5). The competition for labor by coal-related industry in this area will have a direct effect on present industry. Agriculture is the present economic base of much of the Northern Great Plains.

ENVIRONMENTAL IMPACTS OF UNDERGROUND COAL MINING

Acid Mine Drainage

Abandoned underground coal mines and abandoned mine waste disposal sites contribute a large portion of the acid mine discharge. Of the sources of acid mine drainage located and described in Appalachia by the Federal Water Pollution Control Administration between 1964 and 1968, abandoned underground coal mines were found to contribute 52% of the total acid discharge to streams (8). In 1973, acid discharge from abandoned eastern underground coal mines totaled more than 5 million lb./day which was the largest single source of AMD in the U.S. (16).

The large volume of AMD from abandoned underground mines is attributed to fracturing or general subsidence of overlying strata resulting in increased vertical permeability and flow of large volumes of water into the mine void (Figure 6).

Control of acid mine drainage from future underground mining operations could be accomplished through proper selection of mining techniques, water handling and mine sealing. Downdip mining involves the location of mine openings at a high elevation in the seam while development proceeds downdip. Flooding of the mine is automatic after completion of the mining operation thus isolating sulfide minerals in the mine, minimizing oxidation and resulting in better quality discharges than has occurred from the abandoned mines that were developed updip (16). Longwall mining should also be an effective method of improving quality of mine drainage. Controlled fracturing and caving of the roof behind the advancing face reduces void space and inhibits the oxidation of sulfides in the mine.

Subsidence

The two principal underground methods of coal mining in the U.S. are room and pillar and longwall. In room and pillar mining operations, failure of one or more roof supports and failure due to overburden loading on broad roof spans between supporting columns result in collapse of the overlying strata and surface subsidence. The extent of the subsidence zone and the nature of subsidence vary from area to area and depend mainly on the type of mining, width of the mined-out area, thickness of the coal seam, and the depth and characteristics of the overburden.

Surface subsidence may result in excessive damage in highly developed urban areas. Good examples exist in northeastern and in western Pennsylvania. Other land uses are usually less severely affected. In general, lateral stresses result in more severe damage than vertical movement, and they are most intense at the periphery of the subsidence area (17).

Solid Waste (Refuse Banks)

There are between 3,000 and 5,000 refuse banks, containing over three billion tons of refuse, in the eastern coal fields alone. Production of solid waste from all coal mining in 1973 totaled about 110 million tons. A study by the Bureau of Mines estimates that between 1930 and 1971, almost 166,000 acres of land were utilized for disposal of underground mining and processing wastes (18). Of the total, only 20,000 acres were reclaimed.

Refuse banks are a potential source of air and water pollution. When ignited, they provide noxious and lethal gases as mentioned before. Water pollution results from sediment and acid mine drainage.

Underground disposal of coal mine waste is a viable alternative to their disposal on the surface and limits land use impacts. However, experience in this field has been limited in the U.S.

Increased coal production implies increased solid waste that is neither utilized at present nor disposed back underground. The Bureau of Mines estimates that about 10 acres of land are utilized for disposal of coal mine and preparation plant wastes for every million tons of coal produced (17). It is estimated that coal mining wastes will nearly double between 1975 and 1985 (11). However, under the proposed National Energy Plan, they will nearly triple between 1975 and 2000. About three-fourths of the wastes are expected to occur in the eastern regions.

Abandoned Mine Fires

U.S. Bureau of Mines figures show that as of January 1973, there were 59 uncontrolled abandoned mine fires in Appalachia and about 185 uncontrolled fires in the western regions. Abandoned underground mine fires have severe land use implications. They result in surface subsidence while the release of toxic gases is a hazard to human health and to vegetation.

ENVIRONMENTAL IMPACTS OF COAL TRANSPORTATION

The bulk of coal produced in the U.S. is presently being transported mainly by rail (65%), barges (11%), trucks (13%) and Great

Lakes colliers (3%). In addition, transportation of coal by slurry pipelines has been proposed as a method for moving large tonnage of western coal over great distances.

Rail is the primary method for coal transportation in the U.S. All rail movements totaled over 290 million tons in 1973, a 41% increase since 1962 (18). The most significant environmental impacts associated with railroad traffic include: noise, air pollution and congestion. Increased coal production and transportation will only intensify these impacts, particularly congestion problems in western towns.

The channelization of streams, construction of canals and dredging and disposal of dredged spoils in connection with construction and maintenance of waterways for barges have adverse impacts on water quality and in many cases has resulted in the destruction of fresh or coastal wetlands.

The major environmental impacts of trucks are air pollution, noise, highway safety and congestion. In addition, increased truck traffic to accommodate the planned doubling in coal production might necessitate new construction of highways with their attendant environmental impacts.

The major environmental impacts of coal slurry pipelines are almost entirely related to their use of water. They involve water depletion and water quality degradation. Proposed slurry pipelines are expected to obtain their water from ground water sources. Since one ton of water is needed to move one ton of coal, massive amounts of water, in a region that is normally short in water supply, are needed to transport over 100 million tons of coal a year. Without adequate ground water management plans, the construction of slurry pipelines in the West could result in significant ground water problems as well as water quantity and quality problems for surface streams connected with the disturbed aquifers.

ENVIRONMENTAL IMPACTS OF COAL CONVERSION

Air pollution is the most serious environmental problem associated with the conventional burning of coal. In 1974, 390 million tons of coal (about 65% of the total production) were burned by electric utilities for power generation. By 1985, this figure is projected to double to about 800 million tons. At present, nearly two-thirds of the sulfur oxides and one-third of the particulate matter emitted into the atmosphere are from burning coal for electric power generation. In addition, significant amounts of nitrogen oxides, carbon monoxide and hydrocarbons are also emitted in the coal burning process. All of these pollutants are known to have adverse impacts on human health. Carbon dioxide is also released in the coal combustion process. There is mounting concern that carbon dioxide buildup in the atmosphere may result in a "greenhouse" effect causing global climatic changes. It is important that knowledge of the long-term effects of coal development be improved before irreversible effects are encountered.

Gasification and liquefaction of coal may offer major air quality advantages for currently regulated pollutants. However, they present uncertain, potentially serious hazards for pollutants that are not yet regulated (19), particularly organic compounds that are proven carcinogens.

Major increases in electricity generation from conventional coal combustion could have great adverse air quality consequences in the absence of improved combustion and pollution control technologies. In this regard, the National Energy Plan proposes that best available control technology (BACT) be required on all new coal-burning facilities. The same provision has been included in the Clean Air Act Amendments of 1977. Yet, it is projected that sulfur oxides and nitrogen oxides will be higher in 1985 and 2000 than in 1975 (11). In the year 2000, sulfur oxides are projected to be about 12% higher and nitrogen oxides about 61% higher than in 1975. If SO_x and NO_x are to be reduced, continued improvements in BACT will be required. In addition, with planned and proposed increase in coal utilization, increasing amounts of sludges and spent ashes from coal combustion facilities may present a solid waste disposal problem and these wastes may cause a significant potential leachate problem (11). It is projected that in 2000, non-combustible solid wastes from coal burning would increase to 2.7 times the 1975 level and sludges would increase to 8.5 times the 1975 levels (11).

POLICY CONSIDERATIONS

From an environmental standpoint, coal is clearly the dirtiest of all fossil fuels. Severe environmental problems are associated with every phase of the fuel cycle. Table 2 presents a summary of key environmental issues associated with coal mining, preparation, transportation and conventional combustion.

Table 2
KEY ENVIRONMENTAL ISSUES AND REGIONAL CONCERNS
(Federal Regions: 3=Middle Atlantic, 4=South Atlantic, 5=Midwest, 6=Southwest, 8=North Central)

Energy Process	Key Environmental Issues	Regions of Concern
Coal Mining	Stabilization/disposal of underground mining wastes	Regions 3,4,5
	Reclamation of strip-mined land	Water scarce Regions 6,8, parts of 4
	Acid mine drainage	Regions 3,4,5
	Alkaline mine drainage	Primarily Region 8
	Occupational health and safety - underground mining - surface mining	 Regions 3,4,5 Regions 4,6,8
Coal Beneficiation	Suspended solid runoff (final EPA regulations may be less stringent than those assumed in study)	Regions 3,4,5,8
Coal Transportation	Occupational and public health and safety issues (rail accidents)	Primarily Regions 3,4, 5
	Particulate emissions	Highest in Region 5
Conventional Coal Combustion -Elec. Utilities -Indust. Boilers	 Ash and sludge disposal SO_x emissions	 Urban areas Reg. 5 (highest), Reg. 6 (largest increases)

The proposed National Energy Plan, while it "intends to achieve its energy goals without endangering the public health or degrading the environment," its only specific proposals for environmental protection concern strip mining reclamation and air pollutants for which present criteria exist. However, conventional coal combustion and conversion to synthetic gaseous and liquid fuels may result in a much greater range of social and environmental impacts than those presently regulated. In the short term, there can be some temporary trade-offs between coal development and environmental protection. However, in the process of solving this nation's energy problems, we must seek to avoid irreversible and permanent damage to the natural and human environment.

The environmental impacts of increased coal production and utilization, particularly with present technology, are clearly unacceptable. In order to minimize environmental damages more emphasis must be placed upon energy conservation and slower energy growth. While the proposed National Energy Plan represents a step forward in that direction, it could have gone a good deal farther. Energy conservation is more expedient than developing new sources and can be accomplished with less expense than building new capacity. Conservation will minimize the need for more expensive and environmentally harmful supply options and will help in providing time for developing acceptable supply sources. The most conspicuous, benign, and inexhaustible source of alternative energy is solar energy. However, present levels of solar research funding and efforts to disseminate it in the marketplace are inadequate.

Unless we change our emphasis away from centralized fossil and nuclear generation facilities towards the more environmentally benign technologies, levels of many pollutants will increase sharply in the next two decades which may pose great hazards to human health and food production.

REFERENCES

1. U.S. Bureau of Mines, IC-8118, p. 2, 1976.
2. Schmidt, R.A., EPRI Journal, pp. 6-11, August 1977.
3. Office of Technology Assessment, "Analysis of the proposed National Energy Plan," 242 pp., August 1977.
4. Biesecker, J.E. and George, J.R., U.S. Geol. Survey Circular 526, 27 pp., 1966.
5. El-Ashry, M.T. and Mattei, C.M., Proc. Pa. Acad. Sci., 48, p. 30, 1974.
6. Hill, R.D., EPA Water Qual. Off., Pub. No. 14010, 22 pp. 1971.
7. Kinney, E.C., U.S. Fish & Wildlife Service Cir. 191, 27 pp., 1964.
8. Warner, D.L., "Water pollution from mining activities in the U.S.," Prepared for the Fed. Water Qual. Adm., June 1970.
9. Power, J.F., et al., Science, 183, p. 1077, 1974.
10. Curtis, W.R., U.S. Forest Service Paper, Berea, Kentucky, 1969.
11. ERDA, "Draft Annual Environmental Analysis Report," Vol. 1, September 1977.
12. Hadley, R.F. and Keefer, W.R., Miscellaneous Investigations Series, Map I-848-F, U.S. Geol. Survey, 1975.
13. Ellison, R.D., in Reclamation of Western Surface Mined Lands, Ecology Consultants, Inc., pp. 38-52, 1976.
14. U.S. Bureau of Mines, IC-8518, Supp., 1971.
15. U.S. EPA, "First year progress report of a technology assessment of western energy resource development (Draft)," Off. of R&D,

Vol. II-A, p. 483, 1976.
16. U.S. EPA, Office of Water and Hazardous Materials, Report 440/9-75-007, 338 pp., 1975.
17. U.S. Bureau of Mines, IC-8507, 32 pp., 1971.
18. U.S. Bureau of Mines, IC-8706, 90 pp., 1976.
19. Council on Environmental Quality, "Environmental Quality," Seventh Annual Report, p. 212, September 1976.
20. Federal Energy Adm., "Coal: The Other Energy," 11 pp., 1976.
21. Federal Energy Adm., "National Energy Outlook - 1976," Executive Summary, 14 pp., 1976.

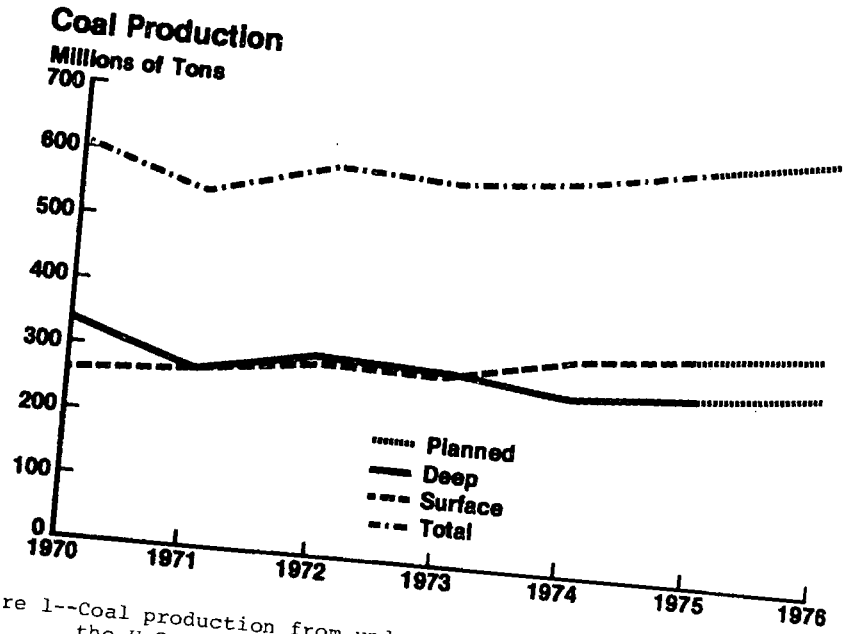

Figure 1--Coal production from underground and surface mines, in the U.S., 1970-1975 (20).

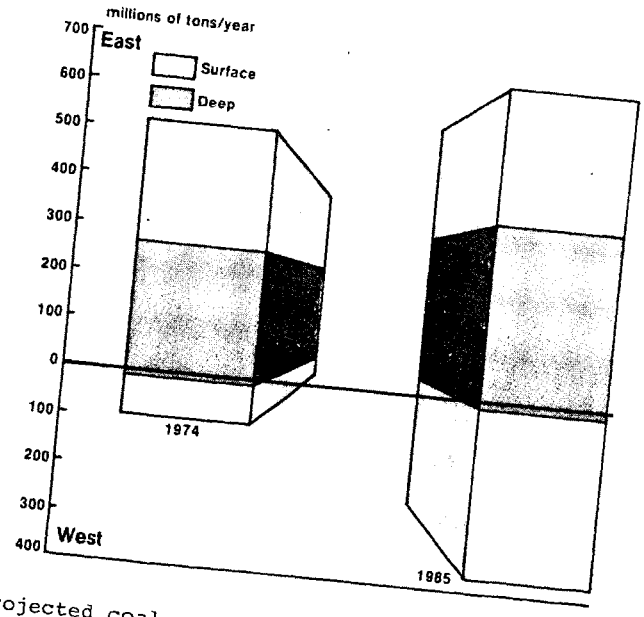

Figure 2--Projected coal production in the U.S., by region, in 1985 (21).

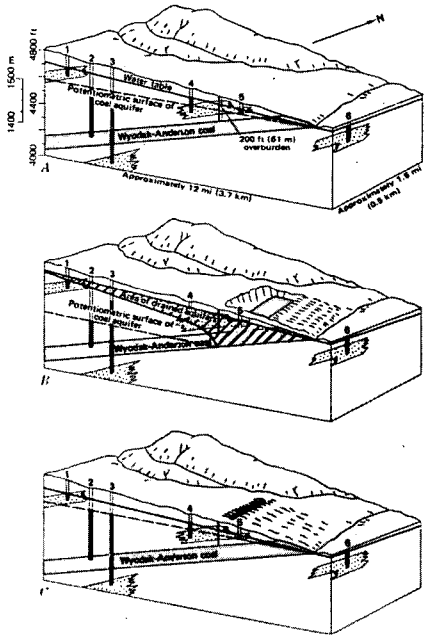

Figure 3--Potential effects of surface mining on shallow aquifers (12). A: before mining, B: after mining, C: after reclamation.

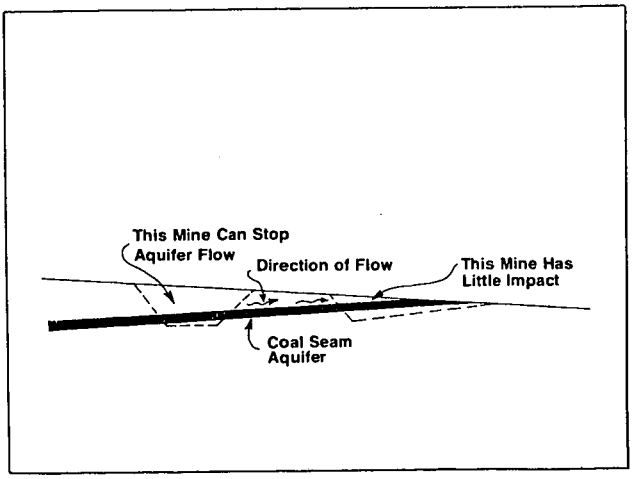

Figure 4--Impact of mine location on shallow aquifers (13).

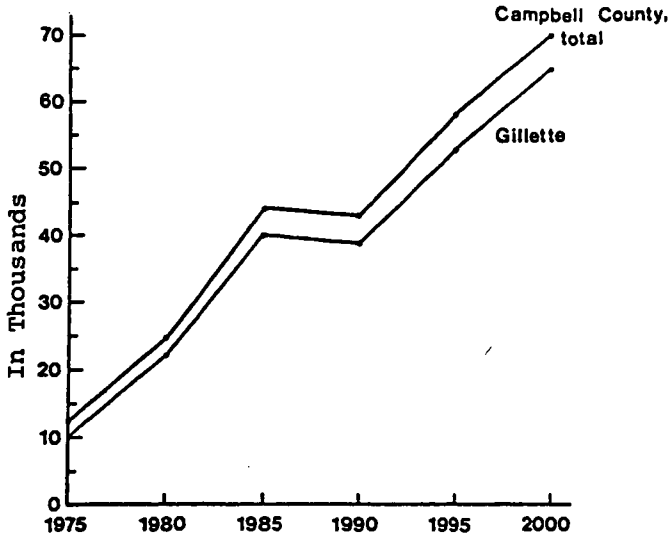

Figure 5--Population estimates for Campbell County and Gillette, Wyoming, 1975-2000 (15).

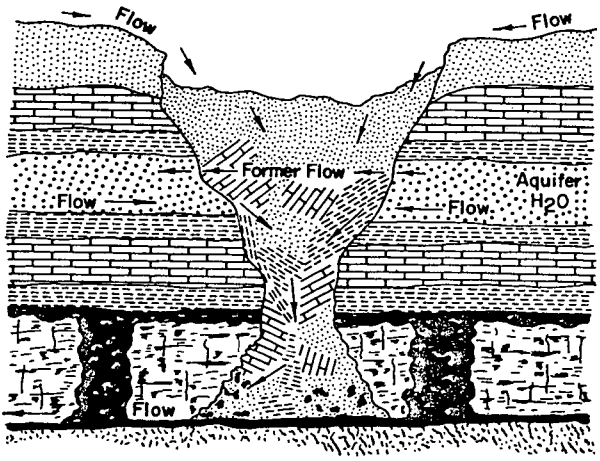

Figure 6--Infiltration of water through collapsed area (16).